

Dissertation
submitted to the
Combined Faculties of the Natural Sciences and Mathematics
of the Ruperto-Carola-University of Heidelberg, Germany
for the degree of
Doctor of Natural Sciences

Put forward by
Giulio Albert Heinrich Schober
born in Düsseldorf
Oral examination: November 30, 2016

Quantum Field Theory of Material Properties:
Its Application to Models of Rashba Spin Splitting

Referees: Prof. Dr. Manfred Salmhofer
Prof. Dr. Andreas Mielke

Quantenfeldtheorie der Materialeigenschaften – Anwendung auf Modelle der Rashba-Spin-Aufspaltung. Das Ziel dieser Arbeit ist es, mikroskopische Feldtheorien – die als solche bereits wissenschaftlich etabliert sind – als ein neues Paradigma der Materialphysik einzuführen. Hierzu entwickeln wir einerseits diejenigen Feldtheorien weiter, auf denen moderne Ab-initio-Rechnungen basieren, und betrachten andererseits deren Anwendung auf die Bismut-Tellur-Halogenide (BiTeX mit $X = \text{I, Br, Cl}$), welche eine prototypische Klasse von Spin-basierten Materialien darstellen. Dazu beginnen wir zunächst mit der Konstruktion von Tight-Binding-Modellen, die zur Approximation der Spin-aufgespaltenen Leitungsbänder von BiTeI verwendet werden können. Danach leiten wir die Theorie der Greens-Funktionen bei endlicher Temperatur systematisch aus deren fundamentalen Bewegungsgleichungen her. Dies ermöglicht es uns ferner, eine kombinierte Methode aus funktionaler Renormierung und Molekularfeldtheorie zu beschreiben, welche allgemein auf Modelle mit mehreren Bändern angewandt werden kann. Speziell für das Rashba-Modell mit einer attraktiven, lokalen Wechselwirkung liefert diese Methode eine unkonventionelle supraleitende Phase: während die Gap-Funktion Singlet-artig ist, hat der Ordnungsparameter gemischte Singlet- und Triplet-Anteile. Weiterhin untersuchen wir die außerordentlichen elektromagnetischen Response-Eigenschaften von BiTeI, die sich aus der Rashba-Spinaufspaltung ergeben, und sagen insbesondere einen Bahn-Paramagnetismus vorher. Schließlich fassen wir den „Functional Approach“ als eine mikroskopische Feldtheorie elektromagnetischer Materialeigenschaften zusammen, die im Einklang mit Ab-initio-Methoden steht.

Quantum Field Theory of Material Properties: Its Application to Models of Rashba Spin Splitting. In this thesis, we argue that microscopic field theories—which as such are already scientifically established—have emerged as a new paradigm in materials physics. We hence seek to elaborate on such field theories which underlie modern *ab initio* calculations, and we apply them to the bismuth tellurohalides (BiTeX with $X = \text{I, Br, Cl}$) as a prototypical class of spin-based materials. For this purpose, we begin by constructing tight-binding models which approximately describe the spin-split conduction bands of BiTeI. Following this, we derive the theory of temperature Green functions systematically from their fundamental equations of motion. This in turn enables us to develop a combined functional renormalization and mean-field approach which is suitable for application to multiband models. For the Rashba model including an attractive, local interaction, this approach yields an unconventional superconducting phase with a singlet gap function and a mixed singlet-triplet order parameter. We further investigate the unusual electromagnetic response of BiTeI, which is caused by the Rashba spin splitting and which includes, in particular, an orbital paramagnetism. Finally, we conclude by summarizing the Functional Approach to electrodynamics of media as a microscopic field theory of electromagnetic material properties which sits in accordance with *ab initio* physics.

Contents

Publications	xi
Introduction	1
I. Models of Rashba spin splitting	7
1. Electrons in periodic potentials	9
1.1. Position and momentum space	9
1.2. Bravais lattice and Brillouin zone	11
1.3. Bloch and Wannier vectors	14
1.4. Bloch-like vectors and atomic orbitals	20
1.5. Single-orbital model	24
1.5.1. Quasi-degenerate perturbation theory	24
1.5.2. Pauli matrix representation	27
2. Tight-binding Rashba model	31
2.1. Symmetries	31
2.1.1. Hermiticity	31
2.1.2. Time-reversal symmetry	32
2.1.3. Spatial inversion symmetry	35
2.1.4. Point-group symmetries	37
2.2. Derivation of Rashba spin splitting	44
2.3. Minimal tight-binding model	47
3. Rashba semiconductor BiTeI	53
3.1. Crystal and band structure	53
3.2. Two-dimensional Rashba model	54
3.3. Effective single-orbital model	57
II. Statistical field theory	67
4. Green function perturbation theory	69
4.1. Basics of second quantization	69
4.2. Temperature Green functions	71
4.3. Green functions on the lattice	75
4.4. Perturbative expansion	79
4.4.1. Gell-Mann–Low theorem	80

4.4.2. Equations of motion	84
4.4.3. Wick theorem	91
4.5. Universal Feynman Graphs	94
4.5.1. Definition	94
4.5.2. Classification	97
4.5.3. Cancellation theorem	101
5. Grassmann field integral	107
5.1. Grassmann algebra	107
5.1.1. Basic definitions	107
5.1.2. Grassmann–Gaussian integral	108
5.2. Green function generator	111
5.3. Connected Green functions	115
5.4. Fully amputated, connected Green functions	125
5.5. One-line-irreducible Green functions	126
A. Nambu formalism	147
III. Functional renormalization and mean-field approach	153
6. Renormalization group equations	155
6.1. Scale dependence	155
6.2. Connected Green function flow	158
6.3. One-line irreducible Green function flow	167
6.4. Level-two truncation and initial-value problem	179
7. Functional renormalization for multiband systems	185
7.1. Flow equations on the lattice	185
7.2. Static-vertex approximation	191
7.3. Fermi surface patching	193
8. Mean-field theory without $SU(2)$ symmetry	197
8.1. Definitions	197
8.2. Symmetries	199
8.3. Mean-field Hamiltonian	201
8.4. Solution for singlet interaction	202
8.4.1. Gap function	203
8.4.2. Bogoliubov transformation	203
8.4.3. Order parameter	207
8.4.4. Singlet and triplet amplitudes	209
8.4.5. Gap equation and critical temperature	210
9. Application to the Rashba model	211
9.1. Model parameters and numerical implementation	211
9.2. Effective interaction and critical scale	214
9.3. Solving the gap equation	217

IV. Summary of further work	223
10. Electrodynamic properties of BiTeI	225
10.1. Optical conductivity	225
10.2. Magneto-optical conductivity	227
10.3. Magnetic susceptibility	231
10.3.1. Thermodynamic calculation	231
10.3.2. Calculation in the Kubo formalism	233
10.3.3. Calculation from Fukuyama's formula	237
11. Functional Approach to electrodynamics of media	239
11.1. Introduction	239
11.2. Universal Response Relations	241
11.3. Relativistic covariance	243
11.4. Refractive index	245
Conclusion	247
References	258
Acknowledgments	259

Publications

While I have compiled this thesis by myself, a large part of the work presented here has been done in collaboration with the authors mentioned below, for which I am sincerely grateful. Following are listed the publications which form the basis of—and which are partly reproduced in—the respective parts of this thesis.

Parts I–III.

- *Functional renormalization and mean-field approach to multiband systems with spin-orbit coupling: Application to the Rashba model with attractive interaction*
with Kay-Uwe Giering, Michael M. Scherer, Carsten Honerkamp,
and Manfred Salmhofer
Phys. Rev. B **93**, 115111 (2016) [Sch+16a]

Part IV, Chapter 10.

- *Ab initio electronic structure and optical conductivity of bismuth tellurohalides*
with Sebastian Schwalbe, René Wirnata, Ronald Starke, and Jens Kortus
e-print available from arXiv:1607.06693 [physics.comp-ph] (2016) [Sch+16b]
- *Enhanced infrared magneto-optical response of the nonmagnetic semiconductor BiTeI driven by bulk Rashba splitting*
with László Demkó, Vilmos Kocsis, Mohammad Saeed Bahramy, Hiroshi Murakawa,
Jong Seok Lee, István Kézsmárki, Ryotaro Arita, Naoto Nagaosa,
and Yoshinori Tokura
Phys. Rev. Lett. **109**, 167401 (2012) [Dem+12]
- *Mechanisms of enhanced orbital dia- and paramagnetism: Application to the Rashba semiconductor BiTeI*
with Hiroshi Murakawa, Mohammad Saeed Bahramy, Ryotaro Arita, Yoshio Kaneko,
Yoshinori Tokura, and Naoto Nagaosa
Phys. Rev. Lett. **108**, 247208 (2012) [Sch+12]
- *Optical response of relativistic electrons in the polar BiTeI semiconductor*
with Jong Seok Lee, Mohammad Saeed Bahramy, Hiroshi Murakawa, Yoshinori Onose,
Ryotaro Arita, Naoto Nagaosa, and Yoshinori Tokura
Phys. Rev. Lett. **107**, 117401 (2011) [Lee+11]

Part IV, Chapter 11.

- *Ab initio materials physics and microscopic electrodynamics of media*
with Ronald Starke
e-print available from arXiv:1606.00445 [cond-mat.mtrl-sci] (2016) [[SS16c](#)]
- *Response theory of the electron-phonon coupling*
with Ronald Starke
e-print available from arXiv:1606.00012 [cond-mat.mtrl-sci] (2016) [[SS16b](#)]
- *Relativistic covariance of Ohm's law*
with Ronald Starke
Int. J. Mod. Phys. D, DOI: 10.1142/S0218271816400101 (2016) [[SS16a](#)]
- *Microscopic theory of the refractive index*
with Ronald Starke
e-print available from arXiv:1510.03404 [cond-mat.mtr-sci] (2015) [[SS15b](#)]
- *Functional approach to electrodynamics of media*
with Ronald Starke
Phot. Nano. Fund. Appl. **14**, 1 (2015) [[SS15a](#)]

Introduction

In constructing a new theory, we shall be careful to insist that they should be precise theories, giving a description from which definite conclusions can be drawn. We do not want to proceed in a fashion that would allow us to change the details of the theory at every place that we find it in conflict with experiment, or with our initial postulates. Any vague theory that is not completely absurd can be patched up by more vague talk at every point that brings up inconsistencies—and if we begin to believe in the talk rather than in the evidence we will be in a sorry state.

R. P. Feynman [FMW95, p. 22]

Classical and quantum field theory form the basis of modern *materials physics*. From a purely conceptual point of view, they have together replaced the traditional picture of materials as being composed of point particles, elementary electric or magnetic dipoles, microscopic elastic springs, etc. Such simplified models were easily accepted even after quantum mechanics had been firmly established, mainly because they can be *visualized* similarly as the macroscopic objects which surround us in everyday life. By contrast, with the advent of *ab initio* materials physics, the starting point of realistic material descriptions became the many-body Schrödinger (or Dirac) equation and the microscopic Maxwell equations. These fundamental equations define the Schrödinger (or Dirac) field and the electromagnetic field, respectively. As such, these microscopic *field theories* do not contain any “objects” or “particles”, and hence they are abstract by their very nature. Even the electrons and photons, which are often cited in this context, are the elementary excitations of the corresponding *quantized fields* (just as “phonons” are the elementary excitations of the quantized displacement field [SS16b]). Here, “elementary excitation” refers to an excited state of the system which exhibits a certain energy difference to the ground state, but does not imply any particle-like nature of these excitations (see Ref. [PG15]). In particular, this implies a strict rejection of the so-called “philosophical realism”. Consequently, field theories can be thought of only in terms of the differential equations which govern the time evolution of the fields from some given initial conditions, as well as in terms of a quantization procedure which promotes the real- or complex-valued classical fields to operator-valued fields satisfying certain (anti)commutation relations. Under this new paradigm, all deductions should be drawn as a matter of principle from the microscopic field equations (in addition, perhaps, to some *empirically motivated* assumptions, such as the high degree of nuclear localization in the case of a crystalline solid [SS16b]).

However, it is not *a priori* clear how the observable properties of materials such as their solidity, their electric and magnetic response, or their optical behavior can be explained by such abstract field theories. In fact, it is precisely the aim of materials physics to deduce such material characteristics from the known microscopic physical laws. Again based on principle, the coupled field theory as defined by the many-body Schrödinger or Dirac equation and by the microscopic Maxwell equations cannot be solved exactly, and even if it were able to be solved, it would not be clear how to extract from the solution statements about the macroscopic behavior of materials. On the practical side, however, several methods have been established which allow for approximate solutions and quantitative predictions of material properties. Above all, *Green function theory* allows one to work with functions of only a few arguments instead of the many-body wave function whose number of arguments equals the particle number [SK12]. (Note that the latter does not count the number of real “particles”, but instead refers to the eigenvalue of the abstract “particle-number operator” or to the corresponding sector of the abstract Fock space.) Already the simplest Green function, the two-point Green function, allows for the calculation of expectation values of all “one-particle operators” such as the charge or the current density in the case of the matter fields [SK12]. Furthermore, as one of the most successful approaches in materials science, *response theory* is concerned with the reaction of a material to an applied (typically electromagnetic) external perturbation. The *Kubo formalism* [Kub57], which gives the concrete formulae for the respective *linear* response functions, already leads to quantitative predictions of electromagnetic properties for an amazing variety of materials, and it is therefore implemented in any modern *ab initio* computer code (such as [Bla+01; Gia+09; KF96]). The success of these theoretical approaches has brought field theories to wide acceptance in spite of their abstract nature.

Apart from the response theory, which mostly deals with time-dependent perturbations of a system that is originally prepared in its ground state, one is also often interested in thermal equilibrium properties and especially in the low-temperature phases of a given material, description of which constitutes a branch of *statistical physics*. Correspondingly, response theory relies on the real-time Green functions (which are typically defined as expectation values of the field operators with respect to the ground state), whereas in statistical physics one deals with the so-called *temperature* Green functions. The latter are defined as expectation values of the field operators with respect to a thermodynamic ensemble as represented by a density matrix. To simplify the perturbation theory, one then usually performs the transition to Green functions in *imaginary time*, also called *Schwinger functions*. The resulting quantum field theory is also called *statistical field theory* [ID89], and we will be mainly concerned in this thesis with the latter type of Green functions. A main pillar of statistical field theory is the *functional renormalization group* (fRG), which has been developed in recent decades into a versatile and unbiased methodology for investigating correlated electron systems [BTW02; Met+12; SH01]. It enables one to study (possibly competing) Fermi liquid instabilities without making potentially restrictive *a priori* assumptions with regard to the ordered phases, and it yields the low-energy effective interactions after *integrating out* the high-energy degrees of freedom in the functional integral formalism. In combination with a Fermi surface patching approximation, this procedure has been applied successfully to models

relevant for the high-temperature superconducting cuprates and iron pnictides, strontium ruthenate, graphene, and many other correlated electron systems (for a recent review of these, see Ref. [Met+12]).

This thesis aims at further developing and improving (quantum) field theoretical techniques as they are presently used in materials physics. Moreover, it seeks to apply these techniques to a special class of materials whose properties are dominated by the spin degree of freedom (for this reason they are sometimes called *spin-based materials*). In accordance with the above remarks about field theories, the spin is also an abstract concept which cannot be visualized as a concrete object. In particular, one cannot generally view the spin as an arrow pointing in a certain direction (or in a superposition of directions), and physical reasoning based on such an idea is necessarily met with skepticism. On a fundamental level, the spin is just an additional index which labels the matter fields (i.e., the Dirac or Schrödinger fields). Within response theory, it makes its effect through an additional, transverse contribution to the electromagnetic current [SS16c, Sct. 3.2.5]. In the work presented here, we restrict ourselves to the non-relativistic Schrödinger equation, where the spin is taken into account by the Pauli spin-orbit term. In particular, we investigate the recently discovered semiconductor BiTeI, which displays *Rashba spin splitting* (RSS) of the energy bands [Ish+11]. Concretely, this means that near the Γ point of the Brillouin zone, the lowest conduction bands of this material can be described approximately by the Rashba Hamiltonian [BR60; Ras60], which reads

$$H_R(\mathbf{k}) = \frac{\hbar^2}{2m^*} (k_x^2 + k_y^2) + \alpha (k_x \sigma_y - k_y \sigma_x),$$

where m^* denotes the effective electron mass, α the Rashba parameter, and σ_x, σ_y the Pauli matrices. The spin splitting is extraordinarily large in BiTeI, with the Rashba parameter being approximately $\alpha = 3.8 \text{ eV \AA}$ [Ish+11] (compared to $\alpha = 0.33 \text{ eV \AA}$ for the Au(111) surface [LMJ96]). Moreover, in contrast to the traditional two-dimensional systems showing RSS [Ast+07; Nit+97], it is a property of the *bulk* energy bands of this material, which results from the large atomic spin-orbit coupling of the Bi atoms and the non-centrosymmetric crystal structure [BAN11; Ish+11]. This giant bulk RSS produces as a result several unconventional electromagnetic properties of this material, which will be discussed in greater detail below. A similar (but smaller) spin splitting has been reported more recently also in the related compounds BiTeBr and BiTeCl [Akr+14; Che+13; Sch+16b]. Due to their unique electronic structure and properties, these bismuth tellurohalides are considered promising candidates [Ras12] for spintronics applications such as the Datta-Das spin transistor [DD90; Koo+09].

In concrete terms, an outline of this thesis can be given as follows. The first Part I is dedicated to the construction of *tight-binding models* which approximate the band structure of BiTeI and can thus be used as an input for numerical simulations of this material's properties. These tight-binding models are conventionally defined by a Hamiltonian matrix $H(\mathbf{R})$ which depends on the site \mathbf{R} of the crystal lattice. It must be emphasized, however, that such a description does not imply that the electrons would “live” on the lattice (and “hop” from one site to the other). Instead, we aim at describing electrons in the periodic potential of the nuclei, where the latter are assumed to be fixed at the

lattice sites. For this purpose, it is simply convenient to work in a certain basis of the state space $L^2(\mathbb{R}^3)$, which is given by the Wannier functions $\Phi_{n\mathbf{R}}(\mathbf{x})$ labeled by the lattice vector \mathbf{R} and an additional band index n . The Hamiltonian matrix must then be identified with the matrix elements of a fundamental Hamiltonian \hat{H} (acting on $L^2(\mathbb{R}^3)$) with respect to these Wannier functions, i.e., $H_{nn'}(\mathbf{R} - \mathbf{R}') = \langle \Phi_{n\mathbf{R}} | \hat{H} | \Phi_{n'\mathbf{R}'} \rangle$. Thus, the electrons still “live”, as it were, in the whole three-dimensional space, which means that their wave function is defined on \mathbb{R}^3 . In this context, it is also important to distinguish between the Bloch wavevector \mathbf{k}_0 , which is restricted to the first Brillouin zone and which labels the Bloch eigenfunctions $\psi_{n\mathbf{k}_0}(\mathbf{x})$ of the fundamental Hamiltonian, and the true wavevector \mathbf{k} , which still ranges over the three-dimensional space (usually, both are denoted by the same symbol \mathbf{k}). In particular, after Fourier’s transformation of the Bloch eigenfunctions, one obtains a set of functions $\psi_{n\mathbf{k}_0}(\mathbf{k})$ of the true wavevector \mathbf{k} , which are labeled by the Bloch wavevector \mathbf{k}_0 . Another related issue is the transformation between the “band basis” and the “orbital basis”, which is commonly employed in fRG applications. Here, the question arises how a Hamiltonian matrix $H_{\mu\mu'}(\mathbf{R})$ depending on the lattice site \mathbf{R} and two *orbital* (or *spin*) indices μ, μ' can be interpreted, and how in turn this relates to the fundamental Hamiltonian. To clarify these issues, we first discuss in Ch. 1 the relations between plane-wave functions, Bloch-functions, Bloch-like functions, Wannier functions and atomic orbitals. Following this discussion, we next show how a Hamiltonian matrix $H_{ss'}(\mathbf{k}_0)$ depending on two spin indices s, s' and a Bloch wavevector \mathbf{k}_0 (as used e.g. in Ref. [Sch+16a]) can be derived in a certain approximation from the fundamental Hamiltonian. In Ch. 2, we investigate the symmetry constraints on this Hamiltonian matrix and show that in the case of small wavevectors, this matrix has to coincide with the Rashba Hamiltonian if one only requires time-reversal symmetry and the crystals symmetries of BiTeI. This further allows us to construct a minimal tight-binding model on the hexagonal lattice which reproduces the RSS near the center of the Brillouin zone. Finally, in Ch. 3 we describe in further detail the crystal and band structure of the material BiTeI and, as the most important result of this first part, derive a two-band tight-binding model which accurately reproduces the dispersion of the lowest conduction bands of BiTeI.

In the following Part II, we systematically develop the theory of temperature Green functions in imaginary time, which make up the central elements of statistical field theory. In accordance with our analysis in the first part, we distinguish between *fundamental Green functions* which depend on the position \mathbf{x} (or the true wavevector \mathbf{k}), and *lattice Green functions* which depend on both the lattice site \mathbf{R} and an additional band index n (or the Bloch wavevector \mathbf{k}_0 and n). Strictly speaking, only the former Green functions can be used to calculate directly typical observables such as the charge or the current densities. In Ch. 4, we first prove the fundamental equations of motion of the temperature Green functions, and then derive from these the ordinary Green function perturbation theory. In particular, we provide explicit proofs of the Gell-Mann–Low theorem, the Wick theorem and the cancellation theorem, which together imply the Feynman graph expansion of the temperature Green functions. Here, we remark that these considerations can be transferred to the ordinary (real-time) Green functions, and that in fact even the Gell-Mann–Low theorem can be proven from the equations of motion as will be shown in Ref. [SS17a]. This in turn implies a certain conceptual simplification, since the usual

derivation of the Gell-Mann–Low theorem for real-time Green functions relies on the *adiabatic assumption*, by which the interacting ground state is adiabatically connected to the non-interacting ground-state [FW71]. In the subsequent Ch. 5, we prove the representation of the partition function and the fermionic temperature Green functions in the Grassmann functional integral formalism. The latter is useful for organizing the Feynman graph expansion in an efficient way, and it also allows for a straightforward definition of the connected and the one-line-irreducible Green functions. We will also provide in this chapter detailed proofs of their mutual relations as well as their respective Feynman graph expansions. Finally, in Appendix A, we will explain the Nambu formalism, which has already been used in the original article [SH01] and which will greatly simplify our derivations in Part II and Part III.

Next, in Part III, we derive the *renormalization group equations* (RGE) for the different types of Green functions as defined in Part II. Here, we follow the lines of the seminal article [SH01] with only very slight simplifications. In particular, we find it helpful to define the Legendre transformation as a relation between different *elements* of the Grassmann algebra of the sources, as this does not require the inversion of any *functional*. Generally, in order to solve these RGE numerically, it is necessary to employ a number of approximations. We therefore offer a summary description of the standard approximations of the level-two truncation, neglecting the self-energy, the static-vertex approximation, and the Fermi surface patching approximation. In particular, we provide the explicit RGE for the momentum-discretized interaction vertex in the *refined projection scheme* proposed in Ref. [Sch+16a]. This allows for projections to be made irrespectively of the band index and hence removes a systematic error in deriving effective interactions for multiband models. Following this, we investigate in Ch. 8 the *mean-field theory* for a time-reversal-invariant Hamiltonian $H_{ss'}(\mathbf{k})$ with a singlet superconducting interaction, thereby generalizing results of Ref. [SU91] to the non-SU(2)-symmetric case. Finally, in Ch. 9, we apply our combined functional renormalization and mean-field approach to the tight-binding Rashba model of Ch. 2 with an attractive, local interaction. While the fRG allows us to predict the superconducting interaction for the electrons near the Fermi energy, mean-field theory itself enables us to predict from this the superconducting gap function and the order parameter, thereby providing a more detailed characterization of the low-temperature phases of the model under consideration. The main results of Part II and Part III have already been published in Ref. [Sch+16a] (albeit without the detailed derivations).

The final Part IV briefly summarizes further work which, owing to time and space, we were unable to describe in further detail here. Nevertheless, this work also represents a major part of the total work performed for this thesis, which has been described in detail in previous publications (see p. xi). The first Ch. 10 summarizes the results concerning the electromagnetic properties of the Rashba semiconductor BiTeI. This work was mainly done in the group of Naoto Nagaosa at the University of Tokyo. In particular, having investigated the optical conductivity, the magneto-optical response and the magnetic susceptibility of this material, we have discovered unconventional effects caused by the giant bulk RSS [Dem+12; Lee+11; Sch+12]. In the more recent work [Sch+16b], we have extended the optical conductivity calculations to the whole class of bismuth

tellurohalides BiTeX ($X = \text{I, Br, Cl}$). Our last Ch. 11 consists of a very short summary of the Functional Approach to electrodynamics of media, which has been developed in collaboration with Ronald Starke at TU Bergakademie Freiberg [SS15a; SS15b; SS16a; SS16b; SS16c]. The Functional Approach denotes a microscopic field theory of electromagnetic material properties which operates in accordance with the common practice in *ab initio* physics. It resolves several conceptual and practical problems of the Standard Approach to electrodynamics in media, and it yields analytical formulae for the calculation of all linear electromagnetic response functions from the microscopic conductivity tensor. Moreover, it provides a new perspective on microscopic wave equations in materials as well as the refractive index.

Throughout this thesis, we pay special attention in adhering consistently to what are established conventions. In particular, we always keep to SI units [BIPM06], except on occasions when we compare our theoretical results to experimental data as they are given in other units.

Part I.

Models of Rashba spin splitting

1. Electrons in periodic potentials

1.1. Position and momentum space

We begin by defining the position and momentum eigenvectors through their real-space wave functions on the three-dimensional space \mathbb{R}^3 (see Ref. [Dir47]):

$$\langle \mathbf{x}' | \mathbf{x} \rangle = \delta^3(\mathbf{x}' - \mathbf{x}), \quad (1.1)$$

$$\langle \mathbf{x}' | \mathbf{k} \rangle = \frac{1}{(2\pi)^{3/2}} e^{i\mathbf{k} \cdot \mathbf{x}'}. \quad (1.2)$$

The position eigenvectors are orthonormal and complete in the sense that

$$\langle \mathbf{x} | \mathbf{x}' \rangle = \delta^3(\mathbf{x} - \mathbf{x}'), \quad (1.3)$$

$$\int d^3\mathbf{x} |\mathbf{x}\rangle \langle \mathbf{x}| = 1. \quad (1.4)$$

Analogous equations hold for the momentum eigenvectors (plane-wave functions),

$$\langle \mathbf{k} | \mathbf{k}' \rangle = \delta^3(\mathbf{k} - \mathbf{k}'), \quad (1.5)$$

$$\int d^3\mathbf{k} |\mathbf{k}\rangle \langle \mathbf{k}| = 1. \quad (1.6)$$

Hence, in particular, the position and momentum eigenvectors are related by

$$|\mathbf{k}\rangle = \int d^3\mathbf{x} |\mathbf{x}\rangle \langle \mathbf{x} | \mathbf{k} \rangle, \quad (1.7)$$

$$|\mathbf{x}\rangle = \int d^3\mathbf{k} |\mathbf{k}\rangle \langle \mathbf{k} | \mathbf{x} \rangle. \quad (1.8)$$

For any state vector $|\psi\rangle$, the wave functions in position/momentum space are defined by

$$\langle \mathbf{x} | \psi \rangle = \psi(\mathbf{x}), \quad (1.9)$$

$$\langle \mathbf{k} | \psi \rangle = \psi(\mathbf{k}). \quad (1.10)$$

Multiplying Eqs. (1.7)–(1.8) with $\langle \psi |$ and taking the complex conjugate, we obtain

$$\psi(\mathbf{k}) = \frac{1}{(2\pi)^{3/2}} \int d^3\mathbf{x} \psi(\mathbf{x}) e^{-i\mathbf{k} \cdot \mathbf{x}}, \quad (1.11)$$

$$\psi(\mathbf{x}) = \frac{1}{(2\pi)^{3/2}} \int d^3\mathbf{k} \psi(\mathbf{k}) e^{i\mathbf{k} \cdot \mathbf{x}}. \quad (1.12)$$

These equations define the (inverse) Fourier transformation of the real- and momentum-space wave functions $\psi(\mathbf{x})$ and $\psi(\mathbf{k})$, respectively.

The dimension of the Dirac delta distribution follows from the condition

$$\int d^3\mathbf{x}' \delta^3(\mathbf{x} - \mathbf{x}') = 1. \quad (1.13)$$

Since the three-dimensional volume element has the unit

$$[d^3\mathbf{x}] = \text{m}^3, \quad (1.14)$$

it follows that

$$[\delta^3(\mathbf{x} - \mathbf{x}')] = \text{m}^{-3}. \quad (1.15)$$

Similarly, the momentum-space volume element has the unit

$$[d^3\mathbf{k}] = \text{m}^{-3}, \quad (1.16)$$

and thus, we obtain

$$[\delta^3(\mathbf{k} - \mathbf{k}')] = \text{m}^3. \quad (1.17)$$

The dimensions of the position and momentum eigenvectors can be deduced from the defining equations (1.1)–(1.2): we find

$$[|\mathbf{x}\rangle] = \text{m}^{-3/2}, \quad (1.18)$$

$$[|\mathbf{k}\rangle] = \text{m}^{3/2}. \quad (1.19)$$

On the other hand, any state vector $|\psi\rangle$, which is normalized such that

$$\langle\psi|\psi\rangle = 1, \quad (1.20)$$

necessarily has to be dimensionless, i.e.,

$$[|\psi\rangle] = 1. \quad (1.21)$$

The corresponding wave functions have the units

$$[\psi(\mathbf{x})] = [\langle\mathbf{x}|\psi\rangle] = \text{m}^{-3/2}, \quad (1.22)$$

$$[\psi(\mathbf{k})] = [\langle\mathbf{k}|\psi\rangle] = \text{m}^{3/2}. \quad (1.23)$$

These are consistent with the normalization conditions

$$\int d^3\mathbf{x} |\psi(\mathbf{x})|^2 = 1, \quad (1.24)$$

$$\int d^3\mathbf{k} |\psi(\mathbf{k})|^2 = 1, \quad (1.25)$$

and with the units of the volume elements given by Eqs. (1.14) and (1.16).

1.2. Bravais lattice and Brillouin zone

Generally, the *direct lattice* Γ in three dimensions is defined as a *Bravais lattice*,

$$\Gamma = \{ \mathbf{R}_{(n_1, n_2, n_3)} = n_1 \mathbf{a}_1 + n_2 \mathbf{a}_2 + n_3 \mathbf{a}_3; (n_1, n_2, n_3) \in \mathbb{Z}^3 \}, \quad (1.26)$$

where $\mathbf{a}_1, \mathbf{a}_2, \mathbf{a}_3$ are three linearly independent *primitive vectors* in \mathbb{R}^3 . The *reciprocal lattice* Γ^{-1} consists of all vectors \mathbf{K} with the property that

$$e^{i\mathbf{K} \cdot \mathbf{R}} = 1 \quad \text{for all } \mathbf{R} \in \Gamma. \quad (1.27)$$

Explicitly, the reciprocal lattice is given by

$$\Gamma^{-1} = \{ \mathbf{K}_{(n_1, n_2, n_3)} = n_1 \mathbf{b}_1 + n_2 \mathbf{b}_2 + n_3 \mathbf{b}_3; (n_1, n_2, n_3) \in \mathbb{Z}^3 \}, \quad (1.28)$$

where the primitive vectors $\mathbf{b}_1, \mathbf{b}_2, \mathbf{b}_3$ of the reciprocal lattice are given by

$$\mathbf{b}_i = \pi \epsilon_{ijk} \frac{\mathbf{a}_j \times \mathbf{a}_k}{|\mathbf{a}_1 \cdot (\mathbf{a}_2 \times \mathbf{a}_3)|}. \quad (1.29)$$

These are uniquely determined by the condition

$$\mathbf{a}_i \cdot \mathbf{b}_j = 2\pi \delta_{ij}, \quad (1.30)$$

where δ_{ij} denotes the Kronecker delta. The *Brillouin zone* (or *dual space*) $\mathcal{B} \subset \mathbb{R}^3$ is typically defined as the region of the three-dimensional space which is closer to the origin ($\mathbf{K} = \mathbf{0}$) than to any other reciprocal lattice vector. More generally, it can be defined as any finite region which has the property that for all $\mathbf{K}, \mathbf{K}' \in \Gamma^{-1}$ with $\mathbf{K} \neq \mathbf{K}'$, the following conditions are fulfilled:

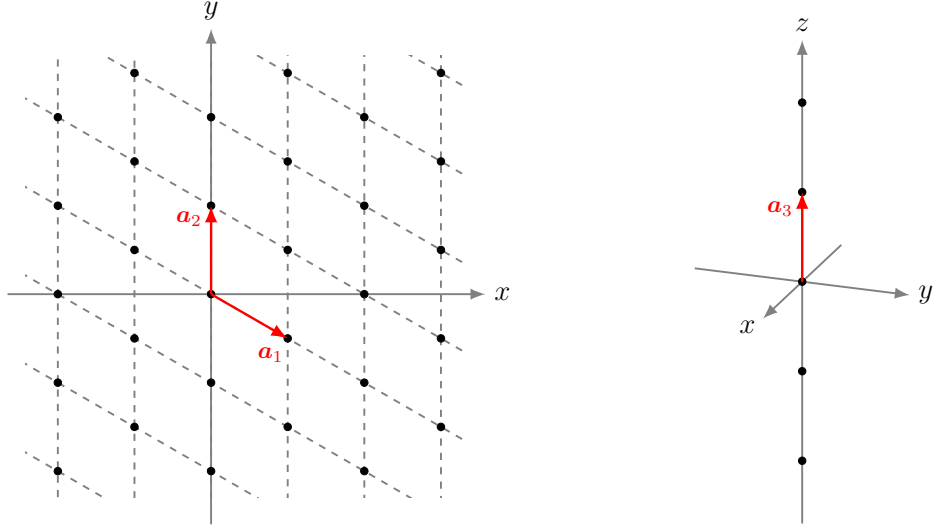
$$\mathcal{B}_{\mathbf{K}} \cap \mathcal{B}_{\mathbf{K}'} = \emptyset, \quad (1.31)$$

$$\bigcup_{\mathbf{K} \in \Gamma^{-1}} \mathcal{B}_{\mathbf{K}} = \mathbb{R}^3. \quad (1.32)$$

Here, we have defined $\mathcal{B}_{\mathbf{K}} = \{ \mathbf{k} + \mathbf{K}; \mathbf{k} \in \mathcal{B} \}$, i.e., $\mathcal{B}_{\mathbf{K}}$ coincides with the Brillouin zone \mathcal{B} shifted by the reciprocal lattice vector \mathbf{K} (such that in particular, $\mathcal{B}_{\mathbf{0}} \equiv \mathcal{B}$).

We now come to the Fourier transformation, which we define directly in the *thermodynamic limit* corresponding to the idealization of an infinite crystal.¹ For any function

¹The technical advantages of working directly in the thermodynamic limit (instead of imposing Born-von-Karman boundary conditions) are that the crystal symmetries are automatically respected, and that the total potential as produced by the nuclei residing at the sites of an infinite lattice is truly periodic. The disadvantages, however, are that an infinite lattice implies also an infinite number of nuclei, and that the thermodynamic limit leads to more singular expressions (such as the Dirac delta distribution in Eq. (1.36)). For a detailed discussion of the Born-von-Karman boundary conditions, see Ref. [SS16b, Appendix A.5].



(a) Two-dimensional projection on the x - y plane. The z axis and the primitive vector \mathbf{a}_3 are perpendicular to the paper plane.

(b) Lattice points in the \mathbf{a}_3 direction.

Figure 1.1: Hexagonal Bravais lattice with primitive vectors $\mathbf{a}_1, \mathbf{a}_2, \mathbf{a}_3$.

$f: \Gamma \rightarrow \mathbb{C}$, the Fourier transform is defined as a function $\hat{f}: \mathcal{B} \rightarrow \mathbb{C}$ given by

$$\hat{f}(\mathbf{k}) = \sum_{\mathbf{R}} f(\mathbf{R}) e^{-i\mathbf{k} \cdot \mathbf{R}}. \quad (1.33)$$

The inverse Fourier transform is then given by

$$f(\mathbf{R}) = \frac{1}{|\mathcal{B}|} \int_{\mathcal{B}} d^3\mathbf{k} \hat{f}(\mathbf{k}) e^{i\mathbf{k} \cdot \mathbf{R}}. \quad (1.34)$$

Here, we have used the following identities, which hold for $\mathbf{R}, \mathbf{R}' \in \Gamma$ and $\mathbf{k}, \mathbf{k}' \in \mathcal{B}$:

$$\delta_{\mathbf{R}, \mathbf{R}'} = \frac{1}{|\mathcal{B}|} \int_{\mathcal{B}} d^3\mathbf{k} e^{i\mathbf{k} \cdot (\mathbf{R} - \mathbf{R}')}, \quad (1.35)$$

$$|\mathcal{B}| \delta^3(\mathbf{k} - \mathbf{k}') = \sum_{\mathbf{R}} e^{i(\mathbf{k} - \mathbf{k}') \cdot \mathbf{R}}. \quad (1.36)$$

Note that $\delta_{\mathbf{R}, \mathbf{R}'}$ denotes the Kronecker delta,

$$\delta_{\mathbf{R}, \mathbf{R}'} = \begin{cases} 1 & \text{if } \mathbf{R} = \mathbf{R}', \\ 0 & \text{otherwise,} \end{cases} \quad (1.37)$$

whereas $\delta^3(\mathbf{k} - \mathbf{k}')$ is the Dirac delta distribution, which has the property that for any

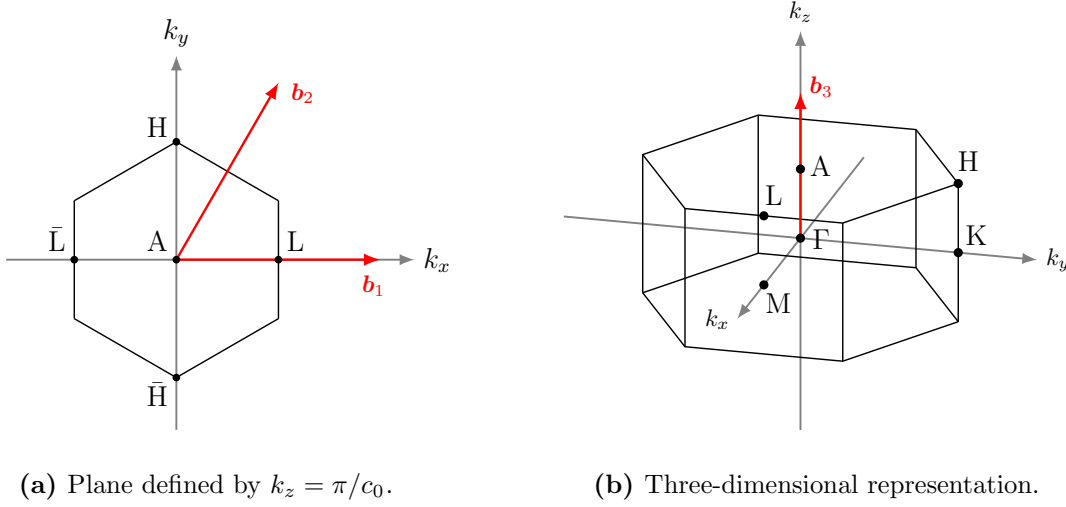


Figure 1.2: Hexagonal Brillouin zone with high-symmetry points, and primitive vectors of the reciprocal lattice $\mathbf{b}_1, \mathbf{b}_2, \mathbf{b}_3$.

function \hat{f} defined on \mathcal{B} ,

$$\hat{f}(\mathbf{k}) = \int_{\mathcal{B}} d^3\mathbf{k}' \delta^3(\mathbf{k} - \mathbf{k}') \hat{f}(\mathbf{k}'). \quad (1.38)$$

In the following, we will omit the “hat” symbol, and hence denote any function on Γ and its Fourier transform on \mathcal{B} by the same symbol, i.e., $\hat{f}(\mathbf{k}) \equiv f(\mathbf{k})$.

Let us consider, in particular, the *hexagonal* Bravais lattice in three dimensions, which describes the crystal structure of the Rashba semiconductor BiTeI (see Sect. 3). In this case, the primitive vectors of the direct lattice are

$$\mathbf{a}_1 = a_0 \begin{pmatrix} \sqrt{3}/2 \\ -1/2 \\ 0 \end{pmatrix}, \quad \mathbf{a}_2 = a_0 \begin{pmatrix} 0 \\ 1 \\ 0 \end{pmatrix}, \quad \mathbf{a}_3 = c_0 \begin{pmatrix} 0 \\ 0 \\ 1 \end{pmatrix}, \quad (1.39)$$

where a_0, c_0 denote the lattice constants, which are given for BiTeI by [BAN11]

$$a_0 = 4.339 \text{ \AA}, \quad c_0 = 6.854 \text{ \AA}. \quad (1.40)$$

The primitive vectors of the reciprocal lattice are then given by

$$\mathbf{b}_1 = \frac{2\pi}{a_0} \begin{pmatrix} 2/\sqrt{3} \\ 0 \\ 0 \end{pmatrix}, \quad \mathbf{b}_2 = \frac{2\pi}{a_0} \begin{pmatrix} 1/\sqrt{3} \\ 1 \\ 0 \end{pmatrix}, \quad \mathbf{b}_3 = \frac{2\pi}{c_0} \begin{pmatrix} 0 \\ 0 \\ 1 \end{pmatrix}. \quad (1.41)$$

The hexagonal Bravais lattice and the corresponding Brillouin zone are shown in Figs. 1.1 and 1.2. In particular, in Fig. 1.2 we have also indicated the high-symmetry points Γ, M, K, A, L, H of the Brillouin zone (we will refer to these in Ch. 3).

1.3. Bloch and Wannier vectors

We consider an electron in the periodic potential V of the nuclei, which is given by

$$V(\mathbf{x}) = \sum_{\mathbf{R} \in \Gamma} v_{\mathbf{R}}(\mathbf{x}). \quad (1.42)$$

In the simplest case, $v_{\mathbf{R}}(\mathbf{x}) \equiv v(\mathbf{x} - \mathbf{R})$ denotes the Coulomb potential generated by a single nucleus with the charge Ze located at the lattice site \mathbf{R} , i.e.,

$$v_{\mathbf{R}}(\mathbf{x}) = \frac{Ze^2}{4\pi\epsilon_0} \frac{1}{|\mathbf{x} - \mathbf{R}|}. \quad (1.43)$$

More generally, the lattice may consist of two or more nuclei per unit cell, such that

$$v_{\mathbf{R}}(\mathbf{x}) = \frac{e^2}{4\pi\epsilon_0} \sum_j \frac{Z_j}{|\mathbf{x} - \mathbf{R} - \mathbf{d}_j|}, \quad (1.44)$$

where j labels the nuclei in the unit cell, which are located at the respective positions $(\mathbf{R} + \mathbf{d}_j)$ and which have the respective charges $(Z_j e)$. For an infinite lattice (i.e., in the thermodynamic limit), the total potential V is lattice-periodic in the sense that

$$V(\mathbf{x} + \mathbf{R}) = V(\mathbf{x}) \quad \forall \mathbf{R} \in \Gamma. \quad (1.45)$$

The electron is described by the Hamiltonian

$$\hat{H} = \frac{|\hat{\mathbf{p}}|^2}{2m} + \hat{V} + \hat{V}_{\text{so}}, \quad (1.46)$$

where $\hat{\mathbf{p}}$ denotes the momentum operator, m the electron mass, and \hat{V} the multiplication operator corresponding to the periodic potential given by Eq. (1.42). Furthermore, \hat{V}_{so} denotes the Pauli spin-orbit term (see e.g. Refs. [Mes62, Ch. XX, §33] and [Win03, Eq. (1.1)]),

$$\hat{V}_{\text{so}} = \frac{\hbar}{4m^2c^2} \boldsymbol{\sigma} \cdot (\nabla \hat{V} \times \hat{\mathbf{p}}), \quad (1.47)$$

where $\boldsymbol{\sigma}$ is the vector of the Pauli matrices. The Hamiltonian (1.46) acts on the one-particle state space

$$\mathcal{H} = L^2(\mathbb{R}^3 \times \{\uparrow, \downarrow\}, \mathbb{C}), \quad (1.48)$$

which consists of all normalizable, complex-valued wave functions $\psi(\mathbf{x}, s)$ which depend on the position $\mathbf{x} \in \mathbb{R}^3$ and the spin $s \in \{\uparrow, \downarrow\}$.

In order to diagonalize the above Hamiltonian, we first define for $\mathbf{R} \in \Gamma$ the *lattice translation operators* $\hat{T}_{\mathbf{R}}$ by their action on wave functions $\psi \in \mathcal{H}$,

$$(\hat{T}_{\mathbf{R}}\psi)(\mathbf{x}, s) = \psi(\mathbf{x} - \mathbf{R}, s). \quad (1.49)$$

These operators have the property that

$$\hat{T}_{\mathbf{R}} \hat{T}_{\mathbf{R}'} = \hat{T}_{\mathbf{R}+\mathbf{R}'}, \quad (1.50)$$

which implies in particular that they are mutually commuting, i.e.,

$$[\hat{T}_{\mathbf{R}}, \hat{T}_{\mathbf{R}'}] = 0. \quad (1.51)$$

The lattice periodicity of V , Eq. (1.45), implies that \hat{H} also commutes with all lattice translation operators,

$$[\hat{T}_{\mathbf{R}}, \hat{H}] = 0. \quad (1.52)$$

Consequently, \hat{H} and all operators $\hat{T}_{\mathbf{R}}$, $\mathbf{R} \in \Gamma$, can be diagonalized simultaneously.

Hence, let us first diagonalize the lattice translation operators. Clearly, the plane-wave functions defined in Sect. 1.1,

$$|\mathbf{k}, s\rangle(\mathbf{x}, s') = \frac{1}{(2\pi)^{3/2}} e^{i\mathbf{k}\cdot\mathbf{x}} \delta_{ss'}, \quad (1.53)$$

are simultaneous eigenvectors of all operators $\hat{T}_{\mathbf{R}}$, since

$$\hat{T}_{\mathbf{R}} |\mathbf{k}, s\rangle = \frac{1}{(2\pi)^{3/2}} e^{i\mathbf{k}\cdot(\mathbf{x}-\mathbf{R})} \delta_{ss'} = e^{-i\mathbf{k}\cdot\mathbf{R}} |\mathbf{k}, s\rangle. \quad (1.54)$$

However, if we are given two plane-wave functions with the momenta \mathbf{k} and \mathbf{k}' , which differ by a reciprocal lattice vector \mathbf{K} , i.e.,

$$\mathbf{k}' = \mathbf{k} + \mathbf{K}, \quad \mathbf{K} \in \Gamma^{-1}, \quad (1.55)$$

then these plane-wave functions necessarily share the same eigenvalue of any translation operator $\hat{T}_{\mathbf{R}}$. This is because

$$e^{-i\mathbf{k}'\cdot\mathbf{R}} = e^{-i\mathbf{k}\cdot\mathbf{R}} e^{-i\mathbf{K}\cdot\mathbf{R}} = e^{-i\mathbf{k}\cdot\mathbf{R}}, \quad (1.56)$$

which follows from the defining property (1.27) of the reciprocal lattice vectors. Therefore, it is natural to define for each *Bloch wavevector* (or *Bloch momentum*) \mathbf{k} in the first Brillouin zone the *Bloch subspace* as the common eigenspace of all lattice translation operators $T_{\mathbf{R}}$ with their corresponding eigenvalues $e^{-i\mathbf{k}\cdot\mathbf{R}}$. Mathematically, we can characterize these Bloch subspaces as

$$\mathcal{H}_{\mathbf{k}} = \hat{P}_{\mathbf{k}} \mathcal{H} \quad (1.57)$$

in terms of the projection operators²

$$\hat{P}_{\mathbf{k}} = |\mathcal{B}| \sum_{\mathbf{K} \in \Gamma^{-1}} \sum_s |\mathbf{k} + \mathbf{K}, s\rangle \langle \mathbf{k} + \mathbf{K}, s|. \quad (1.58)$$

²Strictly speaking, one has to integrate these operators over finite volumes of the Brillouin zone,

$$\hat{P}_{\mathcal{K}} = \frac{1}{|\mathcal{B}|} \int_{\mathcal{K}} d^3\mathbf{k} \hat{P}_{\mathbf{k}}, \quad \mathcal{K} \subseteq \mathcal{B},$$

to obtain genuine projection operators which fulfill the conditions $\hat{P}_{\mathcal{K}}^\dagger = \hat{P}_{\mathcal{K}} = \hat{P}_{\mathcal{K}}^2$.

Here, the normalization factor $|\mathcal{B}|$, which denotes the volume of the Brillouin zone, has been inserted in order to make the projection operators dimensionless (see Sect. 1.1). By definition, these projection operators have the property

$$\hat{T}_{\mathbf{R}} \hat{P}_{\mathbf{k}} = e^{-i\mathbf{k} \cdot \mathbf{R}} \hat{P}_{\mathbf{k}}, \quad (1.59)$$

and hence $\mathcal{H}_{\mathbf{k}}$ can be characterized equivalently as

$$\mathcal{H}_{\mathbf{k}} = \left\{ \psi \in \mathcal{H} : \psi(\mathbf{x} - \mathbf{R}, s) = e^{-i\mathbf{k} \cdot \mathbf{R}} \psi(\mathbf{x}, s) \right\}. \quad (1.60)$$

Furthermore, the subspaces $\mathcal{H}_{\mathbf{k}}$ are orthogonal and complete in the sense that

$$\hat{P}_{\mathbf{k}} \hat{P}_{\mathbf{k}'} = |\mathcal{B}| \delta^3(\mathbf{k} - \mathbf{k}') \hat{P}_{\mathbf{k}}, \quad (1.61)$$

$$\frac{1}{|\mathcal{B}|} \int_{\mathcal{B}} d^3\mathbf{k} \hat{P}_{\mathbf{k}} = 1. \quad (1.62)$$

These equations follow directly from the corresponding properties of the momentum eigenvectors (see Eqs. (1.5) and (1.6)).

We can now diagonalize the Hamiltonian (1.46) separately for each $\mathbf{k} \in \mathcal{B}$ in the subspace $\mathcal{H}_{\mathbf{k}}$. In fact, Eq. (1.52) implies that \hat{H} maps each subspace $\mathcal{H}_{\mathbf{k}}$ into itself, i.e.,

$$\hat{H} |\mathbf{k} + \mathbf{K}', s'\rangle = \sum_{\mathbf{K}, s} |\mathbf{k} + \mathbf{K}, s\rangle H_{\mathbf{K}s, \mathbf{K}'s'}(\mathbf{k}), \quad (1.63)$$

which is equivalent to

$$\langle \mathbf{k} + \mathbf{K}, s | \hat{H} | \mathbf{k}' + \mathbf{K}', s' \rangle = \delta^3(\mathbf{k} - \mathbf{k}') H_{\mathbf{K}s, \mathbf{K}'s'}(\mathbf{k}). \quad (1.64)$$

Consequently, there is an orthonormal basis of eigenvectors $|\Psi_{n\mathbf{k}}\rangle \in \mathcal{H}_{\mathbf{k}}$ satisfying

$$\hat{H} |\Psi_{n\mathbf{k}}\rangle = E_{n\mathbf{k}} |\Psi_{n\mathbf{k}}\rangle, \quad (1.65)$$

or equivalently,

$$\langle \Psi_{n\mathbf{k}} | \hat{H} | \Psi_{n'\mathbf{k}'} \rangle = \delta_{nn'} |\mathcal{B}| \delta^3(\mathbf{k} - \mathbf{k}') E_{n\mathbf{k}}. \quad (1.66)$$

Each vector $|\Psi_{n\mathbf{k}}\rangle$ is called a *Bloch vector*, which is labeled by the Bloch momentum $\mathbf{k} \in \mathcal{B}$ and the *band index* n . The corresponding eigenvalues $E_{n\mathbf{k}}$ as a function of n and \mathbf{k} form the *band structure* of the material. The Bloch vectors are orthonormal and complete in the sense that

$$\langle \Psi_{n\mathbf{k}} | \Psi_{n'\mathbf{k}'} \rangle = \delta_{nn'} |\mathcal{B}| \delta^3(\mathbf{k} - \mathbf{k}'), \quad (1.67)$$

$$\frac{1}{|\mathcal{B}|} \int_{\mathcal{B}} d^3\mathbf{k} \sum_n |\Psi_{n\mathbf{k}}\rangle \langle \Psi_{n\mathbf{k}}| = 1. \quad (1.68)$$

We further note that the Bloch vectors are dimensionless,

$$[|\Psi_{n\mathbf{k}}\rangle] = 1, \quad (1.69)$$

which follows from the condition (1.67).

In order to construct the Bloch vectors $|\Psi_{n\mathbf{k}}\rangle$ explicitly, we write them as linear combinations of the plane-wave basis vectors of the Bloch subspace $\mathcal{H}_{\mathbf{k}}$, i.e.,

$$|\Psi_{n\mathbf{k}}\rangle = |\mathcal{B}|^{1/2} \sum_{\mathbf{K}, s} |\mathbf{k} + \mathbf{K}, s\rangle C_{\mathbf{K}s, n}(\mathbf{k}), \quad (1.70)$$

or equivalently,

$$\langle \mathbf{k} + \mathbf{K}, s | \Psi_{n\mathbf{k}'} \rangle = |\mathcal{B}|^{1/2} \delta^3(\mathbf{k} - \mathbf{k}') C_{\mathbf{K}s, n}(\mathbf{k}), \quad (1.71)$$

with a complex-valued transformation matrix $C_{\mathbf{K}s, n}(\mathbf{k})$. Here, the prefactor $|\mathcal{B}|^{1/2}$ was inserted in order to make this transformation matrix dimensionless. The orthonormality of the momentum eigenvectors and of the Bloch vectors imply that the transformation matrix has to be unitary, i.e.,

$$\sum_{\mathbf{K}, s} C_{\mathbf{K}s, n}^*(\mathbf{k}) C_{\mathbf{K}s, n'}(\mathbf{k}) = \delta_{nn'}. \quad (1.72)$$

Furthermore, by inserting the representation (1.70) into the Schrödinger equation (1.65), we see that this eigenvalue problem is equivalent to (with $E_n(\mathbf{k}) \equiv E_{n\mathbf{k}}$):

$$\sum_{\mathbf{K}', s'} H_{\mathbf{K}s, \mathbf{K}'s'}(\mathbf{k}) C_{\mathbf{K}'s', n}(\mathbf{k}) = E_n(\mathbf{k}) C_{\mathbf{K}s, n}(\mathbf{k}). \quad (1.73)$$

Thus, the matrix $C_{\mathbf{K}s, n}(\mathbf{k})$ represents a unitary transformation which diagonalizes the Hamiltonian matrix, such that

$$\sum_{\mathbf{K}, s} \sum_{\mathbf{K}', s'} C_{\mathbf{K}s, n}^*(\mathbf{k}) H_{\mathbf{K}s, \mathbf{K}'s'}(\mathbf{k}) C_{\mathbf{K}'s', n}(\mathbf{k}) = \delta_{nn'} E_n(\mathbf{k}). \quad (1.74)$$

Given this matrix, the Bloch vectors $|\Psi_{n\mathbf{k}}\rangle$ can be constructed explicitly in terms of the plane-wave vectors $|\mathbf{k} + \mathbf{K}, s\rangle$ by means of Eq. (1.70).

Next, we define the *Wannier vectors* $|\Phi_{n\mathbf{R}}\rangle$ in terms of the Bloch vectors as

$$|\Phi_{n\mathbf{R}}\rangle = \frac{1}{|\mathcal{B}|} \int_{\mathcal{B}} d^3\mathbf{k} |\Psi_{n\mathbf{k}}\rangle e^{-i\mathbf{k}\cdot\mathbf{R}}, \quad (1.75)$$

or conversely,

$$|\Psi_{n\mathbf{k}}\rangle = \sum_{\mathbf{R}} |\Phi_{n\mathbf{R}}\rangle e^{i\mathbf{k}\cdot\mathbf{R}}. \quad (1.76)$$

The Wannier vectors are orthonormal and complete in the sense that

$$\langle \Phi_{n\mathbf{R}} | \Phi_{n'\mathbf{R}'} \rangle = \delta_{n,n'} \delta_{\mathbf{R},\mathbf{R}'}, \quad (1.77)$$

$$\sum_n \sum_{\mathbf{R}} |\Phi_{n\mathbf{R}}\rangle \langle \Phi_{n\mathbf{R}}| = 1. \quad (1.78)$$

This follows directly from the properties (1.67)–(1.68) for the Bloch vectors and, in particular, implies that the Wannier vectors are also dimensionless,

$$[|\Psi_{n\mathbf{R}}\rangle] = 1. \quad (1.79)$$

Under lattice translations, the Wannier vectors transform according to

$$\hat{T}_{\mathbf{R}'} |\Phi_{n\mathbf{R}}\rangle = |\Phi_{n,\mathbf{R}+\mathbf{R}'}\rangle, \quad (1.80)$$

as can be shown easily using the definition (1.75) and the property (1.60) of the Bloch vectors. The transformations defined by Eqs. (1.75)–(1.76) are equivalent to

$$|\Phi_{n\mathbf{R}}\rangle = \frac{1}{|\mathcal{B}|} \int_{\mathcal{B}} d^3\mathbf{k} |\Psi_{n\mathbf{k}}\rangle \langle \Psi_{n\mathbf{k}} | \Phi_{n\mathbf{R}}\rangle, \quad (1.81)$$

$$|\Psi_{n\mathbf{k}}\rangle = \sum_{\mathbf{R}} |\Phi_{n\mathbf{R}}\rangle \langle \Phi_{n\mathbf{R}} | \Psi_{n\mathbf{k}}\rangle, \quad (1.82)$$

with the dimensionless matrix element

$$\langle \Psi_{n\mathbf{k}} | \Phi_{n\mathbf{R}}\rangle = e^{-i\mathbf{k}\cdot\mathbf{R}}. \quad (1.83)$$

Furthermore, the matrix elements of the Hamiltonian in the Wannier basis are given by

$$H_{nn'}(\mathbf{R} - \mathbf{R}') \equiv \langle \Phi_{n\mathbf{R}} | \hat{H} | \Phi_{n'\mathbf{R}'} \rangle = \delta_{nn'} \frac{1}{|\mathcal{B}|} \int_{\mathcal{B}} d^3\mathbf{k} e^{i\mathbf{k}\cdot(\mathbf{R}-\mathbf{R}')} E_{n\mathbf{k}}, \quad (1.84)$$

which follows directly from Eq. (1.66).

Finally, we calculate the matrix elements of the concrete Hamiltonian (1.46) in the plane-wave basis. First, the kinetic term acts on a momentum eigenvector by

$$-\frac{\hbar^2}{2m} \Delta e^{i(\mathbf{k}+\mathbf{K}')\cdot\mathbf{x}} = \frac{\hbar^2|\mathbf{k}+\mathbf{K}'|^2}{2m} e^{i(\mathbf{k}+\mathbf{K}')\cdot\mathbf{x}}. \quad (1.85)$$

The potential $V(\mathbf{x})$ has the lattice periodicity and can therefore be expanded as

$$V(\mathbf{x}) = \sum_{\mathbf{K} \in \Gamma^{-1}} V_{\mathbf{K}} e^{i\mathbf{K}\cdot\mathbf{x}}, \quad (1.86)$$

with complex coefficients $V_{\mathbf{K}}$. Hence, when the potential term acts on a momentum eigenstate, it gives

$$V(\mathbf{x}) e^{i(\mathbf{k}+\mathbf{K}')\cdot\mathbf{x}} = \sum_{\mathbf{K}} V_{\mathbf{K}} e^{i(\mathbf{k}+\mathbf{K}+\mathbf{K}')\cdot\mathbf{x}}. \quad (1.87)$$

Similarly, using that

$$\nabla V(\mathbf{x}) = \sum_{\mathbf{K}} V_{\mathbf{K}} i\mathbf{K} e^{i\mathbf{K}\cdot\mathbf{x}}, \quad (1.88)$$

we find for the Pauli spin-orbit term

$$\begin{aligned} \frac{\hbar}{4m^2c^2} \boldsymbol{\sigma}_{ss'} \cdot \left(\nabla V(\mathbf{x}) \times \frac{\hbar}{i} \nabla \right) e^{i(\mathbf{k}+\mathbf{K}')\cdot\mathbf{x}} = \\ \frac{i\hbar^2}{4m^2c^2} \sum_{\mathbf{K}} V_{\mathbf{K}} \boldsymbol{\sigma}_{ss'} \cdot (\mathbf{K} \times (\mathbf{k} + \mathbf{K}')) e^{i(\mathbf{k}+\mathbf{K}+\mathbf{K}')\cdot\mathbf{x}}. \end{aligned} \quad (1.89)$$

Equations (1.85), (1.87) and (1.89) can be combined into

$$\begin{aligned} \hat{H} |\mathbf{k} + \mathbf{K}', s'\rangle = \sum_{\mathbf{K}, s} |\mathbf{k} + \mathbf{K} + \mathbf{K}', s\rangle \left(\delta_{ss'} \delta_{\mathbf{K}, \mathbf{0}} \frac{\hbar^2 |\mathbf{k} + \mathbf{K}'|^2}{2m} + \delta_{ss'} V_{\mathbf{K}} \right. \\ \left. + \frac{i\hbar^2}{4m^2c^2} V_{\mathbf{K}} \boldsymbol{\sigma}_{ss'} \cdot (\mathbf{K} \times (\mathbf{k} + \mathbf{K}')) \right). \end{aligned} \quad (1.90)$$

By substituting $\mathbf{K} \mapsto \mathbf{K} - \mathbf{K}'$, this is equivalent to

$$\begin{aligned} \hat{H} |\mathbf{k} + \mathbf{K}', s'\rangle = \sum_{\mathbf{K}, s} |\mathbf{k} + \mathbf{K}, s\rangle \left(\delta_{ss'} \delta_{\mathbf{K}-\mathbf{K}', \mathbf{0}} \frac{\hbar^2 |\mathbf{k} + \mathbf{K}'|^2}{2m} + \delta_{ss'} V_{\mathbf{K}-\mathbf{K}'} \right. \\ \left. + \frac{i\hbar^2}{4m^2c^2} V_{\mathbf{K}-\mathbf{K}'} \boldsymbol{\sigma}_{ss'} \cdot ((\mathbf{K} - \mathbf{K}') \times (\mathbf{k} + \mathbf{K}')) \right). \end{aligned} \quad (1.91)$$

By comparing this with Eq. (1.63), we read off the matrix elements of the Hamiltonian in the plane-wave basis:

$$\begin{aligned} H_{\mathbf{K}s, \mathbf{K}'s'}(\mathbf{k}) = \delta_{ss'} \left(\delta_{\mathbf{K}, \mathbf{K}'} \frac{\hbar^2 |\mathbf{k} + \mathbf{K}|^2}{2m} + V_{\mathbf{K}-\mathbf{K}'} \right) \\ + \frac{i\hbar^2}{4m^2c^2} V_{\mathbf{K}-\mathbf{K}'} \boldsymbol{\sigma}_{ss'} \cdot ((\mathbf{K} - \mathbf{K}') \times (\mathbf{k} + \mathbf{K}')). \end{aligned} \quad (1.92)$$

Therefore, the Schrödinger equation (1.65) is equivalent to (see Eq. (1.73))

$$\begin{aligned} \frac{\hbar^2 |\mathbf{k} + \mathbf{K}|^2}{2m} C_{\mathbf{K}s, n}(\mathbf{k}) + \sum_{\mathbf{K}'} V_{\mathbf{K}-\mathbf{K}'} C_{\mathbf{K}'s, n}(\mathbf{k}) \\ + \frac{i\hbar^2}{4m^2c^2} \sum_{\mathbf{K}', s'} V_{\mathbf{K}-\mathbf{K}'} \boldsymbol{\sigma}_{ss'} \cdot ((\mathbf{K} - \mathbf{K}') \times (\mathbf{k} + \mathbf{K}')) C_{\mathbf{K}'s', n}(\mathbf{k}) = E_n(\mathbf{k}) C_{\mathbf{K}s, n}(\mathbf{k}). \end{aligned} \quad (1.93)$$

For each $\mathbf{k} \in \mathcal{B}$, this is a system of coupled linear equations for the coefficients $C_{\mathbf{K}s, n}(\mathbf{k})$ (where $\mathbf{K} \in \Gamma^{-1}$ and $s \in \{\uparrow, \downarrow\}$). Given the solutions of these equations (which are labeled by the band index n), we can construct the Bloch vectors in terms of the plane-wave vectors by means of Eq. (1.70). Finally, we remark that by neglecting the spin-orbit term, Eq. (1.93) agrees with Ref. [AM76, Eq. (8.41)].

1.4. Bloch-like vectors and atomic orbitals

We now rewrite the Hamiltonian (1.46) as

$$\hat{H} = \frac{|\hat{\mathbf{p}}|^2}{2m} + \hat{v} + \Delta\hat{V} + \hat{V}_{\text{so}} \quad (1.94)$$

$$\equiv \hat{h} + \Delta\hat{V} + \hat{V}_{\text{so}}, \quad (1.95)$$

where $\hat{v} \equiv \hat{v}_{\mathbf{0}}$ denotes the Coulomb potential generated by the nuclei within one unit cell which is labeled by $\mathbf{R} = \mathbf{0}$, and where

$$\Delta\hat{V} = \hat{V} - \hat{v}_{\mathbf{0}} = \sum_{\mathbf{R} \neq \mathbf{0}} \hat{v}_{\mathbf{R}} \quad (1.96)$$

is the potential generated by all remaining nuclei. The Hamiltonian

$$\hat{h} = \frac{|\hat{\mathbf{p}}|^2}{2m} + \hat{v} \quad (1.97)$$

describes an electron in the potential of a single or a few nuclei which are concentrated around the origin, disregarding the atomic spin-orbit coupling \hat{V}_{so} (which we will later treat as a perturbation analogously to the term $\Delta\hat{V}$.) We assume that the eigenvalues of \hat{h} as well as the corresponding eigenfunctions are known (in the case of a monatomic lattice, they coincide with the energy levels and atomic orbitals of the hydrogen atom). Thus, we have

$$\hat{h}|\varphi_{\mu s}\rangle = e_{\mu}|\varphi_{\mu s}\rangle, \quad (1.98)$$

where μ is an *orbital* index and s the *spin* index. As we have not included the spin-orbit coupling in \hat{h} , each eigenvalue is at least two-fold degenerate, and the eigenvectors can be chosen to be simultaneous spin eigenvectors, i.e.,

$$\varphi_{\mu s}(\mathbf{x}, s') = \varphi_{\mu}(\mathbf{x}) \delta_{ss'}. \quad (1.99)$$

Note that the index μ labels the eigenvectors and not the eigenenergies, which means that there are in general several orbitals, $\varphi_{\mu_1}, \dots, \varphi_{\mu_d}$, sharing the same eigenvalue, i.e., $e_{\mu_1} = \dots = e_{\mu_d}$. In the following, we will often refer to φ_{μ} as *atomic orbitals* (or *atomic eigenvectors*), although strictly speaking, this labeling is only justified in the case of a monatomic lattice.

Given the atomic eigenvectors $|\varphi_{\mu s}\rangle$, whose position-space wave functions are concentrated around the origin, we further define for each $\mathbf{R} \in \Gamma$ the vectors $|\varphi_{\mu s \mathbf{R}}\rangle$ whose wave functions are shifted by the lattice vector \mathbf{R} , i.e.,

$$\varphi_{\mu s \mathbf{R}}(\mathbf{x}, s') := \varphi_{\mu s}(\mathbf{x} - \mathbf{R}, s'). \quad (1.100)$$

Thus, the wave function of $|\varphi_{\mu s \mathbf{R}}\rangle$ is concentrated around the site \mathbf{R} . Furthermore, we

introduce the *Bloch-like vectors* (also called *Bloch sums*) by the definition [SK54]

$$|\psi_{\mu s \mathbf{k}}\rangle := \frac{1}{\mathcal{N}_{\mu \mathbf{k}}} \sum_{\mathbf{R}} |\varphi_{\mu s \mathbf{R}}\rangle e^{i\mathbf{k} \cdot \mathbf{R}}, \quad (1.101)$$

which is similar to the relation (1.76) between Bloch and Wannier vectors. Here, $\mathcal{N}_{\mu \mathbf{k}}$ is a normalization constant, which will be fixed later. The Bloch-like vectors have the same property (1.60) as the Bloch vectors themselves, i.e.,

$$\psi_{\mu s \mathbf{k}}(\mathbf{x} - \mathbf{R}, s') = e^{-i\mathbf{k} \cdot \mathbf{R}} \psi_{\mu s \mathbf{k}}(\mathbf{x}, s'), \quad (1.102)$$

which implies that the Bloch-like vectors $|\psi_{\mu s \mathbf{k}}\rangle$ also lie in the Bloch subspace $\mathcal{H}_{\mathbf{k}}$. However, in contrast to the Bloch vectors, the Bloch-like vectors are not orthogonal. This was pointed out already by P.-O. Löwdin [Löw50], and can be confirmed easily by the following calculation:

$$\langle \psi_{\mu s \mathbf{k}} | \psi_{\mu' s' \mathbf{k}'} \rangle = \frac{1}{\mathcal{N}_{\mu \mathbf{k}}} \frac{1}{\mathcal{N}_{\mu' \mathbf{k}'}} \sum_{\mathbf{R}, \mathbf{R}'} e^{-i\mathbf{k} \cdot \mathbf{R}} e^{i\mathbf{k}' \cdot \mathbf{R}'} \langle \varphi_{\mu s \mathbf{R}} | \varphi_{\mu' s' \mathbf{R}'} \rangle \quad (1.103)$$

$$= \frac{1}{\mathcal{N}_{\mu \mathbf{k}}} \frac{1}{\mathcal{N}_{\mu' \mathbf{k}'}} \sum_{\mathbf{R}, \mathbf{R}'} e^{-i\mathbf{k} \cdot (\mathbf{R} - \mathbf{R}')} e^{i(\mathbf{k}' - \mathbf{k}) \cdot \mathbf{R}'} \langle \varphi_{\mu s, \mathbf{R} - \mathbf{R}'} | \varphi_{\mu' s' \mathbf{0}} \rangle \quad (1.104)$$

$$= |\mathcal{B}| \delta^3(\mathbf{k} - \mathbf{k}') \frac{1}{\mathcal{N}_{\mu \mathbf{k}}} \frac{1}{\mathcal{N}_{\mu' \mathbf{k}'}} \sum_{\mathbf{R}} e^{-i\mathbf{k} \cdot \mathbf{R}} \langle \varphi_{\mu s \mathbf{R}} | \varphi_{\mu' s' \mathbf{0}} \rangle. \quad (1.105)$$

While for $\mathbf{R} = \mathbf{0}$, the matrix element in Eq. (1.105) diagonalizes as

$$\langle \varphi_{\mu s} | \varphi_{\mu' s'} \rangle = \delta_{\mu \mu'} \delta_{ss'}, \quad (1.106)$$

the same is in general not true for $\mathbf{R} \neq \mathbf{0}$, and therefore,

$$\langle \psi_{\mu s \mathbf{k}} | \psi_{\mu' s' \mathbf{k}'} \rangle \neq |\mathcal{B}| \delta^3(\mathbf{k} - \mathbf{k}') \delta_{\mu \mu'} \delta_{ss'}. \quad (1.107)$$

In particular, this implies that there is no unitary matrix $U_{\mu s, n}(\mathbf{k})$ which mediates between the Bloch vectors (“band basis”) and the Bloch-like vectors (“orbital basis”):

$$|\Psi_{n \mathbf{k}}\rangle \neq \sum_{\mu, s} |\psi_{\mu s \mathbf{k}}\rangle U_{\mu s, n}(\mathbf{k}). \quad (1.108)$$

In actual fact, by Eq. (1.99), the matrix element in Eq. (1.105) only diagonalizes *partly* with respect to the spin indices, i.e.,

$$\langle \varphi_{\mu s \mathbf{R}} | \varphi_{\mu' s' \mathbf{0}} \rangle = \delta_{ss'} \langle \varphi_{\mu \mathbf{R}} | \varphi_{\mu' \mathbf{0}} \rangle. \quad (1.109)$$

This asymmetry between the orbital and spin indices comes from the fact that we have not included \hat{V}_{so} in the unperturbed Hamiltonian \hat{h} . From this, it follows that

$$\langle \psi_{\mu s \mathbf{k}} | \psi_{\mu' s' \mathbf{k}'} \rangle = |\mathcal{B}| \delta^3(\mathbf{k} - \mathbf{k}') \delta_{ss'} S_{\mu \mu'}(\mathbf{k}), \quad (1.110)$$

where we have introduced the *overlap matrix*

$$S_{\mu\mu'}(\mathbf{k}) = \frac{1}{\mathcal{N}_{\mu\mathbf{k}}} \frac{1}{\mathcal{N}_{\mu'\mathbf{k}}} \left(\delta_{\mu\mu'} + \sum_{\mathbf{R} \neq \mathbf{0}} e^{-i\mathbf{k} \cdot \mathbf{R}} \langle \varphi_{\mu\mathbf{R}} | \varphi_{\mu'\mathbf{0}} \rangle \right). \quad (1.111)$$

The normalization constant $\mathcal{N}_{\mu\mathbf{k}}$ is now determined from the condition

$$S_{\mu\mu}(\mathbf{k}) \stackrel{!}{=} 1, \quad (1.112)$$

which yields

$$\mathcal{N}_{\mu\mathbf{k}} = \left(1 + \sum_{\mathbf{R} \neq \mathbf{0}} e^{-i\mathbf{k} \cdot \mathbf{R}} \langle \varphi_{\mu\mathbf{R}} | \varphi_{\mu\mathbf{0}} \rangle \right)^{1/2}. \quad (1.113)$$

Note that $\mathcal{N}_{\mathbf{k}}$ is real-valued and $S_{\mu\mu'}(\mathbf{k})$ is hermitean, as can be shown by substituting $\mathbf{R} \mapsto -\mathbf{R}$ in the summations over direct lattice vectors.

Consider now again the Schrödinger equation (1.65), which constitutes an eigenvalue problem for the Bloch vectors. Let us *assume* that each Bloch vector can be expanded in terms of the Bloch-like vectors as follows (the following presentation closely follows Ref. [Pic12]):

$$|\Psi_{n\mathbf{k}}\rangle = \sum_{\mu, s} |\psi_{\mu s\mathbf{k}}\rangle B_{\mu s, n}(\mathbf{k}), \quad (1.114)$$

or equivalently,

$$\langle \psi_{\mu s\mathbf{k}} | \Psi_{n\mathbf{k}'} \rangle = |\mathcal{B}| \delta^3(\mathbf{k} - \mathbf{k}') B_{\mu s, n}(\mathbf{k}), \quad (1.115)$$

where $B_{\mu s, n}(\mathbf{k})$ is a complex-valued transformation matrix. Then, the Schrödinger equation (1.65) is equivalent to

$$\sum_{\mu', s'} \langle \psi_{\mu s\mathbf{k}} | \hat{H} | \psi_{\mu' s' \mathbf{k}'} \rangle B_{\mu' s', n}(\mathbf{k}) = E_n(\mathbf{k}) \sum_{\mu', s'} \langle \psi_{\mu s\mathbf{k}} | \psi_{\mu' s' \mathbf{k}'} \rangle B_{\mu' s', n}(\mathbf{k}). \quad (1.116)$$

Next, let us calculate the matrix elements of the Hamiltonian with respect to the Bloch-like vectors, which appear on the left-hand side of this equation. By performing the same steps as in Eqs. (1.103)–(1.105), we obtain

$$\langle \psi_{\mu s\mathbf{k}} | \hat{H} | \psi_{\mu' s' \mathbf{k}'} \rangle = |\mathcal{B}| \delta^3(\mathbf{k} - \mathbf{k}') H_{\mu s, \mu' s'}(\mathbf{k}), \quad (1.117)$$

with

$$H_{\mu s, \mu' s'}(\mathbf{k}) = \frac{1}{\mathcal{N}_{\mu\mathbf{k}}} \frac{1}{\mathcal{N}_{\mu'\mathbf{k}}} \sum_{\mathbf{R}} e^{-i\mathbf{k} \cdot \mathbf{R}} \langle \varphi_{\mu s\mathbf{R}} | \hat{H} | \varphi_{\mu' s' \mathbf{0}} \rangle. \quad (1.118)$$

The matrix element with $\mathbf{R} = \mathbf{0}$ can be expressed even more explicitly: we have

$$\hat{H} |\varphi_{\mu s \mathbf{0}}\rangle = (e_{\mu} + \Delta \hat{V} + \hat{V}_{\text{so}}) |\varphi_{\mu s \mathbf{0}}\rangle, \quad (1.119)$$

and consequently,

$$\langle \varphi_{\mu s \mathbf{0}} | \hat{H} | \varphi_{\mu' s' \mathbf{0}} \rangle = \delta_{\mu\mu'} \delta_{ss'} e_{\mu} + \langle \varphi_{\mu s \mathbf{0}} | (\Delta \hat{V} + \hat{V}_{so}) | \varphi_{\mu' s' \mathbf{0}} \rangle. \quad (1.120)$$

Thus, we obtain

$$\begin{aligned} H_{\mu s, \mu' s'}(\mathbf{k}) &= \frac{1}{\mathcal{N}_{\mu \mathbf{k}}} \frac{1}{\mathcal{N}_{\mu' \mathbf{k}}} \left(e_{\mu} \delta_{\mu\mu'} \delta_{ss'} + \langle \varphi_{\mu s \mathbf{0}} | (\Delta \hat{V} + \hat{V}_{so}) | \varphi_{\mu' s' \mathbf{0}} \rangle \right. \\ &\quad \left. + \sum_{\mathbf{R} \neq \mathbf{0}} e^{-i\mathbf{k} \cdot \mathbf{R}} \langle \varphi_{\mu s \mathbf{R}} | \hat{H} | \varphi_{\mu' s' \mathbf{0}} \rangle \right). \end{aligned} \quad (1.121)$$

Using the result (1.117) together with Eq. (1.110), the Schrödinger equation (1.116) turns into

$$\sum_{\mu', s'} H_{\mu s, \mu' s'}(\mathbf{k}) B_{\mu' s', n}(\mathbf{k}) = E_n(\mathbf{k}) \sum_{\mu'} S_{\mu\mu'}(\mathbf{k}) B_{\mu' s, n}(\mathbf{k}). \quad (1.122)$$

Hence, in contrast to the representation (1.73) of the Schrödinger equation in terms of orthogonal plane-wave functions, its representation in terms of non-orthogonal Bloch-like functions leads to a *generalized eigenvalue problem* (see Ref. [Löw50]). Its solution yields the energy bands $E_n(\mathbf{k})$ and the coefficient functions $B_{\mu' s, n}(\mathbf{k})$, by which one can construct the Bloch vectors in terms of the Bloch-like vectors via Eq. (1.114).

With this, we now go on to express the Wannier vectors in terms of the atomic orbitals. Using the definition (1.75) as well as Eqs. (1.101) and (1.114), we obtain

$$|\Phi_{n\mathbf{R}}\rangle = \frac{1}{|\mathcal{B}|} \int_{\mathcal{B}} d^3\mathbf{k} |\Psi_{n\mathbf{k}}\rangle e^{-i\mathbf{k} \cdot \mathbf{R}} \quad (1.123)$$

$$= \sum_{\mu, s} \frac{1}{|\mathcal{B}|} \int_{\mathcal{B}} d^3\mathbf{k} |\psi_{\mu s \mathbf{k}}\rangle B_{\mu s, n}(\mathbf{k}) e^{-i\mathbf{k} \cdot \mathbf{R}} \quad (1.124)$$

$$= \sum_{\mu, s} \sum_{\mathbf{R}'} |\varphi_{\mu s \mathbf{R}'}\rangle \frac{1}{|\mathcal{B}|} \int_{\mathcal{B}} d^3\mathbf{k} \frac{1}{\mathcal{N}_{\mu \mathbf{k}}} B_{\mu s, n}(\mathbf{k}) e^{i\mathbf{k} \cdot (\mathbf{R}' - \mathbf{R})}. \quad (1.125)$$

This equation shows that in general, each Wannier vector $|\Phi_{n\mathbf{R}}\rangle$ is a linear combination of all kinds of atomic orbitals centered at all possible lattice sites. Only if we assume that the overlap between orbitals at different lattice sites is completely negligible, such that $\mathcal{N}_{\mu \mathbf{k}} \approx 1$ and $B_{\mu s, n}(\mathbf{k}) \approx B_{\mu s, n}(\mathbf{0})$, then Eq. (1.125) reduces to

$$|\Phi_{n\mathbf{R}}\rangle \approx \sum_{\mu, s} |\varphi_{\mu s \mathbf{R}}\rangle B_{\mu s, n}(\mathbf{0}). \quad (1.126)$$

In this case, the Wannier vector $|\Phi_{n\mathbf{R}}\rangle$ is obviously concentrated around the lattice site \mathbf{R} , and it is a linear combination of atomic orbitals centered at the same lattice site (cf. [AM76, Ch. 10]).

Finally, we define the *tight-binding limit*, in which the energy bands of the crystal reduce to the atomic energy levels. Intuitively, this limit is reached when the distance between the nuclei forming the lattice is sufficiently large, such that each electron is bound to its respective nucleus and not delocalized in the crystal. More precisely, if the following matrix elements are negligible:

$$\langle \varphi_{\mu s \mathbf{0}} | \varphi_{\mu' s' \mathbf{R}} \rangle \rightarrow 0, \quad (1.127)$$

$$\langle \varphi_{\mu s \mathbf{0}} | \hat{H} | \varphi_{\mu' s' \mathbf{R}} \rangle \rightarrow 0, \quad (1.128)$$

$$\langle \varphi_{\mu s \mathbf{0}} | (\Delta \hat{V} + \hat{V}_{\text{so}}) | \varphi_{\mu' s' \mathbf{0}} \rangle \rightarrow 0, \quad (1.129)$$

then we obtain from Eq. (1.113) that

$$\mathcal{N}_{\mu \mathbf{k}} = 1, \quad (1.130)$$

from Eq. (1.111) that

$$S_{\mu \mu'}(\mathbf{k}) = \delta_{\mu \mu'}, \quad (1.131)$$

and from Eq. (1.121) that

$$H_{\mu s, \mu' s'}(\mathbf{k}) = e_{\mu} \delta_{\mu \mu'} \delta_{ss'}, \quad (1.132)$$

which implies that the energy bands coincide with the atomic energy levels, $E_{\mu}(\mathbf{k}) = e_{\mu}$. In the next section, we will consider the case where the above matrix elements are not completely negligible but assumed to be small (compared to the distance of the atomic energy levels). Under this assumption, we will then derive an approximate expression for the energy bands of the crystal.

1.5. Single-orbital model

1.5.1. Quasi-degenerate perturbation theory

We now restrict ourselves to the simplest case of a single orbital $|\varphi_0\rangle$, which is an eigenvector of the Hamiltonian \hat{h} given by Eq. (1.97) with the corresponding eigenvalue e_0 . We assume that this eigenvalue is separated from all other eigenvalues of \hat{h} by a certain energy difference Δe_0 , and that this eigenvalue has no further degeneracy besides the two-fold spin degeneracy. Thus, we have

$$\hat{h} |\varphi_{0s}\rangle = e_0 |\varphi_{0s}\rangle, \quad (1.133)$$

and the corresponding wave function is diagonal in spin space,

$$\varphi_{0s}(\mathbf{x}, s') = \varphi_0(\mathbf{x}) \delta_{ss'}. \quad (1.134)$$

We further assume that the following conditions are fulfilled:

- (i) The orbitals $\varphi_{\mu s}$ are sufficiently concentrated around the origin, i.e., within the region where ΔV is small. More precisely, we assume that

$$|\langle \varphi_{\mu s} | \Delta \hat{V} | \varphi_{\mu' s'} \rangle| \ll \Delta e_0. \quad (1.135)$$

- (ii) The overlap between orbitals at different lattice sites is small, hence for $\mathbf{R} \neq \mathbf{0}$,

$$|\langle \varphi_{\mu s} | \varphi_{\mu' s'} \rangle| \ll 1, \quad (1.136)$$

$$|\langle \varphi_{\mu s} | \hat{H} | \varphi_{\mu' s'} \rangle| \ll \Delta e_0. \quad (1.137)$$

- (iii) The spin-orbit coupling is small, such that

$$|\langle \varphi_{\mu s} | \hat{V}_{\text{so}} | \varphi_{\mu' s'} \rangle| \ll \Delta e_0. \quad (1.138)$$

If these conditions are fulfilled, then we can derive an effective Hamiltonian $H_{ss'}(\mathbf{k})$ describing a “spin-split energy band”, which approaches the atomic energy e_0 in the tight-binding limit. For this purpose, we split off the atomic eigenvalues from the Hamiltonian (1.121), such that

$$H_{\mu s, \mu' s'}(\mathbf{k}) = \frac{1}{\mathcal{N}_{n\mathbf{k}}^2} e_{\mu} \delta_{\mu\mu'} \delta_{ss'} + H'_{\mu s, \mu' s'}(\mathbf{k}), \quad (1.139)$$

where

$$H'_{\mu s, \mu' s'}(\mathbf{k}) = \frac{1}{\mathcal{N}_{\mu\mathbf{k}}^2} \frac{1}{\mathcal{N}_{\mu'\mathbf{k}}} \left(\langle \varphi_{\mu s} | (\Delta \hat{V} + \hat{V}_{\text{so}}) | \varphi_{\mu' s'} \rangle + \sum_{\mathbf{R} \neq \mathbf{0}} e^{-i\mathbf{k} \cdot \mathbf{R}} \langle \varphi_{\mu s} | \hat{H} | \varphi_{\mu' s'} \rangle \right). \quad (1.140)$$

Now, the conditions (i)–(iii) imply that

$$|H'_{\mu s, \mu' s'}(\mathbf{k})| \ll \Delta e_0, \quad (1.141)$$

and hence we can apply *quasi-degenerate perturbation theory* (see Ref. [Win03, Appendix B]) to bring the Hamiltonian (1.139) into an approximate block-diagonal form. The resulting effective Hamiltonian for the relevant energy bands reads

$$H_{ss'}(\mathbf{k}) = \frac{1}{\mathcal{N}_{0\mathbf{k}}^2} e_0 \delta_{ss'} + H'_{0s, 0s'}(\mathbf{k}) + \sum_{\mu \neq 0} \sum_t H'_{0s, \mu t}(\mathbf{k}) H'_{\mu t, 0s'}(\mathbf{k}) \frac{1}{e_0 - e_{\mu}} + \mathcal{O}(|H'(\mathbf{k})/\Delta e_0|^2). \quad (1.142)$$

Thus, we have shown how one can derive—by starting from the fundamental Hamiltonian (1.46) and applying a number of approximations to it—a Hamiltonian matrix $H_{ss'}(\mathbf{k})$ which depends on two spin indices and one Bloch momentum. The derivation presented here is valid if the conditions described at the beginning of this section are fulfilled.

We now further restrict ourselves to the zero-order terms in the expansion (1.142), i.e.,

$$H_{ss'}(\mathbf{k}) = \frac{1}{\mathcal{N}_{0\mathbf{k}}^2} e_0 \delta_{ss'} + H'_{0s,0s'}(\mathbf{k}) \quad (1.143)$$

$$= \frac{1}{\mathcal{N}_{0\mathbf{k}}^2} \left(e_0 \delta_{ss'} + \langle \varphi_{0s} | \Delta \hat{V} + \hat{V}_{so} | \varphi_{0s'} \rangle + \sum_{\mathbf{R} \neq \mathbf{0}} e^{-i\mathbf{k} \cdot \mathbf{R}} \langle \varphi_{0s\mathbf{R}} | \hat{H} | \varphi_{0s'} \rangle \right), \quad (1.144)$$

where the normalization constant is given by (see Eq. (1.113))

$$\mathcal{N}_{0\mathbf{k}} = \left(1 + \sum_{\mathbf{R} \neq \mathbf{0}} e^{-i\mathbf{k} \cdot \mathbf{R}} \langle \varphi_{0\mathbf{R}} | \varphi_0 \rangle \right)^{1/2}. \quad (1.145)$$

This approximation simply means that all matrix elements $H_{\mu s, \mu' s'}(\mathbf{k})$ with $\mu = 0$ and $\mu' \neq 0$ (or vice versa) are neglected, and thus the Hamiltonian matrix becomes trivially block-diagonal: from Eq. (1.118), we obtain directly

$$H_{ss'}(\mathbf{k}) \equiv H_{0s,0s'}(\mathbf{k}) = \frac{1}{\mathcal{N}_{0\mathbf{k}}^2} \sum_{\mathbf{R}} e^{-i\mathbf{k} \cdot \mathbf{R}} \langle \varphi_{0s\mathbf{R}} | \hat{H} | \varphi_{0s'} \rangle. \quad (1.146)$$

By further applying the same approximation to the overlap matrix, i.e., by assuming that $S_{\mu\mu'}(\mathbf{k}) = \delta_{\mu\mu'}$, the generalized eigenvalue problem (1.122) reduces to an ordinary eigenvalue problem, which reads

$$\sum_{s'} H_{ss'}(\mathbf{k}) U_{s'n}(\mathbf{k}) = E_n(\mathbf{k}) U_{sn}(\mathbf{k}). \quad (1.147)$$

The solution of this eigenvalue problem yields two energy bands, $E_{\pm}(\mathbf{k})$, which approach the atomic energy e_0 in the tight-binding limit (the latter was defined in the previous section). Furthermore, the solution yields the unitary matrix $U_{sn}(\mathbf{k})$ by which one can construct the Bloch vectors in terms of the Bloch-like vectors, i.e.,

$$|\Psi_{n\mathbf{k}}\rangle = \sum_s |\psi_{0s\mathbf{k}}\rangle U_{sn}(\mathbf{k}). \quad (1.148)$$

In particular, in this approximation the Bloch-like vectors are indeed orthonormal. The hermitean matrix $H_{ss'}(\mathbf{k})$ is called the *Hamiltonian matrix in the spin basis*, and the unitary matrix $U_{sn}(\mathbf{k})$ *mediates between the band basis* (Bloch vectors) *and the spin basis* (Bloch-like vectors). We stress again, however, that this is possible only in the zero-order approximation described above, because in general the Bloch-like vectors are not orthogonal.

For later purposes, we further define the inverse Fourier transform of the above Hamiltonian matrix as

$$H_{ss'}(\mathbf{R} - \mathbf{R}') := \frac{1}{|\mathcal{B}|} \int_{\mathcal{B}} d^3\mathbf{k} H_{ss'}(\mathbf{k}) e^{i\mathbf{k} \cdot (\mathbf{R} - \mathbf{R}')}. \quad (1.149)$$

By Eq. (1.146), this is equivalent to

$$H_{ss'}(\mathbf{R} - \mathbf{R}') = \sum_{\mathbf{R}'' \neq \mathbf{0}} \langle \varphi_{0s\mathbf{R}''} | \hat{H} | \varphi_{0s'} \rangle \frac{1}{|\mathcal{B}|} \int_{\mathcal{B}} d^3\mathbf{k} e^{i\mathbf{k} \cdot (\mathbf{R} - \mathbf{R}' - \mathbf{R}'')} \frac{1}{\mathcal{N}_{0\mathbf{k}}^2}. \quad (1.150)$$

By substituting $\mathbf{R} - \mathbf{R}' - \mathbf{R}'' \mapsto \mathbf{R}''$ and using the translation invariance of \hat{H} , we thus arrive at the expression

$$H_{ss'}(\mathbf{R} - \mathbf{R}') = \sum_{\mathbf{R}'' \neq \mathbf{0}} \langle \varphi_{0s, \mathbf{R} - \mathbf{R}''} | \hat{H} | \varphi_{0s', \mathbf{R}'} \rangle \frac{1}{|\mathcal{B}|} \int_{\mathcal{B}} d^3\mathbf{k} e^{i\mathbf{k} \cdot \mathbf{R}''} \frac{1}{\mathcal{N}_{0\mathbf{k}}^2}. \quad (1.151)$$

From this, we conclude that the “Hamiltonian matrix in direct space” $H_{ss'}(\mathbf{R} - \mathbf{R}')$ is in general given by a complicated convolution; only if we assume that $\mathcal{N}_{0\mathbf{k}} = 1$, the above expression simplifies to

$$H_{ss'}(\mathbf{R} - \mathbf{R}') = \langle \varphi_{0s, \mathbf{R}} | \hat{H} | \varphi_{0s', \mathbf{R}'} \rangle, \quad (1.152)$$

which means that $H_{ss'}(\mathbf{R} - \mathbf{R}')$ is given by the matrix elements of the fundamental Hamiltonian \hat{H} with respect to atomic orbitals with the distance vector $(\mathbf{R} - \mathbf{R}')$.

Finally, if we neglect the spin-orbit coupling \hat{V}_{so} , then the effective Hamiltonian (1.144) becomes diagonal in the spin basis,

$$H_{ss'}(\mathbf{k}) = \delta_{ss'} E(\mathbf{k}), \quad (1.153)$$

and the dispersion of the two-fold degenerate band is given by

$$E(\mathbf{k}) = \frac{1}{\mathcal{N}_{0\mathbf{k}}^2} \left(e_0 + \langle \varphi_0 | \Delta \hat{V} | \varphi_0 \rangle + \sum_{\mathbf{R} \neq \mathbf{0}} e^{-i\mathbf{k} \cdot \mathbf{R}} \langle \varphi_{0\mathbf{R}} | \hat{H} | \varphi_0 \rangle \right). \quad (1.154)$$

Using that $\hat{H} = \hat{h} + \Delta \hat{V}$ and $\hat{h} \varphi_0 = e_0$, this is equivalent to

$$\begin{aligned} E(\mathbf{k}) = e_0 + & \left(1 + \sum_{\mathbf{R} \neq \mathbf{0}} e^{-i\mathbf{k} \cdot \mathbf{R}} \langle \varphi_{0\mathbf{R}} | \varphi_0 \rangle \right)^{-1} \\ & \times \left(\langle \varphi_0 | \Delta \hat{V} | \varphi_0 \rangle + \sum_{\mathbf{R} \neq \mathbf{0}} e^{-i\mathbf{k} \cdot \mathbf{R}} \langle \varphi_{0\mathbf{R}} | \Delta \hat{V} | \varphi_0 \rangle \right), \end{aligned} \quad (1.155)$$

which in turn agrees precisely with Ref. [AM76, Eqs. (10.15)–(10.18)].

1.5.2. Pauli matrix representation

Any complex (2×2) matrix can be expanded in terms of the identity matrix $\mathbb{1} \equiv \mathbb{1}_{2 \times 2}$ and the three Pauli matrices,

$$\sigma_x = \begin{pmatrix} 0 & 1 \\ 1 & 0 \end{pmatrix}, \quad \sigma_y = \begin{pmatrix} 0 & -i \\ i & 0 \end{pmatrix}, \quad \sigma_z = \begin{pmatrix} 1 & 0 \\ 0 & -1 \end{pmatrix}. \quad (1.156)$$

In particular, the Hamiltonian matrix in the spin basis (defined by Eq. (1.146)) can be expanded for each $\mathbf{k} \in \mathcal{B}$ as

$$H_{ss'}(\mathbf{k}) = f(\mathbf{k})\delta_{ss'} + \mathbf{g}(\mathbf{k}) \cdot \boldsymbol{\sigma}_{ss'}. \quad (1.157)$$

We call this the *Pauli matrix representation* of the Hamiltonian matrix. For a general (2×2) matrix, the coefficient functions f and $\mathbf{g} = (g_x, g_y, g_z)^T$ are complex-valued, but the hermiticity of the Hamiltonian matrix enforces them to be real-valued (see Sct. 2.1.1). In components, the Pauli matrix representation reads as

$$H = \begin{pmatrix} f + g_z & g_x - ig_y \\ g_x + ig_y & f - g_z \end{pmatrix}, \quad (1.158)$$

where we have suppressed the momentum dependencies. The Hamiltonian matrix in direct space (given by Eq. (1.149)) can be expanded analogously as

$$H_{ss'}(\mathbf{R}) = f(\mathbf{R})\delta_{ss'} + \mathbf{g}(\mathbf{R}) \cdot \boldsymbol{\sigma}_{ss'}. \quad (1.159)$$

The functions $f(\mathbf{R})$, $\mathbf{g}(\mathbf{R})$ are related to $f(\mathbf{k})$, $\mathbf{g}(\mathbf{k})$ by Fourier's transformation, which is precisely analogous to Eq. (1.149).

Next, the (2×2) matrix (1.158) can be diagonalized as

$$\sum_{s,s'} U_{ns}^* H_{ss'} U_{s'n'} = \delta_{nn'} E_{n'}, \quad (1.160)$$

or in matrix notation as

$$U^\dagger H U = E \equiv \begin{pmatrix} E_- & 0 \\ 0 & E_+ \end{pmatrix}. \quad (1.161)$$

The eigenvalues are given explicitly by

$$E_{\mp} = f \mp |\mathbf{g}|, \quad (1.162)$$

and the unitary matrix U reads

$$U = \frac{1}{\sqrt{2|\mathbf{g}|}} \begin{pmatrix} \sqrt{|\mathbf{g}| - g_z} & \sqrt{|\mathbf{g}| + g_z} \\ -\sqrt{|\mathbf{g}| + g_z} e^{i\varphi} & \sqrt{|\mathbf{g}| - g_z} e^{i\varphi} \end{pmatrix}. \quad (1.163)$$

Here, $\varphi \equiv \varphi(\mathbf{g}) \in [0, 2\pi)$ denotes the polar angle of the two-dimensional vector $(g_x, g_y)^T$, which is defined such that

$$e^{i\varphi(\mathbf{g})} = \frac{g_x + ig_y}{\sqrt{g_x^2 + g_y^2}} = \frac{g_x + ig_y}{\sqrt{(|\mathbf{g}| - g_z)(|\mathbf{g}| + g_z)}}. \quad (1.164)$$

The matrix U contains the eigenvectors ψ^\mp of the Hamiltonian matrix (1.158) as column

vectors, hence

$$\psi^- = \frac{1}{\sqrt{2|\mathbf{g}|}} \begin{pmatrix} \sqrt{|\mathbf{g}| - g_z} \\ -\sqrt{|\mathbf{g}| + g_z} e^{i\varphi} \end{pmatrix}, \quad \psi^+ = \frac{1}{\sqrt{2|\mathbf{g}|}} \begin{pmatrix} \sqrt{|\mathbf{g}| + g_z} \\ \sqrt{|\mathbf{g}| - g_z} e^{i\varphi} \end{pmatrix} \quad (1.165)$$

These eigenvectors correspond to the lower (E_-) and to the upper (E_+) energy level, respectively. An important property of the Pauli matrix representation is that the spin expectation value in each eigenstate can be expressed directly in terms of the function \mathbf{g} :

$$\langle \mathbf{s} \rangle^\mp \equiv \frac{\hbar}{2} \sum_{s, s'} [\psi_s^\mp]^* \boldsymbol{\sigma}_{ss'} \psi_{s'}^\mp = \frac{\hbar}{2} \left(\mp \frac{\mathbf{g}}{|\mathbf{g}|} \right). \quad (1.166)$$

Thus, the spin polarization of the upper energy level is given by the normalized vector $\mathbf{g}/|\mathbf{g}|$, and it is opposite to the spin polarization of the lower energy level.

For later purposes, we further derive two properties of the matrix $U = U(\mathbf{k})$ which diagonalizes the Hamiltonian matrix (1.157). The first one follows directly from Eq. (1.161), which is equivalent to

$$H(\mathbf{k}) = U(\mathbf{k}) E(\mathbf{k}) U^\dagger(\mathbf{k}). \quad (1.167)$$

Putting in the representation (1.157) and the eigenvalues (1.162) yields

$$f(\mathbf{k}) \mathbb{1} + \mathbf{g}(\mathbf{k}) \cdot \boldsymbol{\sigma} = U(\mathbf{k}) (f(\mathbf{k}) \mathbb{1} - |\mathbf{g}(\mathbf{k})| \sigma_z) U^\dagger(\mathbf{k}) \quad (1.168)$$

$$= f(\mathbf{k}) \mathbb{1} - |\mathbf{g}(\mathbf{k})| U(\mathbf{k}) \sigma_z U^\dagger(\mathbf{k}). \quad (1.169)$$

Therefore, the following identity holds:

$$U(\mathbf{k}) \sigma_z U^\dagger(\mathbf{k}) = -\frac{\mathbf{g}(\mathbf{k})}{|\mathbf{g}(\mathbf{k})|} \cdot \boldsymbol{\sigma}. \quad (1.170)$$

The second property holds under the assumption of time-reversal symmetry, which requires that (see Sect. 2.1.2, Eq. (2.43))

$$H(\mathbf{k}) = [\mathrm{i}\sigma_y]^\dagger H^*(-\mathbf{k}) \mathrm{i}\sigma_y. \quad (1.171)$$

By using this assumption, we obtain from Eq. (1.161) that

$$E(\mathbf{k}) = U^\dagger(\mathbf{k}) [\mathrm{i}\sigma_y]^\dagger H^*(-\mathbf{k}) [\mathrm{i}\sigma_y] U(\mathbf{k}) \quad (1.172)$$

$$= [\mathrm{i}\sigma_y U(\mathbf{k})]^\dagger H^*(-\mathbf{k}) [\mathrm{i}\sigma_y U(\mathbf{k})], \quad (1.173)$$

and further, by complex conjugation,

$$[\mathrm{i}\sigma_y U^*(\mathbf{k})]^\dagger H(-\mathbf{k}) [\mathrm{i}\sigma_y U^*(\mathbf{k})] = E(\mathbf{k}). \quad (1.174)$$

This implies that $H(-\mathbf{k})$ has the same eigenvalues as $H(\mathbf{k})$, i.e.,

$$E(-\mathbf{k}) = E(\mathbf{k}), \quad (1.175)$$

and that the unitary matrix $[i\sigma_y U^*(\mathbf{k})]$ diagonalizes $H(-\mathbf{k})$. Indeed, from the explicit form of $U(\mathbf{k})$ given by Eq. (1.163), we find by a straightforward calculation that

$$i\sigma_y U^*(\mathbf{k}) = U(-\mathbf{k}) \begin{pmatrix} e^{-i\varphi(-\mathbf{k})} & 0 \\ 0 & -e^{-i\varphi(-\mathbf{k})} \end{pmatrix} = U(-\mathbf{k}) e^{-i\varphi(-\mathbf{k})} \sigma_z. \quad (1.176)$$

This shows that the column vectors of the matrix $[i\sigma_y U^*(\mathbf{k})]$ coincide with the column vectors of $U(-\mathbf{k})$ up to the phase factors.

2. Tight-binding Rashba model

2.1. Symmetries

We now assume that the nuclear potential (1.42), and hence also the fundamental Hamiltonian \hat{H} given by Eq. (1.46), have the following symmetries (besides the invariance under lattice translations): time-reversal symmetry, and the symmetries of the point group C_{3v} of BiTeI (which contains the three-fold rotation C_3 and the mirror reflection σ_v , see Sect. 3.1). In addition, we assume that the orbital $|\varphi_{0s}\rangle$, which is the eigenvector of the atomic Hamiltonian (1.97), is invariant under these very symmetries. Based on these assumptions, we will in the following derive the transformation behavior of the atomic orbitals $|\varphi_{0s\mathbf{R}}\rangle$ centered at arbitrary lattice sites, and of the corresponding Bloch-like vectors $|\psi_{0s\mathbf{k}}\rangle$. Moreover, we will derive the corresponding symmetry constraints on the effective Hamiltonian matrix $H_{ss'}(\mathbf{k})$ as defined in the previous chapter.

2.1.1. Hermiticity

The fundamental Hamiltonian equals its hermitean conjugate,

$$\hat{H} = \hat{H}^\dagger. \quad (2.1)$$

Although this is actually not a symmetry of the Hamiltonian but a general postulate of quantum mechanics, it will be convenient to consider the consequences of this condition together with those of the genuine symmetries. We denote the atomic orbital in terms of which the single-orbital model was defined in Sect. 1.5 by $\varphi_s \equiv \varphi_{0s}$ (omitting the subscript “0” to lighten the notation). Then, the hermiticity of the fundamental Hamiltonian implies that

$$\langle \varphi_{s\mathbf{R}} | \hat{H} | \varphi_{s'} \rangle = \langle \varphi_{s\mathbf{R}} | \hat{H}^\dagger | \varphi_{s'} \rangle \quad (2.2)$$

$$= \langle \varphi_{s'} | \hat{H} | \varphi_{s\mathbf{R}} \rangle^* \quad (2.3)$$

$$= \langle \varphi_{s', -\mathbf{R}} | \hat{H} | \varphi_s \rangle^*, \quad (2.4)$$

where in the last step we have used the lattice translation invariance of \hat{H} . For the

Hamiltonian matrix (1.146), this implies (using that $\mathcal{N}_{\mathbf{k}} = \mathcal{N}_{\mathbf{k}}^*$)

$$H_{ss'}(\mathbf{k}) = \frac{1}{\mathcal{N}_{\mathbf{k}}^2} \sum_{\mathbf{R}} e^{-i\mathbf{k} \cdot \mathbf{R}} \langle \varphi_{s\mathbf{R}} | \hat{H} | \varphi_{s'} \rangle \quad (2.5)$$

$$= \frac{1}{\mathcal{N}_{\mathbf{k}}^2} \sum_{\mathbf{R}} e^{-i\mathbf{k} \cdot \mathbf{R}} \langle \varphi_{s', -\mathbf{R}} | \hat{H} | \varphi_s \rangle^* \quad (2.6)$$

$$= \frac{1}{\mathcal{N}_{\mathbf{k}}^2} \sum_{\mathbf{R}} e^{i\mathbf{k} \cdot \mathbf{R}} \langle \varphi_{s'\mathbf{R}} | \hat{H} | \varphi_s \rangle^* \quad (2.7)$$

$$= \left(\frac{1}{\mathcal{N}_{\mathbf{k}}^2} \sum_{\mathbf{R}} e^{-i\mathbf{k} \cdot \mathbf{R}} \langle \varphi_{s'\mathbf{R}} | \hat{H} | \varphi_s \rangle \right)^* \quad (2.8)$$

$$= H_{s's}^*(\mathbf{k}). \quad (2.9)$$

In matrix notation, this can be written equivalently as

$$H(\mathbf{k}) = H^\dagger(\mathbf{k}). \quad (2.10)$$

Thus, for each \mathbf{k} , the Hamiltonian matrix $H(\mathbf{k})$ is a hermitean (2×2) matrix. Furthermore, by using the Pauli matrix expansion (1.157), we obtain

$$f(\mathbf{k}) \mathbb{1} + \mathbf{g}(\mathbf{k}) \cdot \boldsymbol{\sigma} = f^*(\mathbf{k}) \mathbb{1} + \mathbf{g}^*(\mathbf{k}) \cdot \boldsymbol{\sigma}, \quad (2.11)$$

where we have used the hermiticity of the Pauli matrices. We therefore find

$$f(\mathbf{k}) = f^*(\mathbf{k}), \quad (2.12)$$

$$\mathbf{g}(\mathbf{k}) = \mathbf{g}^*(\mathbf{k}), \quad (2.13)$$

meaning that $f(\mathbf{k})$ and $g_x(\mathbf{k})$, $g_y(\mathbf{k})$, $g_z(\mathbf{k})$ are real-valued functions. By Fourier transformation (see Eq. (1.149)), the above conditions translate into

$$H(\mathbf{R}) = H^\dagger(-\mathbf{R}), \quad (2.14)$$

and respectively

$$f(\mathbf{R}) = f^*(-\mathbf{R}), \quad (2.15)$$

$$\mathbf{g}(\mathbf{R}) = \mathbf{g}^*(-\mathbf{R}), \quad (2.16)$$

for the corresponding functions in direct space.

2.1.2. Time-reversal symmetry

The time-reversal operator $\hat{\Theta}$ (see Ref. [Mes62, Ch. XV, §17–18]) is characterized by its

action on the position, momentum and spin operators:

$$\hat{\Theta}^\dagger \hat{\mathbf{x}} \hat{\Theta} = \hat{\mathbf{x}}, \quad (2.17)$$

$$\hat{\Theta}^\dagger \hat{\mathbf{p}} \hat{\Theta} = -\hat{\mathbf{p}}, \quad (2.18)$$

$$\hat{\Theta}^\dagger \hat{\boldsymbol{\sigma}} \hat{\Theta} = -\hat{\boldsymbol{\sigma}}. \quad (2.19)$$

It is antiunitary, hence $\hat{\Theta}^{-1} = \hat{\Theta}^\dagger$, and

$$\langle \phi | \hat{\Theta} | \psi \rangle = \langle \psi | \hat{\Theta}^\dagger | \phi \rangle, \quad \text{for } \phi, \psi \in \mathcal{H}. \quad (2.20)$$

Furthermore, it can be defined through its action on wave functions $\psi \in \mathcal{H}$ as

$$(\hat{\Theta}\psi)(\mathbf{x}, s) = \sum_{s'} [-i\sigma_y]_{ss'} \psi^*(\mathbf{x}, s'). \quad (2.21)$$

We assume that the atomic wave function $\varphi(\mathbf{x}) \equiv \varphi_0(\mathbf{x})$ (which is defined by Eqs. (1.133)–(1.134)) is real-valued, i.e.,

$$\varphi(\mathbf{x}) = \varphi^*(\mathbf{x}). \quad (2.22)$$

This implies that

$$(\hat{\Theta}\varphi_s)(\mathbf{x}, s') = \sum_{t'} [-i\sigma_y]_{s't'} \varphi_s(\mathbf{x}, t') = \sum_{t'} [-i\sigma_y]_{s't'} \varphi(\mathbf{x}) \delta_{st'} = [-i\sigma_y]_{s's} \varphi(\mathbf{x}) \quad (2.23)$$

$$= \sum_t \varphi(\mathbf{x}) \delta_{s't} [-i\sigma_y]_{ts} = \sum_t \varphi_t(\mathbf{x}, s') [-i\sigma_y]_{ts}, \quad (2.24)$$

and consequently,

$$\hat{\Theta} |\varphi_s\rangle = \sum_t |\varphi_t\rangle [-i\sigma_y]_{ts}. \quad (2.25)$$

From this, we further obtain

$$\hat{\Theta} |\varphi_{s\mathbf{R}}\rangle = \hat{\Theta} \hat{T}_{\mathbf{R}} |\varphi_s\rangle = \hat{T}_{\mathbf{R}} \hat{\Theta} |\varphi_s\rangle = \sum_t \hat{T}_{\mathbf{R}} |\varphi_t\rangle [-i\sigma_y]_{ts} = \sum_t |\varphi_{t\mathbf{R}}\rangle [-i\sigma_y]_{ts}, \quad (2.26)$$

where we have used that the time reversal operator commutes with the lattice translations. The above equation gives the transformation behavior of the vectors $|\varphi_{s\mathbf{R}}\rangle$ under time reversal. Next, consider the Bloch-like vectors defined by Eqs. (1.101) and (1.113), i.e.,

$$|\psi_{s\mathbf{k}}\rangle = \frac{1}{\mathcal{N}_{\mathbf{k}}} \sum_{\mathbf{R}} |\varphi_{s\mathbf{R}}\rangle e^{i\mathbf{k}\cdot\mathbf{R}}, \quad (2.27)$$

with the (spin-independent) normalization constant

$$\mathcal{N}_{\mathbf{k}} = \left(\sum_{\mathbf{R}} e^{-i\mathbf{k}\cdot\mathbf{R}} \langle \varphi_{s\mathbf{R}} | \varphi_s \rangle \right)^{1/2}. \quad (2.28)$$

Using that $\mathcal{N}_{\mathbf{k}}$ is real-valued, we can calculate as

$$\hat{\Theta}|\psi_{s\mathbf{k}}\rangle = \frac{1}{\mathcal{N}_{\mathbf{k}}} \sum_{\mathbf{R}} e^{-i\mathbf{k}\cdot\mathbf{R}} \hat{\Theta}|\varphi_{s\mathbf{R}}\rangle \quad (2.29)$$

$$= \frac{1}{\mathcal{N}_{\mathbf{k}}} \sum_{\mathbf{R}} e^{-i\mathbf{k}\cdot\mathbf{R}} \sum_t |\varphi_{t\mathbf{R}}\rangle [-i\sigma_y]_{ts} \quad (2.30)$$

$$= \sum_t |\psi_{t,-\mathbf{k}}\rangle [-i\sigma_y]_{ts}, \quad (2.31)$$

which gives the transformation law of the Bloch-like vectors under time reversal.

Now, the fundamental Hamiltonian (1.46) is invariant under time reversal provided that the nuclear potential V is real-valued. Hence, we may assume that

$$[\hat{\Theta}, \hat{H}] = 0, \quad (2.32)$$

which is equivalent to

$$\hat{H} = \hat{\Theta}^{-1} \hat{H} \hat{\Theta} = \hat{\Theta}^\dagger \hat{H} \hat{\Theta}. \quad (2.33)$$

For the matrix elements of the Hamiltonian, it follows that

$$\langle \varphi_{s\mathbf{R}} | \hat{H} | \varphi_{s'} \rangle = \langle \varphi_{s\mathbf{R}} | \hat{\Theta}^\dagger \hat{H} \hat{\Theta} | \varphi_{s'} \rangle \quad (2.34)$$

$$= \sum_{t'} [-i\sigma_y]_{t's'} \langle \varphi_{s\mathbf{R}} | \hat{\Theta}^\dagger \hat{H} | \varphi_{t'} \rangle \quad (2.35)$$

$$= \sum_{t'} [-i\sigma_y]_{t's'} \langle \varphi_{t'} | \hat{H} \hat{\Theta} | \varphi_{s\mathbf{R}} \rangle \quad (2.36)$$

$$= \sum_{t,t'} [-i\sigma_y]_{ts} [-i\sigma_y]_{t's'} \langle \varphi_{t'} | \hat{H} | \varphi_{t\mathbf{R}} \rangle \quad (2.37)$$

$$= \sum_{t,t'} [i\sigma_y]_{ts} [i\sigma_y]_{t's'} \langle \varphi_{t\mathbf{R}} | \hat{H} | \varphi_{t'} \rangle^* \quad (2.38)$$

$$= \sum_{t,t'} [i\sigma_y]_{st}^\dagger \langle \varphi_{t\mathbf{R}} | \hat{H} | \varphi_{t'} \rangle^* [i\sigma_y]_{t's'}. \quad (2.39)$$

For the Hamiltonian matrix, this further implies

$$H_{ss'}(\mathbf{k}) = \frac{1}{\mathcal{N}_{\mathbf{k}}^2} \sum_{\mathbf{R}} e^{-i\mathbf{k}\cdot\mathbf{R}} \langle \varphi_{s\mathbf{R}} | \hat{H} | \varphi_{s'} \rangle \quad (2.40)$$

$$= \sum_{t,t'} [i\sigma_y]_{st}^\dagger \left(\frac{1}{\mathcal{N}_{\mathbf{k}}^2} \sum_{\mathbf{R}} e^{i\mathbf{k}\cdot\mathbf{R}} \langle \varphi_{t\mathbf{R}} | \hat{H} | \varphi_{t'} \rangle \right)^* [i\sigma_y]_{t's'} \quad (2.41)$$

$$= \sum_{t,t'} [i\sigma_y]_{st}^\dagger H_{tt'}^*(-\mathbf{k}) [i\sigma_y]_{t's'}. \quad (2.42)$$

Here, we have used that $\mathcal{N}_{\mathbf{k}} = \mathcal{N}_{-\mathbf{k}}$, which follows from Eq. (2.22). In matrix notation, we can write the above condition as

$$H(\mathbf{k}) = [\mathrm{i}\sigma_y]^\dagger H^*(-\mathbf{k}) \mathrm{i}\sigma_y. \quad (2.43)$$

In the Pauli matrix representation, we further obtain

$$f(\mathbf{k}) + \mathbf{g}(\mathbf{k}) \cdot \boldsymbol{\sigma} = f^*(-\mathbf{k}) - \mathbf{g}^*(-\mathbf{k}) \cdot \boldsymbol{\sigma}, \quad (2.44)$$

where we have used that

$$[\mathrm{i}\sigma_y]^\dagger \boldsymbol{\sigma}^* [\mathrm{i}\sigma_y] = -\boldsymbol{\sigma}. \quad (2.45)$$

Hence, time-reversal symmetry yields the conditions

$$f(\mathbf{k}) = f^*(-\mathbf{k}), \quad (2.46)$$

$$\mathbf{g}(\mathbf{k}) = -\mathbf{g}^*(-\mathbf{k}). \quad (2.47)$$

By Fourier transformation, we obtain the equivalent conditions

$$H(\mathbf{R}) = [\mathrm{i}\sigma_y]^\dagger H^*(\mathbf{R}) \mathrm{i}\sigma_y, \quad (2.48)$$

as well as

$$f(\mathbf{R}) = f^*(\mathbf{R}), \quad (2.49)$$

$$\mathbf{g}(\mathbf{R}) = -\mathbf{g}^*(\mathbf{R}), \quad (2.50)$$

for the corresponding functions in direct space.

2.1.3. Spatial inversion symmetry

For the sake of completeness, we also study in this subsection the consequences of the spatial inversion symmetry, although we do *not* assume that the Hamiltonian (1.46) has this symmetry. In fact, the crystal structure of BiTeI (and hence the nuclear potential V acting on the electrons) is not invariant under spatial inversion, and this is one main reason—besides the large atomic spin-orbit coupling of the bismuth atoms—for the Rashba spin splitting of the electronic energy states in this material (see Refs. [Ish+11], [DDJ08, Sct. 16.4], and the discussion in Sct. 2.2).

The operator \hat{P} representing a spatial inversion (see Ref. [Mes62, Ch. XV, §10]) has the properties that

$$\hat{P}^\dagger \hat{\mathbf{x}} \hat{P} = -\hat{\mathbf{x}}, \quad (2.51)$$

$$\hat{P}^\dagger \hat{\mathbf{p}} \hat{P} = -\hat{\mathbf{p}}, \quad (2.52)$$

$$\hat{P}^\dagger \boldsymbol{\sigma} \hat{P} = \boldsymbol{\sigma}. \quad (2.53)$$

It is unitary and self-inverse, i.e.,

$$\hat{P}^\dagger = \hat{P} = \hat{P}^{-1}, \quad (2.54)$$

and it can be defined through its action on $\psi \in \mathcal{H}$ as

$$(\hat{P}\psi)(\mathbf{x}, s) = \psi(-\mathbf{x}, s). \quad (2.55)$$

We assume that the orbital $\varphi \equiv \varphi_0$ is invariant under spatial inversion, such that

$$\varphi(\mathbf{x}) = \varphi(-\mathbf{x}). \quad (2.56)$$

This implies the following transformation behavior of the atomic orbitals:

$$\hat{P}|\varphi_{s\mathbf{R}}\rangle = \hat{P}\hat{T}_{\mathbf{R}}|\varphi_s\rangle = \hat{T}_{-\mathbf{R}}\hat{P}|\varphi_s\rangle = \hat{T}_{-\mathbf{R}}|\varphi_s\rangle = |\varphi_{s,-\mathbf{R}}\rangle. \quad (2.57)$$

For the Bloch-like functions, we then obtain

$$\hat{P}|\psi_{s\mathbf{k}}\rangle = \frac{1}{\mathcal{N}_{\mathbf{k}}} \sum_{\mathbf{R}} e^{-i\mathbf{k}\cdot\mathbf{R}} |\varphi_{s,-\mathbf{R}}\rangle = \frac{1}{\mathcal{N}_{\mathbf{k}}} \sum_{\mathbf{R}} e^{i\mathbf{k}\cdot\mathbf{R}} |\varphi_{s\mathbf{R}}\rangle = |\psi_{s,-\mathbf{k}}\rangle. \quad (2.58)$$

Here, we have used the condition $\mathcal{N}_{\mathbf{k}} = \mathcal{N}_{-\mathbf{k}}$, which also follows from Eq. (2.56).

Now, assume that the system is invariant under spatial inversion, i.e.,

$$[\hat{P}, \hat{H}] = 0. \quad (2.59)$$

This implies for the matrix elements of the fundamental Hamiltonian that

$$\langle\varphi_{s\mathbf{R}}|\hat{H}|\varphi_{s'}\rangle = \langle\varphi_{s\mathbf{R}}|\hat{P}^\dagger\hat{H}\hat{P}|\varphi_{s'}\rangle = \langle\varphi_{s,-\mathbf{R}}|\hat{H}|\varphi_{s'}\rangle, \quad (2.60)$$

and hence for the Hamiltonian matrix that

$$H_{ss'}(\mathbf{k}) = \frac{1}{\mathcal{N}_{\mathbf{k}}^2} \sum_{\mathbf{R}} e^{-i\mathbf{k}\cdot\mathbf{R}} \langle\varphi_{s,-\mathbf{R}}|\hat{H}|\varphi_{s'}\rangle \quad (2.61)$$

$$= \frac{1}{\mathcal{N}_{\mathbf{k}}^2} \sum_{\mathbf{R}} e^{i\mathbf{k}\cdot\mathbf{R}} \langle\varphi_{s\mathbf{R}}|\hat{H}|\varphi_{s'}\rangle = H_{ss'}(-\mathbf{k}), \quad (2.62)$$

which can be written equivalently as

$$H(\mathbf{k}) = H(-\mathbf{k}). \quad (2.63)$$

From the Pauli matrix representation, we thus obtain

$$f(\mathbf{k}) = f(-\mathbf{k}), \quad (2.64)$$

$$g(\mathbf{k}) = g(-\mathbf{k}). \quad (2.65)$$

In direct space, the equivalent conditions read

$$H(\mathbf{R}) = H(-\mathbf{R}), \quad (2.66)$$

as well as

$$f(\mathbf{R}) = f(-\mathbf{R}), \quad (2.67)$$

$$\mathbf{g}(\mathbf{R}) = \mathbf{g}(-\mathbf{R}), \quad (2.68)$$

which can be shown by substituting $\mathbf{k} \mapsto -\mathbf{k}$ in Eq. (1.149) for the Fourier transform.

2.1.4. Point-group symmetries

Finally, we consider the symmetries of the group C_{3v} , which is the point group of BiTeI. These are the rotation by $2\pi/3$ around the z -axis, C_3 , and the reflection through the vertical xz -plane, σ_v (see Refs. [BAN11; Ish+11] and Sct. 3.1).

Three-fold rotation.—The operator \hat{C}_3 implementing a rotation by $2\pi/3$ around the z -axis has the following properties (see Ref. [Mes62, Ch. XIII, §11 and §19]):

$$\hat{C}_3^\dagger \hat{\mathbf{x}} \hat{C}_3 = C_3 \hat{\mathbf{x}}, \quad (2.69)$$

$$\hat{C}_3^\dagger \hat{\mathbf{p}} \hat{C}_3 = C_3 \hat{\mathbf{p}}, \quad (2.70)$$

$$\hat{C}_3^\dagger \boldsymbol{\sigma} \hat{C}_3 = C_3 \boldsymbol{\sigma}, \quad (2.71)$$

where on the right hand side, C_3 denotes the (3×3) matrix

$$C_3 = \begin{pmatrix} \cos \frac{2\pi}{3} & -\sin \frac{2\pi}{3} & 0 \\ \sin \frac{2\pi}{3} & \cos \frac{2\pi}{3} & 0 \\ 0 & 0 & 1 \end{pmatrix} = \begin{pmatrix} -\frac{1}{2} & -\frac{\sqrt{3}}{2} & 0 \\ \frac{\sqrt{3}}{2} & -\frac{1}{2} & 0 \\ 0 & 0 & 1 \end{pmatrix}. \quad (2.72)$$

The operator \hat{C}_3 is unitary and can be defined through its action on $\psi \in \mathcal{H}$ as

$$(\hat{C}_3 \psi)(\mathbf{x}, s) = \sum_{s'} [e^{-i\frac{\pi}{3}\sigma_z}]_{ss'} \psi(C_3^{-1} \mathbf{x}, s'). \quad (2.73)$$

If we identify the spin indices as $\uparrow \equiv +1$, $\downarrow \equiv -1$, such that formally

$$[\sigma_z]_{ss'} = s \delta_{ss'}, \quad (2.74)$$

we can write Eq. (2.73) shorthand as

$$(\hat{C}_3 \psi)(\mathbf{x}, s) = e^{-i\frac{\pi}{3}s} \psi(C_3^{-1} \mathbf{x}, s). \quad (2.75)$$

We assume that the atomic orbital $\varphi \equiv \varphi_0$ (which is concentrated around the origin) is

invariant under this transformation, i.e.,

$$\varphi(\mathbf{x}) = \varphi(C_3^{-1} \mathbf{x}). \quad (2.76)$$

This then implies

$$\hat{C}_3 |\varphi_{s\mathbf{R}}\rangle = \hat{C}_3 \hat{T}_{\mathbf{R}} |\varphi_s\rangle = \hat{T}_{C_3\mathbf{R}} \hat{C}_3 |\varphi_s\rangle = \hat{T}_{C_3\mathbf{R}} |\varphi_s\rangle e^{-i\frac{\pi}{3}s} = |\varphi_{s,C_3\mathbf{R}}\rangle e^{-i\frac{\pi}{3}s}. \quad (2.77)$$

From this, we obtain the invariance of the normalization constant,

$$\mathcal{N}_{\mathbf{k}}^2 = \sum_{\mathbf{R}} e^{-i\mathbf{k}\cdot\mathbf{R}} \langle \varphi_{s\mathbf{R}} | \varphi_s \rangle \quad (2.78)$$

$$= \sum_{\mathbf{R}} e^{-i\mathbf{k}\cdot\mathbf{R}} \langle \varphi_{s\mathbf{R}} | \hat{C}_3^\dagger \hat{C}_3 | \varphi_s \rangle \quad (2.79)$$

$$= \sum_{\mathbf{R}} e^{-i\mathbf{k}\cdot\mathbf{R}} \langle \varphi_{s,C_3\mathbf{R}} | \varphi_s \rangle \quad (2.80)$$

$$= \sum_{\mathbf{R}} e^{-i\mathbf{k}\cdot C_3^{-1}\mathbf{R}} \langle \varphi_{s\mathbf{R}} | \varphi_s \rangle \quad (2.81)$$

$$= \sum_{\mathbf{R}} e^{-i(C_3\mathbf{k})\cdot\mathbf{R}} \langle \varphi_{s\mathbf{R}} | \varphi_s \rangle \quad (2.82)$$

$$= (\mathcal{N}_{C_3\mathbf{k}})^2, \quad (2.83)$$

and subsequently the transformation law of the Bloch-like vectors,

$$\hat{C}_3 |\psi_{s\mathbf{k}}\rangle = |\psi_{s,C_3\mathbf{k}}\rangle e^{-i\frac{\pi}{3}s}. \quad (2.84)$$

A similar calculation using the invariance of the fundamental Hamiltonian, $\hat{H} = \hat{C}_3^\dagger \hat{H} \hat{C}_3$, further yields the constraint on the Hamiltonian matrix,

$$H_{ss'}(\mathbf{k}) = e^{i\frac{\pi}{3}s} H_{ss'}(C_3\mathbf{k}) e^{-i\frac{\pi}{3}s'}, \quad (2.85)$$

which in matrix notation reads

$$H(\mathbf{k}) = e^{i\frac{\pi}{3}\sigma_z} H(C_3\mathbf{k}) e^{-i\frac{\pi}{3}\sigma_z}. \quad (2.86)$$

The Pauli matrix representation then yields

$$f(\mathbf{k}) + \mathbf{g}(\mathbf{k}) \cdot \boldsymbol{\sigma} = f(C_3\mathbf{k}) + \mathbf{g}(C_3\mathbf{k}) \cdot [C_3\boldsymbol{\sigma}], \quad (2.87)$$

where we have used that

$$e^{i\frac{\pi}{3}\sigma_z} \boldsymbol{\sigma} e^{-i\frac{\pi}{3}\sigma_z} = C_3 \boldsymbol{\sigma}. \quad (2.88)$$

Equation (2.87) can be written equivalently as

$$f(\mathbf{k}) + \mathbf{g}(\mathbf{k}) \cdot \boldsymbol{\sigma} = f(C_3\mathbf{k}) + [C_3^{-1}\mathbf{g}](C_3\mathbf{k}) \cdot \boldsymbol{\sigma}, \quad (2.89)$$

from which we obtain directly

$$f(\mathbf{k}) = f(C_3 \mathbf{k}), \quad (2.90)$$

$$\mathbf{g}(\mathbf{k}) = [C_3^{-1} \mathbf{g}](C_3 \mathbf{k}), \quad (2.91)$$

where the second condition can be written equivalently as

$$[C_3 \mathbf{g}](\mathbf{k}) = \mathbf{g}(C_3 \mathbf{k}). \quad (2.92)$$

The corresponding conditions in direct space look precisely the same (thus, they are obtained by simply substituting $\mathbf{k} \mapsto \mathbf{R}$ in Eqs. (2.86) and (2.90)–(2.91)).

Mirror reflection.—A reflection through the vertical xz -plane can be defined as the product of a spatial inversion and a rotation around the y axis by an angle of π (see Ref. [Mes62, Ch. XV, §10]). The corresponding operator \hat{M}_y has the properties

$$\hat{M}_y^\dagger \hat{\mathbf{x}} \hat{M}_y = M_y \hat{\mathbf{x}}, \quad (2.93)$$

$$\hat{M}_y^\dagger \hat{\mathbf{p}} \hat{M}_y = M_y \hat{\mathbf{p}}, \quad (2.94)$$

$$\hat{M}_y^\dagger \boldsymbol{\sigma} \hat{M}_y = -M_y \boldsymbol{\sigma}, \quad (2.95)$$

where on the right hand side, M_y denotes the (3×3) matrix

$$M_y = \begin{pmatrix} 1 & 0 & 0 \\ 0 & -1 & 0 \\ 0 & 0 & 1 \end{pmatrix}. \quad (2.96)$$

Note in particular the sign change in Eq. (2.95), which comes from the fact that a spatial inversion leaves the spin invariant (see Eq. (2.53)). The reflection operator is unitary and self-inverse, i.e.,

$$\hat{M}_y^\dagger = \hat{M}_y = \hat{M}_y^{-1}, \quad (2.97)$$

and its explicit action on $\psi \in \mathcal{H}$ reads as

$$(\hat{M}_y \psi)(\mathbf{x}, s) = \sum_{s'} [\sigma_y]_{ss'} \psi(M_y \mathbf{x}, s'). \quad (2.98)$$

The transformation properties of the basis functions and of the Hamiltonian matrix can be derived analogously as in the case of the three-fold rotation symmetry, with the only difference being the additional sign factor in Eq. (2.95). Thus, assuming that

$$\varphi(\mathbf{x}) = \varphi(M_y \mathbf{x}), \quad (2.99)$$

we obtain

$$\hat{M}_y |\varphi_s \mathbf{R}\rangle = \sum_t |\varphi_t, M_y \mathbf{R}\rangle [\sigma_y]_{ts}, \quad (2.100)$$

as well as

$$\hat{M}_y |\psi_{s\mathbf{k}}\rangle = \sum_t |\psi_{t, M_y \mathbf{k}}\rangle [\sigma_y]_{ts}. \quad (2.101)$$

The invariance of the fundamental Hamiltonian under mirror reflection, $[\hat{M}_y, \hat{H}] = 0$, then translates into the condition on the Hamiltonian matrix

$$H(\mathbf{k}) = \sigma_y H(M_y \mathbf{k}) \sigma_y. \quad (2.102)$$

From the Pauli matrix representation, we further obtain

$$f(\mathbf{k}) = f(M_y \mathbf{k}), \quad (2.103)$$

$$[M_y \mathbf{g}](\mathbf{k}) = -\mathbf{g}(M_y \mathbf{k}), \quad (2.104)$$

where the additional sign in the last equation comes from Eq. (2.95). The corresponding conditions in direct space are again completely analogous (i.e., they are obtained by simply substituting $\mathbf{k} \mapsto \mathbf{R}$). The following Tables 2.1, 2.2 and 2.3 summarize the transformation properties of the basis functions as well as of the Hamiltonian matrices in dual and in direct space, for all the symmetries considered in this section.

	Possible symmetry of the Hamiltonian	Transformation of atomic orbitals	Transformation of Bloch-like vectors
Hermiticity	$\hat{H} = \hat{H}^\dagger$	—	—
Time-reversal	$[\hat{\Theta}, \hat{H}] = 0$	$\hat{\Theta} \varphi_{s,\mathbf{R}}\rangle = \sum_{s'} \varphi_{s',\mathbf{R}}\rangle [-i\sigma_y]_{s's}$	$\hat{\Theta} \psi_{s,\mathbf{k}}\rangle = \sum_{s'} \psi_{s',-\mathbf{k}}\rangle [-i\sigma_y]_{s's}$
(Spatial inversion)	$[\hat{P}, \hat{H}] = 0$	$\hat{P} \varphi_{s,\mathbf{R}}\rangle = \varphi_{s,-\mathbf{R}}\rangle$	$\hat{P} \psi_{s,\mathbf{k}}\rangle = \psi_{s,-\mathbf{k}}\rangle$
Three-fold rotation	$[\hat{C}_3, \hat{H}] = 0$	$\hat{C}_3 \varphi_{s,\mathbf{R}}\rangle = \varphi_{s,C_3\mathbf{R}}\rangle e^{-i\frac{\pi}{3}s}$	$\hat{C}_3 \psi_{s,\mathbf{k}}\rangle = \psi_{s,C_3\mathbf{k}}\rangle e^{-i\frac{\pi}{3}s}$
Mirror reflection	$[\hat{M}_y, \hat{H}] = 0$	$\hat{M}_y \varphi_{s,\mathbf{R}}\rangle = \sum_{s'} \varphi_{s',M_y\mathbf{R}}\rangle [\sigma_y]_{s's}$	$\hat{M}_y \psi_{s,\mathbf{k}}\rangle = \sum_{s'} \psi_{s',M_y\mathbf{k}}\rangle [\sigma_y]_{s's}$

Table 2.1: Possible symmetries of the fundamental Hamiltonian (1.46) and their action on basis functions.

	Hamiltonian matrix	Pauli matrix representation	
Hermiticity	$H(\mathbf{k}) = H^\dagger(\mathbf{k})$	$f(\mathbf{k}) = f^*(\mathbf{k})$	$\mathbf{g}(\mathbf{k}) = \mathbf{g}^*(\mathbf{k})$
Time-reversal	$H(\mathbf{k}) = [\mathrm{i}\sigma_y]^\dagger H^*(-\mathbf{k}) \mathrm{i}\sigma_y$	$f(\mathbf{k}) = f^*(-\mathbf{k})$	$\mathbf{g}(\mathbf{k}) = -\mathbf{g}^*(-\mathbf{k})$
(Spatial inversion)	$H(\mathbf{k}) = H(-\mathbf{k})$	$f(\mathbf{k}) = f(-\mathbf{k})$	$\mathbf{g}(\mathbf{k}) = \mathbf{g}(-\mathbf{k})$
Three-fold rotation	$H(\mathbf{k}) = \mathrm{e}^{\mathrm{i}\frac{\pi}{3}\sigma_z} H(C_3\mathbf{k}) \mathrm{e}^{-\mathrm{i}\frac{\pi}{3}\sigma_z}$	$f(\mathbf{k}) = f(C_3\mathbf{k})$	$[C_3\mathbf{g}](\mathbf{k}) = \mathbf{g}(C_3\mathbf{k})$
Mirror reflection	$H(\mathbf{k}) = \sigma_y H(M_y\mathbf{k}) \sigma_y$	$f(\mathbf{k}) = f(M_y\mathbf{k})$	$[M_y\mathbf{g}](\mathbf{k}) = -\mathbf{g}(M_y\mathbf{k})$

Table 2.2: Symmetries of the Hamiltonian matrix in dual space (defined by Eq. (1.146)).

	Hamiltonian matrix	Pauli matrix representation	
Hermiticity	$H(\mathbf{R}) = H^\dagger(-\mathbf{R})$	$f(\mathbf{R}) = f^*(-\mathbf{R})$	$\mathbf{g}(\mathbf{R}) = \mathbf{g}^*(-\mathbf{R})$
Time-reversal	$H(\mathbf{R}) = [\mathrm{i}\sigma_y]^\dagger H^*(\mathbf{R}) \mathrm{i}\sigma_y$	$f(\mathbf{R}) = f^*(\mathbf{R})$	$\mathbf{g}(\mathbf{R}) = -\mathbf{g}^*(\mathbf{R})$
(Spatial inversion)	$H(\mathbf{R}) = H(-\mathbf{R})$	$f(\mathbf{R}) = f(-\mathbf{R})$	$\mathbf{g}(\mathbf{R}) = \mathbf{g}(-\mathbf{R})$
Three-fold rotation	$H(\mathbf{R}) = \mathrm{e}^{\mathrm{i}\frac{\pi}{3}\sigma_z} H(C_3\mathbf{R}) \mathrm{e}^{-\mathrm{i}\frac{\pi}{3}\sigma_z}$	$f(\mathbf{R}) = f(C_3\mathbf{R})$	$[C_3\mathbf{g}](\mathbf{R}) = \mathbf{g}(C_3\mathbf{R})$
Mirror reflection	$H(\mathbf{R}) = \sigma_y H(M_y\mathbf{R}) \sigma_y$	$f(\mathbf{R}) = f(M_y\mathbf{R})$	$[M_y\mathbf{g}](\mathbf{R}) = -\mathbf{g}(M_y\mathbf{R})$

Table 2.3: Symmetries of the Hamiltonian matrix in direct space (defined by Eq. (1.149)).

2.2. Derivation of Rashba spin splitting

In this section, we investigate in more detail the implications of the hermiticity, the time-reversal symmetry and the symmetries of the point group C_{3v} for the Hamiltonian matrix. Concretely, we will show that by requiring these symmetries, $H_{ss'}(\mathbf{k})$ necessarily coincides near $\mathbf{k} = \mathbf{0}$ with the Rashba Hamiltonian.

Consider again the Hamiltonian matrix (1.146) in the Pauli matrix representation, i.e.,

$$H(\mathbf{k}) = f(\mathbf{k}) \mathbb{1} + \mathbf{g}(\mathbf{k}) \cdot \boldsymbol{\sigma}. \quad (2.105)$$

First, the *hermiticity* implies that $f(\mathbf{k})$ and $\mathbf{g}(\mathbf{k})$ are real-valued functions. Furthermore, by the *time-reversal symmetry*, f is an even function, while \mathbf{g} is an odd function of the Bloch momentum \mathbf{k} , i.e.,

$$f(\mathbf{k}) = f(-\mathbf{k}), \quad (2.106)$$

$$\mathbf{g}(\mathbf{k}) = -\mathbf{g}(-\mathbf{k}). \quad (2.107)$$

If the Hamiltonian was also invariant under spatial inversion symmetry, hence if

$$f(\mathbf{k}) = f(-\mathbf{k}), \quad (2.108)$$

$$\mathbf{g}(\mathbf{k}) = \mathbf{g}(\mathbf{k}), \quad (2.109)$$

then these equations would together imply that

$$\mathbf{g}(\mathbf{k}) = \mathbf{0} \quad \text{for all } \mathbf{k}. \quad (2.110)$$

Thus, the Hamiltonian matrix $H_{ss'}(\mathbf{k}) = f(\mathbf{k}) \delta_{ss'}$ would be spin independent and therefore lead to a single spin-degenerate energy band. From this, we conclude that a spin splitting is only possible if either time-reversal symmetry or inversion symmetry is not preserved. In this thesis, we are concerned with a class of models which are invariant under time-reversal, but which lack inversion symmetry.¹

We now come back to the case of a hermitean and time-reversal invariant Hamiltonian: by expanding the corresponding functions $f(\mathbf{k})$ and $\mathbf{g}(\mathbf{k})$ up to quadratic order in \mathbf{k} , we obtain (with $i, j \in \{x, y, z\}$)

$$f(\mathbf{k}) = f(\mathbf{0}) + \sum_{i,j} F_{ij} k_i k_j, \quad (2.111)$$

$$g_i(\mathbf{k}) = \sum_j G_{ij} k_j. \quad (2.112)$$

¹The simplest model which does not preserve time-reversal symmetry is obtained for a *constant* function $\mathbf{g}(\mathbf{k}) = -\mu \mathbf{B}$. The resulting Hamiltonian $H(\mathbf{k}) = -\mu \mathbf{B} \cdot \boldsymbol{\sigma}$ can be used to describe the Zeeman effect, i.e., the splitting of electronic energy levels under an applied magnetic field \mathbf{B} .

By the hermiticity, F_{ij} and G_{ij} are real matrices. The linear term of f as well as the constant and the quadratic terms of \mathbf{g} vanish by the time-reversal symmetry. Without loss of generality, we can further set $f(\mathbf{0}) = 0$, which just corresponds to a constant energy shift. In matrix notation, Eqs. (2.111)–(2.112) are equivalent to

$$f(\mathbf{k}) = \mathbf{k}^T F \mathbf{k} = (k_x, k_y, k_z) \begin{pmatrix} F_{xx} & F_{xy} & F_{xz} \\ F_{yx} & F_{yy} & F_{yz} \\ F_{zx} & F_{zy} & F_{zz} \end{pmatrix} \begin{pmatrix} k_x \\ k_y \\ k_z \end{pmatrix}, \quad (2.113)$$

and respectively

$$\mathbf{g}(\mathbf{k}) = G \mathbf{k} = \begin{pmatrix} G_{xx} & G_{xy} & G_{xz} \\ G_{yx} & G_{yy} & G_{yz} \\ G_{zx} & G_{zy} & G_{zz} \end{pmatrix} \begin{pmatrix} k_x \\ k_y \\ k_z \end{pmatrix}. \quad (2.114)$$

Next, let us study the consequences of the point-group symmetries. The *three-fold rotation symmetry* implies that

$$f(\mathbf{k}) = f(C_3 \mathbf{k}) = (C_3 \mathbf{k})^T F (C_3 \mathbf{k}) = \mathbf{k}^T (C_3^T F C_3) \mathbf{k} \quad (2.115)$$

for all $\mathbf{k} \in \mathcal{B}$, and hence

$$F = C_3^T F C_3. \quad (2.116)$$

One can convince oneself that for the components this implies

$$F_{xx} = F_{yy}, \quad (2.117)$$

$$F_{xy} = -F_{yx}, \quad (2.118)$$

$$F_{xz} = F_{zx} = F_{yz} = F_{zy} = 0. \quad (2.119)$$

Thus, the matrix F is of the form

$$F = \begin{pmatrix} F_{xx} & F_{xy} & 0 \\ -F_{xy} & F_{xx} & 0 \\ 0 & 0 & F_{zz} \end{pmatrix}. \quad (2.120)$$

Similarly, from the condition

$$\mathbf{g}(\mathbf{k}) = (C_3^T \mathbf{g})(C_3 \mathbf{k}) = C_3^T G (C_3 \mathbf{k}) = (C_3^T G C_3) \mathbf{k}, \quad (2.121)$$

we obtain

$$G = C_3^T G C_3, \quad (2.122)$$

and thus G is of the same form as F , i.e.,

$$G = \begin{pmatrix} G_{xx} & G_{xy} & 0 \\ -G_{xy} & G_{xx} & 0 \\ 0 & 0 & G_{zz} \end{pmatrix}. \quad (2.123)$$

The consequences of the *mirror reflection symmetry* can be deduced analogously: from the condition $f(\mathbf{k}) = f(M_y \mathbf{k})$, we obtain

$$F = M_y^T F M_y, \quad (2.124)$$

which in turn implies that

$$F_{xy} = F_{yx} = F_{xz} = F_{zx} = 0. \quad (2.125)$$

On the other hand, the condition $\mathbf{g}(\mathbf{k}) = -(M_y \mathbf{g})(M_y \mathbf{k})$ yields

$$G = -M_y^T G M_y, \quad (2.126)$$

and hence, taking into account the additional minus sign,

$$G_{xx} = G_{yy} = G_{zz} = G_{xz} = G_{zx} = 0. \quad (2.127)$$

By combining the three-fold rotation and the mirror reflection symmetries, we conclude that the matrices F and G must be of the following form:

$$F = \begin{pmatrix} F_{xx} & 0 & 0 \\ 0 & F_{xx} & 0 \\ 0 & 0 & F_{zz} \end{pmatrix}, \quad G = \begin{pmatrix} 0 & G_{xy} & 0 \\ -G_{xy} & 0 & 0 \\ 0 & 0 & 0 \end{pmatrix}. \quad (2.128)$$

Correspondingly, the Hamiltonian matrix is given up to quadratic order in \mathbf{k} by

$$H(\mathbf{k}) = \mathbf{k}^T F \mathbf{k} + (G \mathbf{k}) \cdot \boldsymbol{\sigma} \quad (2.129)$$

$$= F_{xx}(k_x^2 + k_y^2) + F_{zz}k_z^2 + G_{xy}(k_y\sigma_x - k_x\sigma_y). \quad (2.130)$$

Thus, we have shown that this general form of the Hamiltonian matrix near $\mathbf{k} = \mathbf{0}$ can be deduced directly from the time-reversal symmetry and the symmetries of the point group C_{3v} of the BiTeI crystal.

By further neglecting the k_z dependence, i.e., by setting $f_{zz} = 0$, the above Hamiltonian matrix further reduces to

$$H(\mathbf{k}) = F_{xx}(k_x^2 + k_y^2) - G_{xy}(k_x\sigma_y - k_y\sigma_x). \quad (2.131)$$

This expression coincides precisely with the (two-dimensional) Rashba Hamiltonian, which will be described in more detail in Sect. 3.2. The parameters F_{xx} and G_{xy} are related to the Rashba energy E_R and the Rashba wavevector k_R (see Eq. (3.16)) by

$$F_{xx} = \frac{E_R}{k_R^2}, \quad G_{xy} = -\frac{2E_R}{k_R}, \quad (2.132)$$

or conversely by

$$E_R = \frac{G_{xy}^2}{4F_{xx}}, \quad k_R = -\frac{G_{xy}}{2F_{xx}}. \quad (2.133)$$

In Sct. 3.2, we will see that the Rashba Hamiltonian can be used to approximately describe the dispersion of the lowest conduction bands of BiTeI.

2.3. Minimal tight-binding model

In this section, we construct a *tight-binding model* which approximately coincides near $\mathbf{k} = \mathbf{0}$ with the Rashba Hamiltonian. In general, a tight-binding model is characterized by the condition that the Hamiltonian matrix in direct space, $H(\mathbf{R} - \mathbf{R}')$, vanishes if the distance vector $(\mathbf{R} - \mathbf{R}')$ exceeds a few lattice sites. Here, we even assume that it vanishes unless \mathbf{R} and \mathbf{R}' are *nearest-neighbor* vectors. By further restricting ourselves to a single plane of the hexagonal Bravais lattice (i.e., to the sites $\mathbf{R} = (R_x, R_y, R_z)^T$ with $R_z = 0$), each lattice site has only six nearest neighbors (see Fig. 1.1a), and the corresponding distance vectors are given in terms of the primitive vectors \mathbf{a}_1 and \mathbf{a}_2 by

$$\mathbf{R}_1 = \mathbf{a}_2, \quad (2.134)$$

$$\mathbf{R}_2 = \mathbf{a}_1 + \mathbf{a}_2, \quad (2.135)$$

$$\mathbf{R}_3 = \mathbf{a}_1, \quad (2.136)$$

$$\mathbf{R}_4 = -\mathbf{a}_2, \quad (2.137)$$

$$\mathbf{R}_5 = -\mathbf{a}_1 - \mathbf{a}_2, \quad (2.138)$$

$$\mathbf{R}_6 = -\mathbf{a}_1. \quad (2.139)$$

Thus, we consider a *model* Hamiltonian matrix in direct space, which is of the form

$$H_{ss'}(\mathbf{R}) = \sum_{i=1}^6 H_{ss'}(\mathbf{R}_i) \delta_{\mathbf{R}, \mathbf{R}_i}. \quad (2.140)$$

By Fourier transformation, we obtain from this the Hamiltonian matrix in dual space as

$$H_{ss'}(\mathbf{k}) = \sum_{i=1}^6 H_{ss'}(\mathbf{R}_i) e^{-i\mathbf{k} \cdot \mathbf{R}_i}. \quad (2.141)$$

In the following, we will choose the parameters $H_{ss'}(\mathbf{R}_i)$ in such a way that the resulting Hamiltonian matrix is invariant under time-reversal symmetry and the symmetries of the point group C_{3v} . By the argument of the preceding section, this implies that the Hamiltonian matrix in dual space coincides near $\mathbf{k} = \mathbf{0}$ with the Rashba Hamiltonian.

We start again from the Pauli matrix representation of the Hamiltonian matrix as given by Eq. (1.157). The above expansion (2.140) of the Hamiltonian matrix implies an analogous expansion of the functions $f(\mathbf{R})$ and $g(\mathbf{R})$. Hence, it remains to specify the

parameters $f(\mathbf{R}_i)$ and $g(\mathbf{R}_i)$ ($i = 1, \dots, 6$) in accordance with the symmetry constraints derived in the previous section (see Table 2.3). First, the hermiticity, the time-reversal symmetry and the point-group symmetries imply that $f(\mathbf{R})$ is real-valued and satisfies

$$f(-\mathbf{R}) = f(\mathbf{R}), \quad (2.142)$$

$$f(C_3\mathbf{R}) = f(\mathbf{R}), \quad (2.143)$$

$$f(M_y\mathbf{R}) = f(\mathbf{R}). \quad (2.144)$$

Therefore, if $f(\mathbf{R})$ is restricted to nearest-neighbor vectors within a plane of the hexagonal lattice, it is completely determined by a single real parameter

$$f(\mathbf{R}_1) \equiv -t \in \mathbb{R}. \quad (2.145)$$

By Eqs. (2.142)–(2.144), we then have

$$f(\mathbf{R}_i) = -t \quad \forall i \in \{1, \dots, 6\}. \quad (2.146)$$

Thus, f is given in direct space by

$$f(\mathbf{R}) = \sum_{i=1}^6 f(\mathbf{R}_i) \delta_{\mathbf{R}, \mathbf{R}_i} = -t \sum_{i=1}^6 \delta_{\mathbf{R}, \mathbf{R}_i}, \quad (2.147)$$

and in dual space by

$$f(\mathbf{k}) = -t \sum_{i=1}^6 e^{-i\mathbf{k} \cdot \mathbf{R}_i} = -2t \left\{ \cos(\mathbf{k} \cdot \mathbf{R}_1) + \cos(\mathbf{k} \cdot \mathbf{R}_2) + \cos(\mathbf{k} \cdot \mathbf{R}_3) \right\}. \quad (2.148)$$

In terms of the dimensionless quantity

$$\boldsymbol{\kappa} = a_0 \mathbf{k}, \quad (2.149)$$

where a_0 denotes the lattice constant, we obtain the explicit expression

$$f(\mathbf{k}) = -2t \left\{ \cos(\kappa_y) + \cos\left(\frac{\sqrt{3}}{2}\kappa_x + \frac{1}{2}\kappa_y\right) + \cos\left(\frac{\sqrt{3}}{2}\kappa_x - \frac{1}{2}\kappa_y\right) \right\} \quad (2.150)$$

$$= -2t \left\{ \cos(\kappa_y) + 2 \cos\left(\frac{\sqrt{3}}{2}\kappa_x\right) \cos\left(\frac{1}{2}\kappa_y\right) \right\}. \quad (2.151)$$

Similarly, the symmetries imply that $g(\mathbf{R})$ is purely imaginary, and

$$g(-\mathbf{R}) = -g(\mathbf{R}), \quad (2.152)$$

$$g(C_3\mathbf{R}) = (C_3g)(\mathbf{R}), \quad (2.153)$$

$$g(M_y\mathbf{R}) = -(M_yg)(\mathbf{R}). \quad (2.154)$$

In particular, using that $M_y\mathbf{R}_1 = -\mathbf{R}_1$, we find that

$$(M_yg)(\mathbf{R}_1) = -g(M_y\mathbf{R}_1) = -g(-\mathbf{R}_1) = g(\mathbf{R}_1), \quad (2.155)$$

which in turn implies that

$$g_y(\mathbf{R}_1) = 0. \quad (2.156)$$

As $\mathbf{g}(\mathbf{R})$ is restricted to nearest-neighbor vectors, it is therefore completely determined by only two real parameters $\alpha, \gamma \in \mathbb{R}$ defined as

$$g_x(\mathbf{R}_1) \equiv -i\alpha, \quad g_z(\mathbf{R}_1) \equiv i\gamma. \quad (2.157)$$

Explicitly, the three components of \mathbf{g} are then given by

$$\begin{pmatrix} g_x(\mathbf{R}) \\ g_y(\mathbf{R}) \end{pmatrix} = -i\alpha \left\{ \begin{pmatrix} 1 \\ 0 \end{pmatrix} \delta_{\mathbf{R}, \mathbf{R}_1}^- + \begin{pmatrix} -1/2 \\ \sqrt{3}/2 \end{pmatrix} \delta_{\mathbf{R}, C_3 \mathbf{R}_1}^- + \begin{pmatrix} -1/2 \\ -\sqrt{3}/2 \end{pmatrix} \delta_{\mathbf{R}, C_3^{-1} \mathbf{R}_1}^- \right\}, \quad (2.158)$$

as well as by

$$g_z(\mathbf{R}) = i\gamma \left\{ \delta_{\mathbf{R}, \mathbf{R}_1}^- + \delta_{\mathbf{R}, C_3 \mathbf{R}_1}^- + \delta_{\mathbf{R}, C_3^{-1} \mathbf{R}_1}^- \right\}, \quad (2.159)$$

where we have abbreviated

$$\delta_{\mathbf{R}, \mathbf{R}'}^- = \delta_{\mathbf{R}, \mathbf{R}'} - \delta_{\mathbf{R}, -\mathbf{R}'}. \quad (2.160)$$

By Fourier transformation (see Eq. (2.141)), this is equivalent to

$$\begin{pmatrix} g_x(\mathbf{k}) \\ g_y(\mathbf{k}) \end{pmatrix} = -2\alpha \left\{ \begin{pmatrix} 1 \\ 0 \end{pmatrix} \sin(\mathbf{k} \cdot \mathbf{R}_1) + \begin{pmatrix} -1/2 \\ \sqrt{3}/2 \end{pmatrix} \sin(\mathbf{k} \cdot \mathbf{R}_5) + \begin{pmatrix} -1/2 \\ -\sqrt{3}/2 \end{pmatrix} \sin(\mathbf{k} \cdot \mathbf{R}_3) \right\} \quad (2.161)$$

and respectively

$$g_z(\mathbf{R}) = 2\gamma \left\{ \sin(\mathbf{k} \cdot \mathbf{R}_1) + \sin(\mathbf{k} \cdot \mathbf{R}_5) + \sin(\mathbf{k} \cdot \mathbf{R}_3) \right\}. \quad (2.162)$$

With $\boldsymbol{\kappa}$ defined by Eq. (2.149), we further obtain the explicit expressions

$$g_x(\mathbf{k}) = -2\alpha \left\{ \sin(\kappa_y) - \frac{1}{2} \sin\left(-\frac{\sqrt{3}}{2} \kappa_x - \frac{1}{2} \kappa_y\right) - \frac{1}{2} \sin\left(\frac{\sqrt{3}}{2} \kappa_x - \frac{1}{2} \kappa_y\right) \right\} \quad (2.163)$$

$$= -2\alpha \left\{ \sin(\kappa_y) + \cos\left(\frac{\sqrt{3}}{2} \kappa_x\right) \sin\left(\frac{1}{2} \kappa_y\right) \right\}, \quad (2.164)$$

as well as

$$g_y(\mathbf{k}) = -2\alpha \left\{ \frac{\sqrt{3}}{2} \sin\left(-\frac{\sqrt{3}}{2} \kappa_x - \frac{1}{2} \kappa_y\right) - \frac{\sqrt{3}}{2} \sin\left(\frac{\sqrt{3}}{2} \kappa_x - \frac{1}{2} \kappa_y\right) \right\} \quad (2.165)$$

$$= 2\alpha \sqrt{3} \sin\left(\frac{\sqrt{3}}{2} \kappa_x\right) \cos\left(\frac{1}{2} \kappa_y\right), \quad (2.166)$$

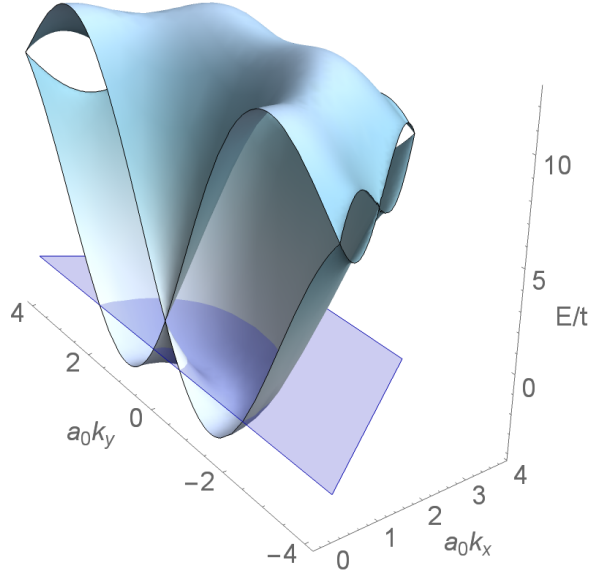


Figure 2.1: Energy bands of the minimal tight-binding model for $\alpha/t = 2$.

and finally also

$$g_z(\mathbf{k}) = 2\gamma \left\{ \sin(\kappa_y) + \sin\left(-\frac{\sqrt{3}}{2}\kappa_x - \frac{1}{2}\kappa_y\right) + \sin\left(\frac{\sqrt{3}}{2}\kappa_x - \frac{1}{2}\kappa_y\right) \right\} \quad (2.167)$$

$$= 2\gamma \left\{ \sin(\kappa_y) - 2 \cos\left(\frac{\sqrt{3}}{2}\kappa_x\right) \sin\left(\frac{1}{2}\kappa_y\right) \right\}. \quad (2.168)$$

In summary, the minimal tight-binding model is defined in dual space by Eq. (2.105), where $f(\mathbf{k})$ and $\mathbf{g}(\mathbf{k})$ are given in terms of the real hopping parameters t , α and γ by Eqs. (2.151) and (2.163)–(2.168), respectively.

The two energy bands of the model are given by (see Eq. (1.162))

$$E_{\pm}(\mathbf{k}) = f(\mathbf{k}) \mp |\mathbf{g}(\mathbf{k})|, \quad (2.169)$$

and they are shown in Fig. 2.1 for the parameter values

$$\alpha/t = 2, \quad \gamma/t = 0. \quad (2.170)$$

Furthermore, Fig. 2.2 shows the *density of states* of the tight-binding model, which is defined as

$$D(E) = \frac{1}{|\mathcal{B}|} \int_{\mathcal{B}} d^2\mathbf{k} [\delta(E - E_-(\mathbf{k})) + \delta(E - E_+(\mathbf{k}))]. \quad (2.171)$$

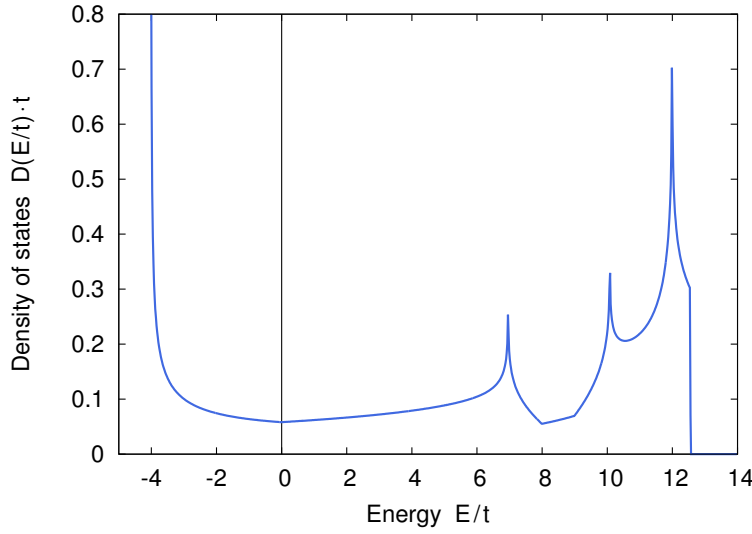


Figure 2.2: Density of states of the minimal tight-binding model for $\alpha/t = 2$. The vertical line marks the position of the band crossing at the center of the Brillouin zone.

From this, we read off the *bandwidth* (i.e., the difference between the maximum and the minimum energy) of the model as

$$(\Delta E)_{\max}/t \approx 16.5. \quad (2.172)$$

Finally, for small wavevectors satisfying

$$|\boldsymbol{\kappa}| \equiv a_0 |\mathbf{k}| \ll 1, \quad (2.173)$$

we can expand the functions $f(\mathbf{k})$ and $\mathbf{g}(\mathbf{k})$ around $\mathbf{k} = \mathbf{0}$. Approximating

$$\sin x \approx x, \quad \cos x \approx 1 - \frac{x^2}{2} \quad (2.174)$$

in Eqs. (2.151) and (2.163)–(2.168), we obtain to second order in $\boldsymbol{\kappa}$ the expansions

$$f(\boldsymbol{\kappa}) = -6t + \frac{3t}{2}(\kappa_x^2 + \kappa_y^2), \quad (2.175)$$

$$g_x(\boldsymbol{\kappa}) = -3\alpha\kappa_y, \quad (2.176)$$

$$g_y(\boldsymbol{\kappa}) = 3\alpha\kappa_x, \quad (2.177)$$

$$g_z(\boldsymbol{\kappa}) = 0. \quad (2.178)$$

Thus, the Hamiltonian matrix in dual space reads to second order in $\boldsymbol{\kappa}$ as

$$H(\mathbf{k}) = \frac{3t}{2}a_0^2(k_x^2 + k_y^2) + 3\alpha a_0(k_x\sigma_y - k_y\sigma_x), \quad (2.179)$$

where we have neglected the constant energy shift $(-6t)$ in Eq. (2.175). As expected,

this expression coincides again precisely with the Rashba Hamiltonian (see Sct. 3.2). The parameters t and α are related to E_R and k_R (see Eq. (3.16)) by

$$t = \frac{2E_R}{3(a_0 k_R)^2}, \quad \alpha = \frac{2E_R}{3a_0 k_R}, \quad (2.180)$$

or conversely by

$$E_R = \frac{3\alpha^2}{2t}, \quad k_R = \frac{\alpha}{a_0 t}. \quad (2.181)$$

The Rashba-type dispersion of the bands near $\mathbf{k} = \mathbf{0}$ can be clearly seen in Fig. 2.1.

3. Rashba semiconductor BiTeI

3.1. Crystal and band structure

The crystal structure of BiTeI can be characterized as follows [BAN11; Ish+11] (see [IUCr05; Wik16] for the general crystallographic classification):

Lattice system: hexagonal,

Lattice type: primitive,

Bravais lattice: hexagonal (hP),

Point group: C_{3v} ,

Space group: $P3m1$ (No. 156),

Crystal system: trigonal,

Crystal family: hexagonal.

The crystal structure of BiTeI is shown schematically in Fig. 3.1. It has a three-fold principal axis C_3 (which defines the z -axis) and three vertical mirror planes σ_v . Correspondingly, the point group of BiTeI is C_{3v} (Schoenflies notation). Each unit cell of BiTeI has a basis consisting of three atoms, bismuth (Bi), tellurium (Te) and iodine (I). These different atom species form layers stacking along the z -axis. Due to the particular arrangement of the Te and I atoms, the crystal structure lacks inversion symmetry.

The strong spin-orbit coupling of the Bi atoms together with the inversion-asymmetric crystal structure of BiTeI leads to a spin splitting of the bulk energy bands of this material [BAN11; Ish+11; Lee+11]. The band structure of BiTeI is shown in Fig. 3.2 in the plane defined by $k_z = \pi/c_0$ (where c_0 denotes the lattice constant in the z -direction; see Fig. 1.2). This band structure is particularly simple, as only two bands are intersected by the Fermi energy. (In the undoped samples considered in Ref. [Dem+12], the Fermi energy lies slightly above the band crossing at the A point.) Near the A point of the Brillouin zone, the two lowest conduction bands can be described by the two-dimensional Rashba Hamiltonian, which will be explained in more detail in the next section. Remarkably, the energy difference between these two bands reaches $\simeq 400$ meV at the minimum of the lower band. In addition, there is a rather mild dispersion of the bands along the Γ –A direction, which is due to a weak interaction between the consec-

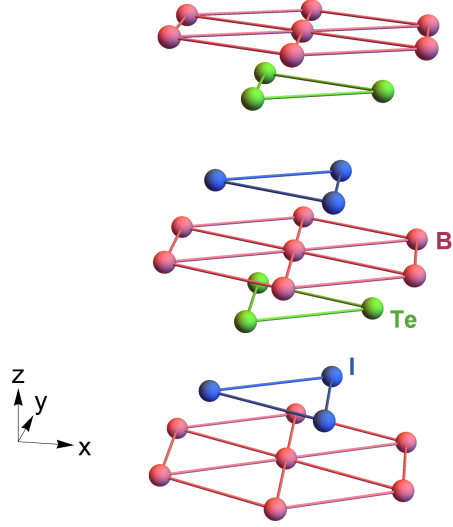


Figure 3.1: Crystal structure of BiTeI.

utive Te–Bi–I layers along the z -axis [Lee+11]. The 12 valence and 6 conduction bands below and above the Fermi energy were derived from the 18-band tight-binding model of Ref. [Ish+11]. This model takes into account Bi-6 p , Te-5 p and I-5 p orbitals and was constructed using maximally localized Wannier functions [Kun+10; Mos+08; SMV01].

3.2. Two-dimensional Rashba model

Near the A point of the Brillouin zone and within the $k_z = \pi/c_0$ plane (see Fig. 1.2), the dispersion of the two lowest conduction bands of BiTeI can be described by the two-dimensional Rashba model [BR60; Ras60]. This is defined by the Hamiltonian

$$\hat{H}_R = \frac{\hat{p}^2}{2m^*} + \frac{\alpha}{\hbar} \mathbf{e}_z \cdot (\hat{\mathbf{p}} \times \boldsymbol{\sigma}) \equiv \frac{\hat{p}^2}{2m^*} + \frac{\alpha}{\hbar} (\hat{p}_x \sigma_y - \hat{p}_y \sigma_x), \quad (3.1)$$

where m^* denotes the effective electron mass and α the Rashba parameter [Bor+13]. The above Hamiltonian acts on wave functions in $L^2(\mathbb{R}^2, \mathbb{C}^2)$, and it can be diagonalized in terms of the momentum eigenvectors (see Sct. 1.1), which are defined by their wave functions as

$$\langle \mathbf{x}, s' | \mathbf{k}, s \rangle = \frac{1}{(2\pi)^{3/2}} e^{i\mathbf{k} \cdot \mathbf{x}} \delta_{ss'}. \quad (3.2)$$

Note that in this section, $\mathbf{k} \in \mathbb{R}^2$ denotes a two-dimensional wavevector. For each \mathbf{k} , the Hamiltonian matrix $(H_R)_{ss'}(\mathbf{k})$ is defined by

$$\hat{H}_R |\mathbf{k}, s'\rangle = \sum_s |\mathbf{k}, s\rangle (H_R)_{ss'}(\mathbf{k}), \quad (3.3)$$

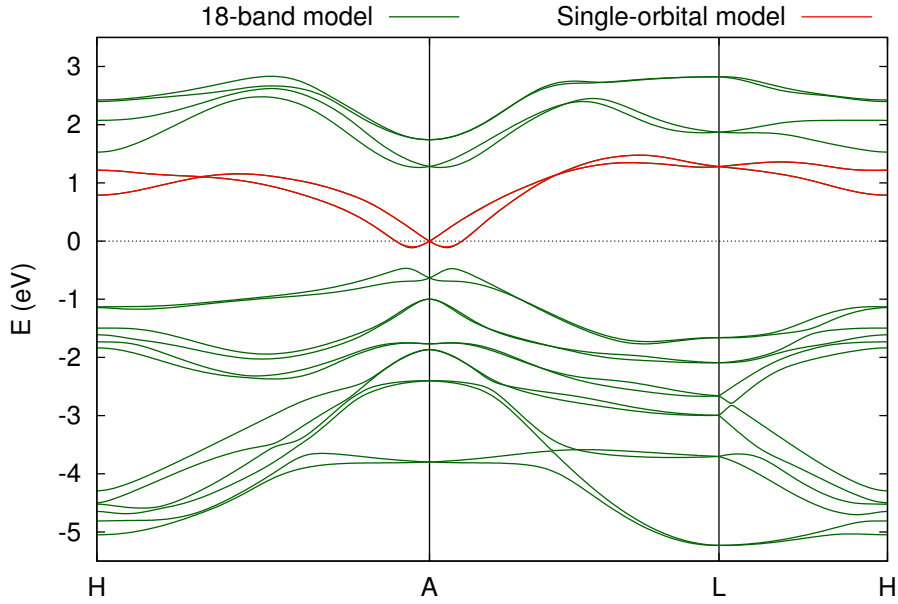


Figure 3.2: Dispersion of the bulk energy bands of BiTeI along the special directions H–A–L–H (see Fig. 1.2). The energy is measured relative to the conduction band crossing at the A point. The 12 valence and 6 conduction bands (green color) have been derived from the 18-band model of Ref. [Ish+11]. The red bands, which accurately reproduce the dispersion of the two lowest conduction bands, have been obtained from the effective single-orbital model of Sct. 3.3 (including up to 10th-nearest-neighbor hopping).

or equivalently by

$$\langle \mathbf{k}, s | \hat{H}_R | \mathbf{k}', s' \rangle = \delta^2(\mathbf{k} - \mathbf{k}') (H_R)_{ss'}(\mathbf{k}). \quad (3.4)$$

From Eq. (3.1), we obtain the explicit form of this Hamiltonian matrix as

$$H_R(\mathbf{k}) = \frac{\hbar^2 |\mathbf{k}|^2}{2m^*} + \alpha (k_x \sigma_y - k_y \sigma_x). \quad (3.5)$$

Furthermore, this hermitean (2×2) matrix can be represented for each \mathbf{k} in terms of the Pauli matrices as in Eq. (1.157), where the coefficient functions are given by

$$f(\mathbf{k}) = \frac{\hbar^2 |\mathbf{k}|^2}{2m^*}, \quad g_x(\mathbf{k}) = -\alpha k_y, \quad g_y(\mathbf{k}) = \alpha k_x, \quad g_z(\mathbf{k}) = 0. \quad (3.6)$$

In particular, the Hamiltonian matrix can be diagonalized for each \mathbf{k} exactly as described in Sct. 1.5.2. We thus obtain the eigenvectors of the Rashba Hamiltonian (3.1) by a unitary transformation,

$$|\mathbf{k}, n\rangle = \sum_s |\mathbf{k}, s\rangle U_{sn}(\mathbf{k}), \quad (3.7)$$

where the matrix $U(\mathbf{k}) \equiv U_{sn}(\mathbf{k})$ is given by Eq. (1.163). For the concrete coefficient functions specified in Eq. (3.6), this matrix simplifies to

$$U(\mathbf{k}) = \frac{1}{\sqrt{2}} \begin{pmatrix} 1 & 1 \\ -ie^{i\varphi(\mathbf{k})} & ie^{i\varphi(\mathbf{k})} \end{pmatrix}, \quad (3.8)$$

where $\varphi(\mathbf{k}) \in [0, 2\pi)$ denotes the polar angle of the two-dimensional vector $(k_x, k_y)^T$,

$$e^{i\varphi(\mathbf{k})} = \frac{k_x + ik_y}{\sqrt{k_x^2 + k_y^2}} = \frac{k_x + ik_y}{\sqrt{(|\mathbf{k}| - k_z)(|\mathbf{k}| + k_z)}}. \quad (3.9)$$

In particular, by Eq. (3.6), $\varphi(\mathbf{k})$ it is related to $\varphi(\mathbf{g})$ (as defined in Eq. (1.164)) by

$$\varphi(\mathbf{g}) = \varphi(\mathbf{k}) + \frac{\pi}{2}. \quad (3.10)$$

The real-space wave functions of the so-defined eigenvectors are given by

$$\langle \mathbf{x}, s | \mathbf{k}, n \rangle = \frac{1}{(2\pi)^{3/2}} e^{i\mathbf{k} \cdot \mathbf{x}} U_{sn}(\mathbf{k}). \quad (3.11)$$

They diagonalize the Hamiltonian (3.1) in the sense that

$$\hat{H} |\mathbf{k}, n\rangle = E_n(\mathbf{k}) |\mathbf{k}, n\rangle, \quad (3.12)$$

or equivalently,

$$\langle \mathbf{k}, n | \hat{H} | \mathbf{k}', n' \rangle = \delta^2(\mathbf{k} - \mathbf{k}') E_n(\mathbf{k}), \quad (3.13)$$

where the eigenvalues are given by

$$E_{\mp}(\mathbf{k}) = \frac{\hbar^2 |\mathbf{k}|^2}{2m^*} \mp \alpha |\mathbf{k}|. \quad (3.14)$$

Hence, $n = -$ labels the lower, and $n = +$ the upper branch of the Rashba dispersion. By further introducing the *Rashba wavevector* k_R and the *Rashba energy* E_R as

$$k_R = \frac{m^* \alpha}{\hbar^2}, \quad E_R = \frac{\hbar^2 k_R^2}{2m^*}, \quad (3.15)$$

the eigenenergies (3.14) can be written equivalently as

$$E_{\mp}(\mathbf{k}) = E_R \left[\left(\frac{|\mathbf{k}|}{k_0} \right)^2 \mp 2 \left(\frac{|\mathbf{k}|}{k_0} \right) \right]. \quad (3.16)$$

As explained in Ref. [Sch+16a], the characteristics of the Rashba model dispersion are: (i) the band crossing at $\mathbf{k} = \mathbf{0}$, (ii) the approximately linear dispersion for small wave vectors, and (iii) the band minimum which is attained on the circle $|\mathbf{k}| = k_R$. The Rashba energy E_R , which equals the energy difference between the band crossing and the minimum of the lower band, is often used to quantify the Rashba spin splitting of the energy bands in real materials [Ish+11].

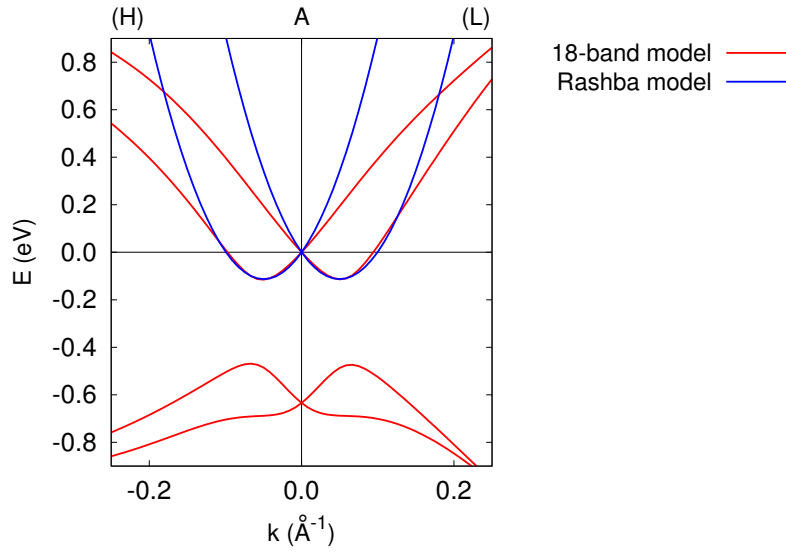


Figure 3.3: Band structure of BiTeI in the 18-band model, and Rashba model dispersion approximating the lowest conduction bands near the A point. The dispersion is shown along the special directions A–H and A–L (see Fig. 1.2).

As mentioned above, the Rashba model can be used to approximately describe the dispersion of the lowest conduction bands of BiTeI near the A point. For this purpose, we choose the parameters from Ref. [BAN11]:

$$E_R = 113 \text{ meV}, \quad k_R = 0.05 \text{ Å}^{-1}, \quad (3.17)$$

or correspondingly,

$$m^* = 0.084 m_e, \quad \alpha = 4.52 \text{ eV Å}, \quad (3.18)$$

where m_e denotes the electron mass. The resulting dispersion of the Rashba model is shown in Fig. 3.3 in comparison with the band structure of BiTeI as calculated from the 18-band model. Note, however, that the Rashba model neglects the dispersion in the k_z direction, which is also present in BiTeI (see Sct. 3.1).

3.3. Effective single-orbital model

The 18-band model of Ref. [Ish+11] is an effective tight-binding model, which is given in the form of an (18×18) Hamiltonian matrix $H_{ij}(\mathbf{R})$. Here, $\mathbf{R} \in \Gamma$ labels the Bravais lattice vector, while $i = (A, \mu, s)$ and $j = (B, \nu, s')$ are multi-indices labeling atom species $A, B \in \{\text{Bi}, \text{Te}, \text{I}\}$, orbitals $\mu, \nu \in \{p_x, p_y, p_z\}$ and spins $s, s' \in \{\uparrow, \downarrow\}$. Note, however, that these indices do not actually refer to atomic orbitals, but to the so-called maximally localized Wannier functions [Kun+10; Mos+08; SMV01]. However, as the

atomic orbitals serve as an “initial guess” for constructing these maximally localized Wannier functions [SMV01], the latter are still labeled by “orbital” indices. The 18-band model contains only up to 6th-nearest-neighbor hoppings, which means that the matrix $H_{ij}(\mathbf{R})$ can be non-zero only for those vectors \mathbf{R} of the hexagonal lattice which can be reached from the origin by six times “hopping” from one site to one of its nearest neighbors. By Fourier transforming the Hamiltonian matrix,

$$H_{ij}(\mathbf{k}) = \sum_{\mathbf{R}} H_{ij}(\mathbf{R}) e^{-i\mathbf{k}\mathbf{R}}, \quad (3.19)$$

and subsequently diagonalizing the resulting matrix in dual space,

$$\sum_j H_{ij}(\mathbf{k}) \Psi_j^n(\mathbf{k}) = E^n(\mathbf{k}) \Psi_i^n(\mathbf{k}), \quad (3.20)$$

we obtain the energy bands $E^n(\mathbf{k})$ and the corresponding eigenvectors $\Psi^n(\mathbf{k})$ of the 18-band model (see Fig. 3.2). These are labeled by a band index $n \in \{1, \dots, 18\}$ in such a way that for any \mathbf{k} ,

$$E^n(\mathbf{k}) \leq E^m(\mathbf{k}), \quad \text{if } n < m. \quad (3.21)$$

As mentioned above, only two bands (with the indices $n = 13$ and $n = 14$) are intersected by the Fermi energy. These are the lowest conduction bands, which are expected to be dominant in determining the low-temperature properties of the material. Therefore, a natural question is whether one can construct a simplified tight-binding model which reproduces only these two conduction bands. In particular, this would be useful for numerical simulations, where the CPU time often scales polynomially with the number of bands. For answering this question, it would at first sight be tempting to simply select the two bands $E^{13}(\mathbf{k})$ and $E^{14}(\mathbf{k})$, and to define the tight-binding model in direct space by taking their inverse Fourier transforms. This procedure, however, does not lead to a Hamiltonian matrix which decays sufficiently fast on the direct lattice, because the energy bands are not analytic functions of the Bloch momentum (see Ref. [Kat04, Sct. VI.7] for general relations between the analyticity of a function and the decay of its Fourier transform). In particular, due to the band crossing at the A point, the two lowest conduction bands are not even differentiable at this point. In the following, we will therefore describe an alternative route to this problem, which allows us to construct a two-band tight-binding model that in fact reproduces accurately the two lowest conduction bands of BiTeI.

For simplicity, we neglect again the k_z dispersion of the energy bands (however, this approximation is not essential for our general procedure). Thus, we assume that \mathbf{k} is restricted to the hexagonal face of the Brillouin zone which contains the A point (see Fig. 1.2a), and \mathbf{R} labels the sites of the two-dimensional lattice as shown in Fig. 1.1a. Furthermore, we denote the two lowest conduction bands (with $n = 13$ and $n = 14$) by $E^-(\mathbf{k})$ and $E^+(\mathbf{k})$, respectively. For the following discussion, it will be important to note that the (18×18) Hamiltonian matrix $H(\mathbf{k})$ as given by Eq. (3.19) is in fact analytic in the wavevector \mathbf{k} (although the energy bands $E^-(\mathbf{k})$ and $E^+(\mathbf{k})$ are not analytic).

Moreover, the spin expectation values in the corresponding eigenstates $\Psi^\pm(\mathbf{k})$ can be calculated as

$$\langle \mathbf{S} \rangle^\pm(\mathbf{k}) = \frac{\hbar}{2} \sum_{A, \mu} \sum_{s, s'} [\Psi_{A\mu s}^\pm(\mathbf{k})]^* \boldsymbol{\sigma}_{ss'} \Psi_{A\mu s'}^\pm(\mathbf{k}). \quad (3.22)$$

However, in contrast to the single-orbital model of Sect. 1.5.2—where the spin expectation values are given by Eq. (1.166)—the vectors $\langle \mathbf{S} \rangle^\pm(\mathbf{k})$ as calculated from the 18-band model by means of Eq. (3.22) are not normalized. In fact, for general \mathbf{k} , we even have

$$|\langle \mathbf{S} \rangle^+(\mathbf{k})| \neq |\langle \mathbf{S} \rangle^-(\mathbf{k})|. \quad (3.23)$$

Nevertheless, the following relation holds in the 18-band model for any \mathbf{k} :

$$\frac{\langle \mathbf{S} \rangle^+(\mathbf{k})}{|\langle \mathbf{S} \rangle^+(\mathbf{k})|} = - \frac{\langle \mathbf{S} \rangle^-(\mathbf{k})}{|\langle \mathbf{S} \rangle^-(\mathbf{k})|}, \quad (3.24)$$

hence the upper and the lower conduction bands have opposite spin orientations.

We can now construct an *effective single-orbital model* $H_{ss'}(\mathbf{k})$, which reproduces the two lowest conduction bands of BiTeI, in three steps as follows:

- (i) First, we identify for each \mathbf{k} the eigenvalues $e^\pm(\mathbf{k})$ and the spin expectation values $\langle \mathbf{s} \rangle^\pm(\mathbf{k})$ of the single-orbital model with the corresponding (normalized) quantities of the 18-band model. This means, we set

$$e^\pm(\mathbf{k}) := E^\pm(\mathbf{k}), \quad (3.25)$$

$$\langle \mathbf{s} \rangle^\pm(\mathbf{k}) := \frac{\hbar}{2} \frac{\langle \mathbf{S} \rangle^\pm(\mathbf{k})}{|\langle \mathbf{S} \rangle^\pm(\mathbf{k})|}. \quad (3.26)$$

By Eqs. (1.162) and (1.166), these conditions are equivalent to

$$f(\mathbf{k}) \pm |g(\mathbf{k})| = E^\pm(\mathbf{k}), \quad (3.27)$$

$$\pm \frac{g(\mathbf{k})}{|g(\mathbf{k})|} = \frac{\langle \mathbf{S} \rangle^\pm(\mathbf{k})}{|\langle \mathbf{S} \rangle^\pm(\mathbf{k})|}, \quad (3.28)$$

where $f(\mathbf{k})$ and $g(\mathbf{k})$ are the coefficient functions in the Pauli matrix representation (see Eq. (1.157)). The above equalities determine these coefficient functions uniquely: by Eq. (3.27), we have

$$f(\mathbf{k}) = \frac{1}{2} (E^+(\mathbf{k}) + E^-(\mathbf{k})), \quad (3.29)$$

$$|g(\mathbf{k})| = \frac{1}{2} (E^+(\mathbf{k}) - E^-(\mathbf{k})), \quad (3.30)$$

and from Eq. (3.28), we obtain

$$g(\mathbf{k}) = |g(\mathbf{k})| \frac{\langle \mathbf{S} \rangle^+(\mathbf{k})}{|\langle \mathbf{S} \rangle^+(\mathbf{k})|} = \frac{1}{2} (E^+(\mathbf{k}) - E^-(\mathbf{k})) \frac{\langle \mathbf{S} \rangle^+(\mathbf{k})}{|\langle \mathbf{S} \rangle^+(\mathbf{k})|}. \quad (3.31)$$

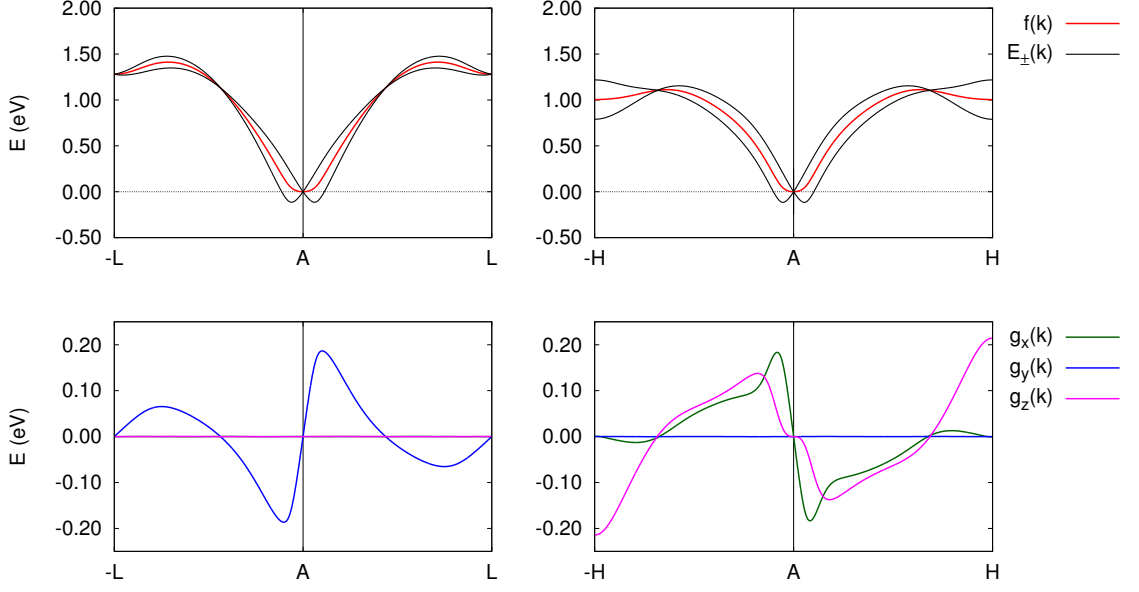


Figure 3.4: Lowest conduction bands $E_{\pm}(\mathbf{k})$ of BiTeI along the special directions $\bar{\text{L}}\text{--A--L}$ (k_x direction) and $\bar{\text{H}}\text{--A--H}$ (k_y direction), and corresponding functions $f(\mathbf{k})$, $\mathbf{g}(\mathbf{k})$ of the effective single-orbital model. Apart from the A point, the bands also cross at the L points and at additional \mathbf{k} points (which are called “accidental” band crossings [Sch+12]).

We remark that by the identity (3.24), we can define \mathbf{g} equivalently as

$$\mathbf{g}(\mathbf{k}) = -\frac{1}{2} (E^+(\mathbf{k}) - E^-(\mathbf{k})) \frac{\langle \mathbf{S} \rangle^-(\mathbf{k})}{|\langle \mathbf{S} \rangle^-(\mathbf{k})|}. \quad (3.32)$$

Thus, we have defined an the effective single-orbital model with the Hamiltonian matrix in dual space

$$H^{\text{eff}}(\mathbf{k}) = f(\mathbf{k}) \mathbb{1} + \mathbf{g}(\mathbf{k}) \cdot \boldsymbol{\sigma}, \quad (3.33)$$

where the functions $f(\mathbf{k})$ and $\mathbf{g}(\mathbf{k})$ are given by Eqs. (3.29) and (3.31), respectively. The crucial point is now that these functions are analytic in the whole Brillouin zone, and hence the so-defined Hamiltonian matrix $H^{\text{eff}}(\mathbf{k})$ is analytic in \mathbf{k} , too. In fact, this can be seen from Fig. 3.4, which shows $f(\mathbf{k})$ and $\mathbf{g}(\mathbf{k})$ along the special directions $\bar{\text{L}}\text{--A--L}$ and $\bar{\text{H}}\text{--A--H}$ (see Fig. 1.2a). Despite the fact that the two lowest conduction bands cross at various \mathbf{k} points, these functions are analytic in the whole Brillouin zone. We further remark that the effective single-orbital model inherits all the symmetries of the 18-band model, hence it is invariant under time-reversal and the C_{3v} point group operations as described in Sect. 2.1.

- (ii) Next, we define the effective Hamiltonian matrix direct space, $H^{\text{eff}}(\mathbf{R})$, by taking the inverse Fourier transform of Eq. (3.33) (analogously to Eq. (1.149)). The matrix $H^{\text{eff}}(\mathbf{R})$ can then again be expanded in terms of the identity matrix and the Pauli matrices as in Eq. (1.159), where the coefficient functions $f(\mathbf{R})$ and $\mathbf{g}(\mathbf{R})$ are the

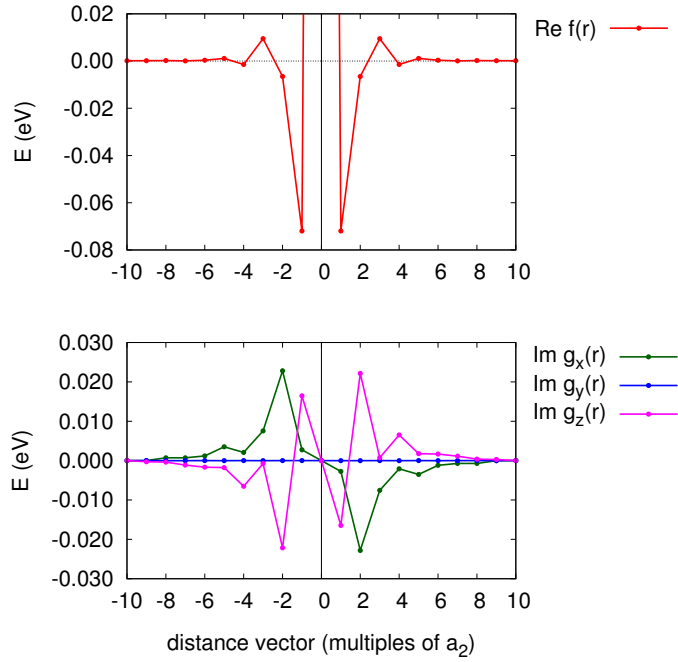


Figure 3.5: Functions $f(\mathbf{R})$ and $\mathbf{g}(\mathbf{R})$ along the y direction of the hexagonal Bravais lattice. The distance vector is given in integer multiples of the primitive vector \mathbf{a}_2 (see Fig. 1.1a). The value of f at $\mathbf{R} = \mathbf{0}$ corresponds to a constant energy shift and can therefore be neglected.

inverse Fourier transforms of Eqs. (3.29) and (3.31), respectively. By the analyticity of $f(\mathbf{k})$ and $\mathbf{g}(\mathbf{k})$, these Fourier transforms decay rapidly with the distance vector \mathbf{R} . This is indeed clearly seen in Fig. 3.5, which shows $f(\mathbf{R})$ and $\mathbf{g}(\mathbf{R})$ along the y direction of the Bravais lattice (see Fig. 1.1a). Furthermore, by the hermiticity and the time-reversal symmetry, $f(\mathbf{R})$ is real-valued and even, while $\mathbf{g}(\mathbf{R})$ is purely imaginary and odd under $\mathbf{R} \mapsto -\mathbf{R}$ (see Table 2.3 in Sect. 2.1).

- (iii) Finally, we construct a tight-binding model by neglecting the entries of $H^{\text{eff}}(\mathbf{R})$ for large distance vectors \mathbf{R} . Due to the rapid decay property of the Hamiltonian matrix, this is indeed a reasonable approximation. For example, let $H^{\leq 10}(\mathbf{R})$ be the Hamiltonian matrix which is (i) equal to $H^{\text{eff}}(\mathbf{R})$ if \mathbf{R} is an n th-nearest-neighbor vector with $n \leq 10$, and (ii) zero otherwise. The Fourier transformation and subsequent diagonalization of this reduced Hamiltonian matrix yields the energy bands of the tight-binding model. As seen in Fig. 3.2, these energy bands agree almost perfectly with the original energy bands of the 18-band model.

In summary, we have derived an effective tight-binding model $H^{\leq 10}(\mathbf{R})$ on the hexagonal Bravais lattice, which takes into account hoppings between up to 10th-nearest-neighbor vectors and which accurately reproduces the dispersion of the two lowest conduction bands of BiTeI.

Before closing this chapter, let us take a closer look at Fig. 3.4, which reveals detailed information about the spin polarization of the lowest conduction bands of BiTeI. In the k_x direction, we have $g_x = g_z = 0$, hence all spins point in the σ_y direction (see Eq. (1.166)). Furthermore, in the vicinity of the A point, g_y depends linearly on the wavevector, i.e., $g_y(\mathbf{k}) \propto k_x$. On the other hand, in the k_y direction near the A point, the spins point in the σ_x direction, and $g_x(\mathbf{k}) \propto -k_y$. These properties are precisely in accordance with the Rashba Hamiltonian (see Eq. (3.6)). At larger wavevectors, there appears an additional out-of-plane spin component (σ_z), which is characteristic of the C_{3v} symmetry and which is described by the effective Hamiltonian $(3k_x^2 - k_y^2)k_y\sigma_z$ [Bah+12].

Finally, for a more comprehensive view of the band structure of BiTeI, we have also plotted the energy bands $E^\pm(\mathbf{k})$ of the 18-band model as well as the functions $f(\mathbf{k})$ and $\mathbf{g}(\mathbf{k})$ on the whole hexagonal face of the Brillouin zone defined by $k_z = \pi/c_0$, see Figs. 3.6–3.11. Clearly, the function $\mathbf{g}(\mathbf{k})$ vanishes wherever the two conduction bands cross. As seen in Figs. 3.11, this does not only happen at the A point in the center of the hexagonal face of the Brillouin zone, but also at the three inequivalent L points at the zone boundaries (see Fig. 1.2). In fact, these are all high-symmetry points with the property that $\mathbf{k} = -\mathbf{k}$, and hence the band crossing at these points is enforced by the time-reversal symmetry. Apart from these points, however, there are additional “accidental” band crossings in the midway between A and L (see Ref. [Sch+12, Supplemental Material]). The time-reversal symmetry and the threefold rotation symmetry imply that these accidental band crossings appear simultaneously at six symmetric positions in the Brillouin zone. Near these points, the two conduction bands form *tilted Dirac cones*, which are characterized by a Fermi surface which consists of two lines instead of a single point (if the Fermi energy is exactly at the band crossings). In Ref. [Sch+12], we have predicted that these tilted Dirac cones may lead to novel phenomena such as a diverging orbital paramagnetism. Finally, we remark that similar features (“type-II Dirac cones”) have been found more recently in the band structure of WTe₂ monolayers [Mue+16].

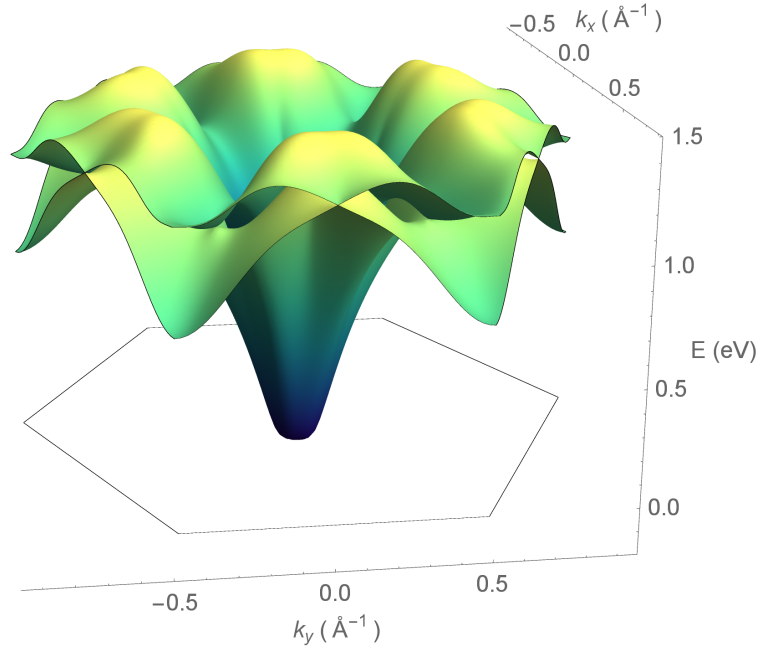


Figure 3.6: Dispersion of the two lowest conduction bands of BiTeI in the hexagonal face of the Brillouin zone which is defined by $k_z = \pi/c_0$ (see Fig. 1.2).

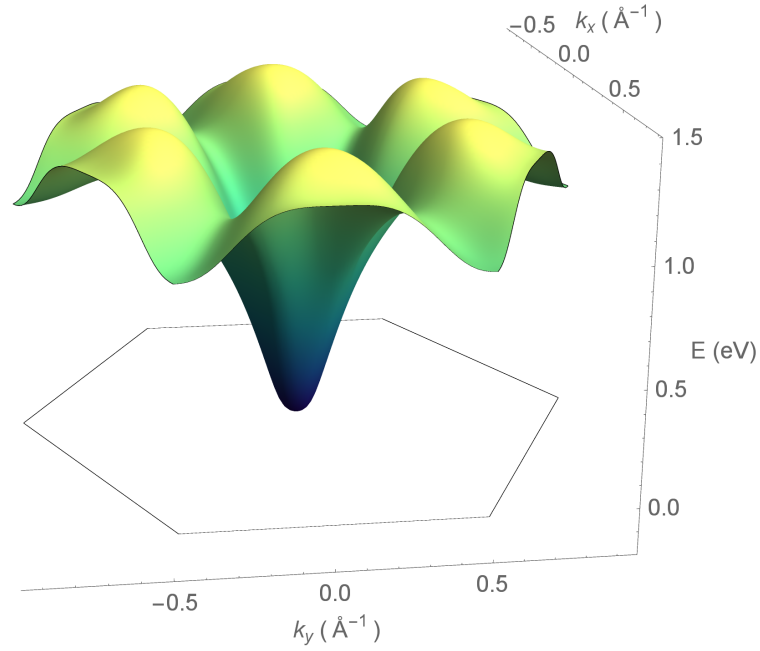


Figure 3.7: Function $f(\mathbf{k})$ of the effective single-orbital model.

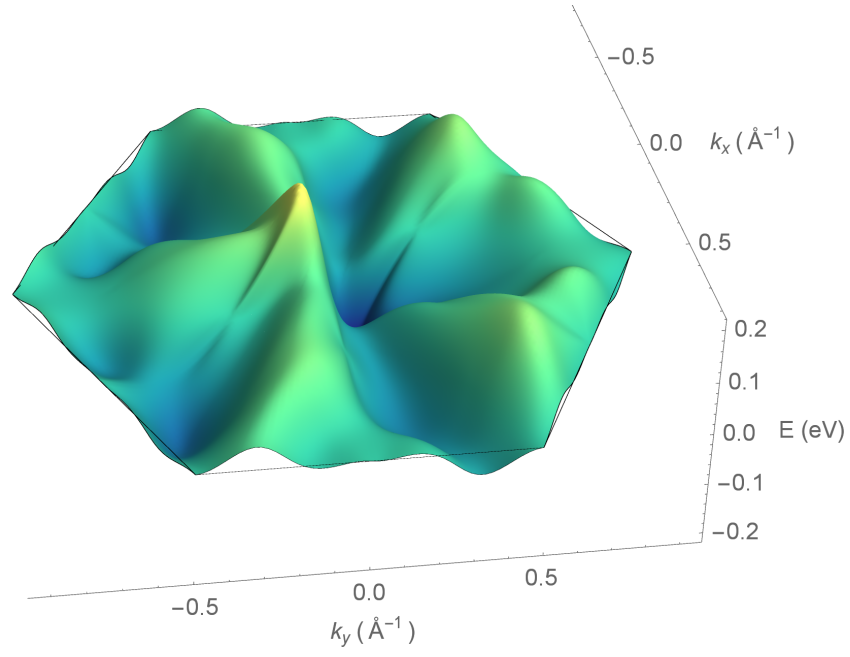


Figure 3.8: Function $g_x(\mathbf{k})$.

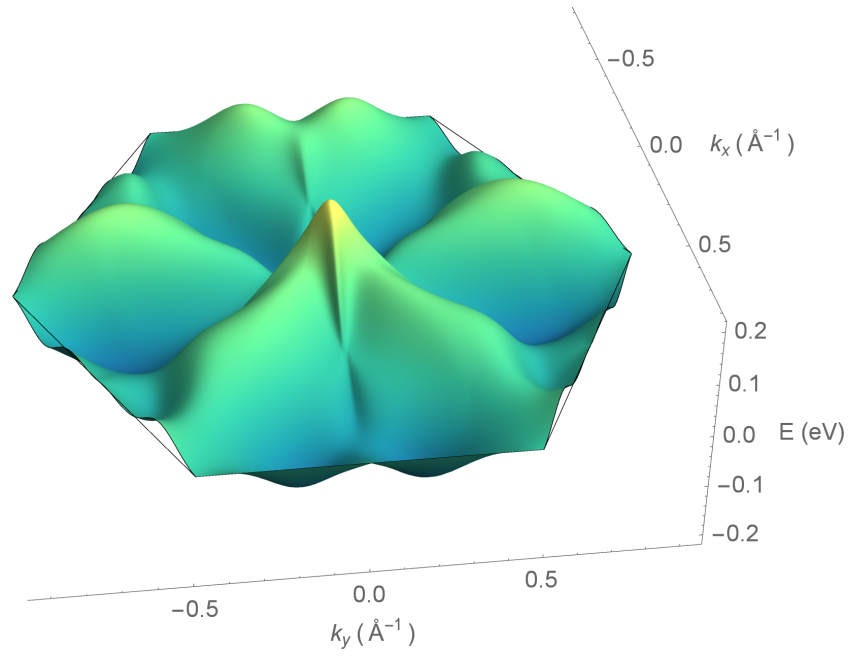


Figure 3.9: Function $g_y(\mathbf{k})$.

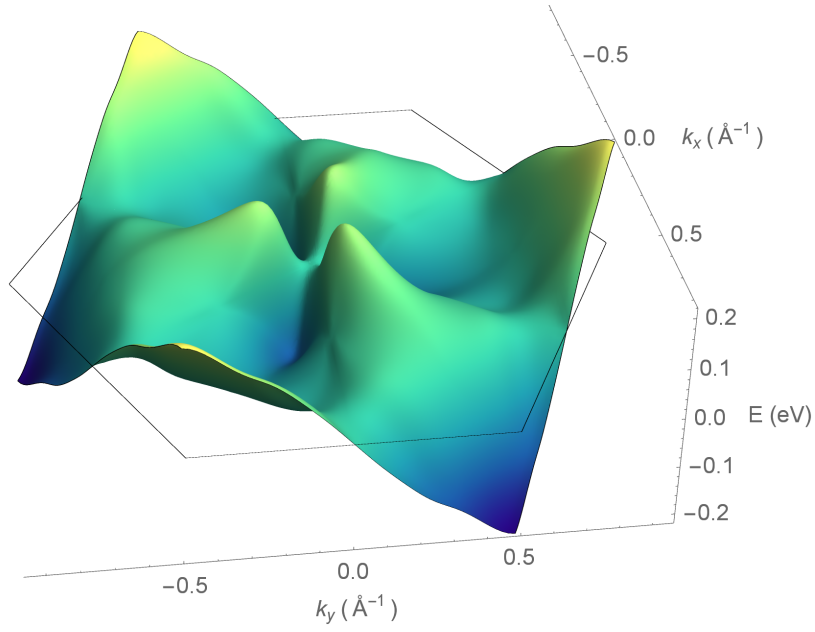


Figure 3.10: Function $g_z(\mathbf{k})$.

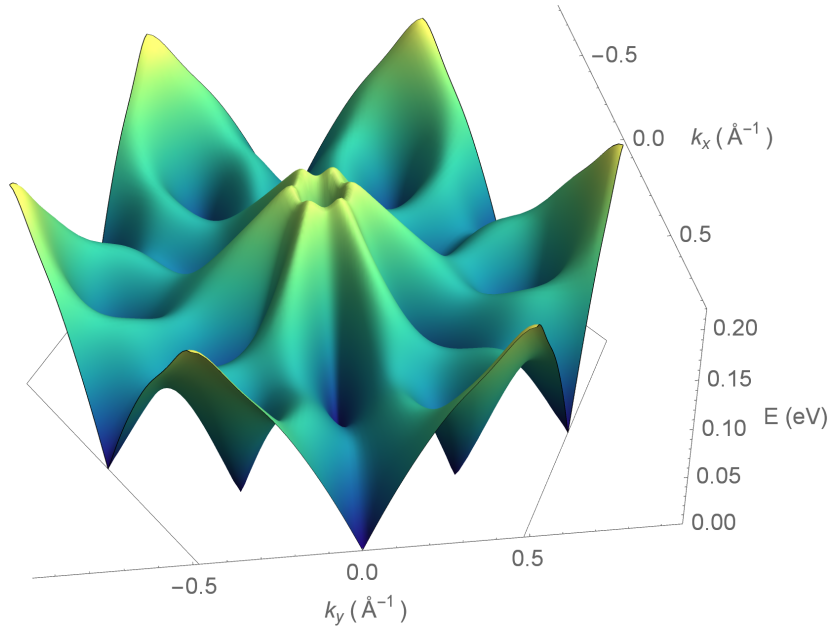


Figure 3.11: Absolute value $|g(\mathbf{k})|$, which equals the energy difference between the spin-split lowest conduction bands of BiTeI.

Part II.

Statistical field theory

4. Green function perturbation theory

4.1. Basics of second quantization

We begin this chapter with a brief introduction of the most important notions of statistical field theory, i.e., field operators (this Sect. 4.1) and temperature Green functions (next Sect. 4.2). Our presentation is partly based on Ref. [FW71, Ch. 7]. We start from the second-quantized electronic Hamiltonian

$$\hat{H} = \hat{H}_0 + \hat{V} \quad (4.1)$$

which acts on the *fermionic Fock space* (see e.g. Refs. [Sal99, Appendix B.1] or [SS16b, Appendix B]). The Hamiltonian consists of a *free part* H_0 and an *interaction part* V . The free part describes (non-interacting) electrons in the *external* periodic potential V_{ext} of the nuclei and is given by the second-quantized form of Eq. (1.46) [note the change in notation: $H \mapsto H_0$ and $V \mapsto V_{\text{ext}}$]. Hence,

$$\begin{aligned} \hat{H}_0 = \int d^3\mathbf{x} \sum_{s,s'} \hat{\psi}^\dagger(\mathbf{x}, s) & \left(\delta_{ss'} \left(-\frac{\hbar^2}{2m} \Delta + V_{\text{ext}}(\mathbf{x}) \right) \right. \\ & \left. + \frac{i\hbar^2}{4m^2c^2} \boldsymbol{\sigma}_{ss'} \cdot ((-\nabla V_{\text{ext}})(\mathbf{x}) \times \nabla) \right) \hat{\psi}(\mathbf{x}, s'). \end{aligned} \quad (4.2)$$

Furthermore, we assume an electron-electron interaction of the form

$$\hat{V} = \frac{1}{2} \int d^3\mathbf{x} \int d^3\mathbf{x}' \sum_{s,s'} \hat{\psi}^\dagger(\mathbf{x}, s) \hat{\psi}^\dagger(\mathbf{x}', s') v(\mathbf{x}, \mathbf{x}') \hat{\psi}(\mathbf{x}', s') \hat{\psi}(\mathbf{x}, s). \quad (4.3)$$

Here, the field operators in position/spin space are defined by

$$\hat{\psi}(\mathbf{x}, s) = \hat{a}(|\mathbf{x}, s\rangle), \quad (4.4)$$

$$\hat{\psi}^\dagger(\mathbf{x}, s) = \hat{a}^\dagger(|\mathbf{x}, s\rangle), \quad (4.5)$$

where $\hat{a}(|\varphi\rangle)$ and $\hat{a}^\dagger(|\varphi\rangle)$ are the fermionic annihilation and creation operators (which can be defined for any one-particle state $|\varphi\rangle$). In Eqs. (4.4)–(4.5), these operators annihilate and create, respectively, a position and spin eigenvector $|\mathbf{x}, s\rangle$, which is defined by its wave function (see Sect. 1.1)

$$\langle \mathbf{y}, s' | \mathbf{x}, s \rangle = \delta^3(\mathbf{x} - \mathbf{y}) \delta_{s,s'}. \quad (4.6)$$

In particular, the above field operators satisfy the *canonical anticommutation relations*

$$[\hat{\psi}(\mathbf{x}, s), \hat{\psi}(\mathbf{x}', s')]_+ = 0, \quad (4.7)$$

$$[\hat{\psi}^\dagger(\mathbf{x}, s), \hat{\psi}^\dagger(\mathbf{x}', s')]_+ = 0, \quad (4.8)$$

$$[\hat{\psi}(\mathbf{x}, s), \hat{\psi}^\dagger(\mathbf{x}', s')]_+ = \langle \mathbf{x}, s | \mathbf{x}', s' \rangle = \delta^3(\mathbf{x} - \mathbf{x}') \delta_{s, s'}, \quad (4.9)$$

where for any two operators \hat{A} and \hat{B} ,

$$[\hat{A}, \hat{B}]_+ = \hat{A}\hat{B} + \hat{B}\hat{A} \quad (4.10)$$

denotes the anticommutator. In general, we assume that the interaction kernel in Eq. (4.3) depends only on the distance of the two spatial arguments,

$$v(\mathbf{x}, \mathbf{x}') \equiv v(|\mathbf{x} - \mathbf{x}'|), \quad (4.11)$$

which implies in particular the symmetry $v(\mathbf{x}, \mathbf{x}') = v(\mathbf{x}', \mathbf{x})$. This assumption is in particular fulfilled for the Coulomb interaction kernel,

$$v(\mathbf{x}, \mathbf{x}') = \frac{e^2}{4\pi\epsilon_0} \frac{1}{|\mathbf{x} - \mathbf{x}'|}. \quad (4.12)$$

Next, we introduce the particle-number operator in second quantization,

$$\hat{N} = \int d^3\mathbf{x} \sum_s \hat{\psi}^\dagger(\mathbf{x}, s) \hat{\psi}(\mathbf{x}, s). \quad (4.13)$$

Subtracting this from the Hamiltonian (4.1) yields

$$\hat{K} = \hat{H} - \mu\hat{N}, \quad (4.14)$$

where μ denotes the chemical potential. The *grand-canonical partition function* at the inverse temperature $\beta = 1/(k_B T)$ is now defined in terms of these operators as

$$Z = \text{Tr} (e^{-\beta(\hat{H} - \mu\hat{N})}) \equiv \text{Tr} (e^{-\beta\hat{K}}). \quad (4.15)$$

Furthermore, for any operator \hat{O} and for $\tau \in \mathbb{R}$ we define the operator

$$\hat{O}(\tau) = e^{\hat{K}\tau/\hbar} \hat{O} e^{-\hat{K}\tau/\hbar}, \quad (4.16)$$

which is *analogous* to the time evolution in the Heisenberg picture under the identification

$$\tau = it. \quad (4.17)$$

Therefore, τ is usually called “imaginary time”. In the following, we will often suppress the spin index s and write, for example,

$$\hat{\psi}(\mathbf{x}) \equiv \hat{\psi}(\mathbf{x}, s). \quad (4.18)$$

It is then obvious how to restore the spin dependencies: one simply has to replace \mathbf{x} by (\mathbf{x}, s) and complement all integrations over \mathbf{x} by summations over s .

Finally, let us analyze the units of the various quantities introduced above (see also Sct. 1.1). Any Fock-space vector $|\Phi\rangle$ is dimensionless,

$$[|\Phi\rangle] = 1, \quad (4.19)$$

which is required by the normalization condition $\langle\Phi|\Phi\rangle = 1$. On the other hand, an N -particle wave function in position space has the dimension (see Eq. (1.22) for $N = 1$)

$$[\Phi(\mathbf{x}_1, \dots, \mathbf{x}_N)] = \text{m}^{-3N/2}, \quad (4.20)$$

which is consistent with the normalization condition

$$\int d^3\mathbf{x}_1 \dots \int d^3\mathbf{x}_N |\Phi(\mathbf{x}_1, \dots, \mathbf{x}_N)|^2 = 1. \quad (4.21)$$

Next, the annihilation and creation operators $\hat{a}^{(\dagger)}(|\varphi\rangle)$ of any one-particle state $|\varphi\rangle$ act on the dimensionless Fock-space vectors and can therefore be regarded as dimensionless operators themselves. On the other hand, the field operators in position space are defined by Eqs. (4.4)–(4.5). Using that the map $|\varphi\rangle \mapsto \hat{a}(|\varphi\rangle)$ is antilinear and $|\varphi\rangle \mapsto \hat{a}^\dagger(|\varphi\rangle)$ is linear, one shows directly the relations

$$\hat{a}(|\varphi\rangle) = \int d^3\mathbf{x} \varphi^*(\mathbf{x}) \hat{\psi}(\mathbf{x}), \quad (4.22)$$

$$\hat{a}^\dagger(|\varphi\rangle) = \int d^3\mathbf{x} \varphi(\mathbf{x}) \hat{\psi}^\dagger(\mathbf{x}). \quad (4.23)$$

These imply that the field operators in position space have the dimension

$$[\hat{\psi}(\mathbf{x})] = [\hat{\psi}^\dagger(\mathbf{x})] = \text{m}^{-3/2}, \quad (4.24)$$

which is consistent with the anticommutation relation (4.9). Note that the time dependence of the field operators as defined by Eq. (4.16) does not change their dimensions.

4.2. Temperature Green functions

In this thesis, we consider only temperature Green functions in imaginary time, also called *Schwinger functions* (see Refs. [BF04; FW71]). These are analogous to the ordinary (real-time) temperature Green functions under the identification (4.17).

Definition 4.1. For $n \geq 1$ and for $\tau_1, \dots, \tau_{2n} \in [0, \hbar\beta]$, the $2n$ -point temperature Green function G^{2n} is defined as

$$G^{2n}(\mathbf{x}_1, \tau_1; \dots; \mathbf{x}_{2n}, \tau_{2n}) = \frac{1}{Z} \text{Tr} \left(e^{-\beta\hat{K}} \mathcal{T} [\hat{\psi}(\mathbf{x}_1, \tau_1) \dots \hat{\psi}(\mathbf{x}_n, \tau_n) \hat{\psi}^\dagger(\mathbf{x}_{n+1}, \tau_{n+1}) \dots \hat{\psi}^\dagger(\mathbf{x}_{2n}, \tau_{2n})] \right), \quad (4.25)$$

where Z is the grand-canonical partition function given by Eq. (4.15).

In the above expression, the time-ordering operator \mathcal{T} is defined with respect to the imaginary-time arguments. Thus, for any m operators $\hat{O}_1(\mathbf{x}_1, \tau_1), \dots, \hat{O}_m(\mathbf{x}_m, \tau_m)$, the time-ordered product is given explicitly by

$$\begin{aligned} \mathcal{T}[\hat{O}_1(\mathbf{x}_1, \tau_1) \dots \hat{O}_m(\mathbf{x}_m, \tau_m)] &= \sum_{\pi \in S_m} \text{sgn}(\pi) \\ &\times \Theta(\tau_{\pi(1)} - \tau_{\pi(2)}) \dots \Theta(\tau_{\pi(m-1)} - \tau_{\pi(m)}) \hat{O}(\mathbf{x}_{\pi(1)}, \tau_{\pi(1)}) \dots \hat{O}(\mathbf{x}_{\pi(m)}, \tau_{\pi(m)}). \end{aligned} \quad (4.26)$$

Here, S_m denotes the symmetric group of m elements, i.e., the group of all permutations of the set $\{1, \dots, m\}$, and $\text{sgn}(\pi)$ is the sign of the permutation π . Furthermore, Θ denotes the Heaviside step function, which is defined as

$$\Theta(\tau_1 - \tau_2) = \begin{cases} 1, & \text{if } \tau_1 > \tau_2, \\ 0, & \text{if } \tau_1 < \tau_2. \end{cases} \quad (4.27)$$

By construction, the Green function G^{2n} is antisymmetric with respect to its first n and with respect to its last n arguments. Furthermore, the temperature Green functions are “antiperiodic” in the following sense:

Proposition 4.2. *For each $i \in \{1, \dots, 2n\}$, the boundary conditions of the temperature Green function G^{2n} at $\tau_i = 0$ and at $\tau_i = \hbar\beta$ are related by*

$$\begin{aligned} G^{2n}(\mathbf{x}_1, \tau_1; \dots; \mathbf{x}_i, \tau_i = 0; \dots; \mathbf{x}_{2n}, \tau_{2n}) &= \\ -G^{2n}(\mathbf{x}_1, \tau_1; \dots; \mathbf{x}_i, \tau_i = \hbar\beta; \dots; \mathbf{x}_{2n}, \tau_{2n}). \end{aligned} \quad (4.28)$$

This equality holds for any values of the spatial variables $\mathbf{x}_1, \dots, \mathbf{x}_{2n} \in \mathbb{R}^3$ and for any values of the other time variables $\tau_1, \dots, \tau_{i-1}, \tau_{i+1}, \dots, \tau_{2n} \in [0, \hbar\beta]$.

Proof. Consider first the case where $i = n + 1$, hence we compare the boundary conditions at $\tau_{n+1} = 0$ and at $\tau_{n+1} = \hbar\beta$. Using the cyclicity of the trace and the definition (4.16), we can calculate as

$$\begin{aligned} &G^{2n}(\mathbf{x}_1, \tau_1; \dots; \mathbf{x}_{n+1}, \tau_{n+1} = 0; \dots; \mathbf{x}_{2n}, \tau_{2n}) \\ &= \frac{1}{Z} \text{Tr} \left(e^{-\beta\hat{K}} \mathcal{T}[\hat{\psi}(\mathbf{x}_1, \tau_1) \dots \hat{\psi}^\dagger(\mathbf{x}_{n+1}, 0)] \right) \end{aligned} \quad (4.29)$$

$$= \frac{1}{Z} \text{Tr} \left(e^{-\beta\hat{K}} \mathcal{T}[\hat{\psi}(\mathbf{x}_1, \tau_1) \dots \hat{\psi}^\dagger(\mathbf{x}_{n+2}, \tau_{n+2})] \hat{\psi}^\dagger(\mathbf{x}_{n+1}, 0) \right) \quad (4.30)$$

$$= \frac{1}{Z} \text{Tr} \left(\hat{\psi}^\dagger(\mathbf{x}_{n+1}, 0) e^{-\beta\hat{K}} \mathcal{T}[\hat{\psi}(\mathbf{x}_1, \tau_1) \dots \hat{\psi}^\dagger(\mathbf{x}_{n+2}, \tau_{n+2})] \right) \quad (4.31)$$

$$= \frac{1}{Z} \text{Tr} \left(e^{-\beta\hat{K}} \hat{\psi}^\dagger(\mathbf{x}_{n+1}, \hbar\beta) \mathcal{T}[\hat{\psi}(\mathbf{x}_1, \tau_1) \dots \hat{\psi}^\dagger(\mathbf{x}_{n+2}, \tau_{n+2})] \right) \quad (4.32)$$

$$= -\frac{1}{Z} \text{Tr} \left(e^{-\beta\hat{K}} \mathcal{T}[\hat{\psi}(\mathbf{x}_1, \tau_1) \dots \hat{\psi}^\dagger(\mathbf{x}_{n+2}, \tau_{n+2}) \hat{\psi}^\dagger(\mathbf{x}_{n+1}, \hbar\beta)] \right) \quad (4.33)$$

$$= -G^{2n}(\mathbf{x}_1, \tau_1; \dots; \mathbf{x}_{n+1}, \tau_{n+1} = \hbar\beta; \dots; \mathbf{x}_{2n}, \tau_{2n}), \quad (4.34)$$

which proves the antiperiodicity in τ_{n+1} . Using the antisymmetry of G^{2n} in its last n arguments, this implies also the antiperiodicity in $\tau_{n+2}, \dots, \tau_{2n}$. By a similar calculation one shows that G^{2n} fulfills antiperiodic boundary conditions with respect to the first n arguments τ_1, \dots, τ_n . \square

We remark that the temperature Green functions were originally defined by Eq. (4.25) only for τ_i in the interval $[0, \hbar\beta]$. Using the boundary condition (4.28), however, G^{2n} can be continued to an antiperiodic function which is defined for all $\tau_i \in \mathbb{R}$: for example, if

$$\tau_i^m = \tau_i^0 + m(\hbar\beta) \quad (4.35)$$

with $\tau_i^0 \in [0, \hbar\beta]$ and $m \in \mathbb{Z}$, we define

$$\begin{aligned} G^{2n}(\mathbf{x}_1, \tau_1; \dots; \mathbf{x}_i, \tau_i^m; \dots; \mathbf{x}_{2n}, \tau_{2n}) := \\ (-1)^m G^{2n}(\mathbf{x}_1, \tau_1; \dots; \mathbf{x}_i, \tau_i^0; \dots; \mathbf{x}_{2n}, \tau_{2n}). \end{aligned} \quad (4.36)$$

The resulting function G^{2n} is antiperiodic in the sense that for all $\tau_i \in \mathbb{R}$,

$$\begin{aligned} G^{2n}(\mathbf{x}_1, \tau_1; \dots; \mathbf{x}_i, \tau_i + \hbar\beta; \dots; \mathbf{x}_{2n}, \tau_{2n}) = \\ - G^{2n}(\mathbf{x}_1, \tau_1; \dots; \mathbf{x}_i, \tau_i; \dots; \mathbf{x}_{2n}, \tau_{2n}). \end{aligned} \quad (4.37)$$

Note, however, that this antiperiodic function G^{2n} is in general not given by Eq. (4.25) anymore, which in fact holds only for $\tau_i \in [0, \hbar\beta]$. This is because the right-hand side of Eq. (4.25) is not antiperiodic for general $\tau_i \in \mathbb{R}$, which becomes immediately clear from the proof of Proposition 4.2, for which the condition $\tau_i \in [0, \hbar\beta]$ is essential. We further mention that the temperature Green functions are generally invariant under translations with respect to the time variables, i.e.,

$$G^{2n}(\mathbf{x}_1, \tau_1; \dots; \mathbf{x}_{2n}, \tau_{2n}) = G^{2n}(\mathbf{x}_1, \tau_1 + a; \dots; \mathbf{x}_{2n}, \tau_{2n} + a) \quad (4.38)$$

for any $a \in \mathbb{R}$. This can be shown directly from the definition (4.25) by using again the cyclicity of the trace. The analogous property does in general not hold for the spatial variables (see, however, the property (4.64) of the lattice Green functions).

Our next remark concerns the conventions we choose for the temperature Green functions. First, while the partition function given by Eq. (4.15) is dimensionless, the $2n$ -point Green function defined by Eq. (4.25) has the unit

$$[G^{2n}(\mathbf{x}_1, \tau_1; \dots; \mathbf{x}_{2n}, \tau_{2n})] = \text{m}^{-3n}, \quad (4.39)$$

which follows from the corresponding dimension (4.24) of the field operators. Furthermore, we define the Fourier transforms of the temperature Green functions as

$$\begin{aligned} G^{2n}(\mathbf{k}_1, \omega_1; \dots; \mathbf{k}_{2n}, \omega_{2n}) = \\ \frac{1}{(2\pi)^{3n/2}} \int d^3\mathbf{x}_1 \dots \int d^3\mathbf{x}_{2n} \frac{1}{(\hbar\beta)^{2n}} \int_0^{\hbar\beta} d\tau_1 \dots \int_0^{\hbar\beta} d\tau_{2n} G^{2n}(\mathbf{x}_1, \tau_1; \dots; \mathbf{x}_{2n}, \tau_{2n}) \\ \times e^{-i\mathbf{k}_1 \cdot \mathbf{x}_1 + i\omega_1 \tau_1} \dots e^{-i\mathbf{k}_n \cdot \mathbf{x}_n + i\omega_n \tau_n} e^{i\mathbf{k}_{n+1} \cdot \mathbf{x}_{n+1} - i\omega_{n+1} \tau_{n+1}} \dots e^{i\mathbf{k}_{2n} \cdot \mathbf{x}_{2n} - i\omega_{2n} \tau_{2n}}, \end{aligned} \quad (4.40)$$

or conversely,

$$\begin{aligned}
 G^{2n}(\mathbf{x}_1, \tau_1; \dots; \mathbf{x}_{2n}, \tau_{2n}) = & \quad (4.41) \\
 \frac{1}{(2\pi)^{3n/2}} \int d^3\mathbf{k}_1 \dots \int d^3\mathbf{k}_{2n} \sum_{\omega_1} \dots \sum_{\omega_{2n}} G^{2n}(\mathbf{k}_1, \omega_1; \dots; \mathbf{k}_{2n}, \omega_{2n}) \\
 \times e^{i\mathbf{k}_1 \cdot \mathbf{x}_1 - i\omega_1 \tau_1} \dots e^{i\mathbf{k}_n \cdot \mathbf{x}_n - i\omega_n \tau_n} e^{-i\mathbf{k}_{n+1} \cdot \mathbf{x}_{n+1} + i\omega_{n+1} \tau_{n+1}} \dots e^{-i\mathbf{k}_{2n} \cdot \mathbf{x}_{2n} + i\omega_{2n} \tau_{2n}},
 \end{aligned}$$

Here, we sum over fermionic Matsubara frequencies,

$$\omega_1, \dots, \omega_{2n} \in \mathbb{M} = \left\{ \frac{(2\ell + 1)\pi}{\hbar\beta}; \ell \in \mathbb{N} \right\}, \quad (4.42)$$

which is due to the antiperiodicity of the temperature Green functions with respect to their time variables. Note that our convention for the Fourier transform with respect to the time variables differs from the usual convention, where the factor $1/(\hbar\beta)$ is put in front of the sum over the Matsubara frequencies. The advantage of our convention is that the temperature Green functions in the momentum/frequency domain have the same dimensions as their respective counterparts in the position/time domain, hence

$$[G^{2n}(\mathbf{k}_1, \omega_1; \dots; \mathbf{k}_{2n}, \omega_{2n})] = m^{-3n}. \quad (4.43)$$

Finally, if we re-introduce the spin indices by substituting $\mathbf{x}_i \mapsto (\mathbf{x}_i, s_i)$, we will usually denote the spin indices as subscripts, i.e.,

$$G_{s_1 \dots s_{2n}}^{2n}(\mathbf{x}_1, \tau_1; \dots; \mathbf{x}_{2n}, \tau_{2n}) \equiv G^{2n}(\mathbf{x}_1, s_1, \tau_1; \dots; \mathbf{x}_{2n}, s_{2n}, \tau_{2n}). \quad (4.44)$$

Before closing this section, let us point out the particular relevance of the two-point Green function, which is defined as

$$G^2(\mathbf{x}_1, \tau_1; \mathbf{x}_2, \tau_2) = \frac{1}{Z} \text{Tr} \left(e^{-\beta \hat{K}} \mathcal{T} [\psi(\mathbf{x}_1, \tau_1) \hat{\psi}^\dagger(\mathbf{x}_2, \tau_2)] \right). \quad (4.45)$$

This simplest Green function already allows us to calculate the thermal expectation value of any “one-particle” operator which is quadratic in the field operators. For example, the thermal expectation value of the charge density operator,

$$\hat{\rho}(\mathbf{x}) = (-e) \hat{\psi}^\dagger(\mathbf{x}) \hat{\psi}(\mathbf{x}), \quad (4.46)$$

is given by the following equal-time limit of the two-point Green function:

$$\langle \hat{\rho}(\mathbf{x}) \rangle \equiv \frac{1}{Z} \text{Tr} (e^{-\beta \hat{H}} \hat{\rho}(\mathbf{x})) = e \lim_{\tau \rightarrow 0^+} G^2(\mathbf{x}, 0; \mathbf{x}, \tau). \quad (4.47)$$

Similarly, one can calculate the thermal expectation value of any “ n -particle” operator (which is of the order $2n$ in the field operators) from a suitable equal-time limit of the $2n$ -point temperature Green function.

4.3. Green functions on the lattice

In many applications, one does not deal directly with the fundamental Green functions which depend on the position $\mathbf{x} \in \mathbb{R}^3$ or on the momentum $\mathbf{k} \in \mathbb{R}^3$ (and from which one can deduce typical observables such as the charge density as explained in the preceding section). Instead, one considers another type of Green functions which depend on the Bravais lattice vector $\mathbf{R} \in \Gamma$ or on the Bloch momentum $\mathbf{k} \in \mathcal{B}$. (Note that we use the same symbol \mathbf{k} for Bloch momenta and ordinary momenta, although they should be strictly distinguished.) In this section, we will give a precise meaning to these “lattice Green functions” and clarify their relations to the fundamental Green functions.

Definition 4.3. The *lattice Green functions in the Wannier basis* are defined for $n \geq 1$ as follows:

$$\begin{aligned} G_{\ell_1 \dots \ell_{2n}}^{2n}(\mathbf{R}_1, \tau_1; \dots; \mathbf{R}_{2n}, \tau_{2n}) = \\ \frac{1}{Z} \text{Tr} \left(e^{-\beta \hat{K}} \mathcal{T} \left[\hat{a}(|\Phi_{\ell_1 \mathbf{R}_1}\rangle, \tau_1) \dots \hat{a}(|\Phi_{\ell_n \mathbf{R}_n}\rangle, \tau_n) \right. \right. \\ \left. \left. \times \hat{a}^\dagger(|\Phi_{\ell_{2n} \mathbf{R}_{2n}}\rangle, \tau_{2n}) \dots \hat{a}^\dagger(|\Phi_{\ell_{n+1} \mathbf{R}_{n+1}}\rangle, \tau_{n+1}) \right] \right), \end{aligned} \quad (4.48)$$

where $|\Phi_{\ell \mathbf{R}}\rangle$ denotes a Wannier vector which is labeled by the band index ℓ and the Bravais lattice vector \mathbf{R} (see Sct. 1.3). Correspondingly, the operators $\hat{a}(|\Phi_{\ell \mathbf{R}}\rangle)$ and $\hat{a}^\dagger(|\Phi_{\ell \mathbf{R}}\rangle)$ annihilate and create this very Wannier vector, and their time evolution is determined by Eq. (4.16).

We first note that in contrast to the fundamental Green functions (cf. Eq. (4.39)), the lattice Green functions are dimensionless,

$$\left[G_{\ell_1 \dots \ell_{2n}}^{2n}(\mathbf{R}_1, \tau_1; \dots; \mathbf{R}_{2n}, \tau_{2n}) \right] = 1. \quad (4.49)$$

Furthermore, with $\Phi_{\ell \mathbf{R}}(\mathbf{x}, s) \equiv \langle \mathbf{x}, s | \Phi_{\ell \mathbf{R}} \rangle$, the *basis transformations* between the Wannier vectors and the position/spin eigenvectors read

$$|\Phi_{\ell \mathbf{R}}\rangle = \int d^3 \mathbf{x} \sum_s |\mathbf{x}, s\rangle \Phi_{\ell \mathbf{R}}(\mathbf{x}, s), \quad (4.50)$$

$$|\mathbf{x}, s\rangle = \sum_{\ell, \mathbf{R}} |\Phi_{\ell \mathbf{R}}\rangle \Phi_{\ell \mathbf{R}}^*(\mathbf{x}, s). \quad (4.51)$$

Therefore, we can express the above annihilation and creation operators of Wannier vectors in terms of the fundamental field operators (4.4)–(4.5) as

$$\hat{a}(|\Phi_{\ell \mathbf{R}}\rangle) = \int d^3 \mathbf{x} \sum_s \Phi_{\ell \mathbf{R}}^*(\mathbf{x}, s) \hat{\psi}(\mathbf{x}, s), \quad (4.52)$$

$$\hat{a}^\dagger(|\Phi_{\ell \mathbf{R}}\rangle) = \int d^3 \mathbf{x} \sum_s \Phi_{\ell \mathbf{R}}(\mathbf{x}, s) \hat{\psi}^\dagger(\mathbf{x}, s), \quad (4.53)$$

or conversely as

$$\hat{\psi}(\mathbf{x}, s) = \sum_{\ell, \mathbf{R}} \Phi_{\ell \mathbf{R}}(\mathbf{x}, s) \hat{a}(|\Phi_{\ell \mathbf{R}}\rangle), \quad (4.54)$$

$$\hat{\psi}^\dagger(\mathbf{x}, s) = \sum_{\ell, \mathbf{R}} \Phi_{\ell \mathbf{R}}^*(\mathbf{x}, s) \hat{a}^\dagger(|\Phi_{\ell \mathbf{R}}\rangle). \quad (4.55)$$

Here, we have used again the antilinearity and linearity, respectively, of the maps $|\varphi\rangle \mapsto \hat{a}(|\varphi\rangle)$ and $|\varphi\rangle \mapsto \hat{a}^\dagger(|\varphi\rangle)$. As a consequence, the lattice Green functions in the Wannier basis are related to the fundamental Green functions (see Definition 4.1) by

$$\begin{aligned} G_{\ell_1 \dots \ell_{2n}}^{2n}(\mathbf{R}_1, \tau_1; \dots; \mathbf{R}_{2n}, \tau_{2n}) = \\ \int d^3 \mathbf{x}_1 \dots \int d^3 \mathbf{x}_{2n} \sum_{s_1, \dots, s_{2n}} G_{s_1 \dots s_{2n}}^{2n}(\mathbf{x}_1, \tau_1; \dots; \mathbf{x}_{2n}, \tau_{2n}) \\ \times \Phi_{\ell_1 \mathbf{R}_1}^*(\mathbf{x}_1, s_1) \dots \Phi_{\ell_n \mathbf{R}_n}^*(\mathbf{x}_n, s_n) \Phi_{\ell_{n+1} \mathbf{R}_{n+1}}(\mathbf{x}_{n+1}, s_{n+1}) \dots \Phi_{\ell_{2n} \mathbf{R}_{2n}}(\mathbf{x}_{2n}, s_{2n}), \end{aligned} \quad (4.56)$$

or conversely, by

$$\begin{aligned} G_{s_1 \dots s_{2n}}^{2n}(\mathbf{x}_1, \tau_1; \dots; \mathbf{x}_{2n}, \tau_{2n}) = \\ \sum_{\ell_1, \mathbf{R}_1} \dots \sum_{\ell_{2n}, \mathbf{R}_{2n}} G_{\ell_1 \dots \ell_{2n}}^{2n}(\mathbf{R}_1, \tau_1; \dots; \mathbf{R}_{2n}, \tau_{2n}) \\ \times \Phi_{\ell_1 \mathbf{R}_1}(\mathbf{x}_1, s_1) \dots \Phi_{\ell_n \mathbf{R}_n}(\mathbf{x}_n, s_n) \Phi_{\ell_{n+1} \mathbf{R}_{n+1}}^*(\mathbf{x}_{n+1}, s_{n+1}) \dots \Phi_{\ell_{2n} \mathbf{R}_{2n}}^*(\mathbf{x}_{2n}, s_{2n}). \end{aligned} \quad (4.57)$$

Thus, in order to reconstruct the fundamental Green functions from the lattice Green functions, one needs to know the Wannier functions to which the latter refer.

Definition 4.4. The *lattice Green functions in the Bloch basis* (or *band basis*) are defined for $n \geq 1$ as

$$\begin{aligned} G_{\ell_1 \dots \ell_{2n}}^{2n}(\mathbf{k}_1, \tau_1; \dots; \mathbf{k}_{2n}, \tau_{2n}) = \\ \frac{1}{Z} \text{Tr} \left(e^{-\beta \hat{K}} \mathcal{T} \left[\hat{a}(|\Psi_{\ell_1 \mathbf{k}_1}\rangle, \tau_1) \dots \hat{a}(|\Psi_{\ell_n \mathbf{k}_n}\rangle, \tau_n) \right. \right. \\ \left. \left. \times \hat{a}^\dagger(|\Psi_{\ell_{n+1} \mathbf{k}_{n+1}}\rangle, \tau_{n+1}) \dots \hat{a}^\dagger(|\Psi_{\ell_{2n} \mathbf{k}_{2n}}\rangle, \tau_{2n}) \right] \right), \end{aligned} \quad (4.58)$$

where $|\Psi_{\ell \mathbf{k}}\rangle$ denotes a Bloch vector which is labeled by the band index ℓ and the Bloch momentum \mathbf{k} (the latter ranges over the first Brillouin zone \mathcal{B}).

Precisely as their counterparts in the Wannier basis, the lattice Green functions in the Bloch basis are also dimensionless,

$$[G_{\ell_1 \dots \ell_{2n}}^{2n}(\mathbf{k}_1, \tau_1; \dots; \mathbf{k}_{2n}, \tau_{2n})] = 1. \quad (4.59)$$

Using the transformations between Bloch and Wannier vectors, Eqs. (1.75)–(1.76), we obtain the following relations between the lattice Green functions in different bases:

$$G_{\ell_1 \dots \ell_{2n}}^{2n}(\mathbf{k}_1, \tau_1; \dots; \mathbf{k}_{2n}, \tau_{2n}) = \sum_{\mathbf{R}_1} \dots \sum_{\mathbf{R}_{2n}} G_{\ell_1 \dots \ell_{2n}}^{2n}(\mathbf{R}_1, \tau_1; \dots; \mathbf{R}_{2n}, \tau_{2n}) \quad (4.60)$$

$$\times e^{-i\mathbf{k}_1 \cdot \mathbf{R}_1} \dots e^{-i\mathbf{k}_n \cdot \mathbf{R}_n} e^{i\mathbf{k}_{n+1} \cdot \mathbf{R}_{n+1}} \dots e^{i\mathbf{k}_{2n} \cdot \mathbf{R}_{2n}},$$

and conversely,

$$G_{\ell_1 \dots \ell_{2n}}^{2n}(\mathbf{R}_1, \tau_1; \dots; \mathbf{R}_{2n}, \tau_{2n}) = \quad (4.61)$$

$$\frac{1}{|\mathcal{B}|^{2n}} \int_{\mathcal{B}} d^3 \mathbf{k}_1 \dots \int_{\mathcal{B}} d^3 \mathbf{k}_{2n} G_{\ell_1 \dots \ell_{2n}}^{2n}(\mathbf{k}_1, \tau_1; \dots; \mathbf{k}_{2n}, \tau_{2n})$$

$$\times e^{i\mathbf{k}_1 \cdot \mathbf{R}_1} \dots e^{i\mathbf{k}_n \cdot \mathbf{R}_n} e^{-i\mathbf{k}_{n+1} \cdot \mathbf{R}_{n+1}} \dots e^{-i\mathbf{k}_{2n} \cdot \mathbf{R}_{2n}}.$$

Furthermore, the lattice Green functions in the Bloch basis are related to the fundamental Green functions in the position/spin domain by

$$G_{\ell_1 \dots \ell_{2n}}^{2n}(\mathbf{k}_1, \tau_1; \dots; \mathbf{k}_{2n}, \tau_{2n}) = \quad (4.62)$$

$$\int d^3 \mathbf{x}_1 \dots \int d^3 \mathbf{x}_{2n} \sum_{s_1, \dots, s_{2n}} G_{s_1 \dots s_{2n}}^{2n}(\mathbf{x}_1, \tau_1; \dots; \mathbf{x}_{2n}, \tau_{2n})$$

$$\times \Psi_{\ell_1 \mathbf{k}_1}^*(\mathbf{x}_1, s_1) \dots \Psi_{\ell_n \mathbf{k}_n}^*(\mathbf{x}_n, s_n) \Psi_{\ell_{n+1} \mathbf{k}_{n+1}}(\mathbf{x}_{n+1}, s_{n+1}) \dots \Psi_{\ell_{2n} \mathbf{k}_{2n}}(\mathbf{x}_{2n}, s_{2n}),$$

and conversely, by

$$G_{s_1 \dots s_{2n}}^{2n}(\mathbf{x}_1, \tau_1; \dots; \mathbf{x}_{2n}, \tau_{2n}) = \quad (4.63)$$

$$\sum_{\ell_1, \dots, \ell_{2n}} \frac{1}{|\mathcal{B}|^{2n}} \int_{\mathcal{B}} d^3 \mathbf{k}_1 \dots \int_{\mathcal{B}} d^3 \mathbf{k}_{2n} G_{\ell_1 \dots \ell_{2n}}^{2n}(\mathbf{k}_1, \tau_1; \dots; \mathbf{k}_{2n}, \tau_{2n})$$

$$\times \Psi_{\ell_1 \mathbf{k}_1}(\mathbf{x}_1, s_1) \dots \Psi_{\ell_n \mathbf{k}_n}(\mathbf{x}_n, s_n) \Psi_{\ell_{n+1} \mathbf{k}_{n+1}}^*(\mathbf{x}_{n+1}, s_{n+1}) \dots \Psi_{\ell_{2n} \mathbf{k}_{2n}}^*(\mathbf{x}_{2n}, s_{2n}).$$

Note that this is not simply a Fourier transformation, but a complicated transformation involving the Bloch functions. Hence, we stress again that the lattice Green functions alone are not sufficient for constructing the fundamental Green functions: in addition, one needs to know the Bloch (or Wannier) functions to which these lattice Green functions refer.

In Sect. 4.2, we mentioned that the temperature Green functions are generally invariant under temporal translations (see Eqs. (4.38)). On the other hand, as a crystalline system is not spatially homogeneous, the corresponding Green functions are generally not invariant under arbitrary spatial translations. They are, however, invariant under the subset of translations which leave the Bravais lattice invariant. The corresponding property of the lattice Green functions is expressed by the following proposition.

Proposition 4.5. *The lattice Green functions are invariant under lattice translations in the following sense:*

$$G_{\ell_1 \dots \ell_{2n}}^{2n}(\mathbf{R}_1, \tau_1; \dots; \mathbf{R}_{2n}, \tau_{2n}) = G_{\ell_1 \dots \ell_{2n}}^{2n}(\mathbf{R}_1 + \mathbf{R}', \tau_1; \dots; \mathbf{R}_{2n} + \mathbf{R}', \tau_{2n}). \quad (4.64)$$

for any vector $\mathbf{R}' \in \Gamma$ of the direct lattice.

Proof. This follows directly from the definition (4.48) of the lattice Green functions, if we use the transformation property (1.80) of Wannier vectors under lattice translations, the corresponding transformation property of the annihilation and creation operators,

$$\hat{a}^{(\dagger)}(|\Phi_{\ell, \mathbf{R}+\mathbf{R}'}\rangle) = \hat{a}^{(\dagger)}(T_{\mathbf{R}'}|\Phi_{\ell, \mathbf{R}}\rangle) = \hat{T}_{\mathbf{R}'} \hat{a}^{(\dagger)}(|\Phi_{\ell, \mathbf{R}}\rangle) \hat{T}_{\mathbf{R}'}^{-1}, \quad (4.65)$$

as well as the invariance of the Hamiltonian under lattice translations, Eq. (1.52). \square

The invariance under lattice translations and under temporal translations implies that the $2n$ -point lattice Green function essentially depends on only $(2n-1)$ lattice vectors and time variables. This means, we can write

$$\begin{aligned} G_{\ell_1 \dots \ell_{2n}}^{2n}(\mathbf{R}_1, \tau_1; \dots; \mathbf{R}_{2n}, \tau_{2n}) \\ = G_{\ell_1 \dots \ell_{2n}}^{2n}(\mathbf{R}_1 - \mathbf{R}_{2n}, \tau_1 - \tau_{2n}; \dots; \mathbf{R}_{2n-1} - \mathbf{R}_{2n}, \tau_{2n-1} - \tau_{2n}; \mathbf{0}, 0) \end{aligned} \quad (4.66)$$

$$\equiv \tilde{G}_{\ell_1 \dots \ell_{2n}}^{2n}(\mathbf{R}_1 - \mathbf{R}_{2n}, \tau_1 - \tau_{2n}; \dots; \mathbf{R}_{2n-1} - \mathbf{R}_{2n}, \tau_{2n-1} - \tau_{2n}), \quad (4.67)$$

where in the last step we have defined a new function of only $(2n-1)$ variables (\mathbf{R}_i, τ_i) . By performing the transition to the corresponding Green functions in the Bloch basis (see Eq. (4.60)) and by Fourier's transformation with respect to the time variables (see Eq. (4.40)), we further obtain

$$\begin{aligned} G_{\ell_1 \dots \ell_{2n}}^{2n}(\mathbf{k}_1, \omega_1; \dots; \mathbf{k}_{2n}, \omega_{2n}) &= \tilde{G}_{\ell_1 \dots \ell_{2n}}^{2n}(\mathbf{k}_1, \omega_1; \dots; \mathbf{k}_{2n-1}, \omega_{2n-1}) \\ &\times \sum_{\mathbf{K}} |\mathcal{B}| \delta^3(\mathbf{K} + \mathbf{k}_1 + \dots + \mathbf{k}_n, \mathbf{k}_{n+1} + \dots + \mathbf{k}_{2n}) \delta_{\omega_1 + \dots + \omega_n, \omega_{n+1} + \dots + \omega_{2n}}, \end{aligned} \quad (4.68)$$

where the Fourier transform of the reduced function \tilde{G}^{2n} is defined as

$$\begin{aligned} \tilde{G}_{\ell_1 \dots \ell_{2n}}^{2n}(\mathbf{k}_1, \omega_1; \dots; \mathbf{k}_{2n-1}, \omega_{2n-1}) &= \\ \sum_{\mathbf{R}_1} \dots \sum_{\mathbf{R}_{2n-1}} \frac{1}{(\hbar\beta)^{2n-1}} \int_0^{\hbar\beta} d\tau_1 \dots \int_0^{\hbar\beta} d\tau_{2n-1} &\tilde{G}_{\ell_1 \dots \ell_{2n}}^{2n}(\mathbf{R}_1, \tau_1; \dots; \mathbf{R}_{2n-1}, \tau_{2n-1}) \\ \times e^{-i\mathbf{k}_1 \cdot \mathbf{R}_1 + i\omega_1 \tau_1} \dots e^{-i\mathbf{k}_n \cdot \mathbf{R}_n + i\omega_n \tau_n} e^{i\mathbf{k}_{n+1} \cdot \mathbf{R}_{n+1} - i\omega_{n+1} \tau_{n+1}} \dots &e^{i\mathbf{k}_{2n-1} \cdot \mathbf{R}_{2n-1} - i\omega_{2n-1} \tau_{2n-1}}. \end{aligned} \quad (4.69)$$

In particular, the condition (4.68) implies that for Bloch momenta, the “momentum conservation” holds only up to a reciprocal lattice vector \mathbf{K} . The latter is fixed by the condition that all Bloch momenta $\mathbf{k}_1, \dots, \mathbf{k}_{2n}$ lie in the first Brillouin zone. In the following, we will not distinguish explicitly between G^{2n} and \tilde{G}^{2n} , and instead denote both functions for simplicity with the same symbol G^{2n} .

Finally, we come back to the *single-orbital model* of Sct. 1.5, for which yet another class of Green functions can be defined: In this case, there is a unitary matrix $U_{s\ell}(\mathbf{k})$ which mediates between the band basis (Bloch vectors) and the spin basis (Bloch-like vectors), see Eq. (1.148). Therefore, one can define the *Green functions in the Bloch momentum/spin basis* (as used e.g. in Ref. [Sch+16a]) as follows:

$$\begin{aligned} G_{s_1 \dots s_{2n}}^{2n}(\mathbf{k}_1, \tau_1; \dots; \mathbf{k}_{2n}, \tau_{2n}) = & \quad (4.70) \\ \frac{1}{Z} \text{Tr} \left(e^{-\beta \hat{K}} \mathcal{T} \left[\hat{a}(|\psi_{0s_1, \mathbf{k}_1}\rangle, \tau_1) \dots \hat{a}(|\psi_{0s_n, \mathbf{k}_n}\rangle, \tau_n) \right. \right. \\ & \left. \left. \times \hat{a}^\dagger(|\psi_{0s_{2n}, \mathbf{k}_{2n}}\rangle, \tau_{2n}) \dots \hat{a}^\dagger(|\psi_{0s_{n+1}, \mathbf{k}_{n+1}}\rangle, \tau_{n+1}) \right] \right). \end{aligned}$$

These are related to the lattice Green functions in the Bloch basis (or band basis) by the well-known equations

$$\begin{aligned} G_{s_1 \dots s_{2n}}^{2n}(\mathbf{k}_1, \tau_1; \dots; \mathbf{k}_{2n}, \tau_{2n}) = & \sum_{\ell_1, \dots, \ell_{2n}} G_{\ell_1 \dots \ell_{2n}}^{2n}(\mathbf{k}_1, \tau_1; \dots; \mathbf{k}_{2n}, \tau_{2n}) \\ & \times U_{s_1 \ell_1}(\mathbf{k}_1) \dots U_{s_n \ell_n}(\mathbf{k}_n) U_{s_{n+1}, \ell_{n+1}}^*(\mathbf{k}_{n+1}) \dots U_{s_{2n}, \ell_{2n}}^*(\mathbf{k}_{2n}), \end{aligned} \quad (4.71)$$

and conversely,

$$\begin{aligned} G_{\ell_1 \dots \ell_{2n}}^{2n}(\mathbf{k}_1, \tau_1; \dots; \mathbf{k}_{2n}, \tau_{2n}) = & \sum_{s_1, \dots, s_{2n}} G_{s_1 \dots s_{2n}}^{2n}(\mathbf{k}_1, \tau_1; \dots; \mathbf{k}_{2n}, \tau_{2n}) \\ & \times U_{s_1 \ell_1}^*(\mathbf{k}_1) \dots U_{s_n \ell_n}^*(\mathbf{k}_n) U_{s_{n+1}, \ell_{n+1}}(\mathbf{k}_{n+1}) \dots U_{s_{2n}, \ell_{2n}}(\mathbf{k}_{2n}). \end{aligned} \quad (4.72)$$

We remark that one can also define the lattice analoga of the so-called connected and one-line-irreducible Green functions, which will be introduced later in Scts. 5.3 and 5.5. Moreover, the Green function perturbation theory as derived in the next section holds analogously also for the lattice Green functions.

4.4. Perturbative expansion

The *Green function perturbation theory* allows one to express all Green functions G^{2n} of the interacting many-body system in terms of the *free* (or *non-interacting*) two-point Green function G_0^2 as well as the interaction kernel v . Here, the non-interacting temperature Green functions G_0^{2n} are defined analogously to Eq. (4.25), but with the full

Hamiltonian (4.1) replaced by the free Hamiltonian (4.2). In concrete terms, we define (analogously to Eq. (4.14))

$$\hat{K}_0 = \hat{H}_0 - \mu \hat{N}. \quad (4.73)$$

Furthermore, for any operator \hat{O} and for $\tau \in \mathbb{R}$, we define the “time evolution in the interaction picture” as (cf. Eq. (4.16))

$$\hat{O}_I(\tau) = e^{\hat{K}_0 \tau / \hbar} \hat{O} e^{-\hat{K}_0 \tau / \hbar}. \quad (4.74)$$

With this, the partition function of the non-interacting system is defined as

$$Z_0 = \text{Tr}(e^{-\beta \hat{K}_0}), \quad (4.75)$$

and for $n \geq 1$, the *non-interacting* temperature Green function G_0^{2n} is defined as

$$\begin{aligned} G_0^{2n}(\mathbf{x}_1, \tau_1; \dots; \mathbf{x}_{2n}, \tau_{2n}) \\ = \frac{1}{Z_0} \text{Tr}(e^{-\beta \hat{K}_0} \mathcal{T}[\hat{\psi}_I(\mathbf{x}_1, \tau_1) \dots \hat{\psi}_I(\mathbf{x}_n, \tau_n) \hat{\psi}_I^\dagger(\mathbf{x}_{2n}, \tau_{2n}) \dots \hat{\psi}_I^\dagger(\mathbf{x}_{n+1}, \tau_{n+1})]) \end{aligned} \quad (4.76)$$

In particular, the free two-point Green function is also called *covariance* and denoted by

$$C(\mathbf{x}_1, \mathbf{x}_2; \tau_1 - \tau_2) \equiv G_0^2(\mathbf{x}_1, \mathbf{x}_2; \tau_1 - \tau_2). \quad (4.77)$$

The perturbative expansion of the full Green functions G^{2n} in terms of the covariance C and the interaction kernel v is based on three fundamental theorems: the *Gell-Mann–Low theorem*, the *Wick theorem*, and the *cancellation theorem* (or their respective analoga for temperature Green functions). For the convenience of the reader, we will explicitly state and prove these three theorems in the following.

4.4.1. Gell-Mann–Low theorem

Theorem 4.6 (Gell-Mann–Low theorem for temperature Green functions). *The partition function of the interacting electron system has the following representation as a formal power series:*

$$Z = \sum_{k=0}^{\infty} \frac{(-\hbar)^{-k}}{k!} \int_0^{\hbar\beta} d\lambda_1 \dots \int_0^{\hbar\beta} d\lambda_k \text{Tr}(e^{-\beta \hat{K}_0} \mathcal{T}[\hat{V}_I(\lambda_1) \dots \hat{V}_I(\lambda_k)]). \quad (4.78)$$

Furthermore, the interacting temperature Green functions are represented by the Gell-Mann–Low formula as follows:

$$\begin{aligned} G^{2n}(\mathbf{x}_1, \tau_1; \dots; \mathbf{x}_{2n}, \tau_{2n}) = \\ \frac{1}{Z} \sum_{k=0}^{\infty} \frac{(-\hbar)^{-k}}{k!} \int_0^{\hbar\beta} d\lambda_1 \dots \int_0^{\hbar\beta} d\lambda_k \text{Tr}(e^{-\beta \hat{K}_0} \mathcal{T}[\hat{V}_I(\lambda_1) \dots \hat{V}_I(\lambda_k) \\ \times \hat{\psi}_I(\mathbf{x}_1, \tau_1) \dots \hat{\psi}_I(\mathbf{x}_n, \tau_n) \hat{\psi}_I^\dagger(\mathbf{x}_{2n}, \tau_{2n}) \dots \hat{\psi}_I^\dagger(\mathbf{x}_{n+1}, \tau_{n+1})]) \end{aligned} \quad (4.79)$$

On the right-hand side of these equations, the interaction operator $\hat{V}_I(\lambda)$ is given in the interaction picture by

$$\hat{V}_I(\lambda) = e^{\hat{K}_0\tau/\hbar} \hat{V} e^{-\hat{K}_0\tau/\hbar} \quad (4.80)$$

$$= \frac{1}{2} \int d^3\mathbf{x} \int d^3\mathbf{x}' \hat{\psi}_I^\dagger(\mathbf{x}, \lambda) \hat{\psi}_I^\dagger(\mathbf{x}', \lambda) v(\mathbf{x}, \mathbf{x}') \hat{\psi}_I(\mathbf{x}', \lambda) \hat{\psi}_I(\mathbf{x}, \lambda), \quad (4.81)$$

and the thermal expectation values are taken with respect to the free Hamiltonian.

Proof. In contrast to the case of real-time Green functions (see Ref. [SS17a]), the proof of the Gell-Mann–Low theorem for temperature Green functions in imaginary time (i.e., Schwinger functions) is rather elementary. Here, we generalize the proof as given for the two-point Green function in Ref. [FW71, Ch. 7]. We begin by noting that the operators $\hat{O}(\tau)$ in the Heisenberg picture and $\hat{O}_I(\tau)$ in the interaction picture (see Eqs. (4.16) and (4.74)) are related by

$$\hat{O}(\tau, \mathbf{x}) = e^{\hat{K}\tau/\hbar} e^{-\hat{K}_0\tau/\hbar} \hat{O}_I(\tau, \mathbf{x}) e^{\hat{K}_0\tau/\hbar} e^{-\hat{K}\tau/\hbar}. \quad (4.82)$$

Equivalently, we can write this as

$$\hat{O}(\tau, \mathbf{x}) = \hat{U}(0, \tau) \hat{O}_I(\tau, \mathbf{x}) \hat{U}(\tau, 0), \quad (4.83)$$

where the (imaginary-time) *evolution operator* is defined for $\tau, \tau' \in \mathbb{R}$ by

$$\hat{U}(\tau, \tau') = e^{\hat{K}_0\tau/\hbar} e^{-\hat{K}(\tau-\tau')/\hbar} e^{-\hat{K}_0\tau'/\hbar}. \quad (4.84)$$

This operator is not unitary, but it satisfies the group property

$$\hat{U}(\tau, \tau') \hat{U}(\tau', \tau'') = \hat{U}(\tau, \tau''). \quad (4.85)$$

Furthermore, the evolution operator fulfills the *equation of motion*

$$(-\hbar) \frac{\partial}{\partial \tau} \hat{U}(\tau, \tau_0) = \hat{V}_I(\tau) \hat{U}(\tau, \tau_0). \quad (4.86)$$

For $\tau > \tau_0$, it follows that $\hat{U}(\tau, \tau_0)$ is the unique solution of the initial value problem defined by Eq. (4.86) and the initial condition

$$\hat{U}(\tau_0, \tau_0) = \hat{1}. \quad (4.87)$$

The formal solution of this initial value problem is given by

$$\hat{U}(\tau_1, \tau_0) = 1 + \sum_{k=1}^{\infty} (-\hbar)^{-k} \int_{\tau_0}^{\tau_1} d\lambda_1 \int_{\tau_0}^{\lambda_1} d\lambda_2 \dots \int_{\tau_0}^{\lambda_{k-1}} d\lambda_k \hat{V}_I(\lambda_1) \dots \hat{V}_I(\lambda_k) \quad (4.88)$$

$$= \sum_{k=0}^{\infty} (-\hbar)^{-k} \int_{\tau_0}^{\tau_1} d\lambda_1 \int_{\tau_0}^{\lambda_1} d\lambda_2 \dots \int_{\tau_0}^{\lambda_{k-1}} d\lambda_k \hat{V}_I(\lambda_1) \dots \hat{V}_I(\lambda_k). \quad (4.89)$$

Using the time-ordering operator as defined by Eq. (4.26), the above expression can be rewritten in an equivalent but more symmetric form as

$$\hat{U}(\tau_1, \tau_0) = \sum_{k=0}^{\infty} \frac{(-\hbar)^{-k}}{k!} \int_{\tau_0}^{\tau_1} d\lambda_1 \dots \int_{\tau_0}^{\tau_1} d\lambda_k \mathcal{T}[\hat{V}_I(\lambda_1) \dots \hat{V}_I(\lambda_k)]. \quad (4.90)$$

With these results, we go on to prove the assertion as follows: First, the partition function is given by

$$Z = \text{Tr}(e^{-\beta \hat{K}}) = \text{Tr}(e^{-\beta \hat{K}_0} \hat{U}(\hbar\beta, 0)). \quad (4.91)$$

Putting the expansion (4.90) into this formula yields directly the desired Eq. (4.78). Next, consider the $2n$ -point Green function. Let us assume, for the moment, that

$$\tau_1 > \dots > \tau_n > \tau_{n+1} > \dots > \tau_{2n}. \quad (4.92)$$

Then, we obtain

$$G^{2n}(\mathbf{x}_1, \tau_1; \dots; \mathbf{x}_{2n}, \tau_{2n}) = (-1)^{n(n-1)/2} \frac{1}{Z} \text{Tr}(e^{-\beta \hat{K}} \hat{\psi}(\mathbf{x}_1, \tau_1) \dots \hat{\psi}^\dagger(\mathbf{x}_{2n}, \tau_{2n})), \quad (4.93)$$

where the sign factor comes from bringing the fermionic field operators into the correct time order. Using Eq. (4.83), we can further transform this expression into

$$G^{2n}(\mathbf{x}_1, \tau_1; \dots; \mathbf{x}_{2n}, \tau_{2n}) \quad (4.94)$$

$$= (-1)^{n(n-1)/2} \frac{1}{Z} \text{Tr}(e^{-\beta \hat{K}_0} \hat{U}(\hbar\beta, 0) [\hat{U}(0, \tau_1) \hat{\psi}_I(\mathbf{x}_1, \tau_1) \hat{U}(\tau_1, 0)] \dots \times [\hat{U}(0, \tau_{2n}) \hat{\psi}_I^\dagger(\mathbf{x}_{2n}, \tau_{2n}) \hat{U}(\tau_{2n}, 0)]) \quad (4.95)$$

$$= (-1)^{n(n-1)/2} \frac{1}{Z} \text{Tr}(e^{-\beta \hat{K}_0} \hat{U}(\hbar\beta, \tau_1) \hat{\psi}_I(\mathbf{x}_1, \tau_1) \hat{U}(\tau_1, \tau_2) \dots \times \hat{U}(\tau_{2n-1}, \tau_{2n}) \hat{\psi}_I^\dagger(\mathbf{x}_{2n}, \tau_{2n}) \hat{U}(\tau_{2n}, 0)). \quad (4.96)$$

The expansion (4.90) of $\hat{U}(\tau_1, \tau_2)$ contains only field operators $\hat{\psi}(\lambda)$ with $\tau_1 \geq \lambda \geq \tau_2$. Therefore, if we expand all operators $\hat{U}(\tau_j, \tau_{j+1})$ in Eq. (4.96), then all fields operators will already be in the correct time order, and hence we obtain

$$G^{2n}(\mathbf{x}_1, \tau_1; \dots; \mathbf{x}_{2n}, \tau_{2n}) = \quad (4.97)$$

$$(-1)^{n(n-1)/2} \frac{1}{Z} \text{Tr}(e^{-\beta \hat{K}_0} \mathcal{T}[\hat{U}(\hbar\beta, \tau_1) \hat{\psi}_I(\mathbf{x}_1, \tau_1) \hat{U}(\tau_1, \tau_2) \dots \times \hat{U}(\tau_{2n-1}, \tau_{2n}) \hat{\psi}_I^\dagger(\mathbf{x}_{2n}, \tau_{2n}) \hat{U}(\tau_{2n}, 0)]) \quad (4.98)$$

Under the time ordering operator, we may change the order of the field operators and move all evolution operators $\hat{U}(\tau_j, \tau_{j+1})$ to the left, which further yields

$$G^{2n}(\mathbf{x}_1, \tau_1; \dots; \mathbf{x}_{2n}, \tau_{2n}) = \quad (4.99)$$

$$(-1)^{n(n-1)/2} \frac{1}{Z} \text{Tr}(e^{-\beta \hat{K}_0} \mathcal{T}[\hat{U}(\hbar\beta, 0) \hat{\psi}_I(\mathbf{x}_1, \tau_1) \dots \hat{\psi}_I^\dagger(\mathbf{x}_{2n}, \tau_{2n})]).$$

Finally, by re-arranging again the field operators, we arrive at

$$G^{2n}(\mathbf{x}_1, \tau_1; \dots; \mathbf{x}_{2n}, \tau_{2n}) = \frac{1}{Z} \text{Tr} \left(e^{-\beta \hat{K}_0} \mathcal{T} [\hat{U}(\hbar\beta, 0) \hat{\psi}_I(\mathbf{x}_1, \tau_1) \dots \hat{\psi}_I(\mathbf{x}_n, \tau_n) \hat{\psi}_I^\dagger(\mathbf{x}_{2n}, \tau_{2n}) \dots \hat{\psi}_I^\dagger(\mathbf{x}_{n+1}, \tau_{n+1})] \right), \quad (4.100)$$

which is equivalent to the Gell-Mann–Low formula. For any other order of the time arguments τ_1, \dots, τ_{2n} than the one assumed in Eq. (4.92), the calculation can be performed analogously and in fact leads to the same result (4.100). This concludes our proof of the Gell-Mann–Low theorem for temperature Green functions. \square

We now introduce some notations by which the Gell-Mann–Low formula can be written in a more compact and symmetric form (for the sake of clarity, we also re-introduce the spin indices): From Eq. (4.81), we obtain

$$\begin{aligned} \int_0^{\hbar\beta} d\lambda \hat{V}_I(\lambda) &= \frac{1}{2} \int d^3\mathbf{x} \int d^3\mathbf{x}' \sum_s \sum_{s'} \int_0^{\hbar\beta} d\lambda \int_0^{\hbar\beta} d\lambda' \\ &\times \hat{\psi}_I^\dagger(\mathbf{x}, s, \lambda) \hat{\psi}_I^\dagger(\mathbf{x}', s', \lambda') v(\mathbf{x}, \mathbf{x}') \delta(\lambda - \lambda') \hat{\psi}_I(\mathbf{x}', s', \lambda') \hat{\psi}_I(\mathbf{x}, s, \lambda). \end{aligned} \quad (4.101)$$

We combine the spatial variable \mathbf{x} , the spin index s and the imaginary-time variable τ into one multi-variable

$$x = (\mathbf{x}, s, \tau). \quad (4.102)$$

Correspondingly, we introduce the shorthand notations

$$\int dx = \int d^3\mathbf{x} \sum_s \frac{1}{\hbar\beta} \int_0^{\hbar\beta} d\tau, \quad (4.103)$$

as well as

$$\delta(x, x') = \delta^3(\mathbf{x} - \mathbf{x}') \delta_{ss'} \hbar\beta \delta(\tau - \tau'), \quad (4.104)$$

and furthermore,

$$v(x, x') = v(\mathbf{x}, \mathbf{x}') \hbar\beta \delta(\tau - \tau'). \quad (4.105)$$

Then, Eq. (4.101) can be written compactly as

$$\int_0^{\hbar\beta} d\lambda \hat{V}_I(\lambda) = \frac{\hbar\beta}{2} \int dx \int dx' \hat{\psi}_I^\dagger(x) \hat{\psi}_I^\dagger(x') v(x, x') \hat{\psi}_I(x') \hat{\psi}_I(x). \quad (4.106)$$

Next, we define the *four-point interaction kernel* as introduced in Ref. [SK12], i.e.,

$$V(x^1, x^2, x^3, x^4) \equiv v(x^2, x^3) \delta(x^1, x^3) \delta(x^2, x^4). \quad (4.107)$$

This allows us to write Eq. (4.106) more symmetrically as

$$\int_0^{\hbar\beta} d\lambda \hat{V}_I(\lambda) = \frac{\hbar\beta}{2} \int dx^1 \int dx^2 \int dx^3 \int dx^4 V(x^1, x^2, x^3, x^4) \hat{\psi}_I^\dagger(x^1) \hat{\psi}_I^\dagger(x^2) \hat{\psi}_I(x^4) \hat{\psi}_I(x^3). \quad (4.108)$$

With these notations, the Gell-Mann–Low formula (4.79) can be written as

$$\begin{aligned}
 G^{2n}(x_1, \dots, x_{2n}) = & \quad (4.109) \\
 & \frac{1}{Z} \sum_{k=0}^{\infty} \frac{(-\beta)^k}{k! 2^k} \left(\prod_{i=1}^k \int dy_i^1 \int dy_i^2 \int dy_i^3 \int dy_i^4 V(y_i^1, y_i^2, y_i^3, y_i^4) \right) \\
 & \times \text{Tr} \left(e^{-\beta \hat{K}_0} \mathcal{T} \left[\hat{\psi}_1^\dagger(y_1^1) \hat{\psi}_1^\dagger(y_1^2) \hat{\psi}_1(y_1^4) \hat{\psi}_1(y_1^3) \dots \hat{\psi}_1^\dagger(y_k^1) \hat{\psi}_1^\dagger(y_k^2) \hat{\psi}_1(y_k^4) \hat{\psi}_1(y_k^3) \right. \right. \\
 & \quad \left. \left. \times \hat{\psi}_1(x_1) \dots \hat{\psi}_1(x_n) \hat{\psi}_1^\dagger(x_{2n}) \dots \hat{\psi}_1^\dagger(x_{n+1}) \right] \right).
 \end{aligned}$$

Finally, the trace in the last line can be rewritten in terms of the free $(2n+4k)$ -point Green functions as

$$\begin{aligned}
 G^{2n}(x_1, \dots, x_{2n}) = & \quad (4.110) \\
 & \frac{1}{Z} \sum_{k=0}^{\infty} \frac{(-\beta)^k}{k! 2^k} \left(\prod_{i=1}^k \int dy_i^1 \int dy_i^2 \int dy_i^3 \int dy_i^4 V(y_i^1, y_i^2, y_i^3, y_i^4) \right) \\
 & \times G_0^{2n+4k}(x_1, \dots, x_n, y_1^3, y_1^4, \dots, y_k^3, y_k^4; x_{n+1}, \dots, x_{2n}, y_1^1, y_1^2, \dots, y_k^1, y_k^2).
 \end{aligned}$$

Similarly, the partition function can be expressed as

$$\begin{aligned}
 Z = & \sum_{k=0}^{\infty} \frac{(-\beta)^k}{k! 2^k} \left(\prod_{i=1}^k \int dy_i^1 \int dy_i^2 \int dy_i^3 \int dy_i^4 V(y_i^1, y_i^2, y_i^3, y_i^4) \right) \\
 & \times G_0^{4k}(y_1^3, y_1^4, \dots, y_k^3, y_k^4; y_1^1, y_1^2, \dots, y_k^1, y_k^2). \quad (4.111)
 \end{aligned}$$

These formulae relate the interacting Green functions G^{2n} to the four-point interaction kernel V and the non-interacting Green functions G_0^{2n+4k} . In the next step, the Wick theorem will allow to derive from this a formal expression of all interacting Green functions in terms of the interaction kernel V and the free two-point Green function G_0^2 . As the Wick theorem is a direct consequence of the equations of motion for the non-interacting temperature Green functions, we will first derive these equations of motion in the following subsection.

4.4.2. Equations of motion

We begin by introducing yet another notation, which will be useful to simplify complicated expressions involving higher $2n$ -point Green functions: we abbreviate

$$G_0^{2n}(1, \dots, 2n) \equiv G_0^{2n}(x_1, \dots, x_{2n}), \quad (4.112)$$

as well as

$$\delta(1, 2) \equiv \delta(x_1, x_2), \quad (4.113)$$

and furthermore,

$$\int d1 f(1) \equiv \int dx_1 f(x_1), \quad (4.114)$$

for any function f depending on the multi-variable $x_1 = (\mathbf{x}_1, s_1, \tau_1)$. In order to keep the notation simple, we will in the following neglect the spin-orbit coupling in the free Hamiltonian (4.2) and correspondingly suppress all the spin indices. All results of this Chapter 4 and the following Chapters 5–7 will, however, hold analogously in the presence of the spin-orbit coupling.

Theorem 4.7 (Equations of motion for non-interacting temperature Green functions). *The free two-point Green function $C \equiv G_0^2$ satisfies the equation of motion*

$$\frac{1}{\hbar} \left(\hbar \frac{\partial}{\partial \tau} - \frac{\hbar^2}{2m} \Delta_{\mathbf{x}} + V_{\text{ext}}(\mathbf{x}) - \mu \right) C(\mathbf{x}, \tau; \mathbf{x}', \tau') = \delta^3(\mathbf{x} - \mathbf{x}') \delta(\tau - \tau'), \quad (4.115)$$

or equivalently,

$$\beta \left(\hbar \frac{\partial}{\partial \tau_1} - \frac{\hbar^2}{2m} \Delta_{\mathbf{x}_1} + V_{\text{ext}}(\mathbf{x}) - \mu \right) C(1, 2) = \delta(1, 2). \quad (4.116)$$

For $n \geq 2$, the equation of motion for the free $2n$ -point Green function reads

$$\begin{aligned} \beta \left(\hbar \frac{\partial}{\partial \tau_1} - \frac{\hbar^2}{2m} \Delta_{\mathbf{x}_1} + V_{\text{ext}}(\mathbf{x}) - \mu \right) G_0^{2n}(1, \dots, 2n) = \\ \sum_{\ell=n+1}^{2n} (-1)^{\ell-n-1} \delta(1, \ell) G_0^{2n-2}(2, \dots, n; n+1, \dots, \check{\ell}, \dots, 2n), \end{aligned} \quad (4.117)$$

where the notation $\check{\ell}$ means that the index ℓ is omitted.

Remarks. i) Equation (4.115) shows that C is indeed a Green function in the mathematical sense, i.e., the inverse of a differential operator. By defining the integral kernel Q of this differential operator such that

$$\begin{aligned} \int d^3 \mathbf{x}' \frac{1}{\hbar \beta} \int_0^{\hbar \beta} d\tau' Q(\mathbf{x}, \tau; \mathbf{x}', \tau') f(\mathbf{x}', \tau') := \\ \beta \left(\hbar \frac{\partial}{\partial \tau} - \frac{\hbar^2}{2m} \Delta_{\mathbf{x}} + V_{\text{ext}}(\mathbf{x}) - \mu \right) f(\mathbf{x}, \tau), \end{aligned} \quad (4.118)$$

we can write Eq. (4.116) equivalently as

$$\int d3 Q(1, 3) C(3, 2) = \delta(1, 2), \quad (4.119)$$

hence C is the inverse integral kernel of Q .

ii) Similar equations can be derived for the derivatives of the Green functions with respect to the other arguments. In particular, the covariance also satisfies

$$\frac{1}{\hbar} \left(-\hbar \frac{\partial}{\partial \tau'} - \frac{\hbar^2}{2m} \Delta_{\mathbf{x}'} + V_{\text{ext}}(\mathbf{x}) - \mu \right) C(\mathbf{x}, \tau; \mathbf{x}', \tau') = \delta^3(\mathbf{x} - \mathbf{x}') \delta(\tau - \tau'), \quad (4.120)$$

which can be shown analogously as Eq. (4.115).

Proof. First, we consider the covariance as defined by

$$\begin{aligned} C(\mathbf{x}, \tau; \mathbf{x}', \tau') = \\ \Theta(\tau - \tau') \langle \hat{\psi}(\mathbf{x}, \tau) \hat{\psi}^\dagger(\mathbf{x}', \tau') \rangle_0 - \Theta(\tau' - \tau) \langle \hat{\psi}^\dagger(\mathbf{x}', \tau') \hat{\psi}(\mathbf{x}, \tau) \rangle_0. \end{aligned} \quad (4.121)$$

Here and in the following, we denote the thermal expectation value with respect to the non-interacting Hamiltonian by

$$\langle \hat{O} \rangle_0 \equiv \text{Tr} (e^{-\beta \hat{K}_0} \hat{O}). \quad (4.122)$$

Moreover, we suppress the index I of the field operators, which indicates their time evolution in the interaction picture. Hence, it is always understood that

$$\hat{\psi}^{(\dagger)}(\mathbf{x}, \tau) \equiv \hat{\psi}_I^{(\dagger)}(\mathbf{x}, \tau) = e^{\hat{K}_0 \tau / \hbar} \hat{\psi}^{(\dagger)}(\mathbf{x}) e^{-\hat{K}_0 \tau / \hbar}, \quad (4.123)$$

with the non-interacting Hamiltonian

$$\hat{K}_0 = \hat{H}_0 - \mu \hat{N} = \int d^3 \mathbf{y} \hat{\psi}^\dagger(\mathbf{y}) \left(-\frac{\hbar^2}{2m} \Delta_{\mathbf{y}} + V_{\text{ext}}(\mathbf{y}) - \mu \right) \hat{\psi}(\mathbf{y}). \quad (4.124)$$

By differentiating Eq. (4.121) with respect to the imaginary-time argument τ and using the distributional identity

$$\partial_\tau \Theta(\tau - \tau') = \delta(\tau - \tau'), \quad (4.125)$$

we obtain the following four terms:

$$\begin{aligned} \partial_\tau C(\mathbf{x}, \tau; \mathbf{x}', \tau') = \\ \delta(\tau - \tau') \langle \hat{\psi}(\mathbf{x}, \tau) \hat{\psi}^\dagger(\mathbf{x}', \tau') \rangle_0 + \delta(\tau' - \tau) \langle \hat{\psi}^\dagger(\mathbf{x}', \tau') \hat{\psi}(\mathbf{x}, \tau) \rangle_0 \\ + \Theta(\tau - \tau') \langle \partial_\tau \hat{\psi}(\mathbf{x}, \tau) \hat{\psi}^\dagger(\mathbf{x}', \tau') \rangle_0 - \Theta(\tau' - \tau) \langle \hat{\psi}^\dagger(\mathbf{x}', \tau') \partial_\tau \hat{\psi}(\mathbf{x}, \tau) \rangle_0. \end{aligned} \quad (4.126)$$

The first two terms can be combined into

$$\delta(\tau - \tau') \langle \hat{\psi}(\mathbf{x}, \tau) \hat{\psi}^\dagger(\mathbf{x}', \tau) + \hat{\psi}^\dagger(\mathbf{x}', \tau) \hat{\psi}(\mathbf{x}, \tau) \rangle_0 = \delta(\tau - \tau') \delta^3(\mathbf{x} - \mathbf{x}'), \quad (4.127)$$

where we have used the canonical anticommutation relations (4.7)–(4.9), which generally hold for the field operators at equal times. The last two terms in Eq. (4.126) can be recombined again by means of the time-ordering operator, thus giving

$$\partial_\tau C(\mathbf{x}, \tau; \mathbf{x}', \tau') = \delta^3(\mathbf{x} - \mathbf{x}') \delta(\tau - \tau') + \langle \mathcal{T} \partial_\tau \hat{\psi}(\mathbf{x}, \tau) \hat{\psi}^\dagger(\mathbf{x}', \tau') \rangle_0. \quad (4.128)$$

Furthermore, the equation of motion for the field operator follows from Eq. (4.123):

$$\partial_\tau \hat{\psi}(\mathbf{x}, \tau) = -\frac{1}{\hbar} e^{\hat{K}_0 \tau / \hbar} [\hat{\psi}(\mathbf{x}), \hat{K}_0]_- e^{-\hat{K}_0 \tau / \hbar}, \quad (4.129)$$

where

$$[\hat{A}, \hat{B}]_- \equiv [\hat{A}, \hat{B}] = \hat{A}\hat{B} - \hat{B}\hat{A} \quad (4.130)$$

denotes the ordinary commutator (cf. Eq. (4.10)). Using the canonical anticommutation relations (4.7)–(4.9), one can show the identity

$$[\hat{\psi}(\mathbf{x}), \hat{\psi}^\dagger(\mathbf{y}) \hat{\psi}(\mathbf{y})]_- = \delta^3(\mathbf{x} - \mathbf{y}) \hat{\psi}(\mathbf{x}), \quad (4.131)$$

which in turn implies

$$[\hat{\psi}(\mathbf{x}), \hat{K}_0]_- = \left(-\frac{\hbar^2}{2m} \Delta_{\mathbf{x}} + V_{\text{ext}}(\mathbf{x}) - \mu \right) \hat{\psi}(\mathbf{x}). \quad (4.132)$$

Therefore, the equation of motion for the field operator reads explicitly as

$$\partial_\tau \hat{\psi}(\mathbf{x}, \tau) = \frac{1}{\hbar} \left(\frac{\hbar^2}{2m} \Delta_{\mathbf{x}} - V_{\text{ext}}(\mathbf{x}) + \mu \right) \hat{\psi}(\mathbf{x}, \tau). \quad (4.133)$$

Putting this result into Eq. (4.128) leads to

$$\partial_\tau C(\mathbf{x}, \tau; \mathbf{x}', \tau') = \delta^3(\mathbf{x} - \mathbf{x}') \delta(\tau - \tau') + \frac{1}{\hbar} \left(\frac{\hbar^2}{2m} \Delta_{\mathbf{x}} - V_{\text{ext}}(\mathbf{x}) + \mu \right) C(\mathbf{x}, \tau; \mathbf{x}', \tau'), \quad (4.134)$$

which is equivalent to the assertion (4.115).

Next, consider the non-interacting $2n$ -point Green function as defined by

$$G_0^{2n}(\mathbf{x}_1, \tau_1; \dots, \mathbf{x}_{2n}, \tau_{2n}) = \langle \mathcal{T} [\hat{\psi}(\mathbf{x}_1, \tau_1) \dots \hat{\psi}(\mathbf{x}_n, \tau_n) \hat{\psi}^\dagger(\mathbf{x}_{2n}, \tau_{2n}) \dots \hat{\psi}^\dagger(\mathbf{x}_{n+1}, \tau_{n+1})] \rangle_0. \quad (4.135)$$

By permuting the fermionic creation operators and using the notation introduced at the beginning of this subsection, we can write this equivalently as

$$G_0^{2n}(1, \dots, 2n) = (-1)^{n(n-1)/2} \langle \mathcal{T} [\hat{\psi}(1) \dots \hat{\psi}(n) \hat{\psi}^\dagger(n+1) \dots \hat{\psi}^\dagger(2n)] \rangle_0. \quad (4.136)$$

In order to write out the time ordering explicitly, we abbreviate the Heaviside step function depending on two imaginary-time arguments as

$$\Theta_{i,j} \equiv \Theta(\tau_i - \tau_j), \quad (4.137)$$

and similarly, we abbreviate the (normalized) Dirac delta distribution as

$$\delta_{i,j} \equiv \hbar\beta \delta(\tau_i - \tau_j). \quad (4.138)$$

Note that this last function depends only on the time variables—in contrast to the function $\delta(i, j)$ defined by Eq. (4.113), which also depends on the spatial variables. With the above notations, we can write Eq. (4.136) explicitly as

$$G_0^{2n}(1, \dots, 2n) = \quad (4.139)$$

$$(-1)^{n(n-1)/2} \sum_{\pi \in S_{2n}} \text{sgn}(\pi) \Theta_{\pi(1), \pi(2)} \dots \Theta_{\pi(2n-1), \pi(2n)} \langle \hat{\psi}^{(\dagger)}(\pi(1)) \dots \psi^{(\dagger)}(\pi(2n)) \rangle_0,$$

where it is understood that

$$\hat{\psi}^{(\dagger)}(i) = \begin{cases} \hat{\psi}(i), & \text{if } 1 \leq i \leq n, \\ \hat{\psi}^\dagger(i), & \text{if } n+1 \leq i \leq 2n. \end{cases} \quad (4.140)$$

Before applying the derivative with respect to the τ_1 variable, we split the sum in Eq. (4.139) into those terms where $\pi(1) = 1$, those where $\pi(2) = 1, \dots$, and those where $\pi(2n) = 1$. Each term can then be rewritten as a sum over all permutations $\sigma \in S_{2n-1}$ of the set $\{2, \dots, 2n\}$, as follows:

$$G_0^{2n}(1, \dots, 2n) = (-1)^{n(n-1)/2} \sum_{\sigma \in S_{2n-1}} \text{sgn}(\sigma) \quad (4.141)$$

$$\times \left(\Theta_{1, \sigma(2)} \Theta_{\sigma(2), \sigma(3)} \dots \Theta_{\sigma(2n-1), \sigma(2n)} \langle \hat{\psi}(1) \hat{\psi}^{(\dagger)}(\sigma(2)) \dots \psi^{(\dagger)}(\sigma(2n)) \rangle_0 \right.$$

$$- \Theta_{\sigma(2), 1} \Theta_{1, \sigma(3)} \dots \Theta_{\sigma(2n-1), \sigma(2n)} \langle \hat{\psi}^{(\dagger)}(\sigma(2)) \hat{\psi}(1) \dots \psi^{(\dagger)}(\sigma(2n)) \rangle_0$$

$$+ \dots$$

$$+ \Theta_{\sigma(2), \sigma(3)} \dots \Theta_{\sigma(2n-1), 1} \Theta_{1, \sigma(2n)} \langle \hat{\psi}^{(\dagger)}(\sigma(2)) \dots \hat{\psi}(1) \hat{\psi}^{(\dagger)}(\sigma(2n)) \rangle_0$$

$$\left. - \Theta_{\sigma(2), \sigma(3)} \dots \Theta_{\sigma(2n-1), \sigma(2n)} \Theta_{\sigma(2n), 1} \langle \hat{\psi}^{(\dagger)}(\sigma(2)) \dots \hat{\psi}^{(\dagger)}(\sigma(2n)) \hat{\psi}(1) \rangle_0 \right).$$

Similarly as in the case of the two-point Green function, the derivative ∂_{τ_1} can act either on one of the Θ functions, or on the field operator $\hat{\psi}(1)$ inside the thermal expectation value. The latter case yields again

$$(-1)^{n(n-1)/2} \langle \mathcal{T} [\partial_{\tau_1} \hat{\psi}(1) \dots \hat{\psi}(n) \hat{\psi}^\dagger(n+1) \dots \hat{\psi}^\dagger(2n)] \rangle_0 \quad (4.142)$$

$$= \frac{1}{\hbar} \left(\frac{\hbar^2}{2m} \Delta_{\mathbf{x}_1} - V_{\text{ext}}(\mathbf{x}_1) + \mu \right) G_0^{2n}(1, \dots, 2n).$$

On the other hand, the terms where the derivative acts on one the Θ functions can be

combined pairwise to give an anticommutator of the field operators. Thus, we obtain

$$\begin{aligned}
& \beta \left(\hbar \frac{\partial}{\partial \tau_1} - \frac{\hbar^2}{2m} \Delta_{\mathbf{x}_1} + V_{\text{ext}}(\mathbf{x}_1) - \mu \right) G_0^{2n}(1, \dots, 2n) = \\
& (-1)^{n(n-1)/2} \sum_{\sigma \in S_{2n-1}} \text{sgn}(\sigma) \\
& \times \left(\delta_{1, \sigma(2)} \Theta_{1, \sigma(3)} \dots \Theta_{\sigma(2n-1), \sigma(2n)} \right. \\
& \quad \times \langle [\hat{\psi}(1), \hat{\psi}^{(\dagger)}(\sigma(2))]_+ \hat{\psi}^{(\dagger)}(\sigma(3)) \dots \hat{\psi}^{(\dagger)}(\sigma(2n)) \rangle_0 \\
& \quad - \delta_{1, \sigma(3)} \Theta_{\sigma(2), 1} \Theta_{1, \sigma(4)} \dots \Theta_{\sigma(2n-1), \sigma(2n)} \\
& \quad \times \langle \hat{\psi}^{(\dagger)}(\sigma(2)) [\hat{\psi}(1), \hat{\psi}^{(\dagger)}(\sigma(3))]_+ \dots \hat{\psi}^{(\dagger)}(\sigma(2n)) \rangle_0 \\
& \quad + \dots \\
& \quad + \delta_{1, \sigma(2n)} \Theta_{\sigma(2), \sigma(3)} \dots \Theta_{\sigma(2n-1), 1} \\
& \quad \times \langle \hat{\psi}^{(\dagger)}(\sigma(2)) \hat{\psi}^{(\dagger)}(\sigma(3)) \dots [\hat{\psi}(1), \hat{\psi}^{(\dagger)}(\sigma(2n))]_+ \rangle_0 \left. \right). \tag{4.143}
\end{aligned}$$

Consider the first term of the sum in brackets: by the canonical anticommutation relations, this vanishes if $\sigma(2) \leq n$. On the other hand, if $\sigma(2) = \ell$ with $n+1 \leq \ell \leq 2n$, we can use that

$$\delta_{1, \ell} [\hat{\psi}(1), \hat{\psi}^{(\dagger)}(\ell)]_+ \equiv \hbar \beta \delta(\tau_1 - \tau_\ell) [\hat{\psi}(\mathbf{x}_1, \tau_1), \hat{\psi}^{(\dagger)}(\mathbf{x}_\ell, \tau_\ell)]_+ \tag{4.144}$$

$$= \hbar \beta \delta(\tau_1 - \tau_\ell) \delta^3(\mathbf{x}_1 - \mathbf{x}_\ell) \equiv \delta(1, \ell). \tag{4.145}$$

Hence, in this latter case, the first term in brackets equals

$$\delta(1, \ell) \Theta_{1, \sigma(3)} \dots \Theta_{\sigma(2n-1), \sigma(2n)} \langle \hat{\psi}^{(\dagger)}(\sigma(3)) \dots \hat{\psi}^{(\dagger)}(\sigma(2n)) \rangle_0. \tag{4.146}$$

Performing the sum over all permutations $\sigma \in S_{2n-1}$ yields for this term

$$\sum_{\ell=n+1}^{2n} \delta(1, \ell) \sum_{\substack{\sigma \in S_{2n-1} \\ \sigma(2)=\ell}} \text{sgn}(\sigma) \Theta_{1, \sigma(3)} \dots \Theta_{\sigma(2n-1), \sigma(2n)} \langle \hat{\psi}^{(\dagger)}(\sigma(3)) \dots \hat{\psi}^{(\dagger)}(\sigma(2n)) \rangle_0. \tag{4.147}$$

Here, we sum over all permutations of the set $\{2, \dots, 2n\}$ which obey the constraint that $\sigma(2) = \ell$. Our aim, however, is to rewrite this expression in terms of a sum over *all* permutations of the reduced set

$$\{2, 3, \dots, \check{\ell}, \dots, 2n\} \equiv \{2, 3, \dots, \ell-1, \ell+1, \dots, 2n\}. \tag{4.148}$$

For this purpose, we decompose each permutation $\sigma \in S_{2n-1}$ into a product

$$\sigma = \sigma' \circ \sigma_\ell, \tag{4.149}$$

where $\sigma_\ell \in S_{2n-1}$ cyclically permutes the variables $(2, \dots, \ell)$, i.e.,

$$(\sigma_\ell(2), \dots, \sigma_\ell(2n)) = (\ell, 2, \dots, \check{\ell}, \dots, 2n), \quad (4.150)$$

and hence we can write

$$(\sigma(2), \dots, \sigma(2n)) = (\sigma'(\ell), \sigma'(2), \dots, \sigma'(\ell-1), \sigma'(\ell+1), \dots, \sigma'(2n)). \quad (4.151)$$

Then, we can replace in Eq. (4.147) the sum over $\sigma \in S_{2n-1}$ by the sum over $\sigma' \in S_{2n-1}$, and the constraint $\sigma(2) = \ell$ by $\sigma'(\ell) = \ell$. Further using that

$$\text{sgn}(\sigma) = \text{sgn}(\sigma') \text{sgn}(\sigma_\ell) = \text{sgn}(\sigma') (-1)^\ell, \quad (4.152)$$

we see that Eq. (4.147) is equivalent to

$$\begin{aligned} & \sum_{\ell=n+1}^{2n} \delta(1, \ell) (-1)^\ell \sum_{\substack{\sigma' \in S_{2n-1} \\ \sigma'(\ell) = \ell}} \text{sgn}(\sigma') \Theta_{1, \sigma'(2)} \dots \Theta_{\sigma'(\ell-1), \sigma'(\ell+1)} \dots \Theta_{\sigma'(2n-1), \sigma'(2n)} \\ & \times \langle \hat{\psi}^{(\dagger)}(\sigma'(2)) \dots \hat{\psi}^{(\dagger)}(\sigma'(\ell-1)) \hat{\psi}^{(\dagger)}(\sigma'(\ell+1)) \dots \hat{\psi}^{(\dagger)}(\sigma'(2n)) \rangle_0. \end{aligned} \quad (4.153)$$

Now, this sum over permutations σ' is obviously equivalent to the sum over all permutations $\pi \in S_{2n-2}$ of the reduced set (4.148), i.e.,

$$\begin{aligned} & \sum_{\ell=n+1}^{2n} \delta(1, \ell) (-1)^\ell \sum_{\pi \in S_{2n-2}} \text{sgn}(\pi) \Theta_{1, \pi(2)} \dots \Theta_{\pi(\ell-1), \pi(\ell+1)} \dots \Theta_{\pi(2n-1), \pi(2n)} \\ & \times \langle \hat{\psi}^{(\dagger)}(\pi(2)) \dots \hat{\psi}^{(\dagger)}(\pi(\ell-1)) \hat{\psi}^{(\dagger)}(\pi(\ell+1)) \dots \hat{\psi}^{(\dagger)}(\pi(2n)) \rangle_0. \end{aligned} \quad (4.154)$$

The remaining terms in the sum of Eq. (4.143) can be evaluated analogously, and thus we arrive at

$$\begin{aligned} & \beta \left(\hbar \frac{\partial}{\partial \tau_1} - \frac{\hbar^2}{2m} \Delta_{\mathbf{x}_1} + V_{\text{ext}}(\mathbf{x}_1) - \mu \right) G_0^{2n}(1, \dots, 2n) = \\ & (-1)^{n(n-1)/2} \sum_{\ell=n+1}^{2n} \delta(1, \ell) (-1)^\ell \sum_{\pi \in S_{2n-2}} \text{sgn}(\pi) \\ & \times \left(\Theta_{1, \pi(2)} \dots \Theta_{\pi(\ell-1), \pi(\ell+1)} \dots \Theta_{\pi(2n-1), \pi(2n)} \right. \\ & \quad + \Theta_{\pi(2), 1} \Theta_{1, \pi(3)} \dots \Theta_{\pi(\ell-1), \pi(\ell+1)} \dots \Theta_{\pi(2n-1), \pi(2n)} \\ & \quad + \dots \\ & \quad \left. + \Theta_{\pi(2), \pi(3)} \dots \Theta_{\pi(\ell-1), \pi(\ell+1)} \dots \Theta_{\pi(2n), 1} \right) \\ & \times \langle \hat{\psi}^{(\dagger)}(\pi(2)) \dots \hat{\psi}^{(\dagger)}(\pi(\ell-1)) \hat{\psi}^{(\dagger)}(\pi(\ell+1)) \dots \hat{\psi}^{(\dagger)}(\pi(2n)) \rangle_0. \end{aligned} \quad (4.155)$$

In the sum over products of Θ functions, the index 1 appears at all possible positions, and hence this sum simply yields

$$\Theta_{\pi(2),\pi(3)} \cdots \Theta_{\pi(\ell-1),\pi(\ell+1)} \cdots \Theta_{\pi(2n-1),\pi(2n)}. \quad (4.156)$$

By resubstituting the non-interacting $(2n-2)$ -point Green function,

$$\begin{aligned} & \sum_{\pi \in S_{2n-2}} \text{sgn}(\pi) \Theta_{\pi(2),\pi(3)} \cdots \Theta_{\pi(\ell-1),\pi(\ell+1)} \cdots \Theta_{\pi(2n-1),\pi(2n)} \\ & \quad \times \langle \hat{\psi}^{(\dagger)}(\pi(2)) \cdots \hat{\psi}^{(\dagger)}(\pi(\ell-1)) \hat{\psi}^{(\dagger)}(\pi(\ell+1)) \cdots \hat{\psi}^{(\dagger)}(\pi(2n)) \rangle_0 \\ & = (-1)^{(n-1)(n-2)/2} G_0^{2n-2}(2, \dots, n; n+1, \dots, \check{\ell}, \dots, 2n), \end{aligned} \quad (4.157)$$

and using that

$$(-1)^{n(n-1)/2} (-1)^{(n-1)(n-2)/2} = (-1)^{(n-1)^2} = (-1)^{n-1} = (-1)^{-n-1}, \quad (4.158)$$

we finally obtain

$$\begin{aligned} & \beta \left(\hbar \frac{\partial}{\partial \tau_1} - \frac{\hbar^2}{2m} \Delta_{\mathbf{x}_1} + V_{\text{ext}}(\mathbf{x}) - \mu \right) G_0^{2n}(1, \dots, 2n) = \\ & \quad \sum_{\ell=n+1}^{2n} (-1)^{\ell-n-1} \delta(1, \ell) G_0^{2n-2}(2, \dots, n; n+1, \dots, \check{\ell}, \dots, 2n), \end{aligned} \quad (4.159)$$

which was the assertion. \square

4.4.3. Wick theorem

Theorem 4.8 (Wick theorem for non-interacting temperature Green functions). *All non-interacting $2n$ -point Green functions factorize into products of two-point Green functions $C \equiv G_0^2$, i.e., for $n \geq 1$,*

$$G_0^{2n}(x_1, \dots, x_{2n}) = \sum_{\pi \in S_n} \text{sgn}(\pi) C(x_1, \pi(x_{n+1})) \cdots C(x_n, \pi(x_{2n})). \quad (4.160)$$

This formula can be written equivalently as

$$G_0^{2n}(x_1, \dots, x_{2n}) = \det \left([C(x_i, x_{n+j})]_{i,j=1,\dots,n} \right) \quad (4.161)$$

in terms of a determinant.

Proof. This follows directly from the equations of motion for the non-interacting Green functions, Theorem 4.7 (see Ref. [SS17a]). We multiply both sides of Eq. (4.117) by the

non-interacting two-point Green function and integrate over the internal variable. Using partial integration and Eq. (4.120), the left-hand side of the equation yields

$$\begin{aligned} & \int d1 \, C(1', 1) \left(\beta \left(\hbar \frac{\partial}{\partial \tau_1} - \frac{\hbar^2}{2m} \Delta_{\mathbf{x}_1} + V_{\text{ext}}(\mathbf{x}_1) - \mu \right) G_0^{2n}(1, \dots, 2n) \right) \\ &= \int d1 \left(\beta \left(-\hbar \frac{\partial}{\partial \tau_1} - \frac{\hbar^2}{2m} \Delta_{\mathbf{x}_1} + V_{\text{ext}}(\mathbf{x}_1) - \mu \right) C(1', 1) \right) G_0^{2n}(1, \dots, 2n) \end{aligned} \quad (4.162)$$

$$= \int d1 \, \delta(1', 1) G_0^{2n}(1, \dots, 2n) \quad (4.163)$$

$$= G_0^{2n}(1', \dots, 2n). \quad (4.164)$$

The evaluation of the right-hand side is even more straightforward, and thus we obtain

$$G_0^{2n}(1', \dots, 2n) = \quad (4.165)$$

$$\sum_{\ell=n+1}^{2n} (-1)^{\ell-n-1} C(1', \ell) G_0^{2n-2}(2, \dots, n; n+1, \dots, \check{\ell}, \dots, 2n),$$

which is equivalent to

$$G_0^{2n}(1, \dots, 2n) = \quad (4.166)$$

$$\sum_{k=1}^n (-1)^{1+k} C(1, n+k) G_0^{2n-2}(2, \dots, n; n+1, \dots, \widetilde{n+k}, \dots, 2n).$$

Now, the assertion follows by induction in n : For $n = 1$, Eq. (4.161) is trivially fulfilled. Assume that it is fulfilled for $(n-1)$, hence

$$\begin{aligned} & G_0^{2n-2}(2, \dots, n; n+1, \dots, \widetilde{n+k}, \dots, 2n) = \\ & \det \left([C(i, n+j)]_{i=2, \dots, n; j=1, \dots, \check{k}, \dots, n} \right). \end{aligned} \quad (4.167)$$

By putting this into Eq. (4.166), the equation of motion turns into the Laplace expansion for the determinant, which shows that the assertion (4.161) holds for n as well. This completes the induction and thus our proof of the Wick theorem. \square

We now come back to the Gell-Mann–Low formula (4.110), which expresses the interacting Green functions in terms of the non-interacting Green functions and the interaction kernel. For the convenience of the reader, we reproduce this formula again here:

$$G^{2n}(x_1, \dots, x_{2n}) = \quad (4.168)$$

$$\begin{aligned} & \frac{1}{Z} \sum_{k=0}^{\infty} \frac{(-\beta)^k}{k! 2^k} \left(\prod_{i=1}^k \int dy_i^1 \int dy_i^2 \int dy_i^3 \int dy_i^4 V(y_i^1, y_i^2, y_i^3, y_i^4) \right) \\ & \times G_0^{2n+4k}(x_1, \dots, x_n, y_1^3, y_1^4, \dots, y_k^3, y_k^4; x_{n+1}, \dots, x_{2n}, y_1^1, y_1^2, \dots, y_k^1, y_k^2). \end{aligned}$$

By the Wick theorem, the non-interacting Green functions factorize into products of two-point functions, i.e.,

$$G_0^{2n+4k}(x_1, \dots, x_n, y_1^3, y_1^4, \dots, y_k^3, y_k^4; x_{n+1}, \dots, x_{2n}, y_1^1, y_1^2, \dots, y_k^1, y_k^2) = \quad (4.169)$$

$$\sum_{\pi \in S_{n+2k}} \text{sgn}(\pi) C(x_1, \pi(x_{n+1})) \dots C(x_n, \pi(x_{2n}))$$

$$\times C(y_1^3, \pi(y_1^1)) C(y_1^4, \pi(y_1^2)) \dots C(y_k^3, \pi(y_k^1)) C(y_k^4, \pi(y_k^2)).$$

Here, we interpret the permutation π to act directly on the set (or more precisely, the tuple) of the $(n + 2k)$ arguments, i.e.,

$$\pi : (x_{n+1}, \dots, x_{2n}, y_1^1, y_1^2, \dots, y_k^1, y_k^2) \mapsto \quad (4.170)$$

$$(\pi(x_{n+1}), \dots, \pi(x_{2n}), \pi(y_1^1), \pi(y_1^2), \dots, \pi(y_k^1), \pi(y_k^2)).$$

By putting Eq. (4.169) into Eq. (4.168), we obtain a formal expression of the interacting Green functions in terms of the covariance C and the interaction kernel V :

$$G^{2n}(x_1, \dots, x_{2n}) = \frac{1}{Z} \sum_{k=0}^{\infty} \frac{1}{k! 2^k} \sum_{\pi \in S_{n+2k}} \text{Val}[n, k, \pi], \quad (4.171)$$

where we have defined

$$\text{Val}[n, k, \pi] \equiv \text{Val}[n, k, \pi](x_1, \dots, x_{2n}) \quad (4.172)$$

$$:= (-\beta)^k \left(\prod_{i=1}^k \int dy_i^1 \int dy_i^2 \int dy_i^3 \int dy_i^4 V(y_i^1, y_i^2, y_i^3, y_i^4) \right) \quad (4.173)$$

$$\times \text{sgn}(\pi) C(x_1, \pi(x_{n+1})) \dots C(x_n, \pi(x_{2n}))$$

$$\times C(y_1^3, \pi(y_1^1)) C(y_1^4, \pi(y_1^2)) \dots C(y_k^3, \pi(y_k^1)) C(y_k^4, \pi(y_k^2)).$$

This last expression is called the *value of the Feynman graph corresponding to the permutation π* , where the arguments n and k indicate that the Feynman graph has $2n$ external slots and k interaction vertices (see Sect. 4.5). Similarly, one can show the formula for the partition function (which appears in the denominator of Eq. (4.171)):

$$Z = \sum_{k=0}^{\infty} \frac{1}{k! 2^k} \sum_{\pi \in S_{2k}} \text{Val}[0, k, \pi], \quad (4.174)$$

where

$$\text{Val}[0, k, \pi] = (-\beta)^k \left(\prod_{i=1}^k \int dy_i^1 \int dy_i^2 \int dy_i^3 \int dy_i^4 V(y_i^1, y_i^2, y_i^3, y_i^4) \right) \quad (4.175)$$

$$\times \text{sgn}(\pi) C(y_1^3, \pi(y_1^1)) C(y_1^4, \pi(y_1^2)) \dots C(y_k^3, \pi(y_k^1)) C(y_k^4, \pi(y_k^2)).$$

Hence, the Feynman graphs appearing in Eq. (4.174) have no external slots and are therefore called *vacuum bubbles*. We will see below (Theorem 4.19) that these terms can be canceled against certain terms in the numerator of Eq. (4.171), which leads to a perturbative expansion of the Green functions in terms of *bubble-free* Feynman graphs.

4.5. Universal Feynman Graphs

4.5.1. Definition

We now come to the graphical representation of the terms $\text{Val}[n, k, \pi]$ which appear in the formal expression (4.171). As mentioned above, we associate with every permutation $\pi \in S_{n+2k}$ a *Feynman graph*, which is constructed as follows (see Table 4.1; cf. [SK12]):

- (i) Each interaction kernel $V(y_i^1, y_i^2, y_i^3, y_i^4)$ is represented by a square with two *internal, outgoing slots* y_i^3, y_i^4 and two *internal, ingoing slots* y_i^1, y_i^2 . These squares are also called “interaction vertices”.
- (ii) We interpret the variables x_1, \dots, x_n as *external, outgoing slots*, and the variables x_{n+1}, \dots, x_{n+2k} as *external, ingoing slots*.
- (iii) Each covariance $C(\cdot, \cdot)$ is represented by an arrow, which connects an (internal or external) outgoing slot with an (internal or external) ingoing slot. These arrows are also called “covariance lines”. Here, the permutation π determines to which ingoing slot each outgoing slot is connected.

Let us illustrate this correspondence between permutations and Feynman graphs by a concrete example. We choose $n = 1$ and $k = 2$, hence we consider Feynman graphs with two external slots (one ingoing, one outgoing) and two interaction vertices. Furthermore, we choose two particular permutations π_1 and $\pi_2 \in S_5$. The first one is the identity permutation,

$$\pi_1 : (x_2, y_1^1, y_1^2, y_2^1, y_2^2) \mapsto (x_2, y_1^1, y_1^2, y_2^1, y_2^2), \quad (4.176)$$

for which $\text{sgn}(\pi_1) = 1$. This yields the value

$$\text{Val}[1, 2, \pi_1] = (-\beta)^2 \int dy_1^1 \int dy_1^2 \int dy_1^3 \int dy_1^4 V(y_1^1, y_1^2, y_1^3, y_1^4) \quad (4.177)$$

$$\times \int dy_2^1 \int dy_2^2 \int dy_2^3 \int dy_2^4 V(y_2^1, y_2^2, y_2^3, y_2^4) \quad (4.178)$$

$$\times C(x_1, x_2) C(y_1^3, y_1^1) C(y_1^4, y_1^2) C(y_2^3, y_2^1) C(y_2^4, y_2^2),$$

which corresponds to the Feynman graph shown in Fig. 4.1a. The covariance lines connect the external slots $x_1 \rightarrow x_2$, as well as the internal slots $y_i^3 \rightarrow y_i^1$ and $y_i^4 \rightarrow y_i^2$ (for $i = 1, 2$). The second permutation which we consider is defined by

$$\pi_2 : (x_2, y_1^1, y_1^2, y_2^1, y_2^2) \mapsto (y_1^1, x_2, y_1^2, y_2^1, y_2^2), \quad (4.179)$$

and it differs from π_1 by the interchange of the first two and the last two arguments. In particular, we also have $\text{sgn}(\pi_2) = 1$. The value of this second permutation is

$$\text{Val}[1, 2, \pi_2] = (-\beta)^2 \int dy_1^1 \int dy_1^2 \int dy_1^3 \int dy_1^4 V(y_1^1, y_1^2, y_1^3, y_1^4) \quad (4.180)$$

$$\times \int dy_2^1 \int dy_2^2 \int dy_2^3 \int dy_2^4 V(y_2^1, y_2^2, y_2^3, y_2^4) \quad (4.181)$$

$$\times C(x_1, y_1^1) C(y_1^3, x_2) C(y_1^4, y_2^1) C(y_2^3, y_2^2) C(y_2^4, y_2^1),$$

which corresponds to the Feynman graph shown in Fig. 4.1b. This latter Feynman graph differs from the former one in that the outgoing slots x_1 and y_1^3 are respectively connected with the ingoing slots y_1^1 and x_2 (instead of the other way around), and similarly, the outgoing slots y_2^3 and y_2^4 are respectively connected with the ingoing slots y_2^2 and y_2^1 .

Finally, we generalize the graphical representation of the four-point interaction kernel V and the covariance C to *all* Green functions by means of the following prescription: any $2n$ -point Green function $G^{2n}(x_1, \dots, x_n; x_{n+1}, \dots, x_{2n})$ shall be represented by a rectangle with n ingoing slots x_1, \dots, x_n and n outgoing slots x_{n+1}, \dots, x_{2n} , as shown in Table 4.1. We call the graphs defined in this way “Universal Feynman Graphs”, because they can be universally used to represent various Green function equations, which we will demonstrate in the following. Thus, the Universal Feynman Graphs may facilitate the communication between different physics communities, where at present different types of graphs are used to represent different Green function equations (such as the ordinary perturbation theory [FW71, Ch. 3, Sct. 9], the relations between ordinary, connected and one-line-irreducible Green functions [NO98, pp. 116ff.], self-consistent Green function equations [Hel+11], or the functional renormalization group equations [Met+12]).

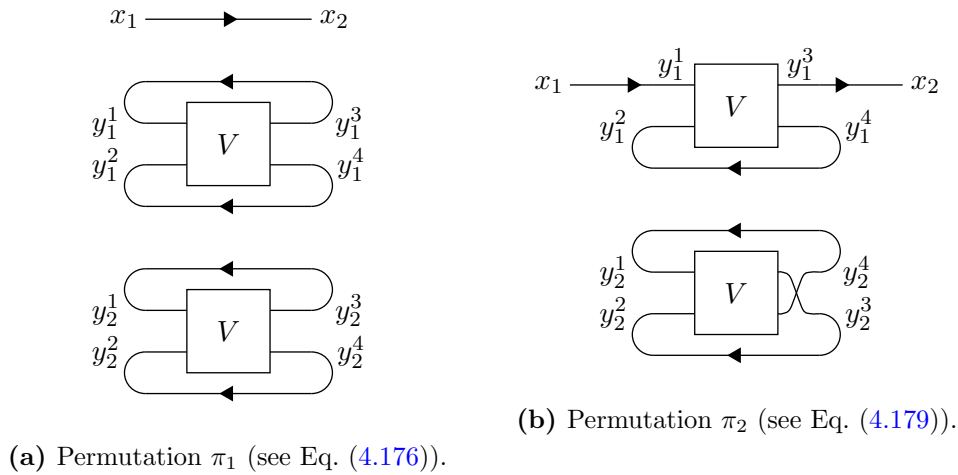


Figure 4.1: Examples of Universal Feynman Graphs and corresponding permutations.

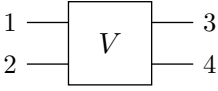
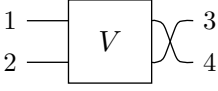
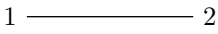

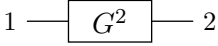
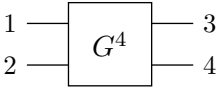
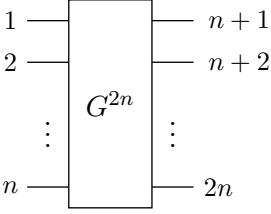
$V(1, 2, 3, 4)$	
$V(1, 2, 4, 3)$	
$\delta(1, 2)$	
$C(1, 2)$	
$G^2(1, 2)$	
$G^4(1, 2, 3, 4)$	
$G^{2n}(1, \dots, n; n+1, \dots, 2n)$	

Table 4.1: Representation of interaction kernels, covariances and interacting Green functions by means of Universal Feynman Graphs.

4.5.2. Classification

Before deriving the perturbative expansion of the interacting Green functions by canceling the denominator in Eq. (4.171) against certain terms in the numerator, we introduce some general notions to classify Feynman graphs.

Definition 4.9. A Feynman graph is called *bubble-free*, if every interaction vertex is connected (through a series of covariance lines and interaction vertices) to *at least one* external slot.

Definition 4.10. A Feynman graph is called *connected*, if it has at least one interaction vertex, and if every interaction vertex is connected (through a series of covariance lines and interaction vertices) to *every* external slot.

Obviously, every connected Feynman graph is bubble-free, but not every bubble-free Feynman graph is connected. Note that in the literature, the term “connected” is usually used for both types of graphs.

Definition 4.11. Consider a connected Feynman graph with $k \geq 1$ interaction vertices. A covariance line of this graph is called

- (i) *internal*, if it connects two internal slots;
- (ii) *external*, if it connects an external slot with an internal slot (or vice versa).

Since a connected Feynman graph does not contain any covariance line which connects two external slots with each other, the above classification is exhaustive, i.e., any covariance line of a connected Feynman graph is either internal or external.

Next, we define the operation of “cutting” an internal covariance line. Consider a connected Feynman graph with $k \geq 1$ interaction vertices and $2n$ external slots, which yields a contribution to the Green function

$$G^{2n}(x_1, \dots, x_n; x_{n+1}, \dots, x_{2n}). \quad (4.182)$$

Let $C(y_1, y_2)$ be an internal covariance line of this graph (connecting the internal, outgoing slot y_1 with the internal, ingoing slot y_2). The operation of *cutting the internal covariance line* is defined by replacing

$$C(y_1, y_2) \mapsto (-1) C(y_1, z_2) C(z_1, y_2), \quad (4.183)$$

where z_1 is a new external, outgoing slot and z_2 a new external, ingoing slot. The resulting Feynman graph (which is not necessarily connected anymore) yields a contribution to (the denominator of) the $(2n + 2)$ -point Green function

$$G^{2n+2}(x_1, \dots, x_n, z_1; x_{n+1}, \dots, x_{2n}, z_2). \quad (4.184)$$

The necessity of including a sign factor in Eq. (4.183) becomes clear if we interpret the operation of cutting a Green function line as a concatenation of two simpler operations (see Fig. 4.2): Assume that the originally given, connected Feynman graph corresponds to a permutation $\pi \in S_{n+2k}$ (Subfigure (a), where we have chosen $n = 1$ and $k = 2$). In the first step, we multiply this Feynman graph by $C(z_1, z_2)$ (Subfigure (b)). Thereby, we obtain a new Feynman graph, which corresponds to a permutation $\sigma \in S_{n+1+2k}$ given explicitly by

$$\begin{aligned} (\sigma(x_{n+1}), \dots, \sigma(x_{2n}), \sigma(z_2), \sigma(y_1^1), \dots, \sigma(y_k^2)) = \\ (\pi(x_{n+1}), \dots, \pi(x_{2n}), z_2, \pi(y_1^1), \dots, \pi(y_k^2)). \end{aligned} \quad (4.185)$$

This permutation σ has the same sign as π , and hence the multiplication of the original Feynman graph by $C(z_1, z_2)$ yields indeed the value of a Feynman graph which contributes to the Green function (4.184). In the next step (Subfigures (c)–(d)), we permute two ingoing slots, namely, we replace

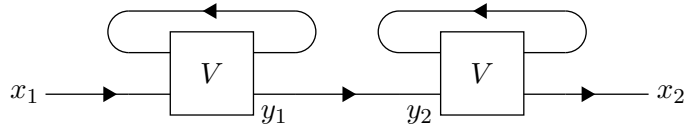
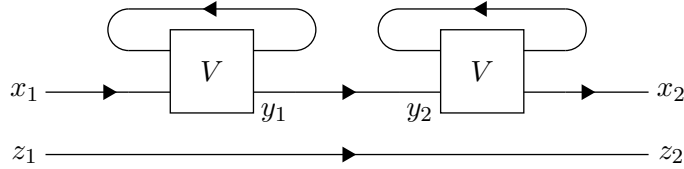
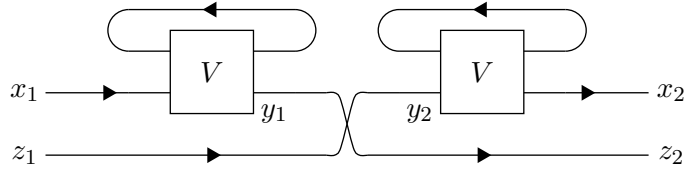
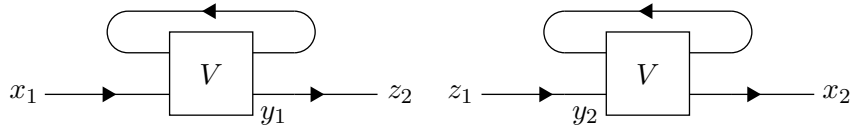
$$C(y_1, y_2) C(z_1, z_2) \mapsto (-1) C(y_1, z_2) C(z_1, y_2). \quad (4.186)$$

The resulting Feynman graph corresponds to another permutation $\sigma' \in S_{n+1+2k}$, which differs from σ by a single transposition:

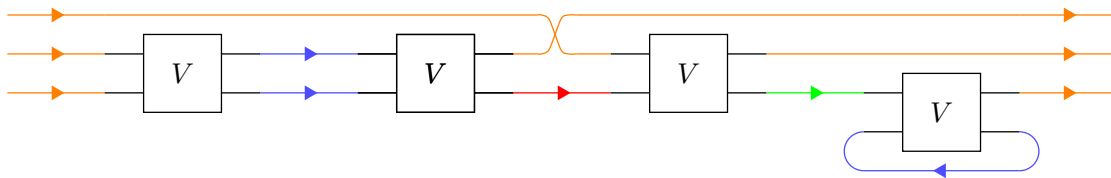
$$(\dots, \sigma'(y_2), \dots, \sigma'(z_2), \dots) = (\dots, \sigma(z_2), \dots, \sigma(y_2), \dots). \quad (4.187)$$

Correspondingly, we have $\text{sgn}(\sigma') = (-1) \text{sgn}(\sigma)$, and the replacement (4.186) indeed yields the value of a Feynman graph which contributes to the Green function (4.184). The concatenation of these two operations (the multiplication with $C(z_1, z_2)$ and the replacement (4.186)) exactly coincides with the operation (4.183) of cutting the internal covariance line. Thus, we have shown that the operation (4.183) indeed transforms any connected Feynman graph which contributes to the $2n$ -point function (4.182) to another Feynman graph which contributes to (the denominator of) the $(2n + 2)$ -point function (4.184).

The operation of cutting internal Green function lines lends itself to another classification of connected Feynman graphs, which we will explain in the following.

(a) Connected Feynman graph corresponding to a permutation $\pi \in S_5$.(b) Feynman graph corresponding to $\sigma \in S_6$, where $\text{sgn}(\sigma) = \text{sgn}(\pi)$.(c) Feynman graph corresponding to $\sigma' \in S_6$, where $\text{sgn}(\sigma') = (-1) \text{sgn}(\sigma)$.

(d) Same Feynman graph as in Subfigure (c).

Figure 4.2: Cutting an internal covariance line.**Figure 4.3:** Classification of the covariance lines of a connected Feynman graph (which contributes to the six-point function): orange = external; blue = internal and non-essential; green = internal extremity line; red = internal torso line.

Definition 4.12. Consider a connected Feynman graph with $2n$ external slots. An *internal* covariance line of this graph is called

- (i) *non-essential*, if by cutting this line the resulting graph remains connected;
- (ii) *essential*, otherwise.

Furthermore, an *essential* covariance line is called

- (ii.a) *extremity line*, if by cutting this line the graph is separated into two parts with $2n_1$ and $2n_2$ external slots, where $n_1 = 1$ and/or $n_2 = 1$ (i.e., at least one part has only two external slots, one ingoing and one outgoing);
- (ii.b) *torso line*, otherwise, i.e., if by cutting this line the graph is separated into two parts with $2n_1$ and $2n_2$ external slots, where $n_1 \geq 2$ and $n_2 \geq 2$.

This classification of internal covariance lines is illustrated for an example Feynman graph in Fig. 4.3. Next, the following simple observation follows directly from the above definitions:

Lemma 4.13. Consider a connected Feynman graph with $2n$ external slots, where $n = 1$ or $n = 2$. Then every essential line is an extremity line.

Proof. The original connected Feynman graph has $2n \leq 4$ external slots. By cutting one essential covariance line, we obtain two Feynman graphs with $2n_1$ and $2n_2$ external slots, respectively, where

$$2n_1 + 2n_2 = 2n + 2 \leq 6. \quad (4.188)$$

This implies that $n_1 = 1$ or $n_2 = 1$, hence the cut line was an extremity line. \square

The above classification of internal covariance lines leads to the following classification of connected Feynman graphs:

Definition 4.14. A connected Feynman graph is called *one-line-reducible*, if it has at least one essential line, and *one-line-irreducible* otherwise.

In the following, we will sometimes omit the “one-line” and simply speak of *reducible* or *irreducible* Feynman graphs. In addition to these already well-established notions, we introduce yet another classification that will prove useful in the following:

Definition 4.15. A connected Feynman graph is called *amputable*, if it has at least one extremity line, and *non-amputable* otherwise.

Obviously, every amputable Feynman graph is reducible (and hence every irreducible graph is non-amputable), but not every reducible Feynman graph is also amputable. However, for $n = 1$ or $n = 2$ these two notions actually coincide:

Lemma 4.16. *Consider a connected Feynman graph with $2n$ external slots, where $n = 1$ or $n = 2$. Then the Feynman graph is reducible if and only if it is amputable.*

Proof. This follows immediately from Lemma 4.13. \square

Finally, we introduce yet another class of graphs, which are called “amputated” (and which are, strictly speaking, not Feynman graphs in the sense of Sect. 4.5.1):

Definition 4.17. Consider a connected Feynman graph with $k \geq 1$ interaction vertices and $2n$ external slots. The value of the corresponding *amputated graph*,

$$\text{Val}_{\text{amp}}[n, k, \pi] \equiv \text{Val}_{\text{amp}}[n, k, \pi](y_1, \dots, y_{2n}), \quad (4.189)$$

is defined such that

$$\begin{aligned} \text{Val}[n, k, \pi](x_1, \dots, x_{2n}) &= \int dy_1 \dots \int dy_{2n} C(x_1, y_1) \dots C(x_n, y_n) \\ &\quad \times \text{Val}_{\text{amp}}[n, k, \pi](y_1, \dots, y_n; y_{n+1}, \dots, y_{2n}) \\ &\quad \times C(y_{n+1}, x_{n+1}) \dots C(y_{2n}, x_{2n}). \end{aligned} \quad (4.190)$$

Hence, the amputated graph is obtained from the given Feynman graph by removing all *external* covariance lines.

We remark that this notion of *amputated* graphs is not directly related to the above notion of *amputable* graphs, as the latter refers only to *internal* covariance lines. However, the notion of amputable graphs can be used to define the following *subclass* of amputated graphs:

Definition 4.18. A *fully amputated* graph is an amputated graph which has no amputable covariance line (i.e., it is non-amputable in the sense of Definition 4.15).

This last notion will be used later to define the so-called fully amputated, connected Green functions (see Sect. 5.4).

4.5.3. Cancellation theorem

We now come back to the formal expression (4.171) of the interacting Green functions in terms of Feynman graphs. As of yet, this formula does not constitute a power series in the interaction, because both the numerator *and* the denominator (which is the partition function Z) are represented separately as power series (see Eq. (4.174)). It turns out, however, that the numerator can be rewritten as a product of two formal power series, one of which cancels precisely against the denominator, thus giving rise to a formal power series of the interacting Green functions in terms of *bubble-free* Feynman graphs. This statement is made precise by the following theorem.

Theorem 4.19 (Cancellation theorem). *For each $n \geq 1$, the interacting temperature Green function G^{2n} can be formally expanded as*

$$G^{2n}(x_1, \dots, x_{2n}) = \sum_{k=0}^{\infty} \frac{1}{k! 2^k} \sum_{\substack{\pi \in S_{n+2k}, \\ \pi \text{ bubble-free}}} \text{Val}[n, k, \pi], \quad (4.191)$$

where for each k , the sum is over all bubble-free Feynman graphs with $2n$ external slots and k interaction vertices.

Remark. If we replace the interaction kernel by

$$V \mapsto \lambda V \quad (4.192)$$

with a dimensionless parameter λ called *interaction strength*, then each term $\text{Val}[n, k, \pi]$ is of the order k in the interaction strength, and hence Eq. (4.191) can be regarded as a formal power series in the interaction strength.

Proof. Every Feynman graph $\pi \in S_{n+2k}$ can be uniquely decomposed into a bubble-free graph $\pi' \in S_{n+2\ell}$ and a vacuum bubble $\sigma \in S_{2(k-\ell)}$, where $\ell \in \{0, \dots, k\}$. Assume, for example, that the first ℓ vertices are connected to the external slots, while the last $(k-\ell)$ vertices form a vacuum bubble, i.e.,

$$\begin{aligned} & (\pi(x_{n+1}), \dots, \pi(x_{2n}), \pi(y_1^1), \pi(y_1^2), \dots, \pi(y_k^1), \pi(y_k^2)) = \\ & (\pi'(x_{n+1}), \dots, \pi'(x_{2n}), \pi'(y_1^1), \pi'(y_1^2), \dots, \pi'(y_\ell^1), \pi'(y_\ell^2), \\ & \sigma(y_{\ell+1}^1), \sigma(y_{\ell+1}^2), \dots, \sigma(y_k^1), \sigma(y_k^2)). \end{aligned} \quad (4.193)$$

Then, the sign of the permutation π equals

$$\text{sgn}(\pi) = \text{sgn}(\pi') \text{sgn}(\sigma), \quad (4.194)$$

and from the definition (4.173) we obtain

$$\text{Val}[n, k, \pi] = \text{Val}[n, \ell, \pi'] \text{Val}[0, k - \ell, \sigma]. \quad (4.195)$$

These equations remain valid if ℓ arbitrary vertices (instead of the first ℓ vertices) are connected to the external slots. Thus, we can write

$$\sum_{\pi \in S_{n+2k}} \text{Val}[n, k, \pi] = \sum_{\ell=0}^k \frac{k!}{\ell! (k-\ell)!} \sum_{\substack{\pi' \in S_{n+2\ell}, \\ \pi' \text{ bubble-free}}} \text{Val}[n, \ell, \pi'] \sum_{\sigma \in S_{2(k-\ell)}} \text{Val}[0, k - \ell, \sigma], \quad (4.196)$$

where the factor $k!/\ell!(k-\ell)!$ counts the number of possibilities by which the k vertices of a given graph can be partitioned into ℓ vertices of a bubble-free graph and $(k-\ell)$

vertices of a vacuum bubble. By putting this result into Eq. (4.171), we find

$$\begin{aligned}
 G^{2n}(x_1, \dots, x_{2n}) &= \frac{1}{Z} \sum_{k=0}^{\infty} \sum_{\ell=0}^k \frac{1}{\ell! 2^\ell} \sum_{\substack{\pi' \in S_{n+2\ell}, \\ \pi' \text{ bubble-free}}} \text{Val}[n, \ell, \pi'] \\
 &\times \frac{1}{(k-\ell)! 2^{k-\ell}} \sum_{\sigma \in S_{2(k-\ell)}} \text{Val}[0, k-\ell, \sigma].
 \end{aligned} \tag{4.197}$$

Finally, by re-arranging the summations according to

$$\sum_{k=0}^{\infty} \sum_{\ell=0}^k f(\ell) g(k-\ell) = \sum_{\ell=0}^{\infty} \sum_{\ell'=0}^{\infty} f(\ell) g(\ell') = \sum_{\ell=0}^{\infty} f(\ell) \sum_{\ell'=0}^{\infty} g(\ell'), \tag{4.198}$$

the second factor in Eq. (4.197) precisely reverts to the expression (4.174) of the partition function and thereby cancels the prefactor $1/Z$, which proves the assertion. \square

The perturbative expansion (4.191) can be further simplified by noting that in each order k , there are several Feynman graphs which have exactly the same value. Concretely, two Feynman graphs have the same value if they can be transformed into each other by (i) simultaneously interchanging the two ingoing and the two outgoing slots of one or more interaction vertices, and/or (ii) interchanging different interaction vertices. The first equality follows from the symmetry

$$V(y^1, y^2, y^3, y^4) = V(y^2, y^1, y^4, y^3) \tag{4.199}$$

of the four-point interaction kernel given by Eq. (4.107). The second equality can be shown from the definition (4.173) by *relabeling* the integration variables (for $i \neq j$)

$$(y_i^1, y_i^2, y_i^3, y_i^4) \leftrightarrow (y_j^1, y_j^2, y_j^3, y_j^4). \tag{4.200}$$

In the k th order, there are precisely $2^k k!$ such *topologically equivalent* Feynman graphs, i.e., graphs which can be transformed into each other by means of the operations (i) and/or (ii), and which therefore have exactly the same value. Consequently, we can simplify Eq. (4.191) by counting each of these equivalent Feynman graphs only once and cancel the prefactor $1/(2^k k!)$ for it. This statement is made precise by the following theorem.

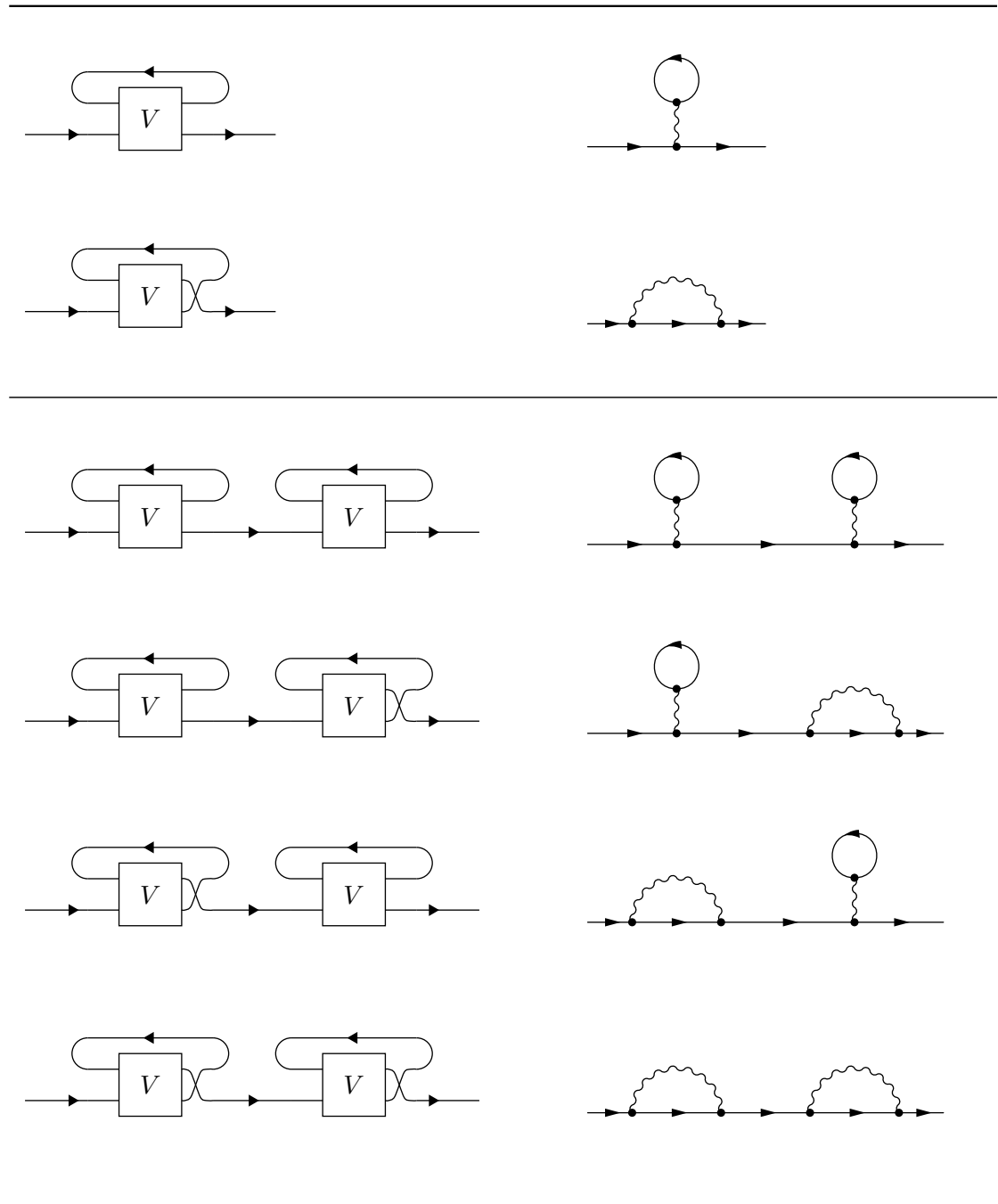
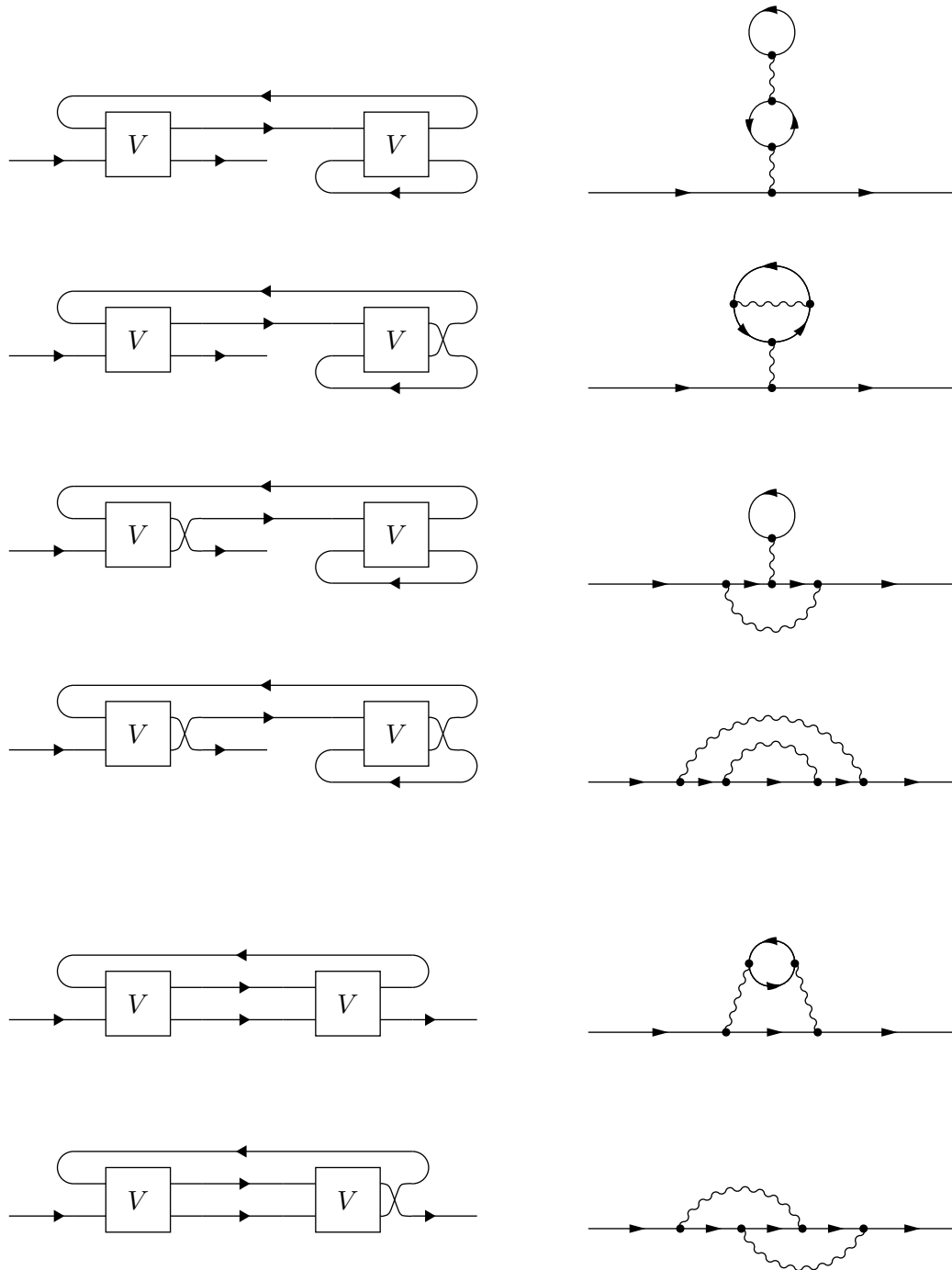


Table 4.2: First- and second-order perturbation theory. *Left column:* Universal Feynman Graphs. *Right column:* traditional Feynman graphs.

**Table 4.2:** First- and second-order perturbation theory (continued).

Theorem 4.20 (Feynman graph expansion of temperature Green functions). *For each $n \geq 1$, the interacting temperature Green function G^{2n} can be formally expanded in terms of the interaction kernel V and the covariance $C \equiv G_0^2$ as*

$$G^{2n}(x_1, \dots, x_{2n}) = \sum_{k=0}^{\infty} \sum'_{\substack{\pi \in S_{n+2k}, \\ \pi \text{ bubble-free}}} \text{Val}[n, k, \pi]. \quad (4.201)$$

Here, for each k , the primed sum is over all topologically distinct bubble-free Feynman graphs with $2n$ external slots and k interaction vertices, and $\text{Val}[n, k, \pi]$ denotes the value of the Feynman graph corresponding to the permutation π as defined by Eq. (4.173).

We remark that in the first order ($k = 1$), there are exactly two topologically distinct bubble-free Feynman graphs, while in the second order ($k = 2$), there are exactly ten such graphs. These first- and second-order Feynman graphs are shown in Table 4.2—both in the Universal Feynman Graph representation (see Sct. 4.5.1) and in the traditional representation (see e.g. Ref. [FW71]).

Finally, let us summarize the advantages of the Universal Feynman Graphs (for the reason of this labeling, see p. 95): (i) they can be universally used for representing various Green function equations, such as the ordinary perturbation theory (this chapter), the relations between ordinary, connected and one-line-irreducible Green functions (next chapter), the equations of motion and self-consistent Green function equations (see Ref. [SK12]), or the functional renormalization group equations (Ch. 6), (ii) they are more clearly arranged than the traditional Feynman graphs, and hence they also reveal certain similarities between different Feynman graphs (see Table 4.2), (iii) they make the correspondence between Feynman graphs and permutations more obvious (see Sct. 4.5.1), and (iv) the value of a given Universal Feynman Graph can be read off easily and without ambiguity (see Eq. (4.173)). Finally, (v) the Universal Feynman Graphs may prevent from the outset any possible misinterpretation of the traditional Feynman graphs in terms of (possibly “virtual”) particle trajectories, and thus they contribute to the overcoming of the physically flawed philosophical realism.

5. Grassmann field integral

5.1. Grassmann algebra

5.1.1. Basic definitions

We consider the Grassmann algebra \mathcal{A} generated by the *Grassmann field variables*

$$\psi(x), \bar{\psi}(x), \quad (5.1)$$

where $x = (\mathbf{x}, s, \tau) \in \mathbb{R}^3 \times \{\uparrow, \downarrow\} \times [0, \hbar\beta)$, and we identify

$$\psi(\mathbf{x}, s, \hbar\beta) \equiv -\psi(\mathbf{x}, s, 0), \quad (5.2)$$

$$\bar{\psi}(\mathbf{x}, s, \hbar\beta) \equiv -\bar{\psi}(\mathbf{x}, s, 0). \quad (5.3)$$

The generators of the Grassmann algebra have the same dimensions as the field operators introduced in the previous chapter (see Eq. (4.24)), i.e.,

$$[\psi(x)] = [\bar{\psi}(x)] = m^{-3/2}. \quad (5.4)$$

Any element $A \in \mathcal{A}$ is called a *Grassmann variable* and can be uniquely expanded in terms of the generators as

$$\begin{aligned} A = & \sum_{n=0}^{\infty} \sum_{m=0}^{\infty} \int dx_1 \dots \int dx_n \int dy_1 \dots \int dy_m \\ & \times f^{n,m}(x_1, \dots, x_n; y_1, \dots, y_m) \bar{\psi}(x_1) \dots \bar{\psi}(x_n) \psi(y_1) \dots \psi(y_m), \end{aligned} \quad (5.5)$$

where the complex coefficient functions $f^{n,m}$ are assumed to be totally antisymmetric with respect to their first n arguments and their last m arguments. In particular, $f^{0,0}$ is called the *constant term* (or *field-independent term*) of the Grassmann variable A .

Let us briefly summarize the most important properties of the Grassmann algebra, which will be used in the following (for details, see Ref. [Sal99, Appendix B.2]). First, the generators of the Grassmann algebra anticommute,

$$\psi(x) \psi(x') = -\psi(x') \psi(x), \quad (5.6)$$

$$\bar{\psi}(x) \bar{\psi}(x') = -\bar{\psi}(x') \bar{\psi}(x), \quad (5.7)$$

$$\psi(x) \bar{\psi}(x') = -\bar{\psi}(x') \psi(x). \quad (5.8)$$

Next, the *differentiation* with respect to these generators is defined for monomials as

$$\begin{aligned} \frac{\delta}{\delta \bar{\psi}(x)} \bar{\psi}(x_1) \dots \bar{\psi}(x_n) \psi(y_1) \dots \psi(y_m) = \\ \sum_{i=1}^n (-1)^{i-1} \delta(x - x_i) \bar{\psi}(x_1) \dots \bar{\psi}(x_{i-1}) \bar{\psi}(x_{i+1}) \dots \bar{\psi}(x_n) \psi(y_1) \dots \psi(y_m), \end{aligned} \quad (5.9)$$

and respectively,

$$\begin{aligned} \frac{\delta}{\delta \psi(y)} \bar{\psi}(x_1) \dots \bar{\psi}(x_n) \psi(y_1) \dots \psi(y_m) = \\ \sum_{j=1}^m (-1)^{n+j-1} \delta(y - y_j) \bar{\psi}(x_1) \dots \bar{\psi}(x_n) \psi(y_1) \dots \psi(y_{j-1}) \psi(y_{j+1}) \dots \psi(y_m). \end{aligned} \quad (5.10)$$

For an arbitrary Grassmann variable $A \in \mathcal{A}$, the corresponding derivatives are defined by expanding A as in Eq. (5.5) and differentiating each monomial separately, i.e., by stipulating the linearity of the Grassmann derivatives. Furthermore, the Grassmann *integration* is defined identically as the differentiation, i.e.,

$$\int d\psi(x) A = \frac{\delta}{\delta \psi(x)} A, \quad \int d\bar{\psi}(x) A = \frac{\delta}{\delta \bar{\psi}(x)} A. \quad (5.11)$$

Finally, the *Grassmann field integral* is defined as

$$\int d\bar{\psi} d\psi = \prod_x \left(\int d\bar{\psi}(x) \int d\psi(x) \right), \quad (5.12)$$

where the formal product ranges over all $x \in \mathbb{R}^3 \times \{\uparrow, \downarrow\} \times [0, \hbar\beta)$. We remark that in this thesis, we use the Grassmann field integral as a heuristic tool, and hence we do not seek to define it as a mathematical object. In fact, the only property of the field integral which we will use is the standard result for Gaussian integrals, which will be explained in the following subsection (see Ref. [SS16b]).

5.1.2. Grassmann–Gaussian integral

Let Q be the inverse integral kernel of the covariance C as defined by Eq. (4.118). We first define the formal product

$$\langle \bar{\psi}, Q\psi \rangle = \int dx \int dx' \bar{\psi}(x) Q(x, x') \psi(x'), \quad (5.13)$$

which is equivalent to

$$\langle \bar{\psi}, Q\psi \rangle = \int d^3\mathbf{x} \sum_s \int d\tau \bar{\psi}(\mathbf{x}, s, \tau) \left(\frac{\partial}{\partial \tau} - \frac{\hbar}{2m} \Delta_{\mathbf{x}} - \frac{\mu}{\hbar} \right) \psi(\mathbf{x}, s, \tau). \quad (5.14)$$

With this, we define a *Grassmann–Gaussian integral* as an expression of the form

$$\frac{1}{\mathcal{N}} \int d\bar{\psi} d\psi e^{-\langle \bar{\psi}, Q \psi \rangle} A, \quad (5.15)$$

with the normalization constant

$$\mathcal{N} = \int d\bar{\psi} d\psi e^{-\langle \bar{\psi}, Q \psi \rangle}, \quad (5.16)$$

where $A \in \mathcal{A}$ may denote any Grassmann variable. The following lemma concerns the fundamental property of such Gaussian integrals (see Ref. [Sal99, Lemma B.7]).

Lemma 5.1 (Factorization property of the Grassmann–Gaussian integral).

The Gaussian integral over a monomial with an equal number of $\bar{\psi}$ and ψ generators yields an antisymmetrized product of covariances, i.e.,

$$\begin{aligned} \frac{1}{\mathcal{N}} \int d\bar{\psi} d\psi e^{-\langle \bar{\psi}, Q \psi \rangle} \psi(x_1) \dots \psi(x_n) \bar{\psi}(x_{2n}) \dots \bar{\psi}(x_{n+1}) = \\ \sum_{\pi \in S_n} \text{sgn}(\pi) C(x_1, \pi(x_{n+1})) \dots C(x_n, \pi(x_{2n})). \end{aligned} \quad (5.17)$$

This formula can be written equivalently in terms of a determinant as

$$\begin{aligned} \frac{1}{\mathcal{N}} \int d\bar{\psi} d\psi e^{-\langle \bar{\psi}, Q \psi \rangle} \psi(x_1) \dots \psi(x_n) \bar{\psi}(x_{2n}) \dots \bar{\psi}(x_{n+1}) = \\ \det \left([C(x_i, x_{n+j})]_{i,j=1,\dots,n} \right). \end{aligned} \quad (5.18)$$

Furthermore, all Gaussian integrals over monomials with a different number of $\bar{\psi}$ and ψ generators vanish.

Before proceeding with the proof, we introduce an additional Grassmann algebra \mathcal{S} (besides \mathcal{A}), which is generated by the elements (also called *sources* or *source fields*)

$$\eta(x), \bar{\eta}(x), \quad (5.19)$$

where again, we identify

$$\eta(\mathbf{x}, s, \hbar\beta) \equiv -\eta(\mathbf{x}, s, 0), \quad (5.20)$$

$$\bar{\eta}(\mathbf{x}, s, \hbar\beta) \equiv -\bar{\eta}(\mathbf{x}, s, 0). \quad (5.21)$$

The elements of \mathcal{S} have the same units as the elements of \mathcal{A} (see Eq. (5.4)), hence

$$[\eta(x)] = [\bar{\eta}(x)] = \text{m}^{-3/2}. \quad (5.22)$$

We further allow for formal multiplications between elements of \mathcal{A} and \mathcal{S} , and we require this multiplication to be anticommutative as well, e.g.,

$$\bar{\psi}(x)\eta(x) = -\eta(x)\bar{\psi}(x). \quad (5.23)$$

In particular, we define the formal inner product

$$\langle \bar{\psi}, \eta \rangle \equiv \int dx \bar{\psi}(x) \eta(x), \quad (5.24)$$

which is a dimensionless quantity. We now proceed with the proof of Lemma 5.1.

Proof. We begin by rewriting the Grassmann–Gaussian integral of Eq. (5.17) using the source fields as follows:

$$\begin{aligned} & \frac{1}{\mathcal{N}} \int d\bar{\psi} d\psi e^{-\langle \bar{\psi}, Q\psi \rangle} \psi(x_1) \dots \psi(x_n) \bar{\psi}(x_{2n}) \dots \bar{\psi}(x_{n+1}) = \\ & \frac{1}{\mathcal{N}} \left(\frac{\delta}{\delta \bar{\eta}(x_1)} \dots \frac{\delta}{\delta \bar{\eta}(x_n)} \frac{\delta}{\delta \eta(x_{2n})} \dots \frac{\delta}{\delta \eta(x_{n+1})} \right) \int d\bar{\psi} d\psi e^{-\langle \bar{\psi}, Q\psi \rangle + \langle \bar{\eta}, \psi \rangle + \langle \eta, \bar{\psi} \rangle} \Big|_{\eta = \bar{\eta} = 0}. \end{aligned} \quad (5.25)$$

Here, the expression on the right-hand side is an element of the Grassmann algebra \mathcal{S} , and the notation $\eta = \bar{\eta} = 0$ indicates that the constant term of this Grassmann variable should be evaluated (see the remark on p. 112). The field integral on the right-hand side can be calculated explicitly by completing the square in the exponent (see Ref. [Sal99, Lemma B.6]). For this purpose, we write

$$\langle \bar{\eta}, \psi \rangle = \langle \bar{\eta}, CQ\psi \rangle = \langle C^T \bar{\eta}, Q\psi \rangle, \quad (5.26)$$

where we have generalized the notation (5.13) in an obvious way, and where we have defined the transpose of the integral kernel C as

$$C^T(x, x') = C(x', x). \quad (5.27)$$

Similarly, we rewrite the last term in the exponent as

$$\langle \eta, \bar{\psi} \rangle = -\langle \bar{\psi}, \eta \rangle = -\langle \bar{\psi}, QC\eta \rangle. \quad (5.28)$$

Thus, we obtain (using [Sal99, Corollary B.2])

$$\int d\bar{\psi} d\psi e^{-\langle \bar{\psi}, Q\psi \rangle + \langle \bar{\eta}, \psi \rangle + \langle \eta, \bar{\psi} \rangle} = e^{-\langle \bar{\eta}, C\eta \rangle} \int d\bar{\psi} d\psi e^{-\langle \bar{\psi} - C^T \bar{\eta}, Q(\psi + C\eta) \rangle} \quad (5.29)$$

$$= e^{-\langle \bar{\eta}, C\eta \rangle} \int d\bar{\psi} d\psi e^{-\langle \bar{\psi}, Q\psi \rangle} \quad (5.30)$$

$$= e^{-\langle \bar{\eta}, C\eta \rangle} \mathcal{N}. \quad (5.31)$$

Putting this result into Eq. (5.25) yields

$$\begin{aligned} & \frac{1}{\mathcal{N}} \int d\bar{\psi} d\psi e^{-\langle \bar{\psi}, Q\psi \rangle} \psi(x_1) \dots \psi(x_n) \bar{\psi}(x_{2n}) \dots \bar{\psi}(x_{n+1}) \\ & = \left(\frac{\delta}{\delta \bar{\eta}(x_1)} \dots \frac{\delta}{\delta \bar{\eta}(x_n)} \frac{\delta}{\delta \eta(x_{2n})} \dots \frac{\delta}{\delta \eta(x_{n+1})} \right) e^{-\langle \bar{\eta}, C\eta \rangle} \Big|_{\eta = \bar{\eta} = 0}. \end{aligned} \quad (5.32)$$

Next, we evaluate the derivatives with respect to the η sources: for $j = 1, \dots, n$, we have

$$\frac{\delta}{\delta \eta(x_{n+j})} e^{-\langle \bar{\eta}, C \eta \rangle} = \left(-\frac{\delta}{\delta \eta(x_{n+j})} \langle \bar{\eta}, C \eta \rangle \right) e^{-\langle \bar{\eta}, C \eta \rangle} \quad (5.33)$$

$$= \left(\int dy_j \bar{\eta}(y_j) C(y_j, x_{n+j}) \right) e^{-\langle \bar{\eta}, C \eta \rangle}. \quad (5.34)$$

Since the factor in front of the exponential does not depend on η anymore, we can successively evaluate all the η derivatives, and thus we obtain

$$\begin{aligned} & \left(\frac{\delta}{\delta \eta(x_{2n})} \cdots \frac{\delta}{\delta \eta(x_{n+1})} \right) e^{-\langle \bar{\eta}, C \eta \rangle} = \\ & \left(\int dy_n \bar{\eta}(y_n) C(y_n, x_{2n}) \right) \cdots \left(\int dy_1 \bar{\eta}(y_1) C(y_1, x_{n+1}) \right) e^{-\langle \bar{\eta}, C \eta \rangle}. \end{aligned} \quad (5.35)$$

By further evaluating the $\bar{\eta}$ derivatives and keeping only the constant term of the resulting expression, we arrive at

$$\begin{aligned} & \left(\frac{\delta}{\delta \bar{\eta}(x_1)} \cdots \frac{\delta}{\delta \bar{\eta}(x_n)} \frac{\delta}{\delta \eta(x_{2n})} \cdots \frac{\delta}{\delta \eta(x_{n+1})} \right) e^{\langle \bar{\eta}, C \eta \rangle} \Big|_{\eta = \bar{\eta} = 0} \\ &= \int dy_1 \cdots \int dy_n C(y_1, x_{n+1}) \cdots C(y_n, x_{2n}) \left(\frac{\delta}{\delta \bar{\eta}(x_1)} \cdots \frac{\delta}{\delta \bar{\eta}(x_n)} \bar{\eta}(y_n) \cdots \bar{\eta}(y_1) \right) \\ &= \int dy_1 \cdots \int dy_n C(y_1, x_{n+1}) \cdots C(y_n, x_{2n}) \sum_{\pi \in S_n} \text{sgn}(\pi) \delta(y_1, \pi(x_1)) \cdots \delta(y_n, \pi(x_n)) \\ &= \sum_{\pi \in S_n} \text{sgn}(\pi) C(\pi(x_1), x_{n+1}) \cdots C(\pi(x_n), x_{2n}), \end{aligned} \quad (5.36)$$

which is equivalent to the assertion (5.17). Finally, the fact that Gaussian integrals over monomials with a different number of $\bar{\psi}$ and ψ generators vanish becomes almost obvious if we consider Eq. (5.32): There, the exponential can be expanded into a sum of monomials which all have an equal number of $\bar{\eta}$ and η sources. If we then take a different number of $\bar{\eta}$ and η derivatives, all resulting terms will be of a different order in η and $\bar{\eta}$, which implies in particular that the constant term vanishes. \square

5.2. Green function generator

In this section, we will prove the *Grassmann field integral representation* of the temperature Green functions. This result establishes the equivalence between the operator formalism (as described in Ch. 4) and the *field integral* (or *functional integral*, *path integral*) formalism of fermionic quantum field theory.

Definition 5.2. The *Green function generator* $\mathcal{Z} \equiv \mathcal{Z}[\bar{\eta}, \eta]$ is an element of the Grassmann algebra \mathcal{S} defined as

$$\mathcal{Z} = \frac{1}{\mathcal{N}} \int d\bar{\psi} d\psi e^{-\langle \bar{\psi}, Q\psi \rangle} e^{-\beta V[\bar{\psi}, \psi] + \langle \bar{\eta}, \psi \rangle + \langle \eta, \bar{\psi} \rangle}, \quad (5.37)$$

with the normalization constant

$$\mathcal{N} = \int d\bar{\psi} d\psi e^{-\langle \bar{\psi}, Q\psi \rangle}. \quad (5.38)$$

Here, $Q = C^{-1}$ is the inverse of the covariance (see Eq. (5.14)), and

$$V[\bar{\psi}, \psi] \equiv \frac{1}{2} \int dx^1 \int dx^2 \int dx^3 \int dx^4 V(x^1, x^2, x^3, x^4) \bar{\psi}(x^1) \bar{\psi}(x^2) \psi(x^4) \psi(x^3), \quad (5.39)$$

with the four-point interaction kernel V given by Eq. (4.107).

Remark. The notation $\mathcal{Z} \equiv \mathcal{Z}[\bar{\eta}, \eta]$ can be used to indicate that \mathcal{Z} is an element of the Grassmann algebra \mathcal{S} generated by $\bar{\eta}(x)$ and $\eta(x)$. In particular, the Green function generator can be expanded (as every element of \mathcal{S}) in terms of the sources as

$$\mathcal{Z}[\bar{\eta}, \eta] = Z + \int dx_1 \int dx_2 f(x_1, x_2) \bar{\eta}(x_1) \eta(x_2) + \dots, \quad (5.40)$$

with a constant term $Z \in \mathbb{C}$, a complex function $f(x_1, x_2) \in \mathbb{C}$, etc. (see Theorem 5.3 for the concrete form of this expansion). In particular, we denote the constant term of this expansion by

$$Z \equiv \mathcal{Z}[0, 0] \equiv \mathcal{Z}[\bar{\eta}, \eta] \big|_{\eta=\bar{\eta}=0}. \quad (5.41)$$

However, the notation $\mathcal{Z} \equiv \mathcal{Z}[\bar{\eta}, \eta]$ does *not* imply that \mathcal{Z} is a *functional* of the sources. In fact, it is not a functional, because η is not an arbitrary function mapping each x to some arbitrary “value” $\eta(x)$. To the contrary, we had defined $\eta(x)$ from the beginning as a fixed element (namely, as one of the generators) of the Grassmann algebra \mathcal{S} . Therefore, one cannot “set $\eta(x)$ to zero” either, and the notation (5.41) for the constant term in the expansion (5.40) is only formal.¹

¹This is in contrast to the bosonic case, where the *generating functional* $\mathcal{Z}[\phi^*, \phi]$ is defined analogously to Eq. (5.37) in terms of arbitrary *functions* ϕ and ϕ^* [NO98]. These functions map each x to some arbitrary complex *values* $\phi(x)$ and $\phi^*(x)$, where $\phi^*(x)$ is the complex conjugate of $\phi(x)$. In particular, $\mathcal{Z}[0, 0]$ is defined by evaluating the functional \mathcal{Z} at the identically vanishing function $\phi(x) \equiv 0$. Hence, only in the bosonic case the term “generating functional” is actually justified. In the fermionic case treated in this thesis, we have therefore replaced it by “Green function generator”. A similar remark applies to the term “functional integral”, which we have replaced here by “Grassmann field integral”.

Theorem 5.3 (Grassmann field integral representation of temperature Green functions). *The constant term of the Green function generator coincides with the grand canonical partition function (4.15), i.e.,*

$$Z = \mathcal{Z}[0, 0]. \quad (5.42)$$

Furthermore, the temperature Green functions (see Definition 4.1) can be represented as Grassmann derivatives of the Green function generator \mathcal{Z} with respect to the sources: for $n \geq 1$,

$$G^{2n}(x_1, \dots, x_{2n}) = \frac{1}{\mathcal{Z}[0, 0]} \left(\frac{\delta}{\delta \bar{\eta}(x_1)} \cdots \frac{\delta}{\delta \bar{\eta}(x_n)} \frac{\delta}{\delta \eta(x_{2n})} \cdots \frac{\delta}{\delta \eta(x_{n+1})} \right) \mathcal{Z}[\bar{\eta}, \eta] \Big|_{\eta = \bar{\eta} = 0}. \quad (5.43)$$

All analogous expressions with a different number of $\bar{\eta}$ and η derivatives vanish, and hence the Green function generator has the formal expansion

$$\begin{aligned} \frac{\mathcal{Z}[\bar{\eta}, \eta]}{\mathcal{Z}[0, 0]} &= 1 + \sum_{n=1}^{\infty} \frac{(-1)^n}{(n!)^2} \int dx_1 \dots \int dx_{2n} G^{2n}(x_1, \dots, x_{2n}) \\ &\quad \times \bar{\eta}(x_1) \dots \bar{\eta}(x_n) \eta(x_{2n}) \dots \eta(x_{n+1}) \end{aligned} \quad (5.44)$$

in terms of the source fields.

Remark. By using the Definition 5.2 of the Green function generator, Eq. (5.43) can be written equivalently as

$$\begin{aligned} G^{2n}(x_1, \dots, x_{2n}) &= \left(\int d\bar{\psi} d\psi e^{-\langle \bar{\psi}, Q \psi \rangle} e^{-\beta V[\bar{\psi}, \psi]} \right)^{-1} \int d\bar{\psi} d\psi e^{-\langle \bar{\psi}, Q \psi \rangle} \\ &\quad \times \psi(x_1) \dots \psi(x_n) \bar{\psi}(x_{2n}) \dots \bar{\psi}(x_{n+1}) e^{-\beta V[\bar{\psi}, \psi]}, \end{aligned} \quad (5.45)$$

where we have canceled the normalization factor \mathcal{N} in the numerator and in the denominator of Eq. (5.43). In particular, the anticommutativity of the Grassmann variables, Eqs. (5.6) and (5.7), now translates into the antisymmetry of the fermionic Green functions G^{2n} with respect to their first n and their last n arguments. Furthermore, by the identifications (5.2)–(5.3), we recover from Eq. (5.45) the antiperiodicity of the temperature Green functions (Proposition 4.2). In fact, these fundamental properties of the temperature Green functions—which can be proven in the operator formalism—actually necessitate the anticommutativity of the Grassmann variables as well as the identifications (5.2)–(5.3) in the field integral formalism.

Proof. To prove the above representation of the temperature Green functions (see Ref. [SS17a]), we first *define* the functions F^{2n} by Eq. (5.45), i.e.,

$$\begin{aligned} F^{2n}(x_1, \dots, x_{2n}) &:= \frac{1}{\mathcal{Z}[0, 0]} \frac{1}{\mathcal{N}} \int d\bar{\psi} d\psi e^{-\langle \bar{\psi}, Q \psi \rangle} \\ &\quad \times \psi(x_1) \dots \psi(x_n) \bar{\psi}(x_{2n}) \dots \bar{\psi}(x_{n+1}) e^{-\beta V[\bar{\psi}, \psi]}. \end{aligned} \quad (5.46)$$

We then show for all $n \geq 1$ that F^{2n} coincides with G^{2n} , where the latter was defined by Eq. (4.25). For this purpose, we expand the exponential in Eq. (5.46) and use the linearity of the Grassmann integral, which yields

$$\begin{aligned}
F^{2n}(x_1, \dots, x_{2n}) = & \quad (5.47) \\
& \frac{1}{\mathcal{Z}[0, 0]} \sum_{k=0}^{\infty} \frac{(-\beta)^k}{k! 2^k} \left(\prod_{i=1}^k \int dy_i^1 \int dy_i^2 \int dy_i^3 \int dy_i^4 V(y_i^1, y_i^2, y_i^3, y_i^4) \right) \\
& \times \frac{1}{\mathcal{N}} \int d\bar{\psi} d\psi e^{-\langle \bar{\psi}, Q \psi \rangle} \\
& \times \psi(x_1) \dots \psi(x_n) \bar{\psi}(x_{2n}) \dots \bar{\psi}(x_{n+1}) \left(\prod_{j=1}^k \bar{\psi}(y_j^1) \bar{\psi}(y_j^2) \psi(y_j^4) \psi(y_j^3) \right). \quad (5.48)
\end{aligned}$$

After re-arranging the Grassmann generators in the last line, we can perform the Gaussian integral by means of Lemma 5.1, i.e.,

$$\begin{aligned}
& \frac{1}{\mathcal{N}} \int d\bar{\psi} d\psi e^{-\langle \bar{\psi}, Q \psi \rangle} \psi(x_1) \dots \psi(x_n) \psi(y_1^3) \psi(y_1^4) \dots \psi(y_k^3) \psi(y_k^4) \\
& \quad \times \bar{\psi}(y_k^2) \bar{\psi}(y_k^1) \dots \bar{\psi}(y_1^2) \bar{\psi}(y_1^1) \bar{\psi}(x_{2n}) \dots \bar{\psi}(x_{n+1}) \\
& = \sum_{\pi \in S_{n+2k}} \text{sgn}(\pi) C(x_1, \pi(x_{n+1})) \dots C(x_n, \pi(x_{2n})) \\
& \quad \times C(y_1^3, \pi(y_1^1)) C(y_1^4, \pi(y_1^2)) \dots C(y_k^3, \pi(y_k^1)) C(y_k^4, \pi(y_k^2)). \quad (5.49)
\end{aligned}$$

Thus, we obtain

$$\begin{aligned}
F^{2n}(x_1, \dots, x_{2n}) = & \quad (5.50) \\
& \frac{1}{\mathcal{Z}[0, 0]} \sum_{k=0}^{\infty} \frac{(-\beta)^k}{k! 2^k} \left(\prod_{i=1}^k \int dy_i^1 \int dy_i^2 \int dy_i^3 \int dy_i^4 V(y_i^1, y_i^2, y_i^3, y_i^4) \right) \\
& \times \sum_{\pi \in S_{n+2k}} \text{sgn}(\pi) C(x_1, \pi(x_{n+1})) \dots C(x_n, \pi(x_{2n})) \\
& \times C(y_1^3, \pi(y_1^1)) C(y_1^4, \pi(y_1^2)) \dots C(y_k^3, \pi(y_k^1)) C(y_k^4, \pi(y_k^2)).
\end{aligned}$$

This expression is equivalent to

$$F^{2n}(x_1, \dots, x_{2n}) = \frac{1}{\mathcal{Z}[0, 0]} \sum_{k=0}^{\infty} \frac{1}{k! 2^k} \sum_{\pi \in S_{n+2k}} \text{Val}[n, k, \pi], \quad (5.51)$$

where $\text{Val}[n, k, \pi]$ was defined by Eq. (4.173). The constant term of the Green function generator can be calculated analogously, and hence we obtain

$$\mathcal{Z}[0, 0] = \sum_{k=0}^{\infty} \frac{1}{k! 2^k} \sum_{\pi \in S_{2k}} \text{Val}[0, k, \pi]. \quad (5.52)$$

The comparison of Eqs. (5.51) and (5.52) with Eqs. (4.171) and (4.174), respectively, shows that $\mathcal{Z}[0, 0]$ coincides with the partition function,

$$\mathcal{Z}[0, 0] = Z, \quad (5.53)$$

and that F^{2n} coincides with the temperature Green function,

$$F^{2n}(x_1, \dots, x_{2n}) = G^{2n}(x_1, \dots, x_{2n}). \quad (5.54)$$

Thus, we have proven the Grassmann field integral representation of the temperature Green functions by showing that this leads precisely to the same Feynman graph expansion as the ordinary Green function perturbation theory.

It remains to prove the vanishing of all expressions which are analogous to Eq. (5.43), but which contain a different number of $\bar{\eta}$ and η derivatives. Indeed, this follows from an analogous calculation as presented above, using the fact that Grassmann–Gaussian integrals over monomials with a different number of $\bar{\psi}$ and ψ generators vanish (see Lemma 5.1). Taken together, these results imply the expansion (5.44) of the Green function generator. The prefactors be checked by conversely deducing Eq. (5.43) from Eq. (5.44), using the identity

$$\begin{aligned} & \left(\frac{\delta}{\delta \bar{\eta}(x_1)} \cdots \frac{\delta}{\delta \bar{\eta}(x_n)} \frac{\delta}{\delta \eta(x_{2n})} \cdots \frac{\delta}{\delta \eta(x_{n+1})} \right) \bar{\eta}(y_1) \cdots \bar{\eta}(y_n) \eta(y_{2n}) \cdots \eta(y_{n+1}) \\ &= (-1)^n \left(\frac{\delta}{\delta \bar{\eta}(x_1)} \cdots \frac{\delta}{\delta \bar{\eta}(x_n)} \frac{\delta}{\delta \eta(x_{2n})} \cdots \frac{\delta}{\delta \eta(x_{n+1})} \right) \eta(y_{n+1}) \cdots \eta(y_{2n}) \bar{\eta}(y_n) \cdots \bar{\eta}(y_1) \\ &= (-1)^n \sum_{\pi \in S_n} \text{sgn}(\pi) \delta(x_1, \pi(y_1)) \cdots \delta(x_n, \pi(y_n)) \\ & \quad \times \sum_{\pi' \in S_n} \text{sgn}(\pi') \delta(x_{n+1}, \pi'(y_{n+1})) \cdots \delta(x_{2n}, \pi'(y_{2n})), \end{aligned} \quad (5.55)$$

as well as the antisymmetry of the Green functions. \square

5.3. Connected Green functions

In contrast to the (ordinary) temperature Green functions, which were in the first place defined in the operator formalism (Definition 4.1) and only afterwards shown to have an equivalent representation in the field integral formalism (Theorem 5.3), the so-called connected Green functions will now be defined directly in the field integral formalism.

Definition 5.4. The *connected Green function generator* $\mathcal{W} \equiv \mathcal{W}[\bar{\eta}, \eta]$ is an element of the Grassmann algebra \mathcal{S} , which is defined as the natural logarithm of the Green function generator \mathcal{Z} divided by its constant term (see Definition 5.2), i.e.,

$$\mathcal{W}[\bar{\eta}, \eta] = \ln \frac{\mathcal{Z}[\bar{\eta}, \eta]}{\mathcal{Z}[0, 0]} = \ln \mathcal{Z}[\bar{\eta}, \eta] - \ln \mathcal{Z}[0, 0]. \quad (5.56)$$

In particular, by our convention, the field-independent term $\mathcal{W}[0, 0]$ vanishes.

Definition 5.5. For $n \geq 1$, the *connected temperature Green functions* G_c^{2n} are defined by taking the Grassmann derivatives of the above generator,

$$G_c^{2n}(x_1, \dots, x_{2n}) = \left(\frac{\delta}{\delta \bar{\eta}(x_1)} \cdots \frac{\delta}{\delta \bar{\eta}(x_n)} \frac{\delta}{\delta \eta(x_{2n})} \cdots \frac{\delta}{\delta \eta(x_{n+1})} \right) \mathcal{W}[\bar{\eta}, \eta] \Big|_{\eta = \bar{\eta} = 0}, \quad (5.57)$$

and subsequently evaluating the field-independent terms.

We remark that in expanding the Green function generator \mathcal{Z} , only monomials with an equal number of $\bar{\eta}$ and η fields appear (see Eq. (5.44)), and hence the same applies to the connected Green function generator \mathcal{W} . Therefore, Eq. (5.57) is equivalent to

$$\begin{aligned} \mathcal{W}[\bar{\eta}, \eta] &= \sum_{n=1}^{\infty} \frac{(-1)^n}{(n!)^2} \int dx_1 \cdots \int dx_{2n} G_c^{2n}(x_1, \dots, x_{2n}) \\ &\quad \times \bar{\eta}(x_1) \cdots \bar{\eta}(x_n) \eta(x_{2n}) \cdots \eta(x_{n+1}). \end{aligned} \quad (5.58)$$

Furthermore, the connected temperature Green functions G_c^{2n} have similar properties as the temperature Green functions G^{2n} themselves: in fact, the former are also antisymmetric with respect to their first n arguments as well as their last n arguments, they satisfy antiperiodic boundary conditions at $\tau_i = 0$ and $\tau_i = \hbar\beta$, and they have the same dimensions as the ordinary Green functions, e.g.,

$$[G_c^{2n}(x_1, \dots, x_{2n})] = m^{-3n}. \quad (5.59)$$

Before deriving the relations between the connected and the ordinary Green functions as well as the Feynman graph expansion of the connected Green functions, we introduce the following notation: for any function $f(x_1, \dots, x_n)$, the antisymmetrization with respect to any subset of arguments, say x_1, \dots, x_m (where $m \leq n$), is denoted as

$$\begin{aligned} \mathbb{A}_{(x_1, \dots, x_m)} f(x_1, \dots, x_m, x_{m+1}, \dots, x_n) &\equiv \\ \frac{1}{m!} \sum_{\pi \in S_m} \text{sgn}(\pi) f(x_{\pi(1)}, \dots, x_{\pi(m)}, x_{m+1}, \dots, x_n). \end{aligned} \quad (5.60)$$

Hence, the subscripts of \mathbb{A} denote the variables with respect to which the function f is antisymmetrized.

Theorem 5.6 (Relations between Green functions and connected Green functions). *The following relations hold between the (ordinary) Green functions G^{2n} and the connected Green functions G_c^{2n} : for $n = 1$,*

$$G^2(x_1, x_2) = G_c^2(x_1, x_2); \quad (5.61)$$

for $n = 2$,

$$\begin{aligned} G^4(x_1, x_2, x_3, x_4) &= G_c^4(x_1, x_2, x_3, x_4) + G_c^2(x_1, x_3) G_c^2(x_2, x_4) - G_c^2(x_1, x_4) G_c^2(x_2, x_3) \\ &\equiv G_c^4(x_1, x_2, x_3, x_4) + 2 \mathbb{A}_{(x_3, x_4)} \{ G_c^2(x_1, x_3) G_c^2(x_2, x_4) \}; \end{aligned} \quad (5.62)$$

for $n = 3$,

$$\begin{aligned} G^6(x_1, x_2, x_3, x_4, x_5, x_6) &= \\ &G_c^6(x_1, x_2, x_3, x_4, x_5, x_6) + 9 \mathbb{A}_{(x_1, x_2, x_3)} \mathbb{A}_{(x_4, x_5, x_6)} \{ G_c^4(x_1, x_2, x_4, x_5) G_c^2(x_3, x_6) \} \\ &+ 6 \mathbb{A}_{(x_4, x_5, x_6)} \{ G_c^2(x_1, x_4) G_c^2(x_2, x_5) G_c^2(x_3, x_6) \}; \end{aligned} \quad (5.63)$$

and similar equations hold for $n > 3$. These relations can be represented graphically by means of Universal Feynman Graphs as shown in Table 5.1.

Proof. We explicitly derive these equations only for $n = 1$ and for $n = 2$; the analogous equations for $n > 2$ can be deduced similarly. Consider first the two-point Green function G^2 , which can be represented in the field integral formalism by Eq. (5.43). Using the relation (5.56) between the Green function generator and the connected Green function generator, we obtain

$$G^2(x_1, x_2) = \frac{1}{\mathcal{Z}[0, 0]} \frac{\delta}{\delta \bar{\eta}(x_1)} \frac{\delta}{\delta \eta(x_2)} \mathcal{Z}[\bar{\eta}, \eta] \Big|_{\eta = \bar{\eta} = 0} \quad (5.64)$$

$$= \frac{\delta}{\delta \bar{\eta}(x_1)} \frac{\delta}{\delta \eta(x_2)} e^{\mathcal{W}[\bar{\eta}, \eta]} \Big|_{\eta = \bar{\eta} = 0} \quad (5.65)$$

$$= \left(\frac{\delta^2 \mathcal{W}}{\delta \bar{\eta}(x_1) \delta \eta(x_2)} + \frac{\delta \mathcal{W}}{\delta \bar{\eta}(x_1)} \frac{\delta \mathcal{W}}{\delta \eta(x_2)} \right) e^{\mathcal{W}[\bar{\eta}, \eta]} \Big|_{\eta = \bar{\eta} = 0} \quad (5.66)$$

$$= G_c^2(x_1, x_2). \quad (5.67)$$

In the last step, we have used that only terms with an equal number of $\bar{\eta}$ and η fields appear in the expansion of $\mathcal{W}[\bar{\eta}, \eta]$ (see Eq. (5.58)), and hence the second term in Eq. (5.66) vanishes by “evaluating” it at $\eta = \bar{\eta} = 0$. Similarly, we obtain

$$G^4(x_1, x_2, x_3, x_4) \quad (5.68)$$

$$= \frac{\delta}{\delta \eta(x_1)} \frac{\delta}{\delta \eta(x_2)} \frac{\delta}{\delta \bar{\eta}(x_4)} \frac{\delta}{\delta \bar{\eta}(x_3)} e^{\mathcal{W}[\bar{\eta}, \eta]} \Big|_{\eta = \bar{\eta} = 0} \quad (5.69)$$

$$= \frac{\delta}{\delta \eta(x_1)} \frac{\delta}{\delta \eta(x_2)} \left(\frac{\delta^2 \mathcal{W}}{\delta \bar{\eta}(x_4) \delta \bar{\eta}(x_3)} + \frac{\delta \mathcal{W}}{\delta \bar{\eta}(x_4)} \frac{\delta \mathcal{W}}{\delta \bar{\eta}(x_3)} \right) \Big|_{\eta = \bar{\eta} = 0} \quad (5.70)$$

$$= G_c^4(x_1, x_2, x_3, x_4) + G_c^2(x_1, x_3) G_c^2(x_2, x_4) - G_c^2(x_1, x_4) G_c^2(x_2, x_3), \quad (5.71)$$

where in the last step, we have neglected again the derivatives of \mathcal{W} with respect to unequal numbers of η and $\bar{\eta}$ fields. \square

$$\begin{aligned}
& \text{---} \boxed{G^2} \text{---} = \text{---} \boxed{G_c^2} \text{---} \\
\\
& \text{---} \boxed{G^4} \text{---} = \text{---} \boxed{G_c^4} \text{---} + \text{---} \boxed{G_c^2} \text{---} - \text{---} \boxed{G_c^2} \text{---} \\
& \hspace{15em} \text{---} \boxed{G_c^2} \text{---} \\
\\
& \text{---} \boxed{G^6} \text{---} = \text{---} \boxed{G_c^6} \text{---} + 9 \mathbb{A} \left\{ \begin{array}{c} \text{---} \boxed{G_c^4} \text{---} \\ \text{---} \boxed{G_c^2} \text{---} \end{array} \right\} \mathbb{A} \\
& \hspace{15em} + 6 \left\{ \begin{array}{c} \text{---} \boxed{G_c^2} \text{---} \\ \text{---} \boxed{G_c^2} \text{---} \\ \text{---} \boxed{G_c^2} \text{---} \end{array} \right\} \mathbb{A}
\end{aligned}$$

Table 5.1: Relations between Green functions and connected Green functions: representation by means of Universal Feynman Graphs.

In Ch. 4, we have shown that the (ordinary) Green functions have a formal perturbative expansion in terms of *bubble-free* Feynman graphs (Theorem 4.19 and Theorem 4.20). In the remainder of this section, we will prove a similar expansion of the connected Green functions in terms of *connected* Feynman graphs (see Definitions 4.9 and 4.10).

Theorem 5.7 (Feynman graph expansion of connected Green functions). *The natural logarithm of the partition function has the following formal expansion in terms of connected vacuum bubbles,*

$$\ln Z = \sum_{k=0}^{\infty} \frac{1}{k! 2^k} \sum_{\substack{\pi \in S_{2k}, \\ \pi \text{ connected}}} \text{Val}[0, k, \pi]. \quad (5.72)$$

Furthermore, the connected temperature Green functions can be expanded in terms of connected Feynman graphs as

$$G_c^{2n}(x_1, \dots, x_{2n}) = \sum_{k=0}^{\infty} \frac{1}{k! 2^k} \sum_{\substack{\pi \in S_{n+2k}, \\ \pi \text{ connected}}} \text{Val}[n, k, \pi], \quad (5.73)$$

where $\text{Val}[n, k, \pi]$ is given explicitly by Eq. (4.173).

Proof. We build on the proof given in Ref. [NO98, pp. 96f. and pp. 106f.], using the so-called *replica technique*: We define for each $P \in \mathbb{N}$ the *auxiliary* Green functions

$$G^{P, 2n}(x_1, \dots, x_{2n}) = \frac{1}{\mathcal{Z}^P[0, 0]} \left(\frac{\delta}{\delta \bar{\eta}(x_1)} \cdots \frac{\delta}{\delta \bar{\eta}(x_n)} \frac{\delta}{\delta \eta(x_{2n})} \cdots \frac{\delta}{\delta \eta(x_{n+1})} \right) \mathcal{Z}^P[\bar{\eta}, \eta] \Big|_{\eta = \bar{\eta} = 0}, \quad (5.74)$$

where $\mathcal{Z}^P[\bar{\eta}, \eta]$ is the Green function generator (5.37) taken to the power of P . In particular, by Theorem 5.3, we recover the ordinary Green functions for $P = 1$,

$$G^{1, 2n}(x_1, \dots, x_{2n}) = G^{2n}(x_1, \dots, x_{2n}). \quad (5.75)$$

Since the expansion of \mathcal{Z} contains only monomials with an equal number of $\bar{\eta}$ and η fields (see Eq. (5.44)), the same applies to \mathcal{Z}^P , and hence Eq. (5.74) is equivalent to

$$\begin{aligned} \frac{\mathcal{Z}^P[\bar{\eta}, \eta]}{\mathcal{Z}^P[0, 0]} &= 1 + \sum_{n=1}^{\infty} \frac{(-1)^n}{(n!)^2} \int dx_1 \dots \int dx_{2n} G^{P, 2n}(x_1, \dots, x_{2n}) \\ &\quad \times \bar{\eta}(x_1) \dots \bar{\eta}(x_n) \eta(x_{2n}) \dots \eta(x_{n+1}). \end{aligned} \quad (5.76)$$

In a first step, we will now derive the perturbative expansion of these auxiliary Green functions, thus generalizing the result of Theorem 4.19 to $P > 1$: From the definition (5.37) of the Green function generator, we obtain

$$\begin{aligned} \mathcal{Z}^P[\bar{\eta}, \eta] &= \frac{1}{\mathcal{N}^P} \left(\prod_p \int d\bar{\psi}_p d\psi_p \right) \exp \left(- \sum_p \langle \bar{\psi}_p, Q \psi_p \rangle \right) \\ &\quad \times \exp \left(-\beta \sum_p V[\bar{\psi}_p, \psi_p] + \sum_p \langle \bar{\eta}, \psi_p \rangle + \sum_p \langle \eta, \bar{\psi}_p \rangle \right), \end{aligned} \quad (5.77)$$

where we have introduced P copies ψ_1, \dots, ψ_P of the Grassmann fields, and where all summations and products range over $p \in \{1, \dots, P\}$. In particular, the normalization constant \mathcal{N}^P is given by

$$\mathcal{N}^P = \left(\prod_p \int d\bar{\psi}_p d\psi_p \right) \exp \left(- \sum_p \langle \bar{\psi}_p, Q \psi_p \rangle \right). \quad (5.78)$$

By putting Eq. (5.77) into Eq. (5.74), performing the η and $\bar{\eta}$ derivatives and evaluating the field-independent term of the resulting expression, we obtain (using Eq. (5.42))

$$\begin{aligned} G^{P, 2n}(x_1, \dots, x_{2n}) = & \quad (5.79) \\ & \frac{1}{Z^P} \frac{1}{\mathcal{N}^P} \left(\prod_p \int d\bar{\psi}_p d\psi_p \right) \exp \left(- \sum_p \langle \bar{\psi}_p, Q \psi_p \rangle \right) \\ & \times \left(\sum_p \psi_p(x_1) \right) \dots \left(\sum_p \psi_p(x_n) \right) \left(\sum_p \bar{\psi}_p(x_{2n}) \right) \dots \left(\sum_p \bar{\psi}_p(x_{n+1}) \right) \\ & \times \exp \left(-\beta \sum_p V[\bar{\psi}_p, \psi_p] \right). \end{aligned}$$

Further expanding the exponential of the interaction term,

$$\begin{aligned} \exp \left(-\beta \sum_q V[\bar{\psi}_q, \psi_q] \right) = & \quad (5.80) \\ \exp \left(-\frac{\beta}{2} \int dy^1 \int dy^2 \int dy^3 \int dy^4 V(y_1, y_2, y_3, y_4) \sum_q \bar{\psi}_q(y^1) \bar{\psi}_q(y^2) \psi_q(y^4) \psi_q(y^3) \right), \end{aligned}$$

into a formal power series leads to the expansion

$$\begin{aligned} G^{P, 2n}(x_1, \dots, x_{2n}) = & \quad (5.81) \\ & \frac{1}{Z^P} \sum_{k=0}^{\infty} \frac{(-\beta)^k}{k! 2^k} \left(\prod_{i=1}^k \int dy_i^1 \int dy_i^2 \int dy_i^3 \int dy_i^4 V(y_i^1, y_i^2, y_i^3, y_i^4) \right) \\ & \times \frac{1}{\mathcal{N}^P} \left(\prod_p \int d\bar{\psi}_p d\psi_p \right) \exp \left(- \sum_p \langle \bar{\psi}_p, Q \psi_p \rangle \right) \\ & \times \left(\sum_p \psi_p(x_1) \right) \dots \left(\sum_p \psi_p(x_n) \right) \left(\sum_p \bar{\psi}_p(x_{2n}) \right) \dots \left(\sum_p \bar{\psi}_p(x_{n+1}) \right) \\ & \times \left(\prod_{j=1}^k \left(\sum_q \bar{\psi}_q(y_j^1) \bar{\psi}_q(y_j^2) \psi_q(y_j^4) \psi_q(y_j^3) \right) \right). \end{aligned}$$

of the auxiliary Green functions. By the linearity of the Grassmann field integral, this

expansion is equivalent to

$$\begin{aligned}
G^{P,2n}(x_1, \dots, x_{2n}) = & \quad (5.82) \\
& \frac{1}{Z^P} \sum_{k=0}^{\infty} \frac{(-\beta)^k}{k! 2^k} \sum_{p_1, \dots, p_{2n}} \sum_{q_1, \dots, q_k} \left(\prod_{i=1}^k \int dy_i^1 \int dy_i^2 \int dy_i^3 \int dy_i^4 V(y_i^1, y_i^2, y_i^3, y_i^4) \right) \\
& \times \frac{1}{\mathcal{N}^P} \left(\prod_p \int d\bar{\psi}_p d\psi_p \right) \exp \left(- \sum_p \langle \bar{\psi}_p, \mathcal{Q} \psi_p \rangle \right) \\
& \times \psi_{p_1}(x_1) \dots \psi_{p_n}(x_n) \bar{\psi}_{p_{2n}}(x_{2n}) \dots \bar{\psi}_{p_{n+1}}(x_{n+1}) \\
& \times \left(\prod_{j=1}^k \bar{\psi}_{q_j}(y_j^1) \bar{\psi}_{q_j}(y_j^2) \psi_{q_j}(y_j^4) \psi_{q_j}(y_j^3) \right).
\end{aligned}$$

We now define a modified covariance \mathcal{C} , which depends not only on two space-time variables x and x' , but also on two field indices $p, p' \in \{1, \dots, P\}$, as follows:

$$\mathcal{C}_{pp'}(x, x') = \begin{cases} C(x, x'), & \text{if } p = p', \\ 0, & \text{otherwise.} \end{cases} \quad (5.83)$$

Its inverse, $\mathcal{Q} = \mathcal{C}^{-1}$, is given by

$$\mathcal{Q}_{pp'}(x, x') = \begin{cases} Q(x, x'), & \text{if } p = p', \\ 0, & \text{otherwise.} \end{cases} \quad (5.84)$$

Furthermore, we define a modified interaction kernel \mathcal{V} as

$$\mathcal{V}_{q^1 q^2 q^3 q^4}(y^1, y^2, y^3, y^4) = \begin{cases} V(y^1, y^2, y^3, y^4), & \text{if } q^1 = q^2 = q^3 = q^4, \\ 0, & \text{otherwise.} \end{cases} \quad (5.85)$$

With these definitions, Eq. (5.82) can be written equivalently as

$$\begin{aligned}
G^{P,2n}(x_1, \dots, x_{2n}) = & \quad (5.86) \\
& \frac{1}{Z^P} \sum_{k=0}^{\infty} \frac{(-\beta)^k}{k! 2^k} \sum_{p_1, \dots, p_{2n}} \left(\prod_{i=1}^k \left(\int dy_i^1 \dots \int dy_i^4 \sum_{q_i^1, \dots, q_i^4} \mathcal{V}_{q_i^1 \dots q_i^4}(y_i^1, \dots, y_i^4) \right) \right) \\
& \times \frac{1}{\mathcal{N}^P} \left(\prod_p \int d\bar{\psi}_p d\psi_p \right) \exp \left(- \sum_{p, p'} \langle \bar{\psi}_p, \mathcal{Q}_{pp'} \psi_{p'} \rangle \right) \\
& \times \psi_{p_1}(x_1) \dots \psi_{p_n}(x_n) \bar{\psi}_{p_{2n}}(x_{2n}) \dots \bar{\psi}_{p_{n+1}}(x_{n+1}) \\
& \times \left(\prod_{j=1}^k \bar{\psi}_{q_j^1}(y_j^1) \bar{\psi}_{q_j^2}(y_j^2) \psi_{q_j^4}(y_j^4) \psi_{q_j^3}(y_j^3) \right).
\end{aligned}$$

To simplify this expression, we define the “external” multi-variables (for $r = 1, \dots, 2n$)

$$X_r \equiv (x_r, p_r), \quad (5.87)$$

as well as the “internal” multi-variables (for $\ell = 1, \dots, 4$ and $i = 1, \dots, k$)

$$Y_i^\ell \equiv (y_i^\ell, q_i^\ell). \quad (5.88)$$

Correspondingly, we combine the integrations over y_i^ℓ and the summations over q_i^ℓ into integrations over the multi-variables Y_i^ℓ ,

$$\int dy_i^\ell \sum_{q_i^\ell} \equiv \int dY_i^\ell. \quad (5.89)$$

Furthermore, the modified interaction kernels can be interpreted as functions of these multi-variables,

$$\mathcal{V}_{q_i^1 \dots q_i^4}(y_i^1, \dots, y_i^4) \equiv \mathcal{V}(Y_i^1, \dots, Y_i^4), \quad (5.90)$$

and similarly the covariances,

$$\mathcal{C}_{pp'}(x, x') \equiv \mathcal{C}(X, X'). \quad (5.91)$$

In addition, we introduce the Grassmann fields

$$\psi_{p_r}(x_r) \equiv \Psi(X_r), \quad (5.92)$$

such that the Grassmann field integral can be written as

$$\prod_p \int d\bar{\psi}_p d\psi_p \equiv \int d\bar{\Psi} d\Psi, \quad (5.93)$$

and the formal inner product as

$$\sum_{p, p'} \langle \bar{\psi}_p, \mathcal{Q}_{pp'} \psi_{p'} \rangle \equiv \langle \bar{\Psi}, \mathcal{Q} \Psi \rangle. \quad (5.94)$$

With these notations, Eq. (5.86) can be written compactly as

$$\begin{aligned} G^{P, 2n}(x_1, \dots, x_{2n}) = & \quad (5.95) \\ & \frac{1}{Z^P} \sum_{k=0}^{\infty} \frac{(-\beta)^k}{k! 2^k} \sum_{p_1, \dots, p_{2n}} \left(\prod_{i=1}^k \int dY_i^1 \dots \int dY_i^4 \mathcal{V}(Y_i^1, \dots, Y_i^4) \right) \\ & \times \frac{1}{\mathcal{N}^P} \int d\bar{\Psi} d\Psi \exp(-\langle \bar{\Psi}, \mathcal{Q} \Psi \rangle) \\ & \times \Psi(X_1) \dots \Psi(X_n) \bar{\Psi}(X_{2n}) \dots \bar{\Psi}(X_{n+1}) \left(\prod_{j=1}^k \bar{\Psi}(Y_j^1) \bar{\Psi}(Y_j^2) \Psi(Y_j^4) \Psi(Y_j^3) \right). \end{aligned}$$

Next, we perform the Grassmann–Gaussian integral by means of Lemma 5.1. After rearranging the Grassmann generators, we thus obtain

$$G^{P,2n}(x_1, \dots, x_{2n}) = \frac{1}{Z^P} \sum_{k=0}^{\infty} \frac{1}{k! 2^k} \sum_{\pi \in S_{n+2k}} \text{Val}^P[n, k, \pi], \quad (5.96)$$

where we have defined

$$\begin{aligned} \text{Val}^P[n, k, \pi] = & \sum_{p_1, \dots, p_{2n}} (-\beta)^k \left(\prod_{i=1}^k \int dY_i^1 \dots \int dY_i^4 \mathcal{V}(Y_i^1, \dots, Y_i^4) \right) \\ & \times \text{sgn}(\pi) \mathcal{C}(X_1, \pi(X_{n+1})) \dots \mathcal{C}(X_n, \pi(X_{2n})) \\ & \times C(Y_1^3, \pi(Y_1^1)) C(Y_1^4, \pi(Y_1^2)) \dots C(Y_k^3, \pi(Y_k^1)) C(Y_k^4, \pi(Y_k^2)), \end{aligned} \quad (5.97)$$

This expression is analogous to—and in fact coincides for $P = 1$ with—the formula (4.173). Similarly, one can show that

$$Z^P = \sum_{k=0}^{\infty} \frac{1}{k! 2^k} \sum_{\pi \in S_{2k}} \text{Val}^P[0, k, \pi]. \quad (5.98)$$

Consequently, by canceling the denominator in Eq. (5.96) analogously as in Theorem 4.19, we arrive at

$$G^{P,2n}(x_1, \dots, x_{2n}) = \sum_{k=0}^{\infty} \frac{1}{k! 2^k} \sum_{\substack{\pi \in S_{n+2k}, \\ \pi \text{ bubble-free}}} \text{Val}^P[n, k, \pi]. \quad (5.99)$$

Hence, we conclude that the auxiliary Green functions $G^{P,2n}$ have a perturbative expansion in terms of bubble-free Feynman graphs, which is analogous to the expansion of the ordinary Green functions G^{2n} . However, in evaluating the Feynman graphs of $G^{P,2n}$, the following modifications have to be taken into account (compare Eqs. (5.97) and (4.173)):

- (i) All external (position, spin and imaginary time) variables x_r are replaced by $X_r = (x_r, p_r)$, and all internal variables y_i^ℓ are replaced by $Y_i^\ell = (y_i^\ell, q_i^\ell)$, where the additional field indices p_i and q_i^ℓ range over the set $\{1, \dots, P\}$.
- (ii) The covariances $C(x_1, x_2)$ are replaced by

$$\mathcal{C}(X_1, X_2) = \delta_{p_1 p_2} C(x_1, x_2), \quad (5.100)$$

and the interaction kernels $V(y^1, \dots, y^4)$ are replaced by

$$\mathcal{V}(Y^1, Y^2, Y^3, Y^4) = \delta_{q^1 q^2} \delta_{q^2 q^3} \delta_{q^3 q^4} V(y^1, y^2, y^3, y^4). \quad (5.101)$$

- (iii) The integrations over the internal variables y_i^ℓ are complemented by summations over the internal indices q_i^ℓ ,

$$\prod_{i=1}^k \int dY_i^1 \dots \int dY_i^4 = \prod_{i=1}^k \int dy_i^1 \dots \int dy_i^4 \sum_{q_i^1, \dots, q_i^4} . \quad (5.102)$$

- (iv) Finally, we have to perform the sum over the external field indices p_1, \dots, p_{2n} in Eq. (5.97). Note, however, that this formula does *not* imply an analogous integration over the external space-time variables x_1, \dots, x_{2n} .

As a consequence of these modifications, the value of any Feynman graph (which corresponds to a permutation π) of the auxiliary Green function $G^{P,2n}$ is related to the value of the corresponding Feynman graph of the ordinary Green function G^{2n} by

$$\text{Val}^P[n, k, \pi] = \text{Val}[n, k, \pi] P^{N_c[n, k, \pi]}, \quad (5.103)$$

where $N_c[n, k, \pi]$ denotes the number of *connected subgraphs* of the Feynman graph π . By putting this result into Eq. (5.98), we obtain

$$Z^P = \sum_{k=0}^{\infty} \frac{1}{k! 2^k} \sum_{\pi \in S_{2k}} \text{Val}[0, k, \pi] P^{N_c[0, k, \pi]}, \quad (5.104)$$

Similarly, putting Eq. (5.103) into Eq. (5.99) yields

$$G^{P,2n}(x_1, \dots, x_{2n}) = \sum_{k=0}^{\infty} \frac{1}{k! 2^k} \sum_{\substack{\pi \in S_{n+2k}, \\ \pi \text{ bubble-free}}} \text{Val}[n, k, \pi] P^{N_c[n, k, \pi]}, \quad (5.105)$$

and thus, by Eq. (5.76),

$$\begin{aligned} \frac{\mathcal{Z}^P[\bar{\eta}, \eta]}{\mathcal{Z}^P[0, 0]} &= 1 + \sum_{n=1}^{\infty} \frac{(-1)^n}{(n!)^2} \int dx_1 \dots \int dx_{2n} \bar{\eta}(x_1) \dots \bar{\eta}(x_n) \eta(x_{2n}) \dots \eta(x_{n+1}) \\ &\quad \times \sum_{k=0}^{\infty} \frac{1}{k! 2^k} \sum_{\substack{\pi \in S_{n+2k}, \\ \pi \text{ bubble-free}}} \text{Val}[n, k, \pi] P^{N_c[n, k, \pi]}. \end{aligned} \quad (5.106)$$

Consider now the expansion

$$Z^P = e^{P \ln Z} = 1 + P \ln Z + \mathcal{O}(P^2), \quad (5.107)$$

in which the natural logarithm of the partition function appears as the P -linear term. From Eq. (5.104), it follows that this P -linear term is given by

$$\ln Z = \sum_{k=1}^{\infty} \frac{1}{k! 2^k} \sum_{\substack{\pi \in S_{2k}, \\ N_c(0, k, \pi)=1}} \text{Val}[0, k, \pi]. \quad (5.108)$$

Here, the condition $N_c(0, k, \pi) = 1$ implies that the Feynman graph corresponding to the permutation π has only one connected subgraph and is therefore connected itself. Hence, Eq. (5.108) is equivalent to the assertion (5.72). Next, consider the analogous expansion

$$\frac{\mathcal{Z}^P[\bar{\eta}, \eta]}{\mathcal{Z}^P[0, 0]} = \exp(P\mathcal{W}[\bar{\eta}, \eta]) = 1 + P\mathcal{W}[\bar{\eta}, \eta] + \mathcal{O}(P^2), \quad (5.109)$$

in which the connected Green function generator (5.56) appears as the P -linear term. From Eq. (5.106), it follows that

$$\begin{aligned} \mathcal{W}[\bar{\eta}, \eta] &= \sum_{n=1}^{\infty} \frac{(-1)^n}{(n!)^2} \int dx_1 \dots \int dx_{2n} \bar{\eta}(x_1) \dots \bar{\eta}(x_n) \eta(x_{2n}) \dots \eta(x_{n+1}) \\ &\times \sum_{k=0}^{\infty} \frac{1}{k! 2^k} \sum_{\substack{\pi \in S_{n+2k}, \\ N_c(n, k, \pi)=1}} \text{Val}[n, k, \pi]. \end{aligned} \quad (5.110)$$

Comparing this formula with Eq. (5.58) shows the assertion (5.73), and this concludes the proof. \square

5.4. Fully amputated, connected Green functions

In this section, we briefly introduce another class of Green functions, which in this thesis do not play an important role by themselves, but which will be needed in the next section for proving the Feynman graph expansion of the so-called one-line-irreducible Green functions. The Green functions of this section are *defined* in terms of their Feynman graph expansions:

Definition 5.8. For $n \geq 1$, the *fully amputated, connected $2n$ -point Green function* Σ^{2n} is defined by its expansion in terms of fully amputated graphs (see Definitions 4.18) as

$$\Sigma^{2n}(x_1, \dots, x_{2n}) = \sum_{k=1}^{\infty} \frac{1}{k! 2^k} \sum_{\substack{\pi \in S_{n+2k}, \\ \pi \text{ non-amputable}}} \text{Val}_{\text{amp}}[n, k, \pi], \quad (5.111)$$

where $\text{Val}_{\text{amp}}[n, k, \pi]$ is given explicitly by Eqs. (4.173) and (4.190).

We remark that for $n = 1$ and for $n = 2$, we can equivalently sum in Eq. (5.111) over all *irreducible* Feynman graphs. This follows directly from Lemma 4.16, which states that for $n \leq 2$, the notions of non-amputable and (one-line-)irreducible graphs coincide. Hence, in particular, Σ^2 coincides with the so-called *irreducible self-energy* [NO98, p. 113],

$$\Sigma^2(x_1, x_2) = \sum_{k=1}^{\infty} \frac{1}{k! 2^k} \sum_{\substack{\pi \in S_{1+2k}, \\ \pi \text{ one-line-irreducible}}} \text{Val}_{\text{amp}}[1, k, \pi]. \quad (5.112)$$

Similarly, the fully amputated, connected four-point function can be characterized as

$$\Sigma^4(x_1, x_2) = \sum_{k=1}^{\infty} \frac{1}{k! 2^k} \sum_{\substack{\pi \in S_{2+2k}, \\ \pi \text{ one-line-irreducible}}} \text{Val}_{\text{amp}}[2, k, \pi]. \quad (5.113)$$

As we will see later, these two equations imply directly the corresponding Feynman graph expansions of the one-line-irreducible two- and four-point Green functions.

Theorem 5.9 (Relations between connected Green functions and fully amputated, connected Green functions). *The following relations hold between the connected Green functions G_c^{2n} and the fully amputated, connected Green functions Σ^{2n} : for $n = 1$,*

$$G_c^2(x_1, x_2) = C(x_1, x_2) + \int dy_1 \int dy_2 C(x_1, y_1) \Sigma^2(y_1, y_2) G_c^2(y_2, x_2); \quad (5.114)$$

and for $n \geq 2$,

$$\begin{aligned} G_c^{2n}(x_1, \dots, x_{2n}) &= \int dy_1 \dots \int dy_{2n} G_c^2(x_1, y_1) \dots G_c^2(x_n, y_n) \\ &\times \Sigma^{2n}(y_1, \dots, y_{2n}) G_c^2(y_{n+1}, x_{n+1}) \dots G_c^2(y_{2n}, x_{2n}). \end{aligned} \quad (5.115)$$

While Eq. (5.114) is an implicit equation for G_c^2 , an explicit equation can be obtained as well by iterating this equation (see proof).

Proof. We first rewrite Eq. (5.114) in a shorthand notation as

$$G_c^2 = C + C \Sigma^2 G_c^2. \quad (5.116)$$

By iterating this equation as in Ref. [NO98, p. 113], we obtain

$$G_c^2 = C + C \Sigma^2 C + C \Sigma^2 C \Sigma^2 C + \dots \quad (5.117)$$

By putting the definition (5.111) of Σ^2 into this expansion and using Eq. (4.190), we see that the right-hand side exactly reproduces the Feynman graph expansion (5.73) of the connected two-point Green function. Similarly, for $n \geq 2$, one can convince oneself that by expanding all Green functions in Eq. (5.115), both sides of the equation produce exactly the same Feynman graphs, and this shows the assertion. \square

5.5. One-line-irreducible Green functions

In this last section, we will define and study the properties of yet another class of Green functions, which will play a central role in the following Part III of this thesis.

We begin by introducing further elements $\bar{\varphi}(x)$, $\varphi(x)$ of the Grassmann algebra \mathcal{S} of the sources as

$$\bar{\varphi}(x) = \frac{\delta \mathcal{W}}{\delta \eta(x)}, \quad (5.118)$$

$$\varphi(x) = \frac{\delta \mathcal{W}}{\delta \bar{\eta}(x)}, \quad (5.119)$$

where $\mathcal{W} = \mathcal{W}[\bar{\eta}, \eta]$ is the connected Green function generator. In the following, we will refer to these particular Grassmann variables as the *new sources* (as opposed to the “old” sources $\eta(x)$ and $\bar{\eta}(x)$). They satisfy again antiperiodic boundary conditions analogously to Eqs. (5.20)–(5.21). Furthermore, the dimensions of the new sources can be deduced from the property

$$\frac{\delta \eta(x)}{\delta \eta(x')} = \delta(x, x'), \quad (5.120)$$

which together with Eq. (4.104) implies that

$$\left[\frac{\delta}{\delta \eta(x)} \right] = [\eta(x)] = \mathfrak{m}^{-3/2}. \quad (5.121)$$

Using that \mathcal{W} is dimensionless, we thus find that

$$[\bar{\varphi}(x)] = [\varphi(x)] = \mathfrak{m}^{-3/2}, \quad (5.122)$$

hence the new sources have the same dimensions as the “old” sources.

Definition 5.10. The *one-line-irreducible Green function generator* Γ is an element of the Grassmann algebra \mathcal{S} , which is defined as the *Legendre transform* of the connected Green function generator \mathcal{W} , i.e.,

$$\Gamma = \mathcal{W} + \langle \bar{\varphi}, \eta \rangle + \langle \varphi, \bar{\eta} \rangle, \quad (5.123)$$

where the Grassmann fields $\varphi(x)$ and $\bar{\varphi}(x)$ are defined by Eqs. (5.118)–(5.119).

Definition 5.11. For $n \geq 1$, the *one-line-irreducible temperature Green functions* Γ^{2n} are defined by taking the Grassmann derivatives of the above generator,

$$\Gamma^{2n}(x_1, \dots, x_{2n}) = \left(\frac{\delta}{\delta \bar{\varphi}(x_1)} \cdots \frac{\delta}{\delta \bar{\varphi}(x_n)} \frac{\delta}{\delta \varphi(x_{2n})} \cdots \frac{\delta}{\delta \varphi(x_{n+1})} \right) \Gamma[\bar{\varphi}, \varphi] \Big|_{\varphi=\bar{\varphi}=0}, \quad (5.124)$$

and subsequently evaluating the field-independent terms.

We *assume* that the new sources $\{\bar{\varphi}(x), \varphi(x)\}$, where $x \in \mathbb{R}^3 \times \{\uparrow, \downarrow\} \times [0, \beta)$, generate again the Grassmann algebra \mathcal{S} , such that every Grassmann variable in \mathcal{S} can be

expanded in terms of these new sources. The derivatives $\delta/\delta\bar{\varphi}(x)$ and $\delta/\delta\varphi(x)$ of any element of \mathcal{S} are then well-defined, and they can be evaluated analogously as in Eqs. (5.9)–(5.10). In particular, we can expand Γ in terms of the new sources as

$$\begin{aligned} \Gamma[\bar{\varphi}, \varphi] &= \sum_{n=1}^{\infty} \frac{(-1)^n}{(n!)^2} \int dx_1 \dots \int dx_{2n} \Gamma^{2n}(x_1, \dots, x_{2n}) \\ &\quad \times \bar{\varphi}(x_1) \dots \bar{\varphi}(x_n) \varphi(x_{n+1}) \dots \varphi(x_{2n}). \end{aligned} \quad (5.125)$$

Note that the expansion (5.58) of \mathcal{W} contains only monomials with an equal number of $\bar{\eta}$ and η fields, and this implies by Eqs. (5.118)–(5.119) and (5.123) that the above expansion of Γ also contains only monomials with an equal number of $\bar{\varphi}$ and φ fields. Furthermore, the one-line-irreducible Green functions Γ^{2n} have similar properties as the (ordinary) Green functions and the connected Green functions: they are antisymmetric with respect to their first n and their last n arguments, they satisfy antiperiodic boundary conditions, and they have the dimensions

$$[\Gamma^{2n}(x_1, \dots, x_{2n})] = m^{-3n}. \quad (5.126)$$

Before studying the one-line-irreducible Green functions in more detail, we will now prove two important properties of the Legendre transformation.

Proposition 5.12 (Involution property of the Legendre transformation). *The old sources coincide with the derivatives of the one-line-irreducible Green function generator Γ with respect to the new sources, i.e.,*

$$\bar{\eta}(x) = \frac{\delta\Gamma}{\delta\varphi(x)}, \quad (5.127)$$

$$\eta(x) = \frac{\delta\Gamma}{\delta\bar{\varphi}(x)}. \quad (5.128)$$

Furthermore, since

$$\mathcal{W} = \Gamma + \langle \bar{\eta}, \varphi \rangle + \langle \eta, \bar{\varphi} \rangle, \quad (5.129)$$

the Legendre transform of Γ is again the connected Green function generator \mathcal{W} .

Proof. First, Eq. (5.127) follows from the definition (5.123) by the product rule,

$$\frac{\delta\Gamma}{\delta\varphi(x)} = \frac{\delta\mathcal{W}}{\delta\varphi(x)} - \left\langle \frac{\delta\eta}{\delta\varphi(x)}, \bar{\varphi} \right\rangle - \left\langle \frac{\delta\bar{\eta}}{\delta\varphi(x)}, \varphi \right\rangle + \bar{\eta}(x), \quad (5.130)$$

together with the chain rule,

$$\frac{\delta\mathcal{W}}{\delta\varphi(x)} = \int dx' \frac{\delta\eta(x')}{\delta\varphi(x)} \frac{\delta\mathcal{W}}{\delta\eta(x')} + \int dx' \frac{\delta\bar{\eta}(x')}{\delta\varphi(x)} \frac{\delta\mathcal{W}}{\delta\bar{\eta}(x')} \quad (5.131)$$

$$= \left\langle \frac{\delta\eta}{\delta\varphi(x)}, \bar{\varphi} \right\rangle + \left\langle \frac{\delta\bar{\eta}}{\delta\varphi(x)}, \varphi \right\rangle. \quad (5.132)$$

Next, Eq. (5.128) can be shown analogously. Finally, since \mathcal{W} is an *even* element of \mathcal{S} (i.e., it contains only monomials with an even number of Grassmann generators), the new sources are *odd* elements of \mathcal{S} . Therefore, Eq. (5.123) is equivalent to

$$\Gamma = \mathcal{W} - \langle \eta, \bar{\varphi} \rangle - \langle \bar{\eta}, \varphi \rangle, \quad (5.133)$$

and this in turn is equivalent to the assertion (5.129). \square

Proposition 5.13. *The matrices of the second derivatives of the generators Γ and \mathcal{W} are inverse to each other in the sense that*

$$\begin{pmatrix} \delta(x, z) & 0 \\ 0 & \delta(x, z) \end{pmatrix} = \int dy \begin{pmatrix} \frac{\delta^2 \Gamma}{\delta \bar{\varphi}(x) \delta \bar{\varphi}(y)} & \frac{\delta^2 \Gamma}{\delta \bar{\varphi}(x) \delta \varphi(y)} \\ \frac{\delta^2 \Gamma}{\delta \varphi(x) \delta \bar{\varphi}(y)} & \frac{\delta^2 \Gamma}{\delta \varphi(x) \delta \varphi(y)} \end{pmatrix} \begin{pmatrix} \frac{\delta^2 \mathcal{W}}{\delta \eta(y) \delta \eta(z)} & \frac{\delta^2 \mathcal{W}}{\delta \eta(y) \delta \bar{\eta}(z)} \\ \frac{\delta^2 \mathcal{W}}{\delta \bar{\eta}(y) \delta \eta(z)} & \frac{\delta^2 \mathcal{W}}{\delta \bar{\eta}(y) \delta \bar{\eta}(z)} \end{pmatrix}. \quad (5.134)$$

This identity can be written equivalently as

$$\delta(X, Z) = \int dY \frac{\delta^2 \Gamma}{\delta \Phi(X) \delta \Phi(Y)} \frac{\delta^2 \mathcal{W}}{\delta H(Y) \delta H(Z)} \quad (5.135)$$

in the Nambu formalism of Appendix A.

Proof. The derivation is particularly simple in the Nambu formalism (see Appendix A): using a functional chain rule, we obtain

$$\delta(X, Z) = \frac{\delta \Phi(Z)}{\delta \Phi(X)} = \frac{\delta}{\delta \Phi(X)} \frac{\delta \mathcal{W}}{\delta H(Z)} = \int dY \frac{\delta H(Y)}{\delta \Phi(X)} \frac{\delta^2 \mathcal{W}}{\delta H(Y) \delta H(Z)} \quad (5.136)$$

$$= \int dY \frac{\delta^2 \Gamma}{\delta \Phi(X) \delta \Phi(Y)} \frac{\delta^2 \mathcal{W}}{\delta H(Y) \delta H(Z)}, \quad (5.137)$$

which coincides with the assertion (5.135). By Eqs. (A.3)–(A.4) and (A.39)–(A.40), this is equivalent to Eq. (5.134). \square

We remark that the involution property of the Legendre transformation (Proposition 5.12) implies also the converse relation, i.e.,

$$\delta(X, Z) = \int dY \frac{\delta^2 \mathcal{W}}{\delta H(X) \delta H(Y)} \frac{\delta^2 \Gamma}{\delta \Phi(Y) \delta \Phi(Z)}. \quad (5.138)$$

These two identities can be written in a shorthand notation as

$$1 = \frac{\delta^2 \Gamma}{\delta \Phi^2} \frac{\delta^2 \mathcal{W}}{\delta H^2} = \frac{\delta^2 \mathcal{W}}{\delta H^2} \frac{\delta^2 \Gamma}{\delta \Phi^2}, \quad (5.139)$$

or equivalently as

$$\frac{\delta^2 \mathcal{W}}{\delta H^2} = \left(\frac{\delta^2 \Gamma}{\delta \Phi^2} \right)^{-1}. \quad (5.140)$$

By taking the field-independent terms of both sides of this equation, we further obtain

$$\left. \frac{\delta^2 \mathcal{W}}{\delta H^2} \right|_{H=0} = \left(\left. \frac{\delta^2 \Gamma}{\delta \Phi^2} \right|_{\Phi=0} \right)^{-1}, \quad (5.141)$$

where we have used that the field-independent term of the inverse equals the inverse of the field-independent term.

Next, we will derive the relations between the connected and the one-line-irreducible Green functions. Our calculations will be facilitated by first deriving the corresponding relations between the Nambu-type Green functions (see Appendix A), and then deducing from these the desired relations between the (usual) Green functions.

Theorem 5.14 (Relations between connected and one-line-irreducible Green functions in the Nambu formalism). *The following relations hold between the connected Green functions \mathbf{G}_c^{2n} and the one-line-irreducible Green functions $\mathbf{\Gamma}^{2n}$ in the Nambu formalism: for $n = 1$,*

$$\delta(X_1, X_2) = \int dY_1 \mathbf{G}_c^2(X_1, Y_1) \mathbf{\Gamma}^2(Y_1, X_2); \quad (5.142)$$

for $n = 2$,

$$\mathbf{G}_c^4(X_1, X_2, X_3, X_4) = \quad (5.143)$$

$$\int dY_1 \dots \int dY_4 \mathbf{G}_c^2(X_1, Y_1) \mathbf{G}_c^2(X_2, Y_2) \mathbf{G}_c^2(X_3, Y_3) \mathbf{G}_c^2(X_4, Y_4) \mathbf{\Gamma}^4(Y_1, Y_2, Y_3, Y_4);$$

for $n = 3$,

$$\mathbf{G}_c^6(X_1, X_2, X_3, X_4, X_5, X_6) = \quad (5.144)$$

$$\begin{aligned} & \int dY_1 \dots \int dY_6 \mathbf{G}_c^2(X_1, Y_1) \mathbf{G}_c^2(X_2, Y_2) \mathbf{G}_c^2(X_3, Y_3) \mathbf{G}_c^2(X_4, Y_4) \\ & \quad \times \mathbf{G}_c^2(X_5, Y_5) \mathbf{G}_c^2(X_6, Y_6) \mathbf{\Gamma}^6(Y_1, Y_2, Y_3, Y_4, Y_5, Y_6) \\ & + 10 \mathbb{A}_{(X_1, \dots, X_6)} \left\{ \int dY_1 \dots \int dY_6 \mathbf{G}_c^2(X_1, Y_1) \mathbf{G}_c^2(X_2, Y_2) \mathbf{G}_c^2(X_3, Y_3) \right. \\ & \quad \times \mathbf{\Gamma}^4(Y_1, Y_2, Y_3, Z) \mathbf{G}_c^2(Z, Z') \mathbf{\Gamma}^4(Z', Y_4, Y_5, Y_6) \\ & \quad \left. \times \mathbf{G}_c^2(Y_4, X_4) \mathbf{G}_c^2(Y_5, X_5) \mathbf{G}_c^2(Y_6, X_6) \right\}. \end{aligned}$$

In general, for $n \geq 2$, we have

$$\mathbf{G}_c^{2n}(X_1, \dots, X_{2n}) = \int dY_1 \dots \int dY_{2n} \mathbf{G}_c^2(X_1, Y_1) \dots \mathbf{G}_c^2(X_{2n}, Y_{2n}) \mathbf{I}^{2n}(Y_1, \dots, Y_{2n}) + \mathcal{R}, \quad (5.145)$$

where the remainder terms denoted by \mathcal{R} have the property that each Feynman graph in their respective expansions contains at least one torso line (see Definition 4.12).

Proof. Our proof is based on Refs. [NO98, pp. 115ff.] and [Zin02, Sct. 7.5]. To simplify the derivations, we first introduce some shorthand notations: we write the Grassmann derivatives of the connected Green function generator as

$$\mathcal{W}(Y_1, \dots, Y_m) \equiv \frac{\delta^m \mathcal{W}}{\delta H(Y_1) \dots \delta H(Y_m)}, \quad (5.146)$$

and the corresponding derivatives of the one-line-irreducible generator as

$$\Gamma(Y_1, \dots, Y_m) \equiv \frac{\delta^m \Gamma}{\delta \Phi(Y_1) \dots \delta \Phi(Y_m)}. \quad (5.147)$$

Moreover, we use the convention of *integrating over all doubly appearing multi-indices*. We now start from the identity

$$\Phi(X_1) = \frac{\delta W}{\delta H(X_1)} \equiv \mathcal{W}(X_1), \quad (5.148)$$

and successively evaluate the n th order Grassmann derivatives of this quantity with respect to the fields $\Phi(X)$. For the first derivative, we thereby obtain

$$\delta(X_2, X_1) = \frac{\delta \Phi(X_1)}{\delta \Phi(X_2)} = \Gamma(X_2, Y_2) \mathcal{W}(Y_2, X_1), \quad (5.149)$$

as shown already above by Eqs. (5.136)–(5.137). The second derivative yields

$$0 = \frac{\delta^2 \Phi(X_1)}{\delta \Phi(X_3) \delta \Phi(X_2)} = \Gamma(X_3, X_2, Y_2) \mathcal{W}(Y_2, X_1) + \Gamma(X_3, Y_3) \Gamma(X_2, Y_2) \mathcal{W}(Y_3, Y_2, X_1), \quad (5.150)$$

where the two terms are respectively produced when the derivative acts on the first factor or on the second factor in Eq. (5.149). Note that both terms are already anti-symmetric with respect to X_2 and X_3 . Applying another derivative yields

$$\begin{aligned} 0 = \frac{\delta^3 \Phi(X_1)}{\Phi(X_4) \Phi(X_3) \Phi(X_2)} &= \Gamma(X_4, X_3, X_2, Y_2) \mathcal{W}(Y_2, X_1) \\ &\quad - \Gamma(X_3, X_2, Y_2) \Gamma(X_4, Y_4) \mathcal{W}(Y_4, Y_2, X_1) \\ &\quad + \Gamma(X_4, X_3, Y_3) \Gamma(X_2, Y_2) \mathcal{W}(Y_3, Y_2, X_1) \\ &\quad + \Gamma(X_4, X_2, Y_2) \Gamma(X_3, Y_3) \mathcal{W}(Y_3, Y_2, X_1) \\ &\quad + \Gamma(X_4, Y_4) \Gamma(X_3, Y_3) \Gamma(X_2, Y_2) \mathcal{W}(Y_4, Y_3, Y_2, X_1). \end{aligned} \quad (5.151)$$

Since the third derivative is antisymmetric in (X_2, X_3, X_4) ,

$$\frac{\delta^3 \Phi(X_1)}{\Phi(X_4) \Phi(X_3) \Phi(X_2)} = \mathbb{A}_{(X_2, X_3, X_4)} \frac{\delta^3 \Phi(X_1)}{\Phi(X_4) \Phi(X_3) \Phi(X_2)}, \quad (5.152)$$

the same applies to the right-hand side of Eq. (5.151). Therefore, we may apply the antisymmetrization operator to the right-hand side of Eq. (5.151) without changing this expression. By antisymmetrizing each term in the sum separately, we thus obtain

$$\begin{aligned} 0 = \mathbb{A}_{(X_2, X_3, X_4)} \Big\{ & \Gamma(X_4, X_3, X_2, Y_2) \mathcal{W}(Y_2, X_1) \\ & + 3 \Gamma(X_4, X_3, Y_3) \Gamma(X_2, Y_2) \mathcal{W}(Y_3, Y_2, X_1) \\ & + \Gamma(X_4, Y_4) \Gamma(X_3, Y_3) \Gamma(X_2, Y_2) \mathcal{W}(Y_4, Y_3, Y_2, X_1) \Big\}. \end{aligned} \quad (5.153)$$

By proceeding further in this way, we obtain after a lengthy calculation

$$\begin{aligned} 0 = \mathbb{A}_{(X_2, \dots, X_5)} \Big\{ & \Gamma(X_5, X_4, X_3, X_2, Y_2) \mathcal{W}(Y_2, X_1) \\ & + 4 \Gamma(X_5, X_4, X_3, Y_3) \Gamma(X_2, Y_2) \mathcal{W}(Y_3, Y_2, X_1) \\ & - 3 \Gamma(X_5, X_4, Y_3) \Gamma(X_3, X_2, Y_2) \mathcal{W}(Y_3, Y_2, X_1) \\ & + 6 \Gamma(X_5, X_4, Y_4) \Gamma(X_3, Y_3) \Gamma(X_2, Y_2) \mathcal{W}(Y_4, Y_3, Y_2, X_1) \\ & + \Gamma(X_5, Y_5) \Gamma(X_4, Y_4) \Gamma(X_3, Y_3) \Gamma(X_2, Y_2) \mathcal{W}(Y_5, Y_4, Y_3, Y_2, X_1) \Big\}, \end{aligned} \quad (5.154)$$

and finally,

$$\begin{aligned} 0 = \mathbb{A}_{(X_2, \dots, X_6)} \Big\{ & \Gamma(X_6, X_5, X_4, X_3, X_2, Y_2) \mathcal{W}(Y_2, X_1) \\ & + 5 \Gamma(X_6, X_5, X_4, X_3, Y_3) \Gamma(X_2, Y_2) \mathcal{W}(Y_3, Y_2, X_1) \\ & - 10 \Gamma(X_6, X_5, X_4, Y_3) \Gamma(X_3, X_2, Y_2) \mathcal{W}(Y_3, Y_2, X_1) \\ & + 10 \Gamma(X_6, X_5, X_4, Y_4) \Gamma(X_3, Y_3) \Gamma(X_2, Y_2) \mathcal{W}(Y_4, Y_3, Y_2, X_1) \\ & - 15 \Gamma(X_6, X_5, Y_4) \Gamma(X_4, X_3, Y_3) \Gamma(X_2, Y_2) \mathcal{W}(Y_4, Y_3, Y_2, X_1) \\ & + 10 \Gamma(X_6, X_5, Y_5) \Gamma(X_4, Y_4) \Gamma(X_3, Y_3) \Gamma(X_2, Y_2) \\ & \quad \times \mathcal{W}(Y_5, Y_4, Y_3, Y_2, X_1) \\ & + \Gamma(X_6, Y_6) \Gamma(X_5, Y_5) \Gamma(X_4, Y_4) \Gamma(X_3, Y_3) \Gamma(X_2, Y_2) \\ & \quad \times \mathcal{W}(Y_6, Y_5, Y_4, Y_3, Y_2, X_1) \Big\}. \end{aligned} \quad (5.155)$$

Our assertions (5.142)–(5.144) now follow by evaluating the field-independent terms of these equations and using Eqs. (A.30) and (A.48):

(i) *Two-point function.* Evaluating the field-independent terms of Eq. (5.149) yields

$$\delta(X_2, X_1) = \mathbf{\Gamma}^2(X_2, Y_2) \mathbf{G}_c^2(Y_2, X_1), \quad (5.156)$$

which is equivalent to the assertion (5.142). In the following, we will also need the converse relation,

$$\delta(Z, Y) = \mathbf{G}_c^2(Z, X) \mathbf{\Gamma}^2(X, Y), \quad (5.157)$$

which can be shown analogously from Eq. (5.138).

(ii) *Four-point function.* Evaluating the field-independent terms of Eq. (5.153) yields

$$\begin{aligned} 0 = & \mathbf{\Gamma}^4(X_4, X_3, X_2, Y_2) \mathbf{G}_c^2(Y_2, X_1) \\ & + \mathbf{\Gamma}^2(X_4, Y_4) \mathbf{\Gamma}^2(X_3, Y_3) \mathbf{\Gamma}^2(X_2, Y_2) \mathbf{G}_c^4(Y_4, Y_3, Y_2, X_1). \end{aligned} \quad (5.158)$$

Here, we have omitted the antisymmetrization operator because both terms on the right-hand side are already antisymmetric in (X_2, X_3, X_4) . By multiplying this equation through with the connected Green functions, integrating over the internal variables and using Eq. (5.157), we further obtain

$$\begin{aligned} \mathbf{G}_c^4(Z_4, Z_3, Z_2, X_1) = & \\ - \mathbf{G}_c^2(Z_4, X_4) \mathbf{G}_c^2(Z_3, X_3) \mathbf{G}_c^2(Z_2, X_2) \mathbf{\Gamma}^4(X_4, X_3, X_2, Y_2) \mathbf{G}_c^2(Y_2, X_1). \end{aligned} \quad (5.159)$$

Finally, renaming variables $(X_1 \mapsto Z_1, Y_2 \mapsto X_1)$ and using the antisymmetry of the two-point function \mathbf{G}_c^2 leads to

$$\begin{aligned} \mathbf{G}_c^4(Z_4, Z_3, Z_2, Z_1) = & \\ \mathbf{G}_c^2(Z_4, X_4) \mathbf{G}_c^2(Z_3, X_3) \mathbf{G}_c(Z_2, X_2) \mathbf{G}_c(Z_1, X_1) \mathbf{\Gamma}^4(X_4, X_3, X_2, X_1), \end{aligned} \quad (5.160)$$

which is equivalent to the assertion (5.143).

(iii) *Six-point function.* From Eq. (5.155), we obtain by evaluating the constant terms,

$$\begin{aligned} 0 = & \mathbf{\Gamma}^6(X_6, X_5, X_4, X_3, X_2, Y_2) \mathbf{G}_c^2(Y_2, X_1) \\ & + 10 \mathbb{A}_{(X_2, \dots, X_6)} \left\{ \mathbf{\Gamma}^4(X_6, X_5, X_4, Y_4) \mathbf{\Gamma}^2(X_3, Y_3) \mathbf{\Gamma}^2(X_2, Y_2) \right. \\ & \quad \left. \times \mathbf{G}_c^4(Y_4, Y_3, Y_2, X_1) \right\} \\ & + \mathbf{\Gamma}^2(X_6, Y_6) \mathbf{\Gamma}^2(X_5, Y_5) \mathbf{\Gamma}^2(X_4, Y_4) \mathbf{\Gamma}^2(X_3, Y_3) \mathbf{\Gamma}^2(X_2, Y_2) \\ & \quad \times \mathbf{G}_c^6(Y_6, Y_5, Y_4, Y_3, Y_2, X_1). \end{aligned} \quad (5.161)$$

Using Eq. (5.157), this further yields

$$\begin{aligned}
& \mathbf{G}_c^6(Z_6, Z_5, Z_4, Z_3, Z_2, X_1) \\
&= -\mathbf{G}_c^2(Z_6, X_6) \mathbf{G}_c^2(Z_5, X_5) \mathbf{G}_c^2(Z_4, X_4) \mathbf{G}_c^2(Z_3, X_3) \mathbf{G}_c^2(Z_2, X_2) \\
&\quad \times \mathbf{I}^6(X_6, X_5, X_4, X_3, X_2, Y_2) \mathbf{G}_c^2(Y_2, X_1) \\
&\quad - 10 \mathbb{A}_{(Z_2, \dots, Z_6)} \left\{ \mathbf{G}_c^2(Z_6, X_6) \mathbf{G}_c^2(Z_5, X_5) \mathbf{G}_c^2(Z_4, X_4) \right. \\
&\quad \left. \times \mathbf{I}^4(X_6, X_5, X_4, Y_4) \mathbf{G}_c^4(Y_4, Z_3, Z_2, X_1) \right\}.
\end{aligned} \tag{5.162}$$

Putting Eq. (5.159) into this formula then leads to

$$\begin{aligned}
& \mathbf{G}_c^6(Z_6, Z_5, Z_4, Z_3, Z_2, X_1) \\
&= -\mathbf{G}_c^2(Z_6, X_6) \mathbf{G}_c^2(Z_5, X_5) \mathbf{G}_c^2(Z_4, X_4) \mathbf{G}_c^2(Z_3, X_3) \mathbf{G}_c^2(Z_2, X_2) \\
&\quad \times \mathbf{I}^6(X_6, X_5, X_4, X_3, X_2, Y_2) \mathbf{G}_c^2(Y_2, X_1) \\
&\quad + 10 \mathbb{A}_{(Z_2, \dots, Z_6)} \left\{ \mathbf{G}_c^2(Z_6, X_6) \mathbf{G}_c^2(Z_5, X_5) \mathbf{G}_c^2(Z_4, X_4) \mathbf{I}^4(X_6, X_5, X_4, Y_4) \right. \\
&\quad \left. \times \mathbf{G}_c^2(Y_4, A_4) \mathbf{G}_c^2(Z_3, A_3) \mathbf{G}_c^2(Z_2, A_2) \mathbf{I}^4(A_4, A_3, A_2, A_1) \mathbf{G}_c^2(A_1, X_1) \right\}.
\end{aligned} \tag{5.163}$$

By renaming variables ($X_1 \mapsto Z_1$, $Y_2 \mapsto X_1$, $A_4 \mapsto Y_3$, $A_3 \mapsto X_3$, $A_2 \mapsto X_2$, $A_1 \mapsto X_1$) and using the antisymmetry of \mathbf{G}_c^2 , we can write this equivalently as

$$\begin{aligned}
& \mathbf{G}_c^6(Z_6, Z_5, Z_4, Z_3, Z_2, Z_1) = \\
& \mathbf{G}_c^2(Z_6, X_6) \mathbf{G}_c^2(Z_5, X_5) \mathbf{G}_c^2(Z_4, X_4) \mathbf{G}_c^2(Z_3, X_3) \mathbf{G}_c^2(Z_2, X_2) \\
&\quad \times \mathbf{G}_c^2(Z_1, X_1) \mathbf{I}^6(X_6, X_5, X_4, X_3, X_2, X_1) \\
&\quad + 10 \mathbb{A}_{(Z_2, \dots, Z_6)} \left\{ \mathbf{G}_c^2(Z_6, X_6) \mathbf{G}_c^2(Z_5, X_5) \mathbf{G}_c^2(Z_4, X_4) \mathbf{I}^4(X_6, X_5, X_4, Y_4) \right. \\
&\quad \left. \times \mathbf{G}_c^2(Y_4, Y_3) \mathbf{I}^4(Y_3, X_3, X_2, X_1) \mathbf{G}_c^2(X_3, Z_3) \mathbf{G}_c^2(X_2, Z_2) \mathbf{G}_c^2(X_1, Z_1) \right\}.
\end{aligned} \tag{5.164}$$

One can convince oneself that the last term is already antisymmetric in all six variables (Z_1, \dots, Z_6), and hence Eq. (5.164) is equivalent to the assertion (5.144). Finally, for $n \geq 2$, Eq. (5.145) follows analogously by iterating the above procedure. \square

Theorem 5.15 (Relations between connected and one-line-irreducible Green functions). *The following relations hold between the connected Green functions G^{2n} and the one-line-irreducible Green functions Γ^{2n} : for $n = 1$,*

$$\delta(x_1, x_2) = \int dy_1 G_c^2(x_1, y_1) \Gamma^2(y_1, x_2); \tag{5.165}$$

for $n = 2$,

$$G_c^4(x_1, x_2, x_3, x_4) = \quad (5.166)$$

$$\int dy_1 \dots \int dy_4 G_c^2(x_1, y_1) G_c^2(x_2, y_2) \Gamma^4(y_1, y_2, y_3, y_4) G_c^2(y_3, x_3) G_c^2(y_4, x_4);$$

for $n = 3$,

$$G_c^6(x_1, x_2, x_3, x_4, x_5, x_6) = \quad (5.167)$$

$$\begin{aligned} & - \int dy_1 \dots \int dy_6 G_c^2(x_1, y_1) G_c^2(x_2, y_2) G_c^2(x_3, y_3) \\ & \quad \times \Gamma^6(y_1, y_2, y_3, y_4, y_5, y_6) G_c^2(y_4, x_4) G_c^2(y_5, x_5) G_c^2(y_6, x_6) \\ & - 9 \mathbb{A}_{(x_1, x_2, x_3)} \mathbb{A}_{(x_4, x_5, x_6)} \left\{ \int dy_1 \dots \int dy_6 G_c^2(x_1, y_1) G_c^2(x_2, y_2) \Gamma^4(y_1, y_2, z, y_6) \right. \\ & \quad \times G_c^2(z, z') G_c^2(y_6, x_6) G_c^2(x_3, y_3) \Gamma^4(z', y_3, y_4, y_5) G_c^2(y_4, x_4) G_c^2(y_5, x_5) \left. \right\}. \end{aligned}$$

In general, for $n \geq 2$, we have

$$G_c^{2n}(x_1, \dots, x_{2n}) = \quad (5.168)$$

$$\begin{aligned} & (-1)^n \int dy_1 \dots \int dy_{2n} G_c^2(x_1, y_1) \dots G_c^2(x_n, y_n) \\ & \quad \times \Gamma^{2n}(y_1, \dots, y_n, y_{n+1}, \dots, y_{2n}) G_c^2(y_{n+1}, x_{n+1}) \dots G_c^2(y_{2n}, x_{2n}) \\ & + \mathcal{R}, \end{aligned}$$

where again, the remainder terms denoted by \mathcal{R} have the property that each Feynman graph in their respective expansions contains at least one torso line (see Definition 4.12). The above relations can be represented graphically by means of Universal Feynman Graphs as shown in Table 5.2.

Proof. We derive these relations from the corresponding equalities for the Nambu-type Green functions (Theorem 5.14). For this purpose, we use the relations (see Appendix A)

$$G_c^2(x_1, +; x_2, -) = G_c^2(x_1, x_2), \quad (5.169)$$

$$G_c^4(x_1, +; x_2, +; x_3, -; x_4, -) = -G_c^4(x_1, x_2, x_3, x_4), \quad (5.170)$$

$$G_c^6(x_1, +; x_2, +; x_3, +; x_4, -; x_5, -; x_6, -) = -G_c^6(x_1, x_2, x_3, x_4, x_5, x_6), \quad (5.171)$$

etc., as well as the analogous relations for the one-line-irreducible Green functions (for which the Nambu indices $+$ and $-$ must be interchanged).

(i) *Two-point function.* From Eq. (5.142), we obtain

$$\delta(x_1, +; x_2, +) = \int dy_1 \sum_{c_1} G_c^2(x_1, +; y_1, c_1) \Gamma^2(y_1, c_1; x_2, +). \quad (5.172)$$

In the sum over Nambu indices, only $c_1 = -$ gives a nonvanishing contribution. Thus,

$$\delta(x_1, x_2) = \int dy_1 \mathbf{G}_c^2(x_1, +; y_1, -) \mathbf{I}^2(y_1, -; x_2, +) \quad (5.173)$$

$$= \int dy_1 G_c^2(x_1, y_1) \Gamma^2(y_1, x_2), \quad (5.174)$$

which coincides with the first identity (5.165).

(ii) *Four-point function.* Equation (5.143) can be written equivalently as

$$\mathbf{G}_c^4(X_1, X_2, X_3, X_4) = \quad (5.175)$$

$$\int dY_1 \dots \int dY_4 \mathbf{G}_c^2(X_1, Y_1) \mathbf{G}_c^2(X_2, Y_2) \mathbf{I}^4(Y_1, Y_2, Y_3, Y_4) \mathbf{G}_c^2(Y_3, X_3) \mathbf{G}_c^2(Y_4, X_4),$$

where we have used the antisymmetry of the Nambu-type two-point function. In particular, this implies

$$\mathbf{G}_c^4(x_1, +; x_2, +; x_3, -; x_4, -) = \quad (5.176)$$

$$\int dy_1 \dots \int dy_4 \sum_{c_1, \dots, c_4} \mathbf{G}_c^2(x_1, +; y_1, c_1) \mathbf{G}_c^2(x_2, +; y_2, c_2) \\ \Gamma^4(y_1, c_1; y_2, c_2; y_3, c_3; y_4, c_4) \mathbf{G}_c^2(y_3, c_3; x_3, -) \mathbf{G}_c^2(y_4, c_4; x_4, -).$$

Here, only the combination of Nambu indices

$$(c_1, c_2, c_3, c_4) = (-, -, +, +) \quad (5.177)$$

gives a nonvanishing contribution to the sum, and this yields

$$\mathbf{G}_c^4(x_1, x_2, x_3, x_4) = \int dy_1 \dots \int dy_4 \quad (5.178)$$

$$\times G_c^2(x_1, y_1) G_c^2(x_2, y_2) \Gamma^4(y_1, y_2, y_3, y_4) G_c^2(y_3, x_3) G_c^2(y_4, x_4),$$

which coincides with the assertion.

(iii) *Six-point function.* We start from Eq. (5.164) in the proof of Theorem 5.14. By using the antisymmetry of \mathbf{G}_c^2 and by renaming the variables, this is equivalent to

$$\mathbf{G}_c^6(X_1, X_2, X_3, X_4, X_5, X_6) = \quad (5.179)$$

$$- \int dY_1 \dots \int dY_6 \mathbf{G}_c^2(X_1, Y_1) \mathbf{G}_c^2(X_2, Y_2) \mathbf{G}_c^2(X_3, Y_3) \\ \times \mathbf{I}^6(Y_1, Y_2, Y_3, Y_4, Y_5, Y_6) \mathbf{G}_c^2(Y_4, X_4) \mathbf{G}_c^2(Y_5, X_5) \mathbf{G}_c^2(Y_6, X_6) \\ + 10 \mathbb{A}_{(X_1, \dots, X_5)} \left\{ \int dY_1 \dots \int dY_6 \mathbf{G}_c^2(X_1, Y_1) \mathbf{G}_c^2(X_2, Y_2) \mathbf{G}_c^2(X_3, Y_3) \mathbf{I}^4(Y_1, Y_2, Y_3, Z) \right. \\ \left. \times \mathbf{G}_c^2(Z, Z') \mathbf{I}^4(Z', Y_4, Y_5, Y_6) \mathbf{G}_c^2(Y_4, X_4) \mathbf{G}_c^2(Y_5, X_5) \mathbf{G}_c^2(Y_6, X_6) \right\}.$$

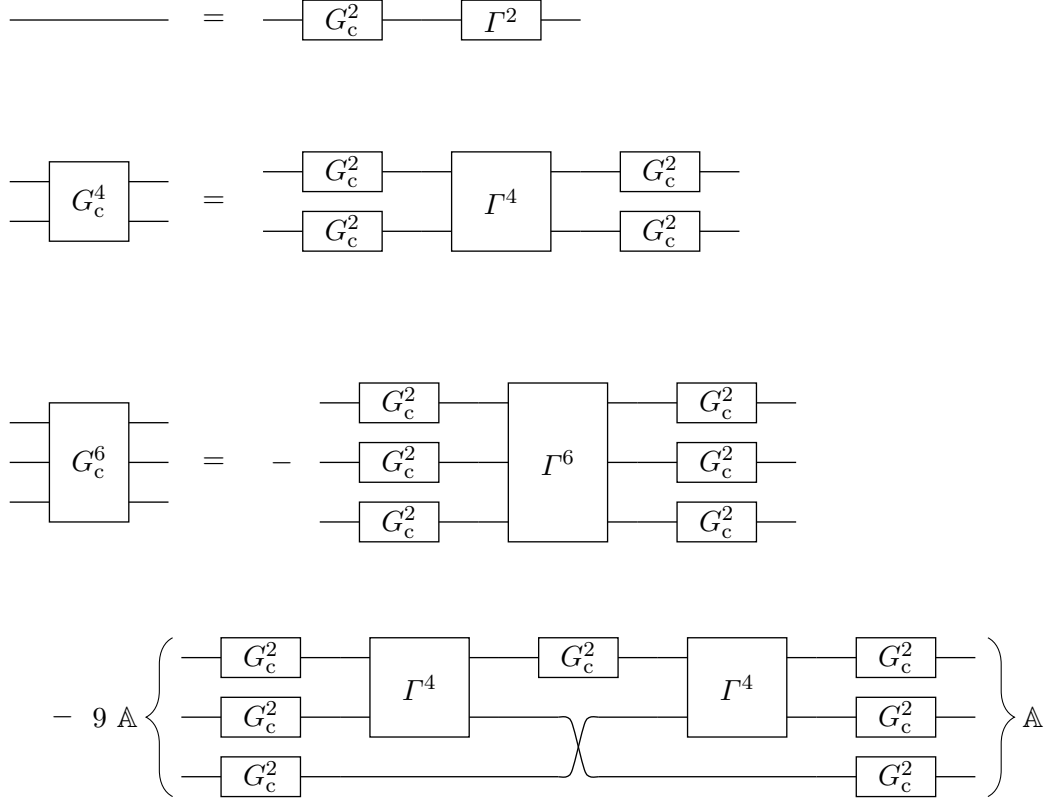


Table 5.2: Relations between connected Green functions and one-line-irreducible Green functions: Universal Feynman Graph representation.

We evaluate this equation for

$$X_1 = (x_1, +), \quad X_2 = (x_2, +), \quad X_3 = (x_3, +), \quad (5.180)$$

$$X_4 = (x_4, -), \quad X_5 = (x_5, -), \quad X_6 = (x_6, -),$$

such that the left-hand side of the equation reverts to $(-1)G_c^6(x_1, x_2, x_3, x_4, x_5, x_6)$. The first term on the right-hand side can be evaluated analogously as in the case of the four-point function, which yields

$$\begin{aligned} & \int dy_1 \dots \int dy_6 G_c^2(x_1, y_1) G_c^2(x_2, y_2) G_c^2(x_3, y_3) \\ & \times \Gamma^6(y_1, y_2, y_3, y_4, y_5, y_6) G_c^2(y_4, x_4) G_c^2(y_5, x_5) G_c^2(y_6, x_6). \end{aligned} \quad (5.181)$$

Next, consider the second term on the right-hand side of Eq. (5.179), which reads

$$\begin{aligned} & \frac{10}{5!} \sum_{\pi \in S_5} \text{sgn}(\pi) \int dY_1 \dots \int dY_6 \\ & \times \mathbf{G}_c^2(X_{\pi(1)}, Y_1) \mathbf{G}_c^2(X_{\pi(2)}, Y_2) \mathbf{G}_c^2(X_{\pi(3)}, Y_3) \mathbf{\Gamma}^4(Y_1, Y_2, Y_3, Z) \\ & \times \mathbf{G}_c^2(Z, Z') \mathbf{\Gamma}^4(Z', Y_4, Y_5, Y_6) \mathbf{G}_c^2(Y_4, X_{\pi(4)}) \mathbf{G}_c^2(Y_5, X_{\pi(5)}) \mathbf{G}_c^2(Y_6, X_6). \end{aligned} \quad (5.182)$$

By the antisymmetry of the two four-point functions in (Y_1, Y_2, Y_3) and respectively in (Y_4, Y_5) , there are always $3!2! = 12$ permutations which give the same contribution. Thus, we need to consider only

$$\frac{5!}{3!2!} = 10 \quad (5.183)$$

representative permutations, provided that we count each of them 12 times. Concretely, we choose the 10 representative permutations π_0, \dots, π_9 which are shown in Table 5.3. Further using that $12 \times 10 / 5! = 1$, we see that the prefactor in Eq. (5.182) cancels out, and hence we are left with the sum

$$\begin{aligned} & \sum_{j=0}^9 \text{sgn}(\pi_j) \int dY_1 \dots \int dY_6 \\ & \times \mathbf{G}_c^2(X_{\pi_j(1)}, Y_1) \mathbf{G}_c^2(X_{\pi_j(2)}, Y_2) \mathbf{G}_c^2(X_{\pi_j(3)}, Y_3) \mathbf{\Gamma}^4(Y_1, Y_2, Y_3, Z) \\ & \times \mathbf{G}_c^2(Z, Z') \mathbf{\Gamma}^4(Z', Y_4, Y_5, Y_6) \mathbf{G}_c^2(Y_4, X_{\pi_j(4)}) \mathbf{G}_c^2(Y_5, X_{\pi_j(5)}) \mathbf{G}_c^2(Y_6, X_6). \end{aligned} \quad (5.184)$$

Consider the first summand with $j = 0$, which corresponds to the identity permutation:

$$\begin{aligned} & \int dY_1 \dots \int dY_6 \mathbf{G}_c^2(X_1, Y_1) \mathbf{G}_c^2(X_2, Y_2) \mathbf{G}_c^2(X_3, Y_3) \mathbf{\Gamma}^4(Y_1, Y_2, Y_3, Z) \\ & \times \mathbf{G}_c^2(Z, Z') \mathbf{\Gamma}^4(Z', Y_4, Y_5, Y_6) \mathbf{G}_c^2(Y_4, X_4) \mathbf{G}_c^2(Y_5, X_5) \mathbf{G}_c^2(Y_6, X_6). \end{aligned} \quad (5.185)$$

By choosing the external Nambu indices as in Eq. (5.180), the product of the connected Green functions \mathbf{G}_c^2 vanishes unless

$$\begin{aligned} Y_1 &= (y_1, -), \quad Y_2 = (y_2, -), \quad Y_3 = (y_3, -), \\ Y_4 &= (y_4, +), \quad Y_5 = (y_5, +), \quad Y_6 = (y_6, +). \end{aligned} \quad (5.186)$$

For this combination of the internal Nambu indices, however, the four-point functions $\mathbf{\Gamma}^4$ vanish. Therefore, the first summand in Eq. (5.184) is zero.

Next, consider the second summand in Eq. (5.184) with $j = 1$ (see Table 5.3): By renaming the variables $Y_3 \leftrightarrow Y_4$, this term equals

$$\begin{aligned} & - \int dY_1 \dots \int dY_6 \mathbf{G}_c^2(X_1, Y_1) \mathbf{G}_c^2(X_2, Y_2) \mathbf{G}_c^2(X_4, Y_4) \mathbf{\Gamma}^4(Y_1, Y_2, Y_4, Z) \\ & \times \mathbf{G}_c^2(Z, Z') \mathbf{\Gamma}^4(Z', Y_3, Y_5, Y_6) \mathbf{G}_c^2(Y_3, X_3) \mathbf{G}_c^2(Y_5, X_5) \mathbf{G}_c^2(Y_6, X_6). \end{aligned} \quad (5.187)$$

In this case, our choice (5.180) of the external Nambu indices implies that

$$\begin{aligned} Y_1 &= (y_1, -), \quad Y_2 = (y_2, -), \quad Y_3 = (y_3, -), \\ Y_4 &= (y_4, +), \quad Y_5 = (y_5, +), \quad Y_6 = (y_6, +), \\ Z &= (z, +), \quad Z' = (z', -), \end{aligned} \quad (5.188)$$

and thus, Eq. (5.187) yields

$$\begin{aligned} & - \int dy_1 \dots \int dy_6 G_c^2(x_1, y_1) G_c^2(x_2, y_2) G_c^2(y_4, x_4) \Gamma^4(y_1, y_2, y_4, z) \\ & \times G_c^2(z, z') \Gamma^4(z', y_3, y_5, y_6) G_c^2(x_3, y_3) G_c^2(y_5, x_5) G_c^2(y_6, x_6). \end{aligned} \quad (5.189)$$

By the antisymmetry of Γ^4 with respect to its last two arguments, this expression equals

$$\begin{aligned} & \int dy_1 \dots \int dy_6 G_c^2(x_1, y_1) G_c^2(x_2, y_2) \Gamma^4(y_1, y_2, z, y_4) G_c^2(z, z') G_c^2(y_4, x_4) \\ & \times G_c^2(x_3, y_3) \Gamma^4(z', y_3, y_5, y_6) G_c^2(y_5, x_5) G_c^2(y_6, x_6). \end{aligned} \quad (5.190)$$

Furthermore, the remaining terms in Eq. (5.184)—i.e., those with $j = 2, \dots, 9$ —can be evaluated analogously. Taking into account also Eq. (5.181), we arrive at

$$\begin{aligned} & (-1) G_c^6(x_1, x_2, x_3, x_4, x_5, x_6) = \\ & \int dy_1 \dots \int dy_6 G_c^2(x_1, y_1) G_c^2(x_2, y_2) G_c^2(x_3, y_3) \\ & \times \Gamma^6(y_1, y_2, y_3, y_4, y_5, y_6) G_c^2(y_4, x_4) G_c^2(y_5, x_5) G_c^2(y_6, x_6) \\ & + \sum_{\pi \in S_3} \text{sgn}(\pi) \sum_{\pi' \in S_3} \text{sgn}(\pi') \int dy_1 \dots \int dy_6 \\ & \times G_c^2(x_{\pi(1)}, y_1) G_c^2(x_{\pi(2)}, y_2) \Gamma^4(y_1, y_2, z, y_4) G_c^2(z, z') G_c^2(y_4, x_{\pi'(4)}) \\ & \times G_c^2(x_{\pi(3)}, y_3) \Gamma^4(z', y_3, y_5, y_6) G_c^2(y_5, x_{\pi'(5)}) G_c^2(y_6, x_{\pi'(6)}), \end{aligned} \quad (5.191)$$

which is equivalent to the assertion (5.167).

Finally, consider the general case where $n \geq 2$. We can write Eq. (5.145) of Theorem 5.14 equivalently as

$$\begin{aligned} & \mathbf{G}_c^{2n}(X_1, \dots, X_{2n}) = \\ & (-1)^n \int dY_1 \dots \int dY_{2n} \mathbf{G}_c^2(X_1, Y_1) \dots \mathbf{G}_c^2(X_n, Y_n) \\ & \times \mathbf{I}^{2n}(Y_1, \dots, Y_n, Y_{n+1}, \dots, Y_{2n}) \mathbf{G}_c^2(Y_{n+1}, X_{n+1}) \dots \mathbf{G}_c^2(Y_{2n}, X_{2n}) \\ & + \mathcal{R}, \end{aligned} \quad (5.192)$$

j	$\text{sgn}(\pi_j)$	$\pi_j(1)$	$\pi_j(2)$	$\pi_j(3)$	$\pi_j(4)$	$\pi_j(5)$
0	+1	1	2	3	4	5
1	-1	1	2	4	3	5
2	+1	1	2	5	3	4
3	+1	1	3	4	2	5
4	-1	1	3	5	2	4
5	+1	1	4	5	2	3
6	-1	2	3	4	1	5
7	+1	2	3	5	1	4
8	-1	2	4	5	1	3
9	+1	3	4	5	1	2

Table 5.3: Representative permutations used for evaluating Eq. (5.182).

where the sign $(-1)^n$ comes from interchanging the arguments of the last n connected Green functions. By choosing the external Nambu indices as

$$X_i = \begin{cases} (x_i, +), & \text{if } i = 1, \dots, n, \\ (x_i, -), & \text{if } i = n + 1, \dots, 2n, \end{cases} \quad (5.193)$$

we see that only the combination of internal Nambu indices given by

$$Y_i = \begin{cases} (y_i, -), & \text{if } i = 1, \dots, n, \\ (y_i, +), & \text{if } i = n + 1, \dots, 2n, \end{cases} \quad (5.194)$$

contributes to the sum, and this implies the assertion (5.168). \square

Corollary 5.16. *The relations (5.165)–(5.168) of Theorem 5.15 can be inverted by simply interchanging the connected and the one-line-irreducible Green functions.*

Proof. This follows from the involution property of the Legendre transformation (Theorem 5.12). In concrete terms, the inverse Green function relations can be proven along the lines of Theorem 5.14 and Theorem 5.15 by only interchanging from the beginning the Green function generators \mathcal{W} and Γ (see [Zin02, Sct. 7.5]). \square

Finally, we are in a position to prove the following theorem, which constitutes the main conclusion of this section.

Theorem 5.17 (Feynman graph expansion of one-line-irreducible Green functions). *The one-line-irreducible two-point Green function Γ^2 is related to the irreducible self-energy Σ^2 (see Sct. 5.4) by*

$$\Gamma^2 = C^{-1} - \Sigma^2. \quad (5.195)$$

Furthermore, for $n \geq 2$, the one-line-irreducible Green function Γ^{2n} is given by $(-1)^n$ times the sum of all amputated, one-line-irreducible graphs (see Definition 4.14), i.e.,

$$\Gamma^{2n} = (-1)^n \sum_{k=1}^{\infty} \frac{1}{k! 2^k} \sum_{\substack{\pi \in S_{n+2k}, \\ \pi \text{ one-line-irreducible}}} \text{Val}_{\text{amp}}[n, k, \pi], \quad (5.196)$$

where $\text{Val}_{\text{amp}}[n, k, \pi]$ is given explicitly by Eqs. (4.173) and (4.190).

Proof. For $n = 1$ and for $n = 2$, the assertion follows immediately from Theorem 5.9 and Theorem 5.15: On the one hand, Eq. (5.116) implies that

$$G_c^2 = (1 - C \Sigma^2)^{-1} C, \quad (5.197)$$

and by inverting this equation, we obtain

$$(G_c^2)^{-1} = C^{-1} (1 - C \Sigma^2) = C^{-1} - \Sigma^2. \quad (5.198)$$

On the other hand, Eq. (5.165) can be written as

$$(G_c^2)^{-1} = \Gamma^2. \quad (5.199)$$

Taken together, these two identities imply Eq. (5.195). Similarly, for $n = 2$, the comparison of Eqs. (5.115) and (5.166) shows that

$$\Gamma^4 = \Sigma^4, \quad (5.200)$$

which by Eq. (5.113) is equivalent to the assertion (5.196).

For general $n \geq 2$, the proof is more complicated. We build on the proof given in Ref. [Zin02, Sct. 7.8], however, employing here the explicit *renormalization group equations* (RGE) for the one-line-irreducible Green functions, which are derived in Sct. 6.3 below. First, Theorem 5.9, Eq. (5.115), and Theorem 5.15, Eq. (5.168), together imply that

$$\Sigma^{2n} = (-1)^n \Gamma^{2n} + \mathcal{R}', \quad (5.201)$$

where the remainder terms denoted by \mathcal{R}' can be expanded in terms of fully amputated Feynman graphs which each contain at least one torso line. In particular, this means that all graphs contained in the second term \mathcal{R}' are (one-line-)reducible. On the other hand, by Eq. (5.111), Σ^{2n} is given by the sum of all non-amputable graphs, which contain as a subset all irreducible graphs. By the above characterization of \mathcal{R}' , all these irreducible graphs must be contained in the first term $(-1)^n \Gamma^{2n}$. Now, if we can show that conversely, all graphs appearing in the expansion of Γ^{2n} are irreducible, then

it follows that the splitting of Eq. (5.201) coincides precisely with the splitting of all non-amputable graphs into those which are irreducible and those which are reducible, respectively, and this would prove the assertion.

Thus, it remains to show that all Feynman graphs appearing in the expansion of Γ^{2n} are one-line-irreducible. For this purpose, we define for each $\varepsilon > 0$ the modified covariance

$$C_\varepsilon(y_1, y_2) = C(y_1, y_2) - \varepsilon \int dz_1 \int dz_2 C(y_1, z_2) C(z_1, y_2). \quad (5.202)$$

First, we show that the inverse of C_ε is given by

$$Q_\varepsilon(y_1, y_2) = Q(y_1, y_2) + \varepsilon + \mathcal{O}(\varepsilon^2). \quad (5.203)$$

In fact, this can be verified as follows:

$$\begin{aligned} \int dy_2 C_\varepsilon(y_1, y_2) Q_\varepsilon(y_2, y_3) &= \delta(y_1, y_3) + \varepsilon \int dy_2 C(y_1, y_2) \\ &\quad - \varepsilon \int dy_2 \int dz_1 \int dz_2 C(y_1, z_2) C(z_1, y_2) Q(y_2, y_3). \end{aligned} \quad (5.204)$$

In the last term, we first perform the integral over y_2 and then over z_1 , hence

$$\int dz_1 \int dy_2 C(z_1, y_2) Q(y_2, y_3) = \int dz_1 \delta(z_1, y_3) = 1. \quad (5.205)$$

This shows that the third term on the right-hand side of Eq. (5.204) cancels against the second term, and thus we obtain the desired identity

$$\int dy_2 C_\varepsilon(y_1, y_2) Q_\varepsilon(y_2, y_3) = \delta(y_1, y_3). \quad (5.206)$$

Next, consider the ε -dependent connected Green functions $G_{c,\varepsilon}^{2n}$ as well as the one-line-irreducible Green functions Γ_ε^{2n} , which are obtained by replacing in their respective Feynman graph expansions all covariance lines by $C \mapsto C_\varepsilon$. We are interested in the derivatives

$$\dot{G}_{c,\varepsilon}^{2n} \Big|_{\varepsilon=0} \equiv \frac{d}{d\varepsilon} G_{c,\varepsilon}^{2n} \Big|_{\varepsilon=0}, \quad (5.207)$$

and respectively

$$\dot{\Gamma}_\varepsilon^{2n} \Big|_{\varepsilon=0} \equiv \frac{d}{d\varepsilon} \Gamma_\varepsilon^{2n} \Big|_{\varepsilon=0}. \quad (5.208)$$

By the linearity of the derivative and by the product rule, these ε derivatives can act on any modified covariance line C_ε of any Feynman graph. Thereby, they produce all possible graphs in which a single covariance line is replaced by

$$C(y_1, y_2) \mapsto \dot{C}_\varepsilon(y_1, y_2) \Big|_{\varepsilon=0} = - \int dz_1 \int dz_2 C(y_1, z_2) C(z_1, y_2), \quad (5.209)$$

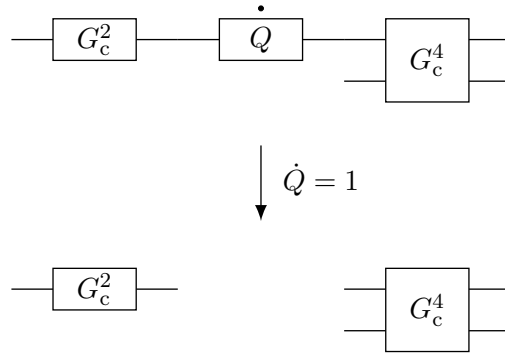


Figure 5.1: Setting $\dot{Q} = 1$ on the right-hand side of the RGE for the *connected* four-point function produces disconnected graphs.

while all other covariance lines remain unchanged,

$$C_\varepsilon(y_1, y_2) \Big|_{\varepsilon=0} = C(y_1, y_2). \quad (5.210)$$

Now, the replacement (5.209) corresponds precisely to the operation of *cutting the covariance line* $C(y_1, y_2)$ (see Sect. 4.5.2) and integrating over the new external arguments z_1 and z_2 . This means, the derivatives (5.207) and (5.208) yield the sums of all (originally connected and respectively one-line-irreducible) Feynman graphs in which one covariance line is cut and the new external arguments are integrated over.

We will now show that all Feynman graphs representing the derivative (5.208) are still connected, which implies that all Feynman graphs representing the original Green function Γ^{2n} are one-line-irreducible. This is in contrast to the Feynman graph expansion of the derivative (5.207), which in fact contains also disconnected graphs. In order to see this explicitly, we will make use of the RGE for the respective Green functions, which are derived in detail in the next chapter 6.

For the sake of understanding, we first consider the connected Green functions (although this theorem is actually only concerned with the one-line-irreducible Green functions): For example, the connected four-point function satisfies the following differential equation (Theorem 6.3, Eq. (6.55) with Λ replaced by ε):

$$\begin{aligned} \dot{G}_{c,\varepsilon}^4(x_1, x_2, x_3, x_4) = & \\ & - \mathbb{A}_{(x_1, x_2)} \int dy_1 \int dy_2 G_{c,\varepsilon}^2(x_1, y_1) \dot{Q}_\varepsilon(y_1, y_2) G_{c,\varepsilon}^4(y_2, x_2, x_3, x_4) \\ & - \mathbb{A}_{(x_3, x_4)} \int dy_1 \int dy_2 G_{c,\varepsilon}^4(x_1, x_2, y_1, x_4) \dot{Q}_\varepsilon(y_1, y_2) G_{c,\varepsilon}^2(y_2, x_3) \\ & + \int dy_1 \int dy_2 G_{c,\varepsilon}^6(x_1, x_2, y_1, x_3, x_4, y_2) \dot{Q}_\varepsilon(y_2, y_1). \end{aligned} \quad (5.211)$$

By evaluating this equation at $\varepsilon = 0$ and using that $\dot{Q}_\varepsilon(x, y)|_{\varepsilon=0} = 1$, we obtain (re-

stricting us for simplicity to the first term)

$$\dot{G}_{c,\varepsilon}^4(x_1, x_2, x_3, x_4)|_{\varepsilon=0} = - \int dy_1 G_c^2(x_1, y_1) \int dy_2 G_c^4(y_2, x_2, x_3, x_4) + \dots \quad (5.212)$$

Hence, by expanding the Green functions on the right-hand side of this equation, we see that already the first term produces disconnected graphs contributing to the derivative of the connected four-point function (see Fig. 5.1).

Next, we will show that the situation is different for the one-line-irreducible Green functions. To begin with, the one-line-irreducible two-point function satisfies the following differential equation (Theorem 6.6):

$$\begin{aligned} \dot{\Gamma}_\varepsilon^4(x_1, x_2, x_3, x_4) = & \quad (5.213) \\ & \int dy_1 \int dy_2 \Gamma_\varepsilon^6(x_1, x_2, y_1, x_3, x_4, y_2) S_\varepsilon(y_2, y_1) \\ & + \frac{1}{2} \int dy_1 \dots \int dy_4 L_\varepsilon(y_1, y_2, y_3, y_4) \Gamma_\varepsilon^4(x_1, x_2, y_1, y_2) \Gamma_\varepsilon^4(y_3, y_4, x_3, x_4) \\ & - 2 \mathbb{A}_{(x_3, x_4)} \int dy_1 \dots \int dy_4 L_\varepsilon(y_3, y_4, y_2, y_1) \Gamma_\varepsilon^4(y_1, x_1, y_3, x_3) \Gamma_\varepsilon^4(x_2, y_2, x_4, y_4). \end{aligned}$$

Here, we have defined the *single-scale Green function*

$$S_\varepsilon(y_2, y_1) = - \int dz_1 \int dz_2 G_{c,\varepsilon}^2(y_2, z_2) \dot{Q}_\varepsilon(z_2, z_1) G_{c,\varepsilon}^2(z_1, y_1), \quad (5.214)$$

as well as the *loop term*

$$L_\varepsilon(y_1, y_2, y_3, y_4) = S_\varepsilon(y_1, y_3) G_{c,\varepsilon}^2(y_2, y_4) + G_{c,\varepsilon}^2(y_1, y_3) S_\varepsilon(y_2, y_4). \quad (5.215)$$

Let us consider the first term on the right-hand side of Eq. (5.213), i.e.,

$$\begin{aligned} \dot{\Gamma}_\varepsilon^4(x_1, x_2, x_3, x_4) = & - \int dy_1 \int dy_2 \int dz_1 \int dz_2 \Gamma_\varepsilon^6(x_1, x_2, y_1, x_3, x_4, y_2) \\ & \times G_{c,\varepsilon}^2(y_2, z_2) \dot{Q}_\varepsilon(z_2, z_1) G_{c,\varepsilon}^2(z_1, y_1) \\ & + \dots \end{aligned} \quad (5.216)$$

For $\varepsilon = 0$, the single-scale Green function becomes disconnected, meaning that

$$S_\varepsilon(y_2, y_1)|_{\varepsilon=0} = - \int dz_2 G_c^2(y_2, z_2) \int dz_1 G_c^2(z_1, y_1). \quad (5.217)$$

For the first term on the right-hand side of Eq. (5.213), this implies

$$\begin{aligned} \dot{\Gamma}_\varepsilon^4(x_1, x_2, x_3, x_4)|_{\varepsilon=0} = & \quad (5.218) \\ & - \int dz_1 \int dz_2 \int dy_1 \int dy_2 G_c^2(z_1, y_1) \Gamma_c^6(x_1, x_2, y_1, x_3, x_4, y_2) G_c^2(y_2, z_2) + \dots \end{aligned}$$

Furthermore, by expanding the connected and the one-line-irreducible Green functions on the right-hand side of this equation, only connected graphs will be produced. (For the connected Green functions, this property was shown by Theorem 5.7; for the one-line-irreducible Green functions Γ^{2n} , it can be shown by induction in n using their relations to the connected Green functions, see Theorem 5.15.) Therefore, all Feynman graphs contributing to the term (5.218) are connected (see Fig. 5.2). One can convince oneself that the same also applies to all other terms on the right-hand side of Eq. (5.213): since the two four-point functions Γ_ε^4 in this equation are connected by S_ε and by $G_{c,\varepsilon}^2$, all Feynman graphs will remain connected even if S_ε becomes disconnected.

More generally, this argument also applies to all higher $2n$ -point Green functions ($n \geq 2$), which follows from the general structure of the RGE (6.69): even if the single-scale Green function becomes disconnected, the resulting graphs on the right-hand side will remain connected. Thus, we have shown that only connected graphs contribute to the derivative (5.208), and hence only one-line-irreducible graphs contribute to Γ^{2n} . This concludes our proof of the Feynman graph expansion of the one-line-irreducible Green functions. \square

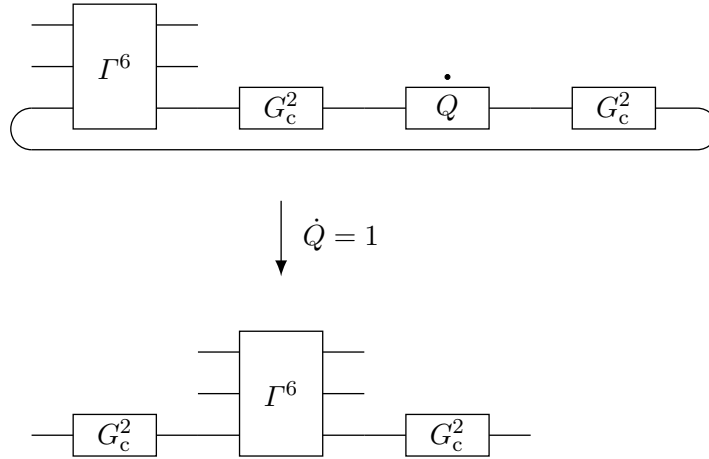


Figure 5.2: Setting $\dot{Q} = 1$ on the right-hand side of the RGE for the *one-line-irreducible* four-point function produces only connected graphs.

A. Nambu formalism

In this appendix, we describe the *Nambu formalism*, which allows us to treat the source fields $\bar{\eta}$ and η (as well as $\bar{\varphi}$ and φ) on an equal footing, and thus to simplify several derivations. This formalism has already been used in the seminal work [SH01] for deriving functional renormalization group equations (cf. also [NO98, pp. 116ff.]).

The Nambu formalism is based on the following notations of the Grassmann field variables (i.e., the generators of the original Grassmann algebra \mathcal{A}),

$$\Psi(x, -) = \bar{\psi}(x), \quad (\text{A.1})$$

$$\Psi(x, +) = \psi(x), \quad (\text{A.2})$$

as well as of the source fields (i.e., the generators of the Grassmann algebra \mathcal{S}),

$$\mathbf{H}(x, -) = \eta(x), \quad (\text{A.3})$$

$$\mathbf{H}(x, +) = \bar{\eta}(x). \quad (\text{A.4})$$

Note that the order of “ $-$ ” and “ $+$ ” is different in the first two and in the last two equations. Moreover, we define the multi-indices

$$X = (x, c), \quad (\text{A.5})$$

which are composed of the spatial, spin and imaginary time variables $x = (\mathbf{x}, s, \tau)$ as well as the additional *Nambu index*

$$c \in \{-, +\}. \quad (\text{A.6})$$

Correspondingly, we define the integration over such multi-indices as

$$\int dX f(X) = \int dx \sum_c f(x, c), \quad (\text{A.7})$$

and the delta distribution as (see also Eqs. (4.103) and (4.104))

$$\delta(X, X') = \delta(x, x') \delta_{cc'}. \quad (\text{A.8})$$

With these notations, the Green function generator (5.37) can be written in a compact

form, as we will now demonstrate. First, we have

$$\langle \eta, \bar{\psi} \rangle + \langle \bar{\eta}, \psi \rangle = \int dx \eta(x) \bar{\psi}(x) + \int dx \bar{\eta}(x) \psi(x) \quad (\text{A.9})$$

$$= \int dx \left(H(x, -) \Psi(x, -) + H(x, +) \Psi(x, +) \right) \quad (\text{A.10})$$

$$= \int dX H(X) \Psi(X) \quad (\text{A.11})$$

$$\equiv \langle H, \Psi \rangle. \quad (\text{A.12})$$

Furthermore, the quadratic term in the exponent can be written as

$$\langle \bar{\psi}, Q \psi \rangle = \int dx_1 \int dx_2 \bar{\psi}(x_1) Q(x_1, x_2) \psi(x_2) \quad (\text{A.13})$$

$$= \frac{1}{2} \int dX_1 \int dX_2 \Psi(X_1) \mathbf{Q}(X_1, X_2) \Psi(X_2) \quad (\text{A.14})$$

$$\equiv \frac{1}{2} \langle \Psi, \mathbf{Q} \Psi \rangle, \quad (\text{A.15})$$

where we have defined the integral kernel

$$\mathbf{Q}(x_1, c_1; x_2, c_2) = \begin{cases} Q(x_1, x_2) & \text{if } (c_1, c_2) = (-, +), \\ -Q(x_2, x_1) & \text{if } (c_1, c_2) = (+, -). \end{cases} \quad (\text{A.16})$$

This integral kernel is antisymmetric in the sense that

$$\mathbf{Q}(X_1, X_2) = -\mathbf{Q}(X_2, X_1), \quad (\text{A.17})$$

and it can be interpreted as a (2×2) matrix with the indices c_1 and c_2 as

$$\mathbf{Q}(X_1, X_2) \equiv \begin{pmatrix} Q(x_1, -; x_2, -) & Q(x_1, -; x_2, +) \\ Q(x_1, +; x_2, -) & Q(x_1, +; x_2, +) \end{pmatrix} \quad (\text{A.18})$$

$$= \begin{pmatrix} 0 & Q(x_1, x_2) \\ -Q(x_2, x_1) & 0 \end{pmatrix}. \quad (\text{A.19})$$

By further denoting the Grassmann field integral as

$$\int d\Psi \equiv \int d\bar{\psi} d\psi, \quad (\text{A.20})$$

we can write the Green function generator (5.37) in the Nambu formalism as

$$\mathcal{Z}[H] = \frac{1}{\mathcal{N}} \int d\Psi e^{-\frac{1}{2} \langle \Psi, \mathbf{Q} \Psi \rangle} e^{-\beta V[\Psi] + \langle H, \Psi \rangle}, \quad (\text{A.21})$$

with the normalization constant

$$\mathcal{N} = \int d\Psi e^{-\frac{1}{2} \langle \Psi, \mathbf{Q} \Psi \rangle}. \quad (\text{A.22})$$

Next, we consider the expansion (5.58) of the connected Green function generator,

$$\mathcal{W}[\mathbf{H}] = \ln \mathcal{Z}[\mathbf{H}] - \ln \mathcal{Z}[0], \quad (\text{A.23})$$

in terms of the connected Green functions. This expansion is obviously equivalent to

$$\begin{aligned} \mathcal{W}[\mathbf{H}] = & \sum_{n=1}^{\infty} \frac{(-1)^n}{(n!)^2} \int dX_1 \dots \int dX_{2n} \tilde{\mathbf{G}}_c^{2n}(X_1, \dots, X_{2n}) \\ & \times \mathbf{H}(X_1) \dots \mathbf{H}(X_n) \mathbf{H}(X_{n+1}) \dots \mathbf{H}(X_{2n}), \end{aligned} \quad (\text{A.24})$$

provided that we define the coefficient functions as

$$\tilde{\mathbf{G}}_c^{2n}(x_1, c_1; \dots; x_{2n}, c_{2n}) = \begin{cases} \mathbf{G}_c^{2n}(x_1, \dots, x_{2n}), & \text{if } c_1 = \dots = c_n = + \text{ and} \\ & c_{n+1} = \dots = c_{2n} = -, \\ 0, & \text{otherwise.} \end{cases} \quad (\text{A.25})$$

By antisymmetrizing these coefficient functions, we obtain the equivalent expression

$$\begin{aligned} \mathcal{W}[\mathbf{H}] = & \sum_{n=1}^{\infty} \frac{(-1)^n}{(n!)^2} (-1)^{n(n-1)/2} \int dX_1 \dots \int dX_{2n} \\ & \times \left(\mathbb{A}_{(X_1, \dots, X_{2n})} \tilde{\mathbf{G}}_c^{2n}(X_1, \dots, X_{2n}) \right) \mathbf{H}(X_1) \dots \mathbf{H}(X_{2n}), \end{aligned} \quad (\text{A.26})$$

where the additional sign factor comes from bringing the anticommuting source fields in Eq. (A.24) into their natural order. For $n \geq 1$, the *connected Green functions in the Nambu formalism* \mathbf{G}_c^{2n} are now defined as

$$\mathbf{G}_c^{2n}(X_1, \dots, X_{2n}) := (-1)^{n(n-1)/2} \frac{(2n)!}{(n!)^2} \mathbb{A}_{(X_1, \dots, X_{2n})} \tilde{\mathbf{G}}_c^{2n}(X_1, \dots, X_{2n}) \quad (\text{A.27})$$

$$= \frac{(-1)^{n(n-1)/2}}{(n!)^2} \sum_{\pi \in S_{2n}} \text{sgn}(\pi) \tilde{\mathbf{G}}_c^{2n}(X_{\pi(1)}, \dots, X_{\pi(2n)}). \quad (\text{A.28})$$

These “Nambu-type” Green functions are totally antisymmetric, i.e., they change sign under the permutation of *any* two arguments. In terms of these functions, the connected Green function generator can be expanded as

$$\mathcal{W}[\mathbf{H}] = \sum_{n=1}^{\infty} \frac{(-1)^n}{(2n)!} \int dX_1 \dots \int dX_{2n} \mathbf{G}_c^{2n}(X_1, \dots, X_{2n}) \mathbf{H}(X_1) \dots \mathbf{H}(X_{2n}). \quad (\text{A.29})$$

In particular, the connected Green functions in the Nambu formalism can be gained back from the connected Green function generator by taking the Grassmann derivatives

$$\mathbf{G}_c^{2n}(X_1, \dots, X_{2n}) = \left(\frac{\delta}{\delta \mathbf{H}(X_1)} \dots \frac{\delta}{\delta \mathbf{H}(X_{2n})} \right) \mathcal{W}[\mathbf{H}] \Big|_{\mathbf{H}=0}. \quad (\text{A.30})$$

Next, we express the “Nambu-type” connected Green functions in terms of the (usual) connected Green functions. For $n = 1$, Eqs. (A.25) and (A.27) imply that

$$\mathbf{G}_c^2(x_1, +; x_2, -) = \tilde{\mathbf{G}}_c^2(x_1, +; x_2, -) - \tilde{\mathbf{G}}_c^2(x_2, -; x_1, +) = G_c^2(x_1, x_2), \quad (\text{A.31})$$

and similarly,

$$\mathbf{G}_c^2(x_1, -; x_2, +) = \tilde{\mathbf{G}}_c^2(x_1, -; x_2, +) - \tilde{\mathbf{G}}_c^2(x_2, +; x_1, -) = -G_c^2(x_2, x_1). \quad (\text{A.32})$$

Moreover, if both Nambu indices are equal, the result vanishes. Thus, we arrive at

$$\mathbf{G}_c^2(x_1, c_1; x_2, c_2) = \begin{cases} -G_c^2(x_2, x_1), & \text{if } (c_1, c_2) = (-, +), \\ G_c^2(x_1, x_2), & \text{if } (c_1, c_2) = (+, -), \\ 0, & \text{otherwise.} \end{cases} \quad (\text{A.33})$$

In matrix notation, these relations can be summarized as

$$\mathbf{G}_c^2(X_1, X_2) = \begin{pmatrix} 0 & -G_c^2(x_2, x_1) \\ G_c^2(x_1, x_2) & 0 \end{pmatrix}. \quad (\text{A.34})$$

Similarly, for $n = 2$, we can calculate as

$$\begin{aligned} & \mathbf{G}_c^4(x_1, +; x_2, +; x_3, -; x_4, -) \\ &= -\frac{1}{4} \left(\tilde{\mathbf{G}}_c^4(x_1, +; x_2, +; x_3, -; x_4, -) - \tilde{\mathbf{G}}_c^4(x_2, +; x_1, +; x_3, -; x_4, -) \right. \\ & \quad \left. - \tilde{\mathbf{G}}_c^4(x_1, +; x_2, +; x_4, -; x_3, -) + \tilde{\mathbf{G}}_c^4(x_2, +; x_1, +; x_4, -; x_3, -) \right) \end{aligned} \quad (\text{A.35})$$

$$\begin{aligned} &= -\frac{1}{4} \left(G_c^4(x_1, x_2, x_3, x_4) - G_c^4(x_2, x_1, x_3, x_4) \right. \\ & \quad \left. - G_c^4(x_1, x_2, x_4, x_3) + G_c^4(x_2, x_1, x_4, x_3) \right) \end{aligned} \quad (\text{A.36})$$

$$= -G_c^4(x_1, x_2, x_3, x_4), \quad (\text{A.37})$$

where we have used the antisymmetry of G_c^4 under the permutation of its first two and its last two arguments. All other combinations of the Nambu indices can be evaluated analogously, and thus we arrive at

$$\mathbf{G}_c^4(x_1, c_1; x_2, c_2; x_3, c_3; x_4, c_4) = \begin{cases} -G_c^4(x_3, x_4, x_1, x_2), & \text{if } (c_1, c_2, c_3, c_4) = (-, -, +, +) \\ G_c^4(x_2, x_4, x_1, x_3), & \text{if } (c_1, c_2, c_3, c_4) = (-, +, -, +), \\ -G_c^4(x_2, x_3, x_1, x_4), & \text{if } (c_1, c_2, c_3, c_4) = (-, +, +, -), \\ -G_c^4(x_1, x_4, x_2, x_3), & \text{if } (c_1, c_2, c_3, c_4) = (+, -, -, +), \\ G_c^4(x_1, x_3, x_2, x_4), & \text{if } (c_1, c_2, c_3, c_4) = (+, -, +, -), \\ -G_c^4(x_1, x_2, x_3, x_4), & \text{if } (c_1, c_2, c_3, c_4) = (+, +, -, -), \\ 0, & \text{otherwise.} \end{cases} \quad (\text{A.38})$$

We go on to rewrite also the Legendre transform in the Nambu formalism. For this purpose, we denote the *new* source fields (defined by Eqs. (5.118)–(5.119)) as

$$\Phi(x, -) = \bar{\varphi}(x), \quad (\text{A.39})$$

$$\Phi(x, +) = \varphi(x). \quad (\text{A.40})$$

Then, Eqs. (5.118)–(5.119) translate into

$$\Phi(X) = \frac{\delta \mathcal{W}}{\delta H(X)}, \quad (\text{A.41})$$

and the Legendre transform (5.123) can be written compactly as

$$\Gamma = \mathcal{W} + \langle \Phi, H \rangle. \quad (\text{A.42})$$

Similarly, Eqs. (5.127)–(5.128) are equivalent to

$$H(X) = \frac{\delta \Gamma}{\delta \Phi(X)}. \quad (\text{A.43})$$

It remains to consider the expansion (5.125) of the one-line-irreducible Green function generator. In fact, this can be rewritten in the Nambu formalism (analogously to the connected Green function generator) as

$$\begin{aligned} \Gamma[\Phi] = & \sum_{n=1}^{\infty} \frac{(-1)^n}{(n!)^2} \int dX_1 \dots \int dX_{2n} \tilde{\Gamma}^{2n}(X_1, \dots, X_{2n}) \\ & \times \Phi(X_1) \dots \Phi(X_n) \Phi(X_{n+1}) \dots \Phi(X_{2n}). \end{aligned} \quad (\text{A.44})$$

In this case, the coefficient functions are defined as (cf. Eq. (A.25))

$$\tilde{\Gamma}^{2n}(x_1, c_1; \dots; x_{2n}, c_{2n}) = \begin{cases} \Gamma^{2n}(x_1, \dots, x_{2n}), & \text{if } c_1 = \dots = c_n = - \text{ and } \\ & c_{n+1} = \dots = c_{2n} = +, \\ 0, & \text{otherwise.} \end{cases} \quad (\text{A.45})$$

Again, an equivalent expansion is obtained by antisymmetrizing these coefficient functions: defining the *one-line-irreducible Green functions in the Nambu formalism* as

$$\Gamma^{2n}(X_1, \dots, X_{2n}) := \frac{(-1)^{(n-1)n/2}}{(n!)^2} \sum_{\pi \in S_{2n}} \text{sgn}(\pi) \tilde{\Gamma}^{2n}(X_{\pi(1)}, \dots, X_{\pi(2n)}), \quad (\text{A.46})$$

the expression (A.44) can be transformed into

$$\Gamma[\Phi] = \sum_{n=1}^{\infty} \frac{(-1)^n}{(2n)!} \int dX_1 \dots \int dX_{2n} \Gamma^{2n}(X_1, \dots, X_{2n}) \Phi(X_1) \dots \Phi(X_{2n}). \quad (\text{A.47})$$

In particular, the one-line-irreducible Green functions in the Nambu formalism can be

represented as the Grassmann derivatives

$$\mathbf{I}^{2n}(X_1, \dots, X_{2n}) = \left(\frac{\delta}{\delta \Phi(X_1)} \cdots \frac{\delta}{\delta \Phi(X_{2n})} \right) \Gamma[\Phi] \Big|_{\Phi=0}. \quad (\text{A.48})$$

Finally, we can express these “Nambu-type” one-line-irreducible Green functions in terms of the (usual) one-line-irreducible Green functions as follows: for $n = 1$,

$$\mathbf{I}^2(x_1, c_1; x_2, c_2) = \begin{cases} \Gamma^2(x_1, x_2) & \text{if } (c_1, c_2) = (-, +), \\ -\Gamma^2(x_2, x_1) & \text{if } (c_1, c_2) = (+, -), \\ 0 & \text{otherwise,} \end{cases} \quad (\text{A.49})$$

and for $n = 2$,

$$\mathbf{I}^4(x_1, c_1; x_2, c_2; x_3, c_3; x_4, c_4) = \begin{cases} -\Gamma^4(x_1, x_2, x_3, x_4), & \text{if } (c_1, c_2, c_3, c_4) = (-, -, +, +), \\ \Gamma^4(x_1, x_3, x_2, x_4), & \text{if } (c_1, c_2, c_3, c_4) = (-, +, -, +), \\ -\Gamma^4(x_1, x_4, x_2, x_3), & \text{if } (c_1, c_2, c_3, c_4) = (-, +, +, -), \\ -\Gamma^4(x_2, x_3, x_1, x_4), & \text{if } (c_1, c_2, c_3, c_4) = (+, -, -, +), \\ \Gamma^4(x_2, x_4, x_1, x_3), & \text{if } (c_1, c_2, c_3, c_4) = (+, -, +, -), \\ -\Gamma^4(x_3, x_4, x_1, x_2), & \text{if } (c_1, c_2, c_3, c_4) = (+, +, -, -), \\ 0, & \text{otherwise.} \end{cases} \quad (\text{A.50})$$

These above equalities may be compared to the respective Eqs. (A.33) and (A.38) for the connected Green functions. The corresponding differences stem from the different definitions of the old and the new sources in the Nambu formalism, Eqs. (A.3)–(A.4) and Eqs. (A.39)–(A.40), respectively.

Part III.

**Functional renormalization and
mean-field approach**

6. Renormalization group equations

In this chapter, we derive the *renormalization group equations* (RGE) for the connected and for the one-line-irreducible Green functions. These have already been used in the proof of the Feynman graph expansion of the one-line-irreducible Green functions (Theorem 5.17). Since the solution of the RGE is not just a function of some continuous parameter Λ (i.e., a single number $f(\Lambda)$ for each Λ), but a whole set of Green functions for each Λ , the corresponding differential equations are also referred to as *functional* RGE. These form the basis of the *functional renormalization group* (fRG) method, which we will use in the following chapters to study the low-temperature phases of the Rashba model with an attractive interaction. The derivations in this chapter follow closely the seminal article [SH01] with only very slight modifications.

6.1. Scale dependence

We introduce a *scale-dependent covariance* C_Λ for each $\Lambda > 0$ in such a way that it satisfies the *initial condition*

$$\lim_{\Lambda \rightarrow \infty} C_\Lambda(x_1, x_2) = 0, \quad (6.1)$$

as well as the *final condition*

$$\lim_{\Lambda \rightarrow 0} C_\Lambda(x_1, x_2) = C(x_1, x_2). \quad (6.2)$$

In typical fRG applications, Λ is associated with an *energy scale*, and hence the above limits are referred to as the *ultraviolet limit* and the *infrared limit*, respectively (see Ch. 7). The inverse of the scale-dependent covariance is denoted by $Q_\Lambda = C_\Lambda^{-1}$. Furthermore, the Green function generator at the scale Λ is defined as (see Definition 5.2)

$$\mathcal{Z}_\Lambda[\bar{\eta}, \eta] = \frac{1}{\mathcal{N}_\Lambda} \int d\bar{\psi} d\psi e^{-\langle \bar{\psi}, Q_\Lambda \psi \rangle} e^{-\beta V[\bar{\psi}, \psi] + \langle \bar{\eta}, \psi \rangle + \langle \eta, \bar{\psi} \rangle}, \quad (6.3)$$

with the normalization constant

$$\mathcal{N}_\Lambda = \int d\bar{\psi} d\psi e^{-\langle \bar{\psi}, Q_\Lambda \psi \rangle}. \quad (6.4)$$

The logarithm of \mathcal{Z}_Λ divided by its field-independent term yields the connected Green function generator at the scale Λ (see Definition 5.4),

$$\mathcal{W}_\Lambda[\bar{\eta}, \eta] = \ln \mathcal{Z}_\Lambda[\bar{\eta}, \eta] - \ln \mathcal{Z}_\Lambda[0, 0]. \quad (6.5)$$

Moreover, the scale dependence of the covariance induces a scale dependence of all interacting Green functions through their respective Feynman graph expansions. In particular, the connected Green functions at the scale Λ are the coefficient functions of the connected Green function generator at the same scale, i.e.,

$$\begin{aligned} \mathcal{W}_\Lambda = \sum_{n=1}^{\infty} \frac{(-1)^n}{(n!)^2} \int dx_1 \dots \int dx_{2n} G_{c,\Lambda}^{2n}(x_1, \dots, x_{2n}) \\ \times \bar{\eta}(x_1) \dots \bar{\eta}(x_n) \eta(x_{2n}) \dots \eta(x_{n+1}). \end{aligned} \quad (6.6)$$

Concretely, these scale-dependent connected Green functions can be represented as the sums of all connected Feynman graphs, in which all covariance lines attain a scale dependence, i.e., $C \mapsto C_\Lambda$. Thus, one can convince oneself that the connected Green functions satisfy the initial conditions

$$\lim_{\Lambda \rightarrow \infty} G_{c,\Lambda}^{2n}(x_1, \dots, x_{2n}) = 0, \quad (6.7)$$

as well as the final conditions

$$\lim_{\Lambda \rightarrow 0} G_{c,\Lambda}^{2n}(x_1, \dots, x_{2n}) = G_c^{2n}(x_1, \dots, x_{2n}). \quad (6.8)$$

Next, the Legendre transform at the scale Λ is defined as (see Definition 5.10)

$$\Gamma_\Lambda = \mathcal{W}_\Lambda + \langle \bar{\varphi}_\Lambda, \eta \rangle + \langle \varphi_\Lambda, \bar{\eta} \rangle, \quad (6.9)$$

where the new source fields are given by

$$\bar{\varphi}_\Lambda(x) = \frac{\delta \mathcal{W}_\Lambda}{\delta \eta(x)}, \quad (6.10)$$

$$\varphi_\Lambda(x) = \frac{\delta \mathcal{W}_\Lambda}{\delta \bar{\eta}(x)}. \quad (6.11)$$

Note, in particular, that these Grassmann variables are scale dependent, too. Correspondingly, the one-line-irreducible Green functions at the scale Λ are defined such that

$$\begin{aligned} \Gamma_\Lambda = \sum_{n=1}^{\infty} \frac{(-1)^n}{(n!)^2} \int dx_1 \dots \int dx_{2n} \Gamma_\Lambda^{2n}(x_1, \dots, x_{2n}) \\ \times \bar{\varphi}_\Lambda(x_1) \dots \bar{\varphi}_\Lambda(x_n) \varphi_\Lambda(x_{2n}) \dots \varphi_\Lambda(x_{n+1}). \end{aligned} \quad (6.12)$$

In perturbation theory, these Green functions are represented as the sums of all one-line-irreducible Feynman graphs with scale-dependent covariance lines. However, as explained in Ref. [Sch+16a], the above definitions are only formal: since C_Λ is in general not invertible, the Legendre transform and in particular the two-point function

$$\Gamma_\Lambda^2 = (G_{c,\Lambda}^2)^{-1} \quad (6.13)$$

are actually not well-defined. This becomes particularly obvious in the limit $\Lambda \rightarrow \infty$, where C_Λ and consequently also $G_{c,\Lambda}^2$ vanish identically. Nevertheless, for $n \geq 2$, the

Table 6.1: Two first-order Feynman graphs contributing to the one-line-irreducible four-point Green function Γ^4 . Only these first-order graphs are relevant for evaluating the initial condition of Γ^4 , because all higher-order Feynman graphs contain at least one covariance line which vanishes in the ultraviolet limit.

one-line-irreducible Green functions Γ_Λ^{2n} can be defined even in the ultraviolet limit, because the inverse of C_Λ does not appear in their Feynman graph expansions (see Theorem 5.17). Concretely, the one-line-irreducible four-point function ($n = 2$) satisfies the initial condition (see Table 6.1)

$$\lim_{\Lambda \rightarrow \infty} \Gamma_\Lambda^4(x_1, x_2, x_3, x_4) = -\beta (V(x_1, x_2, x_3, x_4) - V(x_1, x_2, x_4, x_3)), \quad (6.14)$$

where V denotes the four-point interaction kernel as given by Eq. (4.107). If we assume that the latter is antisymmetric with respect to its last two arguments, then Eq. (6.14) further simplifies to

$$\lim_{\Lambda \rightarrow \infty} \Gamma_\Lambda^4(x_1, x_2, x_3, x_4) = -2\beta V(x_1, x_2, x_3, x_4). \quad (6.15)$$

Note the prefactor $(-\beta)$ in the above equations, which is contained in any first-order Feynman graph (see Eq. (4.173)), and which is consistent with the different dimensions of the quantities Γ^4 and V (see Eqs. (5.126) and (4.107), which respectively imply that $[\Gamma^4(x_1, \dots, x_4)] = \text{m}^{-6}$ and $[V(x_1, \dots, x_4)] = \text{J m}^{-6}$). For $n \geq 3$, the corresponding initial conditions read

$$\lim_{\Lambda \rightarrow \infty} \Gamma_\Lambda^{2n}(x_1, \dots, x_{2n}) = 0 \quad (n \geq 3), \quad (6.16)$$

because all Feynman graphs contributing to these Green functions contain at least one covariance line. By contrast, the limit $\Lambda \rightarrow 0$ is well-defined for all n , and simply yields back the original one-line-irreducible Green functions:

$$\lim_{\Lambda \rightarrow 0} \Gamma_\Lambda^{2n}(x_1, \dots, x_{2n}) = \Gamma^{2n}(x_1, \dots, x_{2n}) \quad (n \geq 1). \quad (6.17)$$

We will come back to these limits in Sect. 6.4, where we will formulate an initial-value problem for the scale-dependent (one-line-irreducible) four-point function.

6.2. Connected Green function flow

In this section, we derive the RGE for the scale-dependent connected Green functions $G_{c,\Lambda}^{2n}$ (see Sct. 5.3). These RGE form an infinite hierarchy of coupled differential equations, one for each n . Instead of deriving them one after the other, however, we will start directly from the connected Green function generator \mathcal{W}_Λ and derive a differential equation for it. Afterwards, we will perform an expansion in the source fields, and thereby simultaneously obtain the corresponding differential equations for all the coefficient functions of \mathcal{W}_Λ , which coincide with the scale-dependent connected Green functions. Furthermore, analogously as in Ch. 5, our calculations will be facilitated by first deriving the RGE for the Nambu-type Green functions, and then deducing from these the desired equations for the connected Green functions themselves (see Ref. [SH01]).

In the Nambu formalism (see Appendix A of Part II), the scale-dependent Green function generator (6.3) can be written as

$$\mathcal{Z}_\Lambda = \frac{1}{\mathcal{N}_\Lambda} \int d\Psi e^{-\frac{1}{2}\langle\Psi, \mathbf{Q}_\Lambda \Psi\rangle} e^{-\beta V[\Psi] + \langle\mathbf{H}, \Psi\rangle}. \quad (6.18)$$

The connected Green function generator is defined by Eq. (6.5), which is equivalent to

$$e^{\mathcal{W}_\Lambda} = \frac{\mathcal{Z}_\Lambda}{\mathcal{Z}_\Lambda[0]}, \quad (6.19)$$

where $\mathcal{Z}_\Lambda[0]$ denotes the field-independent term of \mathcal{Z}_Λ . Let us introduce some further notations, which will be needed in the following. First, we define the matrix

$$\widetilde{\mathcal{W}}_\Lambda(X, Y) = \frac{\delta^2 \mathcal{W}_\Lambda}{\delta \mathbf{H}(X) \delta \mathbf{H}(Y)} - \frac{\delta^2 \mathcal{W}_\Lambda}{\delta \mathbf{H}(X) \delta \mathbf{H}(Y)} \Big|_{\mathbf{H}=0} \quad (6.20)$$

as the second Grassmann derivative of \mathcal{W}_Λ subtracted by the field-independent terms. More compactly, we can write this as

$$\widetilde{\mathcal{W}}_\Lambda = \frac{\delta^2 \mathcal{W}_\Lambda}{\delta \mathbf{H}^2} - \frac{\delta^2 \mathcal{W}_\Lambda}{\delta \mathbf{H}^2} \Big|_{\mathbf{H}=0}. \quad (6.21)$$

Next, for any two *two-point quantities* (i.e., quantities depending on two arguments) $A \equiv A(X, Y)$ and $B \equiv B(X, Y)$, we define their product as

$$(AB)(X, Y) := \int dZ A(X, Z) B(Z, Y), \quad (6.22)$$

and the trace as

$$\text{Tr}[A] := \int dX A(X, X), \quad (6.23)$$

such that in particular,

$$\text{Tr}[AB] = \int dX \int dY A(X, Y) B(Y, X). \quad (6.24)$$

Finally, we denote the derivative of any quantity with respect to the scale parameter Λ by a dot, for example,

$$\dot{\mathcal{W}}_\Lambda \equiv \frac{d}{d\Lambda} \mathcal{W}_\Lambda, \quad (6.25)$$

in the case of the connected Green function generator.

Theorem 6.1 (RGE for connected Green function generator). *The scale-dependent connected Green function generator \mathcal{W}_Λ satisfies the following differential equation:*

$$\dot{\mathcal{W}}_\Lambda = -\frac{1}{2} \left\langle \frac{\delta \mathcal{W}_\Lambda}{\delta H}, \dot{\mathbf{Q}}_\Lambda \frac{\delta \mathcal{W}_\Lambda}{\delta H} \right\rangle + \frac{1}{2} \text{Tr} \left[\dot{\mathbf{Q}}_\Lambda \widetilde{\mathcal{W}}_\Lambda \right], \quad (6.26)$$

where $\widetilde{\mathcal{W}}_\Lambda$ is defined by Eq. (6.20). By expanding \mathcal{W}_Λ into a sum of monomials of the order $2n$ in the source fields,

$$\mathcal{W}_\Lambda = \sum_{n=1}^{\infty} \mathcal{W}_\Lambda^{(2n)}, \quad (6.27)$$

and similarly its derivatives,

$$\widetilde{\mathcal{W}}_\Lambda(X, Y) = \sum_{n=1}^{\infty} \widetilde{\mathcal{W}}_\Lambda^{(2n)}(X, Y), \quad (6.28)$$

the RGE is equivalent to

$$\dot{\mathcal{W}}_\Lambda^{(2n)} = -\frac{1}{2} \sum_{k=1}^n \left\langle \frac{\delta \mathcal{W}_\Lambda^{(2k)}}{\delta H}, \dot{\mathbf{Q}}_\Lambda \frac{\delta \mathcal{W}_\Lambda^{(2n+2-2k)}}{\delta H} \right\rangle + \frac{1}{2} \text{Tr} \left[\dot{\mathbf{Q}}_\Lambda \widetilde{\mathcal{W}}_\Lambda^{(2n)} \right], \quad (6.29)$$

which constitutes an infinite hierarchy of coupled differential equations for the monomials in the source fields.

Proof. First, we note that by Definition 5.4, the generator \mathcal{W}_Λ does not contain any field-independent term. Since \mathcal{W}_Λ is an even element of the Grassmann algebra \mathcal{S} , the right-hand side of Eq. (6.26) does not contain any field-independent term either. Thus, we do not have to consider any constant terms at all, which in fact slightly simplifies the derivation. Taking the scale derivative of both sides of Eq. (6.19) yields

$$\dot{\mathcal{W}}_\Lambda e^{\mathcal{W}_\Lambda} = \frac{\dot{\mathcal{Z}}_\Lambda \mathcal{Z}_\Lambda[0] - \mathcal{Z}_\Lambda \dot{\mathcal{Z}}_\Lambda[0]}{\mathcal{Z}_\Lambda[0]^2} \quad (6.30)$$

$$= \frac{\dot{\mathcal{Z}}_\Lambda}{\mathcal{Z}_\Lambda[0]} - \frac{\mathcal{Z}_\Lambda \dot{\mathcal{Z}}_\Lambda[0]}{\mathcal{Z}_\Lambda[0]^2} \quad (6.31)$$

The Green function generator (6.18) depends on the scale parameter Λ through the normalization constant \mathcal{N}_Λ and through the inverse covariance \mathbf{Q}_Λ . Hence, in principle, the scale derivative can act on each of these two quantities, and therefore generates two different types of terms. However, the two terms in the numerator of Eq. (6.30) which

are produced when the scale derivative acts on the respective normalization constant \mathcal{N}_Λ (in $\dot{\mathcal{Z}}_\Lambda$ or in $\dot{\mathcal{Z}}_\Lambda[0]$) cancel each other. Therefore, we only need to consider the terms where the scale derivative acts on \mathbf{Q}_Λ . For the first term in Eq. (6.31), we thus obtain

$$\begin{aligned} & \frac{1}{\mathcal{Z}_\Lambda[0]} \frac{1}{\mathcal{N}_\Lambda} \frac{d}{d\Lambda} \int d\Psi e^{-\frac{1}{2}\langle\Psi, \mathbf{Q}_\Lambda \Psi\rangle} e^{-\beta V[\Psi] + \langle H, \Psi\rangle} \\ &= \frac{1}{\mathcal{Z}_\Lambda[0]} \frac{1}{\mathcal{N}_\Lambda} \left(-\frac{1}{2}\right) \int d\Psi \langle\Psi, \dot{\mathbf{Q}}_\Lambda \Psi\rangle e^{-\frac{1}{2}\langle\Psi, \mathbf{Q}_\Lambda \Psi\rangle} e^{-\beta V[\Psi] + \langle H, \Psi\rangle} \end{aligned} \quad (6.32)$$

$$= \frac{1}{\mathcal{Z}_\Lambda[0]} \left(-\frac{1}{2}\right) \left\langle \frac{\delta}{\delta H}, \dot{\mathbf{Q}}_\Lambda \frac{\delta}{\delta H} \right\rangle \mathcal{Z}_\Lambda \quad (6.33)$$

$$= -\frac{1}{2} \left\langle \frac{\delta}{\delta H}, \dot{\mathbf{Q}}_\Lambda \frac{\delta}{\delta H} \right\rangle e^{\mathcal{W}_\Lambda}. \quad (6.34)$$

We can further transform this expression as follows:

$$(6.34) = -\frac{1}{2} \int dX \int dY \dot{\mathbf{Q}}_\Lambda(X, Y) \frac{\delta}{\delta H(X)} \frac{\delta}{\delta H(Y)} e^{\mathcal{W}_\Lambda} \quad (6.35)$$

$$= -\frac{1}{2} \int dX \int dY \dot{\mathbf{Q}}_\Lambda(X, Y) \left(\frac{\delta \mathcal{W}_\Lambda}{\delta H(X)} \frac{\delta \mathcal{W}_\Lambda}{\delta H(Y)} + \frac{\delta^2 \mathcal{W}_\Lambda}{\delta H(X) \delta H(Y)} \right) e^{\mathcal{W}_\Lambda} \quad (6.36)$$

$$= -\frac{1}{2} \left\langle \frac{\delta \mathcal{W}_\Lambda}{\delta H}, \dot{\mathbf{Q}}_\Lambda \frac{\delta \mathcal{W}_\Lambda}{\delta H} \right\rangle e^{\mathcal{W}_\Lambda} + \frac{1}{2} \text{Tr} \left[\dot{\mathbf{Q}}_\Lambda \frac{\delta^2 \mathcal{W}_\Lambda}{\delta H^2} \right] e^{\mathcal{W}_\Lambda}. \quad (6.37)$$

Next, consider the second term in Eq. (6.31):

$$-\frac{\mathcal{Z}_\Lambda \dot{\mathcal{Z}}_\Lambda[0]}{\mathcal{Z}_\Lambda[0]^2} = -\frac{\dot{\mathcal{Z}}_\Lambda[0]}{\mathcal{Z}_\Lambda[0]} e^{\mathcal{W}_\Lambda} = -\frac{\dot{\mathcal{Z}}_\Lambda}{\mathcal{Z}_\Lambda[0]} \Big|_{H=0} e^{\mathcal{W}_\Lambda}. \quad (6.38)$$

The first factor on the right-hand side of this equation is just the constant part of the first term in Eq. (6.31) (with the opposite sign), and hence by Eq. (6.37) equals

$$-\frac{1}{2} \text{Tr} \left[\dot{\mathbf{Q}}_\Lambda \frac{\delta^2 \mathcal{W}_\Lambda}{\delta H^2} \Big|_{H=0} \right]. \quad (6.39)$$

(Here, we have used that the first term in Eq. (6.37) has no constant part, because \mathcal{W}_Λ is an even element of \mathcal{S} .) By putting Eqs. (6.37) and (6.39) into Eq. (6.31) as well as by canceling the overall factor $e^{\mathcal{W}_\Lambda}$, we arrive at

$$\dot{\mathcal{W}}_\Lambda = -\frac{1}{2} \left\langle \frac{\delta \mathcal{W}_\Lambda}{\delta H}, \dot{\mathbf{Q}}_\Lambda \frac{\delta \mathcal{W}_\Lambda}{\delta H} \right\rangle + \frac{1}{2} \text{Tr} \left[\dot{\mathbf{Q}}_\Lambda \left(\frac{\delta^2 \mathcal{W}_\Lambda}{\delta H^2} - \frac{\delta^2 \mathcal{W}_\Lambda}{\delta H^2} \Big|_{H=0} \right) \right], \quad (6.40)$$

which is equivalent to the assertion (6.26). Finally, by expanding \mathcal{W}_Λ and $\widetilde{\mathcal{W}}_\Lambda$ in the source fields and equating the terms on both sides of Eq. (6.26) which are of the same order in the fields, we obtain the hierarchy of equations (6.29). \square

Theorem 6.2 (RGE for connected Green functions in the Nambu formalism). *The Nambu-type connected Green functions $\mathbf{G}_{c,\Lambda}^{2n}$ satisfy the following hierarchy of coupled differential equations (for $n \geq 1$):*

$$\begin{aligned} \dot{\mathbf{G}}_{c,\Lambda}^{2n}(X_1, \dots, X_{2n}) = & \quad (6.41) \\ & \frac{1}{2} \mathbb{A}_{(X_1, \dots, X_{2n})} \sum_{\substack{k, \ell \geq 1, \\ k+\ell-1=n}} \binom{2n}{2k-1} \int dY_1 \int dY_2 \dot{\mathbf{Q}}_{\Lambda}(Y_1, Y_2) \\ & \times \mathbf{G}_{c,\Lambda}^{2k}(Y_1, X_1, \dots, X_{2k-1}) \mathbf{G}_{c,\Lambda}^{2\ell}(Y_2, X_{2k}, \dots, X_{2n}) \\ & - \frac{1}{2} \int dY_1 \int dY_2 \dot{\mathbf{Q}}_{\Lambda}(Y_1, Y_2) \mathbf{G}_{c,\Lambda}^{2n+2}(Y_1, Y_2, X_1, \dots, X_{2n}). \end{aligned}$$

In particular, for $n = 1$, this implies

$$\begin{aligned} \dot{\mathbf{G}}_{c,\Lambda}^2(X_1, X_2) = & \int dY_1 \int dY_2 \dot{\mathbf{Q}}_{\Lambda}(Y_1, Y_2) \mathbf{G}_{c,\Lambda}^2(Y_1, X_1) \mathbf{G}_{c,\Lambda}^2(Y_2, X_2) \\ & - \frac{1}{2} \int dY_1 \int dY_2 \dot{\mathbf{Q}}_{\Lambda}(Y_1, Y_2) \mathbf{G}_{c,\Lambda}^4(Y_1, Y_2, X_1, X_2); \end{aligned} \quad (6.42)$$

and for $n = 2$,

$$\begin{aligned} \dot{\mathbf{G}}_{c,\Lambda}^4(X_1, X_2, X_3, X_4) = & \quad (6.43) \\ & 4 \mathbb{A}_{(X_1, \dots, X_4)} \int dY_1 \int dY_2 \dot{\mathbf{Q}}_{\Lambda}(Y_1, Y_2) \mathbf{G}_{c,\Lambda}^2(Y_1, X_1) \mathbf{G}_{c,\Lambda}^4(Y_2, X_2, X_3, X_4) \\ & - \frac{1}{2} \int dY_1 \int dY_2 \dot{\mathbf{Q}}_{\Lambda}(Y_1, Y_2) \mathbf{G}_{c,\Lambda}^6(Y_1, Y_2, X_1, X_2, X_3, X_4). \end{aligned}$$

In these equations, \mathbb{A} denotes the antisymmetrization operator as defined by Eq. (5.60).

Proof. We begin by expanding the right-hand sides of Eqs. (6.27) and (6.28) in terms of the source fields. By Eq. (A.29), we have

$$\mathcal{W}_{\Lambda}^{(2n)} = \frac{(-1)^n}{(2n)!} \int dX_1 \dots \int dX_{2n} \mathbf{G}_{c,\Lambda}^{2n}(X_1, \dots, X_{2n}) \mathbf{H}(X_1) \dots \mathbf{H}(X_{2n}). \quad (6.44)$$

Furthermore, from Eq. (6.20), we obtain

$$\widetilde{\mathcal{W}}_{\Lambda}^{(2n)}(X, Y) = \frac{\delta^2}{\delta \mathbf{H}(X) \delta \mathbf{H}(Y)} \mathcal{W}_{\Lambda}^{(2n+2)} \quad (6.45)$$

$$\begin{aligned} &= \frac{(-1)^{n+1}}{(2n+2)!} \int dX_1 \dots \int dX_{2n+2} \mathbf{G}_{c,\Lambda}^{2n+2}(X_1, \dots, X_{2n+2}) \\ &\quad \times \frac{\delta^2}{\delta \mathbf{H}(X) \delta \mathbf{H}(Y)} \left(\mathbf{H}(X_1) \dots \mathbf{H}(X_{2n+2}) \right). \end{aligned} \quad (6.46)$$

Here, the derivative with respect to $H(Y)$ can act on each of the $(2n+2)$ fields in brackets, and after that, the derivative with respect to $H(X)$ can act on each of the remaining $(2n+1)$ fields. By the antisymmetry of the Nambu-type Green function, all $(2n+2) \times (2n+1)$ resulting terms are equal, and thus we find

$$\begin{aligned} \widetilde{\mathcal{W}}_{\Lambda}^{(2n)}(X, Y) &= \frac{(-1)^{n+1}}{(2n)!} \int dX_1 \dots \int dX_{2n} \\ &\times \mathbf{G}_{c, \Lambda}^{2n+2}(Y, X, X_1, \dots, X_{2n}) H(X_1) \dots H(X_{2n}). \end{aligned} \quad (6.47)$$

Next, we put the above expansions (6.44) and (6.47) into the RGE hierarchy as given by Eq. (6.29). Then, the second term on the right-hand side yields

$$\frac{1}{2} \text{Tr} \left[\dot{\mathbf{Q}}_{\Lambda} \widetilde{\mathcal{W}}_{\Lambda}^{(2n)} \right] = \frac{1}{2} \int dY_1 \int dY_2 \dot{\mathbf{Q}}_{\Lambda}(Y_1, Y_2) \widetilde{\mathcal{W}}_{\Lambda}^{(2n)}(Y_2, Y_1) \quad (6.48)$$

$$\begin{aligned} &= -\frac{1}{2} \frac{(-1)^n}{(2n)!} \int dX_1 \dots \int dX_{2n} \\ &\times \left(\int dY_1 \int dY_2 \dot{\mathbf{Q}}_{\Lambda}(Y_1, Y_2) \mathbf{G}_{c, \Lambda}^{2n+2}(Y_1, Y_2, X_1, \dots, X_{2n}) \right) H(X_1) \dots H(X_{2n}). \end{aligned} \quad (6.49)$$

Furthermore, the first term on the right-hand side of Eq. (6.29) is equivalent to

$$-\frac{1}{2} \sum_{\substack{k, \ell \geq 1, \\ k+\ell-1=n}} \left\langle \frac{\delta \mathcal{W}_{\Lambda}^{(2k)}}{\delta H}, \dot{\mathbf{Q}}_{\Lambda} \frac{\delta \mathcal{W}_{\Lambda}^{(2\ell)}}{\delta H} \right\rangle. \quad (6.50)$$

Similarly as Eq. (6.47), one shows that

$$\begin{aligned} \frac{\delta \mathcal{W}_{\Lambda}^{(2k)}}{\delta H(X)} &= \frac{(-1)^k}{(2k-1)!} \int dX_1 \dots \int dX_{2k-1} \\ &\times \mathbf{G}_{c, \Lambda}^{2k}(X, X_1, \dots, X_{2k-1}) H(X_1) \dots H(X_{2k-1}), \end{aligned} \quad (6.51)$$

and hence we obtain

$$\begin{aligned} &-\frac{1}{2} \left\langle \frac{\delta \mathcal{W}_{\Lambda}^{(2k)}}{\delta H}, \dot{\mathbf{Q}}_{\Lambda} \frac{\delta \mathcal{W}_{\Lambda}^{(2\ell)}}{\delta H} \right\rangle = \\ &\frac{1}{2} \frac{(-1)^n}{(2n)!} \binom{2n}{2k-1} \int dX_1 \dots \int dX_{2n} \int dY_1 \int dY_2 \dot{\mathbf{Q}}_{\Lambda}(Y_1, Y_2) \\ &\times \mathbf{G}_{c, \Lambda}^{2k}(Y_1, X_1, \dots, X_{2k-1}) \mathbf{G}_{c, \Lambda}^{2\ell}(Y_2, X_{2k}, \dots, X_{2n}) H(X_1) \dots H(X_{2n}). \end{aligned} \quad (6.52)$$

Here, we have used the condition $2k+2\ell-2=2n$, which implies in particular that

$$\frac{(2n)!}{(2k-1)!(2\ell-1)!} = \binom{2n}{2k-1}. \quad (6.53)$$

By putting all these results (Eqs. (6.44), (6.49) and (6.52)) into Eq. (6.29) and equating the antisymmetrized coefficient functions for each n , we arrive at the RGE (6.41). For $n = 1$, this in turn implies immediately Eq. (6.42). (There, the antisymmetrization operator has been omitted because the right-hand side is already antisymmetric.) For $n = 2$, one only has to convince oneself that the two terms with $k = 1$ and $k = 2$ are equal, which then implies Eq. (6.43). \square

From the above RGE for the Nambu-type connected Green functions, one can derive the corresponding hierarchy of RGE for the connected Green functions themselves. Here, we explicitly state these equations only for $n = 1$ and for $n = 2$:

Theorem 6.3 (RGE for connected Green functions). *The connected two- and four-point Green functions satisfy the following differential equations:*

$$\begin{aligned} \dot{G}_{c,\Lambda}^2(x_1, x_2) = & - \int dy_1 \int dy_2 G_{c,\Lambda}^2(x_1, y_1) \dot{Q}_\Lambda(y_1, y_2) G_{c,\Lambda}^2(y_2, x_2) \\ & + \int dy_1 \int dy_2 G_{c,\Lambda}^4(x_1, y_1, x_2, y_2) \dot{Q}_\Lambda(y_2, y_1), \end{aligned} \quad (6.54)$$

and respectively,

$$\begin{aligned} \dot{G}_{c,\Lambda}^4(x_1, x_2, x_3, x_4) = & \\ & - \mathbb{A}_{(x_1, x_2)} \int dy_1 \int dy_2 G_{c,\Lambda}^2(x_1, y_1) \dot{Q}_\Lambda(y_1, y_2) G_{c,\Lambda}^4(y_2, x_2, x_3, x_4) \\ & - \mathbb{A}_{(x_3, x_4)} \int dy_1 \int dy_2 G_{c,\Lambda}^4(x_1, x_2, y_1, y_2) \dot{Q}_\Lambda(y_1, y_2) G_{c,\Lambda}^2(y_2, x_3, x_4) \\ & + \int dy_1 \int dy_2 G_{c,\Lambda}^6(x_1, x_2, y_1, x_3, x_4, y_2) \dot{Q}_\Lambda(y_2, y_1). \end{aligned} \quad (6.55)$$

The graphical representation of these equations by means of Universal Feynman Graphs (see Sect. 4.5) is shown in Table 6.3.

Proof. We derive these equations from Theorem 6.2, using the relations (A.16) as well as (5.169)–(5.171) between the Nambu-type and the usual connected Green functions.

(i) *Two-point function.* From Eq. (6.42), we obtain

$$\begin{aligned} \dot{G}_{c,\Lambda}^2(x_1, +; x_2, -) = & \\ & \int dy_1 \int dy_2 \sum_{c_1, c_2} \dot{Q}_\Lambda(y_1, c_1; y_2, c_2) \mathbf{G}_{c,\Lambda}^2(y_1, c_1; x_1, +) \mathbf{G}_{c,\Lambda}^2(y_2, c_2; x_2, -) \\ & - \frac{1}{2} \int dy_1 \int dy_2 \sum_{c_1, c_2} \dot{Q}_\Lambda(y_1, c_1; y_2, c_2) \mathbf{G}_{c,\Lambda}^4(y_1, c_1; y_2, c_2; x_1, +; x_2, -). \end{aligned} \quad (6.56)$$

j	$\text{sgn}(\pi_j)$	$\pi_j(1)$	$\pi_j(2)$	$\pi_j(3)$	$\pi_j(4)$
0	+1	1	2	3	4
1	-1	2	1	3	4
2	+1	3	1	2	4
3	-1	4	1	2	3

Table 6.2: Representative permutations used for evaluating Eq. (6.60).

In the first term on the right-hand side, only the combination of Nambu indices $(c_1, c_2) = (-, +)$ gives a nonvanishing contribution, whereas in the second term, the two contributions from $(c_1, c_2) = (+, -)$ and $(c_1, c_2) = (-, +)$ are equal. It follows that

$$\begin{aligned} \dot{G}_{c,\Lambda}^2(x_1, x_2) = & - \int dy_1 \int dy_2 \dot{Q}_\Lambda(y_1, y_2) G_{c,\Lambda}^2(x_1, y_1) G_{c,\Lambda}^2(y_2, x_2) \\ & + \int dy_1 \int dy_2 \dot{Q}_\Lambda(y_2, y_1) G_{c,\Lambda}^4(y_1, x_1, y_2, x_2), \end{aligned} \quad (6.57)$$

which is equivalent to the assertion (6.54).

(ii) *Four-point function.* We evaluate Eq. (6.43) for

$$X_1 = (x_1, +), \quad X_2 = (x_2, +), \quad X_3 = (x_3, -), \quad X_4 = (x_4, -), \quad (6.58)$$

such that the left-hand side reverts to $(-1)\dot{G}_{c,\Lambda}^4(x_1, x_2, x_3, x_4)$. The second term on the right-hand side can be evaluated analogously as in the case $n = 1$ and yields

$$- \int dy_1 \int dy_2 \dot{Q}_\Lambda(y_2, y_1) G_{c,\Lambda}^6(y_1, x_1, x_2, y_2, x_3, x_4). \quad (6.59)$$

Next, consider the first term on the right-hand side of Eq. (6.43), which reads explicitly

$$\begin{aligned} & \frac{4}{4!} \sum_{\pi \in S_4} \text{sgn}(\pi) \int dY_1 \int dY_2 \\ & \times \dot{Q}_\Lambda(Y_1, Y_2) G_{c,\Lambda}^2(Y_1, X_{\pi(1)}) G_{c,\Lambda}^4(Y_2, X_{\pi(2)}, X_{\pi(3)}, X_{\pi(4)}). \end{aligned} \quad (6.60)$$

By the antisymmetry of the Nambu-type four-point function, there are always $3! = 6$ permutations which give the same contribution. Therefore, only

$$\frac{4!}{3!} = 4 \quad (6.61)$$

representative permutations need to be considered, provided that we count each of them six times. We choose the four representative permutations π_0, \dots, π_3 which are shown in Table 6.2. Using that $6 \times 4 / 4! = 1$, we see that the prefactor in Eq. (6.60) cancels

out, and thus we are left with the sum

$$\begin{aligned} & \sum_{j=0}^3 \text{sgn}(\pi_j) \int dY_1 \int dY_2 \\ & \times \dot{Q}_\Lambda(Y_1, Y_2) G_{c,\Lambda}^2(Y_1, X_{\pi_j(1)}) G_{c,\Lambda}^4(Y_2, X_{\pi_j(2)}, X_{\pi_j(3)}, X_{\pi_j(4)}) . \end{aligned} \quad (6.62)$$

Consider the first summand with $j = 0$, which corresponds to the identity permutation:

$$\int dY_1 \int dY_2 \dot{Q}_\Lambda(Y_1, Y_2) G_{c,\Lambda}^2(Y_1, X_1) G_{c,\Lambda}^4(Y_2, X_2, X_3, X_4) . \quad (6.63)$$

By choosing the external Nambu indices as in Eq. (6.58), this yields

$$\int dy_1 \int dy_2 \dot{Q}_\Lambda(y_1, y_2) G_{c,\Lambda}^2(x_1, y_1) G_{c,\Lambda}^4(y_2, x_2, x_3, x_4) . \quad (6.64)$$

The remaining terms in Eq. (6.62)—i.e., those with $j = 1, 2, 3$ —can be evaluated analogously. Taking into account also Eq. (6.59), we arrive at

$$\begin{aligned} & (-1) \dot{G}_{c,\Lambda}^4(x_1, x_2, x_3, x_4) = \\ & - \int dy_1 \int dy_2 \dot{Q}_\Lambda(y_2, y_1) G_{c,\Lambda}^6(y_1, x_1, x_2, y_2, x_3, x_4) \\ & + \sum_{\pi \in S_2} \text{sgn}(\pi) \int dy_1 \int dy_2 \dot{Q}_\Lambda(y_1, y_2) G_{c,\Lambda}^2(x_{\pi(1)}, y_1) G_{c,\Lambda}^4(y_2, x_{\pi(2)}, x_3, x_4) \\ & + \sum_{\pi \in S_2} \text{sgn}(\pi) \int dy_1 \int dy_2 \dot{Q}_\Lambda(y_2, y_1) G_{c,\Lambda}^2(y_1, x_{\pi(3)}) G_{c,\Lambda}^4(x_1, x_2, y_2, x_{\pi(4)}) , \end{aligned} \quad (6.65)$$

which is equivalent to the assertion (6.55). \square

The diagram shows the expansion of a four-point function with a dot on the external line. The left side is a box labeled G_c^4 with a dot above the top-right external line. This is equal to the sum of four terms, each preceded by a minus sign, and a final term preceded by a plus sign. The four terms are:

- A box labeled G_c^2 followed by a box labeled \dot{Q} followed by a box labeled G_c^4 .
- A box labeled G_c^2 followed by a box labeled \dot{Q} followed by a box labeled G_c^4 with a dot above the top-right external line.
- A box labeled G_c^4 followed by a box labeled \dot{Q} followed by a box labeled G_c^2 .
- A box labeled G_c^4 followed by a box labeled \dot{Q} followed by a box labeled G_c^2 with a dot above the top-right external line.

The plus sign term is a box labeled G_c^6 followed by a box labeled \dot{Q} .

Table 6.3: RGE for the connected two- and four-point Green functions (Theorem 6.3): representation by means of Universal Feynman Graphs (see Sct. 4.5).

6.3. One-line irreducible Green function flow

In this section, we will derive the RGE for the one-line-irreducible Green functions Γ^{2n} (see Sect. 5.5), which in principle also constitute an infinite hierarchy of coupled differential equations. For the sake of brevity, however, we will restrict ourselves to $n = 1$ and $n = 2$, i.e., we will only derive the RGE for the one-line-irreducible two- and four-point functions. Our procedure is analogous as in the previous section: we will first derive a differential equation for the one-line-irreducible generator Γ_Λ , subsequently deduce the RGE for the Nambu-type Green functions, and finally derive the RGE for the one-line-irreducible Green functions themselves (see Ref. [SH01]).

The scale-dependent one-line-irreducible Green function generator Γ_Λ is defined as the Legendre transform of the connected Green function generator \mathcal{W}_Λ (see Eqs. (6.9)–(6.11), and Appendix A of Part II):

$$\Gamma_\Lambda = \mathcal{W}_\Lambda - \langle H, \Phi_\Lambda \rangle, \quad (6.66)$$

where the new sources Φ_Λ are defined as

$$\Phi_\Lambda(x) = \frac{\delta \mathcal{W}_\Lambda}{\delta H(x)}. \quad (6.67)$$

We stress again that by this definition, the source fields Φ_Λ themselves are scale dependent. Furthermore, in analogy to Eq. (6.20), we define the matrix

$$\tilde{\Gamma}_\Lambda(X, Y) = \frac{\delta^2 \Gamma_\Lambda}{\delta \Phi_\Lambda(X) \delta \Phi_\Lambda(Y)} - \frac{\delta^2 \Gamma_\Lambda}{\delta \Phi_\Lambda(X) \delta \Phi_\Lambda(Y)} \Big|_{\Phi_\Lambda=0}, \quad (6.68)$$

which is the second Grassmann derivative of Γ_Λ subtracted by the constant terms.

Theorem 6.4 (RGE for one-line-irreducible Green function generator). *The scale-dependent one-line-irreducible Green function generator Γ_Λ satisfies the following differential equation:*

$$\dot{\Gamma}_\Lambda + \left\langle \frac{\delta \Gamma_\Lambda}{\delta \Phi_\Lambda}, \dot{\Phi}_\Lambda \right\rangle = -\frac{1}{2} \langle \Phi_\Lambda, \dot{\mathbf{Q}}_\Lambda \Phi_\Lambda \rangle + \frac{1}{2} \sum_{p=0}^{\infty} (-1)^p \text{Tr} \left[\mathbf{S}_\Lambda \tilde{\Gamma}_\Lambda (\mathbf{G}_\Lambda^2 \tilde{\Gamma}_\Lambda)^p \right], \quad (6.69)$$

where $\tilde{\Gamma}_\Lambda$ is defined by Eq. (6.68), and where \mathbf{S}_Λ denotes the single-scale Green function in the Nambu formalism, which is defined as

$$\mathbf{S}_\Lambda = -\mathbf{G}_\Lambda^2 \dot{\mathbf{Q}}_\Lambda \mathbf{G}_\Lambda^2. \quad (6.70)$$

By expanding Γ_Λ into a sum of monomials of the order $2n$ in the fields,

$$\Gamma_\Lambda = \sum_{n=1}^{\infty} \Gamma_\Lambda^{(2n)}, \quad (6.71)$$

and similarly its derivatives,

$$\tilde{\Gamma}_\Lambda(X, Y) = \sum_{n=1}^{\infty} \tilde{\Gamma}_\Lambda^{(2n)}(X, Y), \quad (6.72)$$

the RGE (6.69) is equivalent to a hierarchy of coupled differential equations for these monomials, which is given by

$$\dot{\Gamma}_\Lambda^{(2)} + \left\langle \frac{\delta \Gamma_\Lambda^{(2)}}{\delta \Phi_\Lambda}, \dot{\Phi}_\Lambda \right\rangle = -\frac{1}{2} \langle \Phi_\Lambda, \dot{\mathbf{Q}}_\Lambda \Phi_\Lambda \rangle + \frac{1}{2} \text{Tr} [\mathbf{S}_\Lambda \tilde{\Gamma}_\Lambda^{(2)}], \quad (6.73)$$

$$\dot{\Gamma}_\Lambda^{(4)} + \left\langle \frac{\delta \Gamma_\Lambda^{(4)}}{\delta \Phi_\Lambda}, \dot{\Phi}_\Lambda \right\rangle = \frac{1}{2} \text{Tr} [\mathbf{S}_\Lambda \tilde{\Gamma}_\Lambda^{(4)}] - \frac{1}{2} \text{Tr} [\mathbf{S}_\Lambda \tilde{\Gamma}_\Lambda^{(2)} \mathbf{G}_\Lambda^2 \tilde{\Gamma}_\Lambda^{(2)}], \quad (6.74)$$

and by similar equations for $n \geq 3$.

Remark. Before proceeding with the proof, we compare our RGE (6.69) with the corresponding equation in the original article [SH01, Eq. (48)]. First, since we had defined both \mathcal{W}_Λ and Γ_Λ as *elements* of the Grassmann algebra \mathcal{S} of the sources, we did not need to invert any *functional* for defining the (scale-dependent) Legendre transform (see the remark on p. 112). This difference in the definition of the Legendre transform accounts for the additional term on the left-hand side of our RGE (6.69). On the other hand, by our Definitions 5.4 and 5.10, neither \mathcal{W}_Λ nor Γ_Λ has any field-independent term, and this explains the missing constant term on the right-hand side of Eq. (6.69). Despite these differences, the resulting RGE for the one-line-irreducible Green functions (which are stated in Theorem 6.5 and Theorem 6.6) will agree again with the corresponding equations in Ref. [SH01].

Proof. The scale derivative of the Legendre transform (6.66) contains two terms, because both \mathcal{W}_Λ and the source fields Φ_Λ are scale dependent:

$$\dot{\Gamma}_\Lambda = \dot{\mathcal{W}}_\Lambda - \langle \mathbf{H}, \dot{\Phi}_\Lambda \rangle = \dot{\mathcal{W}}_\Lambda - \left\langle \frac{\delta \Gamma_\Lambda}{\delta \Phi_\Lambda}, \dot{\Phi}_\Lambda \right\rangle. \quad (6.75)$$

By using the RGE (6.26) for \mathcal{W}_Λ , the definition (6.67) of the source fields Φ_Λ , and Eqs. (5.140)–(5.141), we obtain the following RGE for Γ_Λ :

$$\begin{aligned} \dot{\Gamma}_\Lambda + \left\langle \frac{\delta \Gamma_\Lambda}{\delta \Phi_\Lambda}, \dot{\Phi}_\Lambda \right\rangle = \\ -\frac{1}{2} \langle \Phi_\Lambda, \dot{\mathbf{Q}}_\Lambda \Phi_\Lambda \rangle + \frac{1}{2} \text{Tr} \left[\dot{\mathbf{Q}}_\Lambda \left(\left(\frac{\delta^2 \Gamma_\Lambda}{\delta \Phi_\Lambda^2} \right)^{-1} - \left(\frac{\delta^2 \Gamma_\Lambda}{\delta \Phi_\Lambda^2} \right)^{-1} \Big|_{\Phi_\Lambda=0} \right) \right]. \end{aligned} \quad (6.76)$$

In order to evaluate the right-hand side of this equation, we have to calculate the inverse of the second derivative of Γ_Λ . First, we note that the field-independent term,

$$\left(\frac{\delta^2 \Gamma_\Lambda}{\delta \Phi_\Lambda^2} \right)^{-1} \Big|_{\Phi_\Lambda=0} = \frac{\delta^2 \mathcal{W}_\Lambda}{\delta \mathbf{H}^2} \Big|_{\mathbf{H}=0} = \mathbf{G}_{c,\Lambda}^2 = \mathbf{G}_\Lambda^2, \quad (6.77)$$

coincides with the (connected) two-point Green function in the Nambu formalism (see Eq. (5.61)). Furthermore, Eq. (6.68) can be written in matrix form as

$$\tilde{\Gamma}_\Lambda = \frac{\delta^2 \Gamma_\Lambda}{\delta \Phi_\Lambda^2} - \mathbf{\Gamma}_\Lambda^2. \quad (6.78)$$

By Theorem 5.14, Eq. (5.142), we have

$$\mathbf{\Gamma}_\Lambda^2 = (\mathbf{G}_\Lambda^2)^{-1}, \quad (6.79)$$

and hence, Eq. (6.78) is equivalent to

$$\frac{\delta^2 \Gamma_\Lambda}{\delta \Phi_\Lambda^2} = (\mathbf{G}_\Lambda^2)^{-1} + \tilde{\Gamma}_\Lambda = (\mathbf{G}_\Lambda^2)^{-1} (1 + \mathbf{G}_\Lambda^2 \tilde{\Gamma}_\Lambda). \quad (6.80)$$

Now, the inverse of this second derivative can be expressed as a geometric series:

$$\left(\frac{\delta^2 \Gamma_\Lambda}{\delta \Phi_\Lambda^2} \right)^{-1} = (1 + \mathbf{G}_\Lambda^2 \tilde{\Gamma}_\Lambda)^{-1} \mathbf{G}_\Lambda^2 = \sum_{p=0}^{\infty} (-1)^p (\mathbf{G}_\Lambda^2 \tilde{\Gamma}_\Lambda)^p \mathbf{G}_\Lambda^2. \quad (6.81)$$

Taking into account also Eq. (6.77), we find that

$$\left(\frac{\delta^2 \Gamma_\Lambda}{\delta \Phi_\Lambda^2} \right)^{-1} - \left(\frac{\delta^2 \Gamma_\Lambda}{\delta \Phi_\Lambda^2} \right)^{-1} \Big|_{\Phi_\Lambda=0} = \sum_{p=1}^{\infty} (-1)^p (\mathbf{G}_\Lambda^2 \tilde{\Gamma}_\Lambda)^p \mathbf{G}_\Lambda^2. \quad (6.82)$$

Thus, the RGE (6.76) is equivalent to

$$\dot{\Gamma}_\Lambda + \left\langle \frac{\delta \Gamma_\Lambda}{\delta \Phi_\Lambda}, \dot{\Phi}_\Lambda \right\rangle = -\frac{1}{2} \langle \Phi_\Lambda, \dot{\mathbf{Q}}_\Lambda \Phi_\Lambda \rangle + \frac{1}{2} \sum_{p=1}^{\infty} (-1)^p \text{Tr} \left[\dot{\mathbf{Q}}_\Lambda (\mathbf{G}_\Lambda^2 \tilde{\Gamma}_\Lambda)^p \mathbf{G}_\Lambda^2 \right]. \quad (6.83)$$

By the cyclicity of the trace and by the definition (6.70), the last term is equivalent to

$$\frac{1}{2} \sum_{p=1}^{\infty} (-1)^p \text{Tr} \left[\mathbf{G}_\Lambda^2 \dot{\mathbf{Q}}_\Lambda (\mathbf{G}_\Lambda^2 \tilde{\Gamma}_\Lambda)^p \right] = -\frac{1}{2} \sum_{p=1}^{\infty} (-1)^p \text{Tr} \left[\mathbf{S}_\Lambda \tilde{\Gamma}_\Lambda (\mathbf{G}_\Lambda^2 \tilde{\Gamma}_\Lambda)^{p-1} \right] \quad (6.84)$$

$$= \frac{1}{2} \sum_{p=0}^{\infty} (-1)^p \text{Tr} \left[\mathbf{S}_\Lambda \tilde{\Gamma}_\Lambda (\mathbf{G}_\Lambda^2 \tilde{\Gamma}_\Lambda)^p \right], \quad (6.85)$$

which yields the RGE (6.69). Finally, by expanding Γ_Λ and $\tilde{\Gamma}_\Lambda$ into monomials and equating the terms on both sides of Eq. (6.69) which are of the order two ($n = 1$) and respectively four ($n = 2$) in the fields, we obtain Eqs. (6.73) and (6.74). \square

Theorem 6.5 (RGE for one-line-irreducible Green functions in the Nambu formalism). *The Nambu-type one-line-irreducible Green functions $\mathbf{\Gamma}^{2n}$ satisfy the following differential equations: for $n = 1$,*

$$\dot{\mathbf{\Gamma}}_\Lambda^2(X_1, X_2) = \dot{\mathbf{Q}}_\Lambda(X_1, X_2) - \frac{1}{2} \int dY_1 \int dY_2 \mathbf{S}_\Lambda(Y_1, Y_2) \mathbf{\Gamma}_\Lambda^4(Y_1, Y_2, X_1, X_2), \quad (6.86)$$

and for $n = 2$,

$$\begin{aligned} \dot{\Gamma}_{\Lambda}^4(X_1, \dots, X_4) = & \\ & - \frac{1}{2} \int dY_1 \int dY_2 \mathbf{S}_{\Lambda}(Y_1, Y_2) \mathbf{\Gamma}_{\Lambda}^6(Y_1, Y_2, X_1, X_2, X_3, X_4) \\ & - \frac{1}{2} \int dY_1 \dots \int dY_4 \mathbf{L}_{\Lambda}(Y_1, \dots, Y_4) \mathbf{B}_{\Lambda}(Y_1, \dots, Y_4; X_1, \dots, X_4). \end{aligned} \quad (6.87)$$

In these equations, the single-scale Green function \mathbf{S}_{Λ} is given by Eq. (6.70). Furthermore, we have defined the loop term in the Nambu formalism \mathbf{L}_{Λ} as

$$\mathbf{L}_{\Lambda}(Y_1, \dots, Y_4) = \mathbf{S}_{\Lambda}(Y_1, Y_3) \mathbf{G}_{\Lambda}^2(Y_2, Y_4) + \mathbf{G}_{\Lambda}^2(Y_1, Y_3) \mathbf{S}_{\Lambda}(Y_2, Y_4), \quad (6.88)$$

and the vertex bilinear \mathbf{B}_{Λ} as

$$\begin{aligned} \mathbf{B}_{\Lambda}(Y_1, \dots, Y_4; X_1, \dots, X_4) = & \mathbf{\Gamma}_{\Lambda}^4(Y_2, Y_3, X_1, X_2) \mathbf{\Gamma}_{\Lambda}^4(Y_1, Y_4, X_3, X_4) \\ & - \mathbf{\Gamma}_{\Lambda}^4(Y_2, Y_3, X_1, X_3) \mathbf{\Gamma}_{\Lambda}^4(Y_1, Y_4, X_2, X_4) \\ & + \mathbf{\Gamma}_{\Lambda}^4(Y_2, Y_3, X_1, X_4) \mathbf{\Gamma}_{\Lambda}^4(Y_1, Y_4, X_2, X_3). \end{aligned} \quad (6.89)$$

Similar equations can be derived for $n \geq 3$.

Proof. We first expand the right-hand sides of Eqs. (6.71) and (6.72) in terms of the source fields: By Eq. (A.47), we have

$$\Gamma_{\Lambda}^{(2n)} = \frac{(-1)^n}{(2n)!} \int dX_1 \dots \int dX_{2n} \mathbf{\Gamma}_{\Lambda}^{2n}(X_1, \dots, X_{2n}) \Phi_{\Lambda}(X_1) \dots \Phi_{\Lambda}(X_{2n}). \quad (6.90)$$

The corresponding expression of the second derivative can be derived analogously as Eq. (6.47) and is given by

$$\begin{aligned} \tilde{\Gamma}_{\Lambda}^{(2n)}(X, Y) = & \frac{(-1)^{n+1}}{(2n)!} \int dX_1 \dots \int dX_{2n} \\ & \times \mathbf{\Gamma}_{\Lambda}^{2n+2}(Y, X, X_1, \dots, X_{2n}) \Phi_{\Lambda}(X_1) \dots \Phi_{\Lambda}(X_{2n}). \end{aligned} \quad (6.91)$$

Next, we expand the left-hand side of the RGE (6.69), i.e.,

$$\dot{\Gamma}_{\Lambda} + \left\langle \frac{\delta \Gamma_{\Lambda}}{\delta \Phi_{\Lambda}}, \dot{\Phi}_{\Lambda} \right\rangle = \sum_{n=1}^{\infty} \left(\dot{\Gamma}_{\Lambda}^{(2n)} + \left\langle \frac{\delta \Gamma_{\Lambda}^{(2n)}}{\delta \Phi_{\Lambda}}, \dot{\Phi}_{\Lambda} \right\rangle \right). \quad (6.92)$$

When a scale derivative is applied to Eq. (6.90), it can act either on the coefficient function or on the source fields. Thus, we obtain

$$\begin{aligned} \dot{\Gamma}_{\Lambda}^{(2n)} = & \frac{(-1)^n}{(2n)!} \int dX_1 \dots \int dX_{2n} \dot{\mathbf{\Gamma}}_{\Lambda}^{2n}(X_1, \dots, X_{2n}) \Phi_{\Lambda}(X_1) \dots \Phi_{\Lambda}(X_{2n}) \\ & + \frac{(-1)^n}{(2n)!} \int dX_1 \dots \int dX_{2n} \mathbf{\Gamma}_{\Lambda}^{2n}(X_1, \dots, X_{2n}) \frac{d}{d\Lambda} \left(\Phi_{\Lambda}(X_1) \dots \Phi_{\Lambda}(X_{2n}) \right). \end{aligned} \quad (6.93)$$

Furthermore, since $\Gamma_\Lambda^{(2n)}$ is an even element of the Grassmann algebra \mathcal{S} , we have

$$\left\langle \frac{\delta \Gamma_\Lambda^{(2n)}}{\delta \Phi_\Lambda}, \dot{\Phi}_\Lambda \right\rangle = - \left\langle \dot{\Phi}_\Lambda, \frac{\delta \Gamma_\Lambda^{(2n)}}{\delta \Phi_\Lambda} \right\rangle = - \int dY \dot{\Phi}_\Lambda(Y) \frac{\delta \Gamma_\Lambda^{(2n)}}{\delta \Phi_\Lambda(Y)}. \quad (6.94)$$

Plugging the expansion (6.90) into this equation yields

$$\begin{aligned} \left\langle \frac{\delta \Gamma_\Lambda^{(2n)}}{\delta \Phi_\Lambda}, \dot{\Phi}_\Lambda \right\rangle &= - \frac{(-1)^n}{(2n)!} \int dX_1 \dots \int dX_{2n} \mathbf{I}_\Lambda^{2n}(X_1, \dots, X_{2n}) \\ &\quad \times \int dY \dot{\Phi}_\Lambda(Y) \frac{\delta}{\delta \Phi_\Lambda(Y)} \left(\Phi_\Lambda(X_1) \dots \Phi_\Lambda(X_{2n}) \right). \end{aligned} \quad (6.95)$$

Now, the important observation is that

$$\int dY \dot{\Phi}_\Lambda(Y) \frac{\delta}{\delta \Phi_\Lambda(Y)} \left(\Phi_\Lambda(X_1) \dots \Phi_\Lambda(X_{2n}) \right) = \frac{d}{d\Lambda} \left(\Phi_\Lambda(X_1) \dots \Phi_\Lambda(X_{2n}) \right). \quad (6.96)$$

In fact, this identity is almost obvious, as both sides of it are equal to

$$\sum_{i=1}^{2n} \Phi_\Lambda(X_1) \dots \Phi_\Lambda(X_{i-1}) \dot{\Phi}_\Lambda(X_i) \Phi_\Lambda(X_{i+1}) \dots \Phi_\Lambda(X_{2n}). \quad (6.97)$$

Therefore, Eq. (6.95) precisely cancels the second term on the right-hand side of Eq. (6.93), and we obtain the desired identity

$$\begin{aligned} \dot{\Gamma}_\Lambda^{(2n)} + \left\langle \frac{\delta \Gamma_\Lambda^{(2n)}}{\delta \Phi_\Lambda}, \dot{\Phi}_\Lambda \right\rangle &= \\ \frac{(-1)^n}{(2n)!} \int dX_1 \dots \int dX_{2n} \dot{\mathbf{I}}_\Lambda^{2n}(X_1, \dots, X_{2n}) \Phi_\Lambda(X_1) \dots \Phi_\Lambda(X_{2n}), \end{aligned} \quad (6.98)$$

where the scale derivative on the right-hand side acts only on the coefficient function but not on the source fields.

With these prerequisites, we now derive the RGE (6.86)–(6.87) for the two- and four-point functions starting from Eqs. (6.73)–(6.74) of Theorem 6.4:

(i) *Two-point function.* By Eq. (6.98), the left-hand side of Eq. (6.73) is given by

$$\dot{\Gamma}_\Lambda^{(2)} + \left\langle \frac{\delta \Gamma_\Lambda^{(2)}}{\delta \Phi_\Lambda}, \dot{\Phi}_\Lambda \right\rangle = - \frac{1}{2} \int dX_1 \int dX_2 \dot{\mathbf{I}}_\Lambda^2(X_1, X_2) \Phi_\Lambda(X_1) \Phi_\Lambda(X_2). \quad (6.99)$$

The first term on the right-hand side of Eq. (6.73) reads

$$- \frac{1}{2} \langle \Phi_\Lambda, \dot{\mathbf{Q}}_\Lambda \Phi_\Lambda \rangle = - \frac{1}{2} \int dX_1 \int dX_2 \dot{\mathbf{Q}}_\Lambda(X_1, X_2) \Phi_\Lambda(X_1) \Phi_\Lambda(X_2), \quad (6.100)$$

and for the second term, we obtain from Eq. (6.91),

$$\begin{aligned} \frac{1}{2} \text{Tr} \left[\mathbf{S}_\Lambda \tilde{\Gamma}_\Lambda^{(2)} \right] &= \frac{1}{2} \int dY_1 \int dY_2 \mathbf{S}_\Lambda(Y_1, Y_2) \tilde{\mathbf{F}}_\Lambda^{(2)}(Y_2, Y_1) \\ &= \frac{1}{4} \int dX_1 \int dX_2 \left(\int dY_1 \int dY_2 \mathbf{S}_\Lambda(Y_1, Y_2) \mathbf{F}_\Lambda^4(Y_1, Y_2, X_1, X_2) \right) \Phi_\Lambda(X_1) \Phi_\Lambda(X_2). \end{aligned} \quad (6.101)$$

Equating the antisymmetric coefficient functions on both sides of the equation yields

$$\dot{\mathbf{I}}_\Lambda^2(X_1, X_2) = \dot{\mathbf{Q}}_\Lambda(X_1, X_2) - \frac{1}{2} \int dY_1 \int dY_2 \mathbf{S}_\Lambda(Y_1, Y_2) \mathbf{F}_\Lambda^4(Y_1, Y_2, X_1, X_2), \quad (6.102)$$

which coincides with the assertion (6.86).

(ii) *Four-point function.* By Eq. (6.98), the left-hand side of Eq. (6.74) is given by

$$\dot{\Gamma}_\Lambda^{(4)} + \left\langle \frac{\delta \Gamma_\Lambda^{(4)}}{\delta \Phi_\Lambda}, \dot{\Phi}_\Lambda \right\rangle = \frac{1}{4!} \int dX_1 \dots \int dX_4 \dot{\mathbf{I}}_\Lambda^4(X_1, \dots, X_4) \Phi_\Lambda(X_1) \dots \Phi_\Lambda(X_4). \quad (6.103)$$

The first term on the right-hand side of Eq. (6.74) can be expressed analogously to Eq. (6.101) as

$$\begin{aligned} \frac{1}{2} \text{Tr} \left[\mathbf{S}_\Lambda \tilde{\Gamma}_\Lambda^{(4)} \right] &= -\frac{1}{2} \frac{1}{4!} \int dX_1 \dots \int dX_4 \Phi_\Lambda(X_1) \dots \Phi_\Lambda(X_4) \\ &\quad \times \left(\int dY_1 \int dY_2 \mathbf{S}_\Lambda(Y_1, Y_2) \mathbf{F}_\Lambda^6(Y_1, Y_2, X_1, \dots, X_4) \right). \end{aligned} \quad (6.104)$$

For the second term, we obtain from Eq. (6.91),

$$\begin{aligned} &-\frac{1}{2} \text{Tr} \left[\mathbf{S}_\Lambda \tilde{\mathbf{F}}_\Lambda^{(2)} \mathbf{G}_\Lambda^2 \tilde{\mathbf{F}}_\Lambda^{(2)} \right] \\ &= -\frac{1}{2} \int dY_1 \dots \int dY_4 \mathbf{S}_\Lambda(Y_1, Y_3) \tilde{\mathbf{F}}_\Lambda^{(2)}(Y_3, Y_2) \mathbf{G}_\Lambda^2(Y_2, Y_4) \tilde{\mathbf{F}}_\Lambda^{(2)}(Y_4, Y_1) \end{aligned} \quad (6.105)$$

$$= -\frac{1}{2} \int dX_1 \dots \int dX_4 \mathbf{T}_\Lambda^4(X_1, \dots, X_4) \Phi_\Lambda(X_1) \dots \Phi_\Lambda(X_4), \quad (6.106)$$

where we have defined

$$\begin{aligned} \mathbf{T}_\Lambda^4(X_1, X_2, X_3, X_4) &= \frac{1}{4} \int dY_1 \dots \int dY_4 \mathbf{S}_\Lambda(Y_1, Y_3) \mathbf{G}_\Lambda^2(Y_2, Y_4) \\ &\quad \times \mathbf{F}_\Lambda^4(Y_2, Y_3, X_1, X_2) \mathbf{F}_\Lambda^4(Y_1, Y_4, X_3, X_4). \end{aligned} \quad (6.107)$$

Equating the antisymmetrized coefficient functions on both sides of Eq. (6.74) yields

$$\begin{aligned} \dot{\mathbf{I}}_\Lambda^4(X_1, X_2, X_3, X_4) &= -\frac{1}{2} \int dY_1 \int dY_2 \mathbf{S}_\Lambda(Y_1, Y_2) \mathbf{F}_\Lambda^6(Y_1, Y_2, X_1, X_2, X_3, X_4) \\ &\quad - \frac{4!}{2} \mathbb{A}_{(X_1, X_2, X_3, X_4)} \mathbf{T}_\Lambda^4(X_1, X_2, X_3, X_4). \end{aligned} \quad (6.108)$$

In order to derive a more explicit expression for the second term on the right-hand side of this equation, we introduce some abbreviations: for $k, \ell \in \{1, \dots, 4\}$, let

$$\mathbf{A}_{k,\ell} \equiv \mathbf{\Gamma}_{\Lambda}^4(Y_2, Y_3, X_k, X_{\ell}), \quad (6.109)$$

$$\mathbf{B}_{k,\ell} \equiv \mathbf{\Gamma}_{\Lambda}^4(Y_1, Y_4, X_k, X_{\ell}). \quad (6.110)$$

Then, we can write

$$\mathbb{A}_{(X_1, \dots, X_4)} \mathbf{T}_{\Lambda}^4(X_1, \dots, X_4) = \quad (6.111)$$

$$\frac{1}{4} \int dY_1 \dots dY_4 \mathbf{S}_{\Lambda}(Y_1, Y_3) \mathbf{G}_{\Lambda}^2(Y_2, Y_4) \mathbb{A}_{(X_1, \dots, X_4)} \{ \mathbf{A}_{1,2} \mathbf{B}_{3,4} \},$$

and it remains to evaluate

$$\mathbb{A}_{(X_1, \dots, X_4)} \{ \mathbf{A}_{1,2} \mathbf{B}_{3,4} \} = \frac{1}{4!} \sum_{\pi \in S_4} \text{sgn}(\pi) \mathbf{A}_{\pi(1), \pi(2)} \mathbf{B}_{\pi(3), \pi(4)}. \quad (6.112)$$

The antisymmetry of $\mathbf{\Gamma}_{\Lambda}^4$ implies the conditions

$$\mathbf{A}_{k,\ell} = -\mathbf{A}_{\ell,k}, \quad (6.113)$$

$$\mathbf{B}_{k,\ell} = -\mathbf{B}_{\ell,k}. \quad (6.114)$$

Consequently, there are always four permutations in the sum of Eq. (6.112) which yield the same contribution, e.g.,

$$\mathbf{A}_{1,2} \mathbf{B}_{3,4} = -\mathbf{A}_{2,1} \mathbf{B}_{3,4} = -\mathbf{A}_{1,2} \mathbf{B}_{4,3} = \mathbf{A}_{2,1} \mathbf{B}_{4,3}. \quad (6.115)$$

Thus, we are left with only six different terms:

$$\mathbb{A}_{(X_1, \dots, X_4)} \{ \mathbf{A}_{1,2} \mathbf{B}_{3,4} \} = \quad (6.116)$$

$$\frac{4}{4!} \left(\mathbf{A}_{1,2} \mathbf{B}_{3,4} + \mathbf{A}_{3,4} \mathbf{B}_{1,2} - \mathbf{A}_{1,3} \mathbf{B}_{2,4} - \mathbf{A}_{2,4} \mathbf{B}_{1,3} + \mathbf{A}_{1,4} \mathbf{B}_{2,3} + \mathbf{A}_{2,3} \mathbf{B}_{1,4} \right).$$

By putting this result into Eq. (6.111) and by renaming in every second term the integration variables as $Y_1 \leftrightarrow Y_2$ and $Y_3 \leftrightarrow Y_4$, we arrive at

$$\mathbb{A}_{(X_1, \dots, X_4)} \mathbf{T}_{\Lambda}^4(X_1, \dots, X_4) = \quad (6.117)$$

$$\begin{aligned} & \frac{1}{4!} \int dY_1 \dots dY_4 \left(\mathbf{S}_{\Lambda}(Y_1, Y_3) \mathbf{G}_{\Lambda}^2(Y_2, Y_4) + \mathbf{G}_{\Lambda}^2(Y_1, Y_3) \mathbf{S}_{\Lambda}(Y_2, Y_4) \right) \\ & \times \left(\mathbf{A}_{1,2} \mathbf{B}_{3,4} - \mathbf{A}_{1,3} \mathbf{B}_{2,4} + \mathbf{A}_{1,4} \mathbf{B}_{2,3} \right). \end{aligned}$$

This is equivalent to

$$\begin{aligned} & \mathbb{A}_{(X_1, \dots, X_4)} \mathbf{T}_{\Lambda}^4(X_1, \dots, X_4) \\ & = \frac{1}{4!} \int dY_1 \dots dY_4 \mathbf{L}_{\Lambda}(Y_1, \dots, Y_4) \mathbf{B}_{\Lambda}(Y_1, \dots, Y_4; X_1, \dots, X_4), \end{aligned} \quad (6.118)$$

with L_Λ and B_Λ defined by Eqs. (6.88) and (6.89), respectively. Combining this result with Eq. (6.108) shows the assertion (6.87). \square

Theorem 6.6 (RGE for one-line-irreducible Green functions). *The one-line-irreducible two- and four-point functions satisfy the following differential equations:*

$$\dot{\Gamma}_\Lambda^2(x_1, x_2) = \dot{Q}_\Lambda(x_1, x_2) + \int dy_1 \int dy_2 \Gamma_\Lambda^4(x_1, y_1, x_2, y_2) S_\Lambda(y_2, y_1), \quad (6.119)$$

and respectively,

$$\begin{aligned} \dot{\Gamma}_\Lambda^4(x_1, \dots, x_4) = & \int dy_1 \int dy_2 \Gamma_\Lambda^6(x_1, x_2, y_1, x_3, x_4, y_2) S_\Lambda(y_2, y_1) \\ & + \Phi_\Lambda^{\text{pp}}(x_1, \dots, x_4) + \Phi_\Lambda^{\text{ph,c}}(x_1, \dots, x_4) + \Phi_\Lambda^{\text{ph,d}}(x_1, \dots, x_4). \end{aligned} \quad (6.120)$$

Here, the last three terms on the right-hand side are called the particle-particle term, the crossed particle-hole term and the direct particle-hole term, and they are given by

$$\begin{aligned} \Phi_\Lambda^{\text{pp}}(x_1, x_2, x_3, x_4) = & \frac{1}{2} \int dy_1 \dots \int dy_4 L_\Lambda(y_1, y_2, y_3, y_4) \\ & \times \Gamma_\Lambda^4(x_1, x_2, y_1, y_2) \Gamma_\Lambda^4(y_3, y_4, x_3, x_4), \end{aligned} \quad (6.121)$$

$$\begin{aligned} \Phi_\Lambda^{\text{ph,c}}(x_1, x_2, x_3, x_4) = & - \int dy_1 \dots \int dy_4 L_\Lambda(y_3, y_4, y_2, y_1) \\ & \times \Gamma_\Lambda^4(y_1, x_1, y_3, x_3) \Gamma_\Lambda^4(x_2, y_2, x_4, y_4), \end{aligned} \quad (6.122)$$

$$\Phi_\Lambda^{\text{ph,d}}(x_1, x_2, x_3, x_4) = -\Phi_\Lambda^{\text{ph,c}}(x_1, x_2, x_4, x_3). \quad (6.123)$$

Furthermore, we have defined the single-scale Green function S_Λ as

$$S_\Lambda = -G_\Lambda^2 \dot{Q}_\Lambda G_\Lambda^2, \quad (6.124)$$

and the loop term L_Λ as

$$L_\Lambda(y_1, y_2, y_3, y_4) = S_\Lambda(y_1, y_3) G_\Lambda^2(y_2, y_4) + G_\Lambda^2(y_1, y_3) S_\Lambda(y_2, y_4). \quad (6.125)$$

The graphical representation of these equations in terms of Universal Feynman Graphs (see Sct. 4.5) is shown in Table 6.4.

Proof. We derive these equations from Theorem 6.5 by using the following relations between Nambu-type Green functions and usual Green functions: Eq. (A.16) for the inverse covariance, Eq. (5.169) for the (connected) two-point Green function, and

$$\Gamma_\Lambda^2(x_1, -; x_2, +) = \Gamma_\Lambda^2(x_1, x_2), \quad (6.126)$$

$$\Gamma_\Lambda^4(x_1, -; x_2, -; x_3, +; x_4, +) = -\Gamma_\Lambda^4(x_1, x_2, x_3, x_4), \quad (6.127)$$

$$\Gamma_\Lambda^6(x_1, -; x_2, -; x_3, -; x_4, +; x_5, +; x_6, +) = -\Gamma_\Lambda^6(x_1, x_2, x_3, x_4, x_5, x_6) \quad (6.128)$$

for the one-line-irreducible Green functions (relations which follow from Eqs. (A.45) and (A.46)). Furthermore, regarding the single-scale Green function, Eqs. (6.70) and (6.124) together imply that

$$\begin{aligned} & \mathbf{S}_\Lambda(x_1, +; x_2, -) \\ &= - \int dy_1 \int dy_2 \sum_{c_1, c_2} \mathbf{G}_\Lambda^2(x_1, +; y_1, c_1) \dot{\mathbf{Q}}_\Lambda(y_1, c_1; y_2, c_2) \mathbf{G}_\Lambda^2(y_2, c_2; x_2, -) \end{aligned} \quad (6.129)$$

$$= - \int dy_1 \int dy_2 \mathbf{G}_\Lambda^2(x_1, +; y_1, -) \dot{\mathbf{Q}}_\Lambda(y_1, -; y_2, +) \mathbf{G}_\Lambda^2(y_2, +; x_2, -) \quad (6.130)$$

$$= - \int dy_1 \int dy_2 G_\Lambda^2(x_1, y_1) Q_\Lambda(y_1, y_2) G_\Lambda^2(y_2, x_2) \quad (6.131)$$

$$= S_\Lambda(x_1, x_2). \quad (6.132)$$

Similarly, for the loop term we obtain from Eqs. (6.88) and (6.125) that

$$\mathbf{L}_\Lambda(x_1, +; x_2, +; x_3, -; x_4, -) \quad (6.133)$$

$$= \mathbf{S}_\Lambda(x_1, +; x_3, -) \mathbf{G}_\Lambda^2(x_2, +; x_4, -) + \mathbf{G}_\Lambda^2(x_1, +; x_3, -) \mathbf{S}_\Lambda(x_2, +; x_4, -) \quad (6.134)$$

$$= S_\Lambda(x_1, x_3) G_\Lambda^2(x_2, x_4) + G_\Lambda^2(x_1, x_3) S_\Lambda(x_2, x_4) \quad (6.135)$$

$$= L_\Lambda(x_1, x_2, x_3, x_4). \quad (6.136)$$

For all other combinations of Nambu indices, the corresponding relations can be derived analogously by using the antisymmetry of \mathbf{S}_Λ and of \mathbf{G}_Λ^2 (see Appendix A of Part II). We now go on to evaluate Eqs. (6.86) and (6.87) for particular combinations of the external Nambu indices.

(i) *Two-point function.* First, Eq. (6.86) yields

$$\begin{aligned} & \dot{\mathbf{I}}_\Lambda^2(x_1, -; x_2, +) = \dot{\mathbf{Q}}_\Lambda(x_1, -; x_2, +) \\ & - \frac{1}{2} \int dy_1 \int dy_2 \sum_{c_1, c_2} \mathbf{S}_\Lambda(y_1, c_1; y_2, c_2) \mathbf{I}_\Lambda^4(y_1, c_1; y_2, c_2; x_1, -; x_2, +). \end{aligned} \quad (6.137)$$

In the second term, both $(c_1, c_2) = (-, +)$ and $(c_1, c_2) = (+, -)$ give the same contribution, and thus we obtain

$$\dot{\mathbf{I}}_\Lambda^2(x_1, x_2) = \dot{\mathbf{Q}}_\Lambda(x_1, x_2) + \int dy_1 \int dy_2 S_\Lambda(y_2, y_1) \Gamma_\Lambda^4(y_1, x_1, y_2, x_2), \quad (6.138)$$

which is equivalent to the assertion (6.119).

(ii) *Four-point function.* Next, we evaluate Eq. (6.87) for

$$X_1 = (x_1, -), \quad X_2 = (x_2, -), \quad X_3 = (x_3, +), \quad X_4 = (x_4, +), \quad (6.139)$$

such that the left-hand side reverts to $(-1)\dot{\Gamma}_\Lambda^4(x_1, x_2, x_3, x_4)$. The first term on the right-hand side can be evaluated analogously as in the case of the two-point function, and hence we obtain

$$\begin{aligned} \dot{\Gamma}_\Lambda^4(x_1, x_2, x_3, x_4) &= \int dy_1 \int dy_2 S_\Lambda(y_2, y_1) \Gamma_\Lambda^4(y_1, x_1, x_2, y_2, x_3, x_4) \\ &\quad + \frac{1}{2} \int dy_1 \dots \int dy_4 \sum_{c_1, \dots, c_4} \mathbf{L}_\Lambda(y_1, c_1; \dots; y_4, c_4) \\ &\quad \times \mathbf{B}_\Lambda(y_1, c_1; \dots; y_4, c_4; x_1, -; x_2, -; x_3, +; x_4, +). \end{aligned} \quad (6.140)$$

The vertex bilinear \mathbf{B}_Λ as defined by Eq. (6.89) consists of three terms, whose respective contributions to the right-hand side of the above RGE are called the *particle-particle term*, the *crossed particle-hole term* and the *direct particle-hole term*. It remains to show that these terms coincide with Eqs. (6.121), (6.122) and (6.123), respectively.

(ii.a) *Particle-particle term.* Putting the first term of Eq. (6.89) into Eq. (6.140) yields the particle-particle term:

$$\begin{aligned} \Phi_\Lambda^{\text{pp}}(x_1, x_2, x_3, x_4) &= \frac{1}{2} \int dy_1 \dots \int dy_4 \sum_{c_1, \dots, c_4} \mathbf{L}_\Lambda(y_1, c_1; y_2, c_2; y_3, c_3; y_4, c_4) \\ &\quad \times \mathbf{\Gamma}_\Lambda^4(y_2, c_2; y_3, c_3; x_1, -; x_2, -) \mathbf{\Gamma}_\Lambda^4(y_1, c_1; y_4, c_4; x_3, +; x_4, +). \end{aligned} \quad (6.141)$$

The product of the two $\mathbf{\Gamma}_\Lambda^4$ functions vanishes unless $(c_1, c_2, c_3, c_4) = (-, +, +, -)$, from which we obtain

$$\begin{aligned} \Phi_\Lambda^{\text{pp}}(x_1, x_2, x_3, x_4) &= -\frac{1}{2} \int dy_1 \dots \int dy_4 L_\Lambda(y_3, y_2, y_1, y_4) \\ &\quad \times \Gamma_\Lambda^4(x_1, x_2, y_2, y_3) \Gamma_\Lambda^4(y_1, y_4, x_3, x_4). \end{aligned} \quad (6.142)$$

By renaming the integration variables and using the antisymmetry of Γ_Λ in its last two arguments, this implies Eq. (6.121).

(ii.b) *Crossed particle-hole term.* This term is obtained by putting the second line of Eq. (6.89) into Eq. (6.140), i.e.,

$$\begin{aligned} \Phi_\Lambda^{\text{ph,c}}(x_1, x_2, x_3, x_4) &= -\frac{1}{2} \int dy_1 \dots \int dy_4 \sum_{c_1, \dots, c_4} \mathbf{L}_\Lambda(y_1, c_1; y_2, c_2; y_3, c_3; y_4, c_4) \\ &\quad \times \mathbf{\Gamma}_\Lambda^4(y_2, c_2; y_3, c_3; x_1, -; x_3, +) \mathbf{\Gamma}_\Lambda^4(y_1, c_1; y_4, c_4; x_2, -; x_4, +). \end{aligned} \quad (6.143)$$

The loop term \mathbf{L}_Λ vanishes unless $c_1 \neq c_3$ and $c_2 \neq c_4$, while the product of the two functions $\mathbf{\Gamma}_\Lambda^4$ vanishes unless $c_2 \neq c_3$ and $c_1 \neq c_4$. This implies that $c_1 = c_2$ as well

as $c_3 = c_4$, and hence only two terms contribute to the sum:

$$\begin{aligned}
\Phi_{\Lambda}^{\text{ph,c}}(x_1, x_2, x_3, x_4) = & \quad (6.144) \\
& -\frac{1}{2} \int dy_1 \dots \int dy_4 \mathbf{L}_{\Lambda}(y_1, -; y_2, -; y_3, +; y_4, +) \\
& \quad \times \mathbf{\Gamma}_{\Lambda}^4(y_2, -; y_3, +; x_1, -; x_3, +) \mathbf{\Gamma}_{\Lambda}^4(y_1, -; y_4, +; x_2, -; x_4, +) \\
& -\frac{1}{2} \int dy_1 \dots \int dy_4 \mathbf{L}_{\Lambda}(y_1, +; y_2, +; y_3, -; y_4, -) \\
& \quad \times \mathbf{\Gamma}_{\Lambda}^4(y_2, +; y_3, -; x_1, -; x_3, +) \mathbf{\Gamma}_{\Lambda}^4(y_1, +; y_4, -; x_2, -; x_4, +).
\end{aligned}$$

One can convince oneself that both terms are in fact equal, and thus we obtain

$$\begin{aligned}
\Phi_{\Lambda}^{\text{ph,c}}(x_1, x_2, x_3, x_4) = & - \int dy_1 \dots \int dy_4 L_{\Lambda}(y_3, y_4, y_1, y_2) \\
& \times \Gamma_{\Lambda}^4(y_2, x_1, y_3, x_3) \Gamma_{\Lambda}^4(y_1, x_2, y_4, x_4), \quad (6.145)
\end{aligned}$$

which is equivalent to Eq. (6.122).

(ii.c) *Direct particle-hole term.* Finally, putting the third line of Eq. (6.89) into Eq. (6.140) yields

$$\begin{aligned}
\Phi_{\Lambda}^{\text{ph,d}}(x_1, x_2, x_3, x_4) = & \frac{1}{2} \int dy_1 \dots \int dy_4 \sum_{c_1, \dots, c_4} \mathbf{L}_{\Lambda}(y_1, c_1; y_2, c_2; y_3, c_3; y_4, c_4) \\
& \times \mathbf{\Gamma}_{\Lambda}(y_2, c_2; y_3, c_3; x_1, -; x_4, +) \mathbf{\Gamma}_{\Lambda}(y_1, c_1; y_4, c_4; x_2, -; x_3, +). \quad (6.146)
\end{aligned}$$

By comparing this expression with Eq. (6.143), we see that

$$\Phi_{\Lambda}^{\text{ph,d}}(x_1, x_2, x_3, x_4) = -\Phi_{\Lambda}^{\text{ph,c}}(x_1, x_2, x_4, x_3), \quad (6.147)$$

which completes the proof. \square

$$\text{---} \boxed{\overset{\bullet}{\Gamma^2}} \text{---} = \text{---} \boxed{\overset{\bullet}{Q}} \text{---} + \text{---} \boxed{\Gamma^4} \text{---} \boxed{S} \text{---}$$

$$\text{---} \boxed{\overset{\bullet}{\Gamma^4}} \text{---} = \frac{1}{2} \text{---} \boxed{\Gamma^4} \text{---} \boxed{L} \text{---} \boxed{\Gamma^4} \text{---}$$

$$- \text{---} \boxed{\Gamma^4} \text{---} \boxed{L} \text{---} \boxed{\Gamma^4} \text{---}$$

$$+ \text{---} \boxed{\Gamma^4} \text{---} \boxed{L} \text{---} \boxed{\Gamma^4} \text{---}$$

$$\text{---} \boxed{L} \text{---} = \text{---} \boxed{S} \text{---} + \text{---} \boxed{G^2} \text{---}$$

$$\text{---} \boxed{S} \text{---} = - \text{---} \boxed{G^2} \text{---} \boxed{\overset{\bullet}{Q}} \text{---} \boxed{G^2} \text{---}$$

Table 6.4: RGE for the one-line-irreducible Green functions (Theorem 6.6). Here, we have omitted the term with the six-point function on the right-hand side of Eq. (6.120), which corresponds to the level-two truncation of Sct. 6.4. The three terms on the right-hand side of the second equation are the particle-particle term, the crossed particle-hole term and the direct particle-hole term (in this order).

6.4. Level-two truncation and initial-value problem

In the previous two sections, we have derived the RGE for the connected and for the one-line-irreducible Green functions, respectively. In this section, we will first comment on the consistency of these two schemes and, after that, introduce the *level-two truncation* as a standard approximation to these equations, which allows us to reduce the infinite hierarchy of RGE to a closed system of finitely many coupled differential equations. To this, we will add appropriate initial conditions, and thereby formulate an *initial-value problem* for the scale-dependent interacting Green functions.

First, we remark that it is even *a priori* clear that the two RGE hierarchies for the connected and for the one-line-irreducible Green functions (Theorems 6.3 and 6.6) are consistent with each other, as both have been derived analytically starting from the respective Definitions 5.4 and 5.10 of the generators \mathcal{W}_Λ and Γ_Λ . On the other hand, one can also convince oneself directly that each of these two hierarchies can be derived from the respective other one by using the relations between the connected and the one-line-irreducible Green functions (Theorem 5.15). For the sake of understanding, we now demonstrate this by deriving the RGE for Γ_Λ^2 (given by Eq. (6.119)) directly from the RGE for $G_{c,\Lambda}^2$ (given by Eq. (6.54)). For this purpose, we introduce the following notations (see also Eqs. (6.22)–(6.23)): Let A and B be two-point quantities, and let C and D be four-point quantities. Then, we define the two-point quantity AB as

$$(AB)(x_1, x_2) = \int dy A(x_1, y) B(y, x_2), \quad (6.148)$$

the four-point quantity $A \otimes B$ as

$$(A \otimes B)(x_1, x_2, x_3, x_4) = A(x_1, x_3) B(x_2, x_4), \quad (6.149)$$

the two-point quantity $\text{Tr}[CA]$ as

$$\text{Tr}[CA](x_1, x_2) = \int dy_1 \int dy_2 C(x_1, y_1, x_2, y_2) A(y_2, y_1), \quad (6.150)$$

and the four-point quantity CD as

$$(CD)(x_1, x_2, x_3, x_4) = \int dy_1 \int dy_2 C(x_1, x_2, y_1, y_2) D(y_1, y_2, x_3, x_4). \quad (6.151)$$

Each of these operations has a straightforward graphical representation in terms of Universal Feynman graphs (see Sect. 4.5). With these notations, we can write the relations (5.165)–(5.166) between the connected and the one-line-irreducible Green functions as

$$1 = G_c^2 \Gamma^2 = G^2 \Gamma^2, \quad (6.152)$$

and respectively,

$$G_c^4 = (G^2 \otimes G^2) \Gamma^4 (G^2 \otimes G^2), \quad (6.153)$$

where we have used Eq. (5.61). Since Eq. (6.152) holds at any scale Λ , we can also take

the Λ derivative to obtain

$$0 = \dot{G}_\Lambda^2 \Gamma_\Lambda^2 + G_\Lambda^2 \dot{\Gamma}_\Lambda^2, \quad (6.154)$$

from which we further deduce

$$\dot{\Gamma}_\Lambda^2 = -\Gamma_\Lambda^2 \dot{G}_\Lambda^2 \Gamma_\Lambda^2. \quad (6.155)$$

Now, the RGE (6.54) for the (connected) two-point function can be written compactly as (suppressing the Λ dependencies in the notation)

$$\dot{G}^2 = -G^2 \dot{Q} G^2 + \text{Tr}[G_c^4 \dot{Q}]. \quad (6.156)$$

Multiplying this equation from left and from right with Γ^2 and using Eq. (6.155) yields

$$-\dot{\Gamma}^2 = -\dot{Q} + \Gamma^2 \text{Tr}[G_c^4 \dot{Q}] \Gamma^2. \quad (6.157)$$

The last term can be transformed as follows (see Table 6.5):

$$\Gamma^2 \text{Tr}[G_c^4 \dot{Q}] \Gamma^2 = \Gamma^2 \text{Tr}[(G^2 \otimes G^2) \Gamma^4 (G^2 \otimes G^2) \dot{Q}] \Gamma^2 \quad (6.158)$$

$$= \Gamma^2 G^2 \text{Tr}[\Gamma^4 (G^2 \dot{Q} G^2)] G^2 \Gamma^2 \quad (6.159)$$

$$= -\text{Tr}[\Gamma^4 S], \quad (6.160)$$

where in the last line, we have substituted the single-scale Green function as given by Eq. (6.124). By putting Eq. (6.160) into Eq. (6.157), we arrive at

$$\dot{\Gamma}^2 = \dot{Q} + \text{Tr}[\Gamma^4 S], \quad (6.161)$$

which is precisely the RGE (6.119) for the one-line-irreducible two-point function Γ^2 . Similarly, it would be possible to derive all RGE for the one-line-irreducible Green functions Γ^{2n} from the corresponding RGE for the connected Green functions G_c^{2n} , and vice versa (although for larger n , such a derivation would be very cumbersome).

Thus, we have shown that the two infinite hierarchies for G_c^{2n} and for Γ^{2n} are completely equivalent. In practice, however, one usually does not deal with such infinite hierarchies of differential equations, but with certain approximations applied to them. Typically, one *truncates* these hierarchies at some particular n_0 , which means that one neglects all $2n$ -point functions with $n > n_0$. In this way, one can obtain a finite, closed set of differential equations, which one may then seek to solve numerically. However, we remark that on the level of such approximations, the truncated hierarchies of the connected and of the one-line-irreducible Green functions are not equivalent anymore.

We now introduce a standard truncation for the one-line-irreducible Green functions, which is called the *level-two truncation*. In this approximation, one neglects all $2n$ -point functions with $n \geq 3$, i.e., one sets

$$\Gamma_\Lambda^{2n}(x_1, \dots, x_{2n}) \equiv 0 \quad \text{for } n \geq 3. \quad (6.162)$$

Thereby, one obtains two coupled differential equations for the one-line-irreducible two- and four-point functions, which are represented graphically in Table 6.4. However, the disadvantage of the RGE for the one-line-irreducible two-point function Γ_Λ^2 is that it holds only formally, because for $\Lambda > 0$ the covariance C_Λ is in general not invertible. Hence, in particular, it is not possible to define an initial value for Γ_Λ^2 (see the discussion in Sect. 6.1). In order to cure this problem, we now replace the RGE for Γ_Λ^2 with the equivalent equation for the (connected) two-point Green function G_Λ^2 . Thereby, we obtain a closed system of coupled differential equations for G_Λ^2 and Γ_Λ^4 , which lends itself to a well-defined initial-value problem.

Theorem 6.7 (Initial-value problem in the level-two truncation). *Consider the coupled differential equations for the (connected) two-point Green function G_Λ^2 and the one-line-irreducible four-point function Γ_Λ^4 given by*

$$\begin{aligned} \dot{G}_\Lambda^2(x_1, x_2) = & \quad (6.163) \\ S_\Lambda(x_1, x_2) - \int dy_1 \dots \int dy_4 G_\Lambda^2(x_1, y_1) \Gamma_\Lambda^4(y_1, y_3, y_2, y_4) S_\Lambda(y_4, y_3) G_\Lambda^2(y_2, x_2), \end{aligned}$$

and respectively

$$\begin{aligned} \dot{\Gamma}_\Lambda^4(x_1, \dots, x_4) = & \quad (6.164) \\ \frac{1}{2} \int dy_1 \dots \int dy_4 L_\Lambda(y_1, y_2, y_3, y_4) \Gamma_\Lambda^4(x_1, x_2, y_1, y_2) \Gamma_\Lambda^4(y_3, y_4, x_3, x_4), \\ - 2 \mathbb{A}_{(x_3, x_4)} \int dy_1 \dots \int dy_4 L_\Lambda(y_3, y_4, y_2, y_1) \Gamma_\Lambda^4(y_1, x_1, y_3, x_3) \Gamma_\Lambda^4(x_2, y_2, x_4, y_4). \end{aligned}$$

Here, the loop term is defined as

$$L_\Lambda = S_\Lambda \otimes G_\Lambda^2 + G_\Lambda^2 \otimes S_\Lambda, \quad (6.165)$$

the single-scale Green function as

$$S_\Lambda = -G_\Lambda^2 \dot{Q}_\Lambda G_\Lambda^2, \quad (6.166)$$

and $Q_\Lambda = C_\Lambda^{-1}$ denotes the inverse covariance. Together, these equations constitute a closed system of coupled differential equations for G_Λ^2 and Γ_Λ^4 . Furthermore, the respective initial conditions of these functions read as

$$\lim_{\Lambda \rightarrow \infty} G_\Lambda^2(x_1, x_2) = 0, \quad (6.167)$$

$$\lim_{\Lambda \rightarrow \infty} \Gamma_\Lambda^4(x_1, x_2, x_3, x_4) = -2\beta V(x_1, x_2, x_3, x_4), \quad (6.168)$$

where β denotes the inverse temperature and V the four-point interaction kernel as defined by Eq. (4.107). Now, let G_Λ^2 and Γ_Λ^4 be the uniquely determined functions which

solve this initial-value problem. If the limiting functions

$$\lim_{\Lambda \rightarrow 0} G_{\Lambda}^2(x_1, x_2), \quad (6.169)$$

$$\lim_{\Lambda \rightarrow 0} \Gamma_{\Lambda}^4(x_1, \dots, x_4) \quad (6.170)$$

exist, then they can be regarded as approximations to the two-point Green function G^2 and to the one-line-irreducible four-point function Γ^4 of the interacting electron system.

Proof. First, Eq. (6.163) can be shown from the RGE (6.54) for G_{Λ}^2 by identifying the first term on the right-hand side with the single-scale Green function, and by replacing in the second term $G_{c,\Lambda}^4$ by Γ_{Λ}^4 as in Eqs. (6.158)–(6.160). Next, Eq. (6.164) follows from the RGE (6.120) for Γ_{Λ}^4 by neglecting the term with the six-point function. Finally, the initial conditions (6.167)–(6.168) have already been shown before in Eqs. (6.7) and (6.15), respectively. \square

In the following, we will consider an even stricter approximation to the RGE hierarchy, which is obtained by *neglecting the self-energy*. Recall that the (irreducible) self-energy Σ_{Λ}^2 at the scale Λ satisfies the equation (which follows from Eqs. (5.165) and (5.195))

$$(G_{\Lambda}^2)^{-1} = (C_{\Lambda})^{-1} - \Sigma_{\Lambda}^2. \quad (6.171)$$

Hence, neglecting the self-energy is equivalent to identifying the (connected) two-point Green function with the covariance,

$$G_{\Lambda}^2 \equiv C_{\Lambda}. \quad (6.172)$$

The above initial-value problem then further simplifies as follows.

Theorem 6.8 (Initial-value problem in the level-two truncation without self-energy). *Consider the differential equation for the one-line-irreducible four-point function given by*

$$\dot{\Gamma}_{\Lambda}^4(x_1, \dots, x_4) = \quad (6.173)$$

$$\begin{aligned} & \frac{1}{2} \int dy_1 \dots \int dy_4 L_{\Lambda}(y_1, y_2, y_3, y_4) \Gamma_{\Lambda}^4(x_1, x_2, y_1, y_2) \Gamma_{\Lambda}^4(y_3, y_4, x_3, x_4), \\ & - 2 \mathbb{A}_{(x_3, x_4)} \int dy_1 \dots \int dy_4 L_{\Lambda}(y_3, y_4, y_2, y_1) \Gamma_{\Lambda}^4(y_1, x_1, y_3, x_3) \Gamma_{\Lambda}^4(x_2, y_2, x_4, y_4), \end{aligned}$$

where the loop term is given by

$$L_{\Lambda} = S_{\Lambda} \otimes C_{\Lambda} + C_{\Lambda} \otimes S_{\Lambda}, \quad (6.174)$$

and the single-scale Green function equals

$$S_{\Lambda} = -C_{\Lambda} \dot{Q}_{\Lambda} C_{\Lambda} = \dot{C}_{\Lambda}. \quad (6.175)$$

Furthermore, let Γ_Λ^4 be the unique solution of this differential equation which satisfies the initial condition

$$\lim_{\Lambda \rightarrow \infty} \Gamma_\Lambda^4(x_1, x_2, x_3, x_4) = -2\beta V(x_1, x_2, x_3, x_4) \quad (6.176)$$

in terms of the four-point interaction kernel. If the limit

$$\lim_{\Lambda \rightarrow 0} \Gamma_\Lambda^4(x_1, \dots, x_4) \quad (6.177)$$

exists, then it can be regarded as an approximation to the one-line-irreducible four-point Green function of the interacting electron system.

Proof. All these equations follow directly from Theorem 6.7 by setting the self-energy to zero and replacing the two-point function by the covariance as in Eq. (6.172). \square

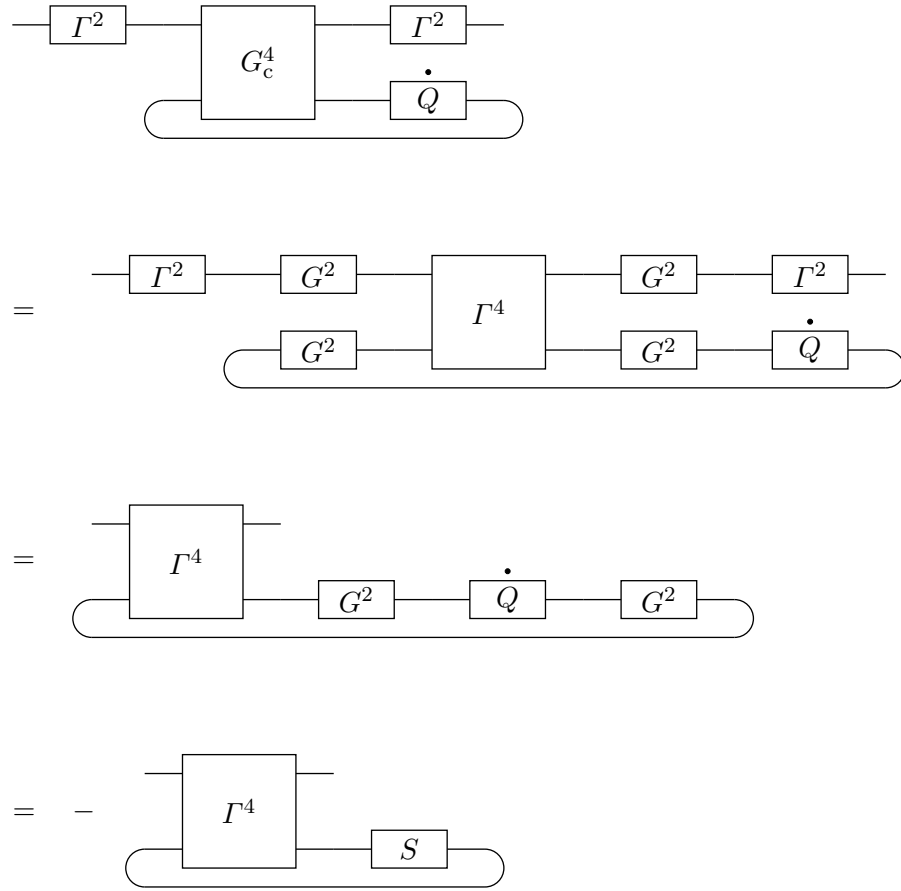


Table 6.5: Calculating with Universal Feynman Graphs: Eqs. (6.158)–(6.160).

7. Functional renormalization for multiband systems

7.1. Flow equations on the lattice

We now come back to the lattice Green functions as defined in Sect. 4.3. Our aim in this chapter is to derive the RGE for these lattice Green functions, and to bring these RGE—by a number of suitable approximations—into a form which allows us to solve them numerically. Later, in Ch. 9, we will apply these approximate RGE for the lattice Green functions to the Rashba tight-binding model as defined in Sect. 2.3.

First, the *lattice covariance in the Bloch basis* (or *band basis*) is defined as

$$C_{nn'}(\mathbf{k}, \mathbf{k}'; \tau - \tau') = \frac{1}{Z_0} \text{Tr} \left(e^{-\beta \hat{K}_0} \mathcal{T} [\hat{a}_n(\mathbf{k}, \tau) \hat{a}_{n'}^\dagger(\mathbf{k}', \tau')] \right), \quad (7.1)$$

where $\hat{K}_0 = \hat{H}_0 - \mu \hat{N}$ is given in terms of the non-interacting Hamiltonian (4.2) and the particle-number operator (4.13), and where Z_0 denotes the partition function of the non-interacting system (see Eq. (4.75)). Furthermore, we have abbreviated the annihilation and creation operators of Bloch vectors as

$$\hat{a}_n(\mathbf{k}, \tau) = \hat{a}(|\Psi_{n\mathbf{k}}\rangle, \tau), \quad (7.2)$$

$$\hat{a}_n^\dagger(\mathbf{k}, \tau) = \hat{a}^\dagger(|\Psi_{n\mathbf{k}}\rangle, \tau), \quad (7.3)$$

where the time evolution of these operators is defined in the interaction picture by Eq. (4.74). Next, we derive an explicit expression for this lattice covariance: The free Hamiltonian subtracted by the particle-number operator can be expressed in the Bloch basis of Sect. 1.3 as

$$\hat{K}_0 = \frac{1}{|\mathcal{B}|} \int_{\mathcal{B}} d^3\mathbf{k} \sum_n e_n(\mathbf{k}) \hat{a}_n^\dagger(\mathbf{k}) \hat{a}_n(\mathbf{k}), \quad (7.4)$$

where we have defined

$$e_n(\mathbf{k}) := E_n(\mathbf{k}) - \mu \quad (7.5)$$

as the Bloch eigenenergies measured relatively to the chemical potential. By using Eq. (7.4), one can show that the time evolution of the Bloch annihilators and creators is

given explicitly by

$$\hat{a}_n(\mathbf{k}, \tau) = \hat{a}_n(\mathbf{k}) e^{-\tau e_n(\mathbf{k})/\hbar}, \quad (7.6)$$

$$\hat{a}_n^\dagger(\mathbf{k}, \tau) = \hat{a}_n^\dagger(\mathbf{k}) e^{\tau e_n(\mathbf{k})/\hbar}. \quad (7.7)$$

Furthermore, by putting this into Eq. (7.1), we find after a short calculation

$$C_{nn'}(\mathbf{k}, \mathbf{k}'; \tau - \tau') = \delta_{nn'} |\mathcal{B}| \delta^3(\mathbf{k} - \mathbf{k}') C_n(\mathbf{k}, \tau - \tau'), \quad (7.8)$$

where the reduced covariance (which depends on only one Bloch momentum) is given explicitly by (see Ref. [Mah90, Eq. (3.2.9)])

$$C_n(\mathbf{k}, \tau - \tau') = e^{-(\tau - \tau') e_n(\mathbf{k})/\hbar} (\Theta(\tau - \tau') - f_n(\mathbf{k})), \quad (7.9)$$

with the Heaviside step function Θ and the Fermi distribution function

$$f_n(\mathbf{k}) \equiv f(e_n(\mathbf{k})) = \left(e^{\beta e_n(\mathbf{k})} + 1 \right)^{-1}. \quad (7.10)$$

By Fourier transforming Eq. (7.9) with respect to the time variables (in accordance with Eq. (4.69)), we then arrive at (see Ref. [Mah90, Eq. (3.2.11)])

$$C_n(\mathbf{k}, \omega) = \frac{1}{\hbar\beta} \int_0^{\hbar\beta} d\tau C_n(\mathbf{k}, \tau) e^{i\omega\tau} = -\frac{1}{\beta} \frac{1}{i\hbar\omega - e_n(\mathbf{k})}, \quad (7.11)$$

where ω labels the fermionic Matsubara frequencies. We remark that this result can be derived even more straightforwardly from the equation of motion (4.115) of the covariance (see Ref. [Sch+16a, Eqs. (41)–(47)]).

In order to set up the renormalization group flow, we now introduce a scale-dependent covariance (see Sect. 6.1) by means of a *regulator function* χ_Λ (defined for $\Lambda > 0$), which appears in the denominator of the above expression:

$$(C_\Lambda)_n(\mathbf{k}, \omega) := -\frac{1}{\beta} \frac{\chi_\Lambda(e_n(\mathbf{k}))}{i\hbar\omega - e_n(\mathbf{k})}. \quad (7.12)$$

This particular regulator function depends only on the Bloch momentum \mathbf{k} , not on the Matsubara frequency ω . As explained in Ref. [Sch+16a], the regulator function can be chosen as a *strict cut-off function*, which is a smooth function with the properties that

$$\chi_\Lambda(e) = \begin{cases} 0, & \text{if } |e| < 0.5\Lambda, \\ 1, & \text{if } |e| > 1.5\Lambda. \end{cases} \quad (7.13)$$

For this choice, the numerator of Eq. (7.12) vanishes if

$$|e_n(\mathbf{k})| \equiv |E_n(\mathbf{k}) - \mu| < 0.5\Lambda, \quad (7.14)$$

which means that all momenta inside a shell of thickness Λ around the Fermi lines are

cut off. (For the concrete implementation of the RG equations, we will use instead a non-strict regulator function; see Eq. (9.7) below). In the case of a strict cut-off function, the scale-dependent covariance (7.12) approaches the original covariance (7.11) in the *infrared limit* $\Lambda \rightarrow 0$. Moreover, by defining the *ultraviolet scale* Λ_0 much larger than the bandwidth of the model, such that

$$|E_n(\mathbf{k}) - \mu| < 0.5\Lambda_0 \quad \text{for all } n \text{ and } \mathbf{k}, \quad (7.15)$$

the covariance vanishes identically at this scale, i.e., $C_{\Lambda_0} = 0$. Thus, the scale-dependent covariance has precisely the properties (6.1) and (6.2) as required in Sect. 6.1. Furthermore, as explained in Sect. 6.1, the scale-dependence of the covariance induces a scale dependence of all interacting Green functions, which then satisfy the hierarchy of RGE derived in the previous chapter.

As a matter of principle, the lattice Green functions satisfy RGE which are formally identical to the RGE of the fundamental Green functions. However, the RGE of the lattice Green functions can be further simplified by employing the invariance of the lattice Green functions under lattice translations (see Proposition 4.5). Concretely, this implies that the lattice covariance depends on only one Bloch momentum, and similarly, every $2n$ -point lattice Green function depends on only $(2n - 1)$ Bloch momenta (see Eq. (4.68)). In particular, the lattice version of the one-line-irreducible four-point Green function in the Bloch basis is of the form

$$(\Gamma_{\Lambda}^4)_{n_1 n_2 n_3 n_4}(k_1, k_2, k_3, k_4) = (\Gamma_{\Lambda}^4)_{n_1 n_2 n_3 n_4}(k_1, k_2, k_3) \delta(k_1 + k_2, k_3 + k_4), \quad (7.16)$$

where we have introduced the multi-variable

$$k = (\mathbf{k}, \omega), \quad (7.17)$$

which consists of a Bloch momentum \mathbf{k} and a fermionic Matsubara frequency ω . Correspondingly, we define the integration over such multi-variables as

$$\int dk = \frac{1}{|\mathcal{B}|} \int_{\mathcal{B}} d^3 \mathbf{k} \sum_{\omega \in \mathbb{M}}, \quad (7.18)$$

and we define the multi-variable delta distribution as

$$\delta(k, k') = |\mathcal{B}| \delta^3(\mathbf{k} - \mathbf{k}') \delta_{\omega, \omega'}. \quad (7.19)$$

Furthermore, we introduce the lattice version of the four-point interaction kernel (in the Bloch basis) as

$$\begin{aligned} V_{n_1 \dots n_4}(\mathbf{k}_1, \omega_1; \dots; \mathbf{k}_4, \omega_4) = \\ \int d^3 \mathbf{x}_1 \dots \int d^3 \mathbf{x}_4 \sum_{s_1, \dots, s_4} V_{s_1 \dots s_4}(\mathbf{x}_1, \omega_1; \dots; \mathbf{x}_4, \omega_4) \\ \times \Psi_{n_1 \mathbf{k}_1}^*(\mathbf{x}_1, s_1) \Psi_{n_2 \mathbf{k}_2}^*(\mathbf{x}_2, s_2) \Psi_{n_3 \mathbf{k}_3}(\mathbf{x}_3, s_3) \Psi_{n_4 \mathbf{k}_4}(\mathbf{x}_4, s_4), \end{aligned} \quad (7.20)$$

which is analogous to Eq. (4.62). This lattice interaction kernel also has the property (7.16) and, moreover, it provides the initial condition for the lattice version of the one-line-irreducible four-point function (cf. Eq. (6.15)), i.e.,

$$\lim_{\Lambda \rightarrow \infty} (\Gamma_{\Lambda}^4)_{n_1 \dots n_4}(k_1, \dots, k_4) = -2\beta V_{n_1 \dots n_4}(k_1, \dots, k_4). \quad (7.21)$$

In the following, it will be convenient to rescale the four-point function in such a way that its initial condition is precisely given by the four-point interaction kernel. Hence, we define the *interaction vertex* (or *effective interaction*) at the scale Λ as

$$V_{\Lambda} := -\frac{1}{2\beta} \Gamma_{\Lambda}^4, \quad (7.22)$$

such that its initial condition is given by

$$\lim_{\Lambda \rightarrow \infty} (V_{\Lambda})_{n_1 \dots n_4}(k_1, \dots, k_4) = V_{n_1 \dots n_4}(k_1, \dots, k_4). \quad (7.23)$$

Correspondingly, we reformulate the RGE (6.173) in terms of this interaction vertex as

$$\begin{aligned} \dot{V}_{\Lambda}(x_1, \dots, x_4) = & \quad (7.24) \\ & -\beta \int dy_1 \dots \int dy_4 L_{\Lambda}(y_1, y_2, y_3, y_4) V_{\Lambda}(x_1, x_2, y_1, y_2) V_{\Lambda}(y_3, y_4, x_3, x_4), \\ & + 4\beta \mathbb{A}_{(x_3, x_4)} \int dy_1 \dots \int dy_4 L_{\Lambda}(y_3, y_4, y_2, y_1) V_{\Lambda}(y_1, x_1, y_3, x_3) V_{\Lambda}(x_2, y_2, x_4, y_4), \end{aligned}$$

Next, we will use the lattice translation invariance to simplify this equation.

Theorem 7.1 (RGE for lattice interaction vertex). *In the level-two truncation and by neglecting the self-energy, the lattice interaction vertex in the Bloch basis satisfies the following differential equation:*

$$(\dot{V}_{\Lambda})_{n_1 n_2 n_3 n_4}(p_1, p_2, p_3) = [\Phi_{\Lambda}^{\text{pp}} + \Phi_{\Lambda}^{\text{ph,c}} + \Phi_{\Lambda}^{\text{ph,d}}]_{n_1 n_2 n_3 n_4}(p_1, p_2, p_3), \quad (7.25)$$

where the three terms on the right-hand side are given by

$$\begin{aligned} (\Phi_{\Lambda}^{\text{pp}})_{n_1 n_2 n_3 n_4}(p_1, p_2, p_3) = & -\beta \sum_{\ell_1, \ell_2} \int dk_1 \int dk_2 \delta(p_1 + p_2 - k_1, k_2) (L_{\Lambda})_{\ell_1 \ell_2}(k_1, k_2) \\ & \times (V_{\Lambda})_{n_1 n_2 \ell_1 \ell_2}(p_1, p_2, k_1) (V_{\Lambda})_{\ell_1 \ell_2 n_3 n_4}(k_1, k_2, p_3), \quad (7.26) \end{aligned}$$

$$\begin{aligned} (\Phi_{\Lambda}^{\text{ph,c}})_{n_1 n_2 n_3 n_4}(p_1, p_2, p_3) = & -2\beta \sum_{\ell_1, \ell_2} \int dk_1 \int dk_2 \delta(p_1 - p_3 + k_1, k_2) (L_{\Lambda})_{\ell_2 \ell_1}(k_2, k_1) \\ & \times (V_{\Lambda})_{\ell_1 n_1 \ell_2 n_3}(k_1, p_1, k_2) (V_{\Lambda})_{n_2 \ell_2 \ell_1 n_4}(p_2, k_2, k_1), \quad (7.27) \end{aligned}$$

$$(\Phi_{\Lambda}^{\text{ph,d}})_{n_1 n_2 n_3 n_4}(p_1, p_2, p_3) = -(\Phi_{\Lambda}^{\text{ph,c}})_{n_2 n_1 n_3 n_4}(p_2, p_1, p_3), \quad (7.28)$$

with the single-scale Green function

$$(S_\Lambda)_\ell(k) = (\dot{C}_\Lambda)_\ell(k), \quad (7.29)$$

and the loop term

$$(L_\Lambda)_{\ell_1\ell_2}(k_1, k_2) = (S_\Lambda)_{\ell_1}(k_1) (C_\Lambda)_{\ell_2}(k_2) + (C_\Lambda)_{\ell_1}(k_1) (S_\Lambda)_{\ell_2}(k_2) \quad (7.30)$$

$$= \frac{d}{d\Lambda} ((C_\Lambda)_{\ell_1}(k_1) (C_\Lambda)_{\ell_2}(k_2)). \quad (7.31)$$

In particular, since $k_2 = (\mathbf{k}_2, \omega_2)$ is fixed in each term in Eqs. (7.26)–(7.27) by momentum conservation, the right-hand side of the RGE effectively requires only a summation over two band indices ℓ_1, ℓ_2 and an integration over one multi-variable $k_1 = (\mathbf{k}_1, \omega_1)$.

Proof. By performing a “basis transformation” using Eqs. (4.62)–(4.63), we obtain from Eq. (7.24) the RGE for the lattice interaction kernel:

$$(\dot{V}_\Lambda)_{n_1n_2n_3n_4}(p_1, p_2, p_3, p_4) = [\Phi_\Lambda^{\text{pp}} + \Phi_\Lambda^{\text{ph,c}} + \Phi_\Lambda^{\text{ph,d}}]_{n_1n_2n_3n_4}(p_1, p_2, p_3, p_4), \quad (7.32)$$

where the particle-particle term, the crossed particle-hole term and the direct particle-hole term are given respectively by

$$\begin{aligned} (\Phi_\Lambda^{\text{pp}})_{n_1n_2n_3n_4}(p_1, p_2, p_3, p_4) &= -\beta \sum_{\ell_1, \dots, \ell_4} \int dk_1 \dots \int dk_4 (L_\Lambda)_{\ell_1\ell_2\ell_3\ell_4}(k_1, k_2, k_3, k_4) \\ &\quad \times (V_\Lambda)_{n_1n_2\ell_1\ell_2}(p_1, p_2, k_1, k_2) (V_\Lambda)_{\ell_3\ell_4n_3n_4}(k_3, k_4, p_3, p_4), \end{aligned} \quad (7.33)$$

$$\begin{aligned} (\Phi_\Lambda^{\text{ph,c}})_{n_1n_2n_3n_4}(p_1, p_2, p_3, p_4) &= 2\beta \sum_{\ell_1, \dots, \ell_4} \int dk_1 \dots \int dk_4 (L_\Lambda)_{\ell_3\ell_4\ell_2\ell_1}(k_3, k_4, k_2, k_1) \\ &\quad \times (V_\Lambda)_{\ell_1n_1\ell_3n_3}(k_1, p_1, k_3, p_3) (V_\Lambda)_{n_2\ell_2n_4\ell_4}(p_2, k_2, p_4, k_4), \end{aligned} \quad (7.34)$$

$$(\Phi_\Lambda^{\text{ph,d}})_{n_1n_2n_3n_4}(p_1, p_2, p_3, p_4) = -(\Phi_\Lambda^{\text{ph,c}})_{n_1n_2n_4n_3}(p_1, p_2, p_4, p_3). \quad (7.35)$$

Furthermore, the property (7.8) of the lattice covariance implies the corresponding property of the single-scale Green function,

$$(S_\Lambda)_{\ell_1\ell_2}(k_1, k_2) = \delta_{\ell_1\ell_2} \delta(k_1, k_2) (S_\Lambda)_{\ell_1}(k_1), \quad (7.36)$$

as well as of the loop term,

$$(L_\Lambda)_{\ell_1\ell_2\ell_3\ell_4}(k_1, k_2, k_3, k_4) = \delta_{\ell_1\ell_3} \delta(k_1, k_3) \delta_{\ell_2\ell_4} \delta(k_2, k_4) (L_\Lambda)_{\ell_1\ell_2}(k_1, k_2). \quad (7.37)$$

We now put these results together with Eq. (7.16) into the above RGE (7.32). Then,

the left-hand side of the RGE turns into

$$(\dot{V}_\Lambda)_{n_1 \dots n_4}(p_1, p_2, p_3, p_4) = (\dot{V}_\Lambda)_{n_1 \dots n_4}(p_1, p_2, p_3) \delta(p_1 + p_2, p_3 + p_4), \quad (7.38)$$

whereas the three terms on the right-hand side have to be evaluated separately.

(i) *Particle-particle term.* For the first term, Eq. (7.33), we obtain

$$\begin{aligned} \Phi_\Lambda^{\text{pp}}(p_1, p_2, p_3, p_4)_{n_1 n_2 n_3 n_4} &= -\beta \sum_{\ell_1, \ell_2} \int dk_1 \int dk_2 (L_\Lambda)_{\ell_1 \ell_2}(k_1, k_2) \\ &\times (V_\Lambda)_{n_1 n_2 \ell_1 \ell_2}(p_1, p_2, k_1) \delta(p_1 + p_2, k_1 + k_2) (V_\Lambda)_{\ell_1 \ell_2 n_3 n_4}(k_1, k_2, p_3) \delta(k_1 + k_2, p_3 + p_4). \end{aligned} \quad (7.39)$$

The product of the two delta distributions equals

$$\delta(p_1 + p_2 - k_1, k_2) \delta(p_1 + p_2, p_3 + p_4), \quad (7.40)$$

and thus we obtain

$$(\Phi_\Lambda^{\text{pp}})_{n_1 n_2 n_3 n_4}(p_1, p_2, p_3, p_4) = (\Phi_\Lambda^{\text{pp}})_{n_1 n_2 n_3 n_4}(p_1, p_2, p_3) \delta(p_1 + p_2, p_3 + p_4), \quad (7.41)$$

with the function Φ_Λ^{pp} on the right-hand side given by Eq. (7.26).

(ii) *Crossed particle-hole term.* First, by using the antisymmetry of V_Λ under the exchange of its last two arguments, Eq. (7.34) can be written equivalently as

$$\begin{aligned} (\Phi_\Lambda^{\text{ph,c}})_{n_1 n_2 n_3 n_4}(p_1, p_2, p_3, p_4) &= -2\beta \sum_{\ell_1, \dots, \ell_4} \int dk_1 \dots \int dk_4 (L_\Lambda)_{\ell_3 \ell_4 \ell_2 \ell_1}(k_3, k_4, k_2, k_1) \\ &\times (V_\Lambda)_{\ell_1 n_1 \ell_3 n_3}(k_1, p_1, k_3, p_3) (V_\Lambda)_{n_2 \ell_2 \ell_4 n_4}(p_2, k_2, k_4, p_4). \end{aligned} \quad (7.42)$$

This formula turns out to be more useful than Eq. (7.34), because the external momentum p_4 appears as the last argument of V_Λ , which can be eliminated by the momentum conservation. Next, by using Eqs. (7.16) and (7.36)–(7.37), we obtain

$$\begin{aligned} (\Phi_\Lambda^{\text{ph,c}})_{n_1 n_2 n_3 n_4}(p_1, p_2, p_3, p_4) &= -2\beta \sum_{\ell_1, \ell_2} \int dk_1 \int dk_2 (L_\Lambda)_{\ell_2 \ell_1}(k_2, k_1) \\ &\times (V_\Lambda)_{\ell_1 n_1 \ell_2 n_3}(k_1, p_1, k_2) \delta(k_1 + p_1, k_2 + p_3) (V_\Lambda)_{n_2 \ell_2 \ell_1 n_4}(p_2, k_2, k_1) \delta(p_2 + k_2, k_1 + p_4). \end{aligned} \quad (7.43)$$

The product of the two delta distributions equals

$$\delta(p_1 - p_3 + k_1, k_2) \delta(p_1 + p_2, p_3 + p_4), \quad (7.44)$$

which in turn leads to

$$(\Phi_{\Lambda}^{\text{ph},c})_{n_1 n_2 n_3 n_4}(p_1, p_2, p_3, p_4) = (\Phi_{\Lambda}^{\text{ph},c})_{n_1 n_2 n_3 n_4}(p_1, p_2, p_3) \delta(p_1 + p_2, p_3 + p_4), \quad (7.45)$$

where $\Phi_{\Lambda}^{\text{ph},c}$ on the right-hand side is given by Eq. (7.27).

(iii) *Direct particle-hole term.* Since V_{Λ} and L_{Λ} are invariant under the simultaneous exchange of their first two and their last two arguments, the same applies to the crossed particle hole term (7.34). Therefore, Eq. (7.35) is equivalent to

$$(\Phi_{\Lambda}^{\text{ph},d})_{n_1 n_2 n_3 n_4}(p_1, p_2, p_3, p_4) = -(\Phi_{\Lambda}^{\text{ph},c})_{n_2 n_1 n_3 n_4}(p_2, p_1, p_3, p_4). \quad (7.46)$$

By combining this with Eq. (7.45), we obtain

$$(\Phi_{\Lambda}^{\text{ph},d})_{n_1 n_2 n_3 n_4}(p_1, p_2, p_3, p_4) = (\Phi_{\Lambda}^{\text{ph},d})_{n_1 n_2 n_3 n_4}(p_1, p_2, p_3) \delta(p_1 + p_2, p_3 + p_4), \quad (7.47)$$

where $\Phi_{\Lambda}^{\text{ph},c}$ on the right-hand side is given by Eq. (7.28). Finally, by combining all results derived in (i)–(iii) together with Eq. (7.38) and by canceling the delta distribution $\delta(p_1 + p_2, p_3 + p_4)$ from both sides of the RGE, we arrive at the assertion (7.25). \square

7.2. Static-vertex approximation

To further simplify the RGE, we now employ the *static-vertex approximation*, by which the frequency dependencies of the interaction vertex are entirely neglected. This means, we replace

$$(V_{\Lambda})_{n_1 \dots n_4}(\mathbf{p}_1, \omega_1; \mathbf{p}_2, \omega_2; \mathbf{p}_3, \omega_3) \mapsto (V_{\Lambda})_{n_1 \dots n_4}(\mathbf{p}_1, 0; \mathbf{p}_2, 0; \mathbf{p}_3, 0) \quad (7.48)$$

$$\equiv (V_{\Lambda})_{n_1 \dots n_4}(\mathbf{p}_1, \mathbf{p}_2, \mathbf{p}_3). \quad (7.49)$$

After this replacement, we can perform the remaining frequency summations on the right-hand side of the RGE analytically, and thereby derive the approximate RGE for the static interaction vertex.

Theorem 7.2 (RGE for static interaction vertex). *In the static-vertex approximation, the RGE for the lattice interaction vertex reduces to*

$$(\dot{V}_{\Lambda})_{n_1 n_2 n_3 n_4}(\mathbf{p}_1, \mathbf{p}_2, \mathbf{p}_3) = [\Phi_{\Lambda}^{\text{pp}} + \Phi_{\Lambda}^{\text{ph},c} + \Phi_{\Lambda}^{\text{ph},d}]_{n_1 n_2 n_3 n_4}(\mathbf{p}_1, \mathbf{p}_2, \mathbf{p}_3), \quad (7.50)$$

where the three terms on the right-hand side are given by

$$(\Phi_{\Lambda}^{\text{pp}})_{n_1 n_2 n_3 n_4}(\mathbf{p}_1, \mathbf{p}_2, \mathbf{p}_3) = \quad (7.51)$$

$$\begin{aligned} & - \sum_{\ell_1, \ell_2} \frac{1}{|\mathcal{B}|} \int_{\mathcal{B}} d^3 \mathbf{k}_1 \int_{\mathcal{B}} d^3 \mathbf{k}_2 \sum_{\mathbf{K}} \delta^3(\mathbf{K} + \mathbf{p}_1 + \mathbf{p}_2 - \mathbf{k}_1, \mathbf{k}_2) \\ & \times (L_{\Lambda}^{-})_{\ell_1 \ell_2}(\mathbf{k}_1, \mathbf{k}_2) (V_{\Lambda})_{n_1 n_2 \ell_1 \ell_2}(\mathbf{p}_1, \mathbf{p}_2, \mathbf{k}_1) (V_{\Lambda})_{\ell_1 \ell_2 n_3 n_4}(\mathbf{k}_1, \mathbf{k}_2, \mathbf{p}_3), \end{aligned}$$

$$(\Phi_{\Lambda}^{\text{ph,c}})_{n_1 n_2 n_3 n_4}(\mathbf{p}_1, \mathbf{p}_2, \mathbf{p}_3) = \quad (7.52)$$

$$\begin{aligned} & - 2 \sum_{\ell_1, \ell_2} \frac{1}{|\mathcal{B}|} \int_{\mathcal{B}} d^3 \mathbf{k}_1 \int_{\mathcal{B}} d^3 \mathbf{k}_2 \sum_{\mathbf{K}} \delta^3(\mathbf{K} + \mathbf{p}_1 - \mathbf{p}_3 + \mathbf{k}_1, \mathbf{k}_2) \\ & \times (L_{\Lambda}^{+})_{\ell_2 \ell_1}(\mathbf{k}_2, \mathbf{k}_1) (V_{\Lambda})_{\ell_1 n_1 \ell_2 n_3}(\mathbf{k}_1, \mathbf{p}_1, \mathbf{k}_2) (V_{\Lambda})_{n_2 \ell_2 \ell_1 n_4}(\mathbf{p}_2, \mathbf{k}_2, \mathbf{k}_1). \end{aligned}$$

$$(\Phi_{\Lambda}^{\text{ph,d}})_{n_1 n_2 n_3 n_4}(\mathbf{p}_1, \mathbf{p}_2, \mathbf{p}_3) = -(\Phi_{\Lambda}^{\text{ph,c}})_{n_2 n_1 n_3 n_4}(\mathbf{p}_2, \mathbf{p}_1, \mathbf{p}_3). \quad (7.53)$$

Here, the particle-particle loop L_{Λ}^{-} and the particle-hole loop L_{Λ}^{+} are given by

$$(L_{\Lambda}^{\mp})_{\ell_1 \ell_2}(\mathbf{k}_1, \mathbf{k}_2) = \frac{d}{d\Lambda} \left(\chi_{\Lambda}(e_{\ell_1}(\mathbf{k}_1)) \chi_{\Lambda}(e_{\ell_2}(\mathbf{k}_2)) \right) (F_{\Lambda}^{\mp})_{\ell_1 \ell_2}(\mathbf{k}_1, \mathbf{k}_2), \quad (7.54)$$

in terms of the functions F_{Λ}^{\mp} as defined by

$$F_{\ell_1 \ell_2}^{-}(\mathbf{k}_1, \mathbf{k}_2) = \frac{1 - f(e_{\ell_1}(\mathbf{k}_1)) - f(e_{\ell_2}(\mathbf{k}_2))}{e_{\ell_1}(\mathbf{k}_1) + e_{\ell_2}(\mathbf{k}_2)}, \quad (7.55)$$

and by

$$F_{\ell_1 \ell_2}^{+}(\mathbf{k}_1, \mathbf{k}_2) = \frac{f(e_{\ell_1}(\mathbf{k}_1)) - f(e_{\ell_2}(\mathbf{k}_2))}{e_{\ell_1}(\mathbf{k}_1) - e_{\ell_2}(\mathbf{k}_2)}. \quad (7.56)$$

Furthermore, $e_{\ell}(\mathbf{k}) = E_{\ell}(\mathbf{k}) - \mu$ are the Bloch energies subtracted by the chemical potential, and $f(e) = (e^{\beta e} + 1)^{-1}$ denotes the Fermi distribution function. The reciprocal lattice vector \mathbf{K} is fixed in each term in Eqs. (7.51)–(7.52) by the condition that all external Bloch momenta $\mathbf{p}_1, \mathbf{p}_2, \mathbf{p}_3$ and all internal Bloch momenta $\mathbf{k}_1, \mathbf{k}_2$ must lie in the first Brillouin zone.

Proof. The RGE (7.50) follows directly from the more general Eq. (7.25) by employing the static-vertex approximation. Hence, it only remains to evaluate the internal frequency summations in Eqs. (7.26)–(7.28), and to show that they produce the expres-

sions (7.54)–(7.56) for the loop terms:

$$(L_{\Lambda}^{\mp})_{\ell_1 \ell_2}(\mathbf{k}_1, \mathbf{k}_2) = \beta \sum_{\omega_1, \omega_2 \in \mathbb{M}} \delta_{\mp \omega_1, \omega_2} (L_{\Lambda})_{\ell_1 \ell_2}(\mathbf{k}_1, \omega_1; \mathbf{k}_2, \omega_2) \quad (7.57)$$

$$= \beta \sum_{\omega \in \mathbb{M}} (L_{\Lambda})_{\ell_1 \ell_2}(\mathbf{k}_1, \omega; \mathbf{k}_2, \mp \omega) \quad (7.58)$$

$$= \beta \sum_{\omega \in \mathbb{M}} \frac{d}{d\Lambda} \left((C_{\Lambda})_{\ell_1}(\mathbf{k}_1, \omega) (C_{\Lambda})_{\ell_2}(\mathbf{k}_2, \mp \omega) \right) \quad (7.59)$$

$$= \frac{d}{d\Lambda} \left(\chi_{\Lambda}(e_{\ell_1}(\mathbf{k}_1)) \chi_{\Lambda}(e_{\ell_2}(\mathbf{k}_2)) \right) \frac{1}{\beta} \sum_{\omega \in \mathbb{M}} \frac{1}{i\hbar\omega - e_{\ell_1}(\mathbf{k}_1)} \frac{1}{\mp i\hbar\omega - e_{\ell_2}(\mathbf{k}_2)}, \quad (7.60)$$

where in the last step, we have used the explicit expression (7.11) of the covariance. Now, the frequency summations can be evaluated by means of the residue theorem (see Ref. [Mah90, Sct. 3.5]) as

$$\mp \frac{1}{\beta} \sum_{\omega \in \mathbb{M}} \frac{1}{i\hbar\omega - e_{\ell_1}(\mathbf{k}_1)} \frac{1}{i\hbar\omega \pm e_{\ell_2}(\mathbf{k}_2)} = \mp \frac{f(e_{\ell_1}(\mathbf{k}_1)) - f(\mp e_{\ell_2}(\mathbf{k}_2))}{e_{\ell_1}(\mathbf{k}_1) \pm e_{\ell_2}(\mathbf{k}_2)}. \quad (7.61)$$

Taking into account the property

$$f(-e) = 1 - f(e) \quad (7.62)$$

of the Fermi distribution function, this shows the assertion. \square

7.3. Fermi surface patching

Finally, in order to make the RGE amenable to a numerical solution for the Rashba tight-binding model (see Ch. 9), we employ yet another approximation, namely, we discretize the Bloch momentum dependencies of the interaction vertex. In concrete terms, we employ the so-called *Fermi surface patching* approximation, which we will now briefly explain (for details, see Ref. [Sch+16a, Sct. III.B and Appendix C]). First, we divide the Brillouin zone \mathcal{B} into N disjoint *patches*,

$$\mathcal{B} = \bigcup_{i=1}^N \mathcal{B}_i, \quad (7.63)$$

and we choose one *representative momentum* for each patch,

$$\boldsymbol{\pi}_i \in \mathcal{B}_i, \quad (7.64)$$

which typically lies on a Fermi surface within that patch. Then, we assume the effective

interaction to be *constant on each patch*, such that

$$(V_\Lambda)_{n_1 \dots n_4}(\mathbf{p}_1, \mathbf{p}_2, \mathbf{p}_3) = \sum_{i_1=1}^N \sum_{i_2=1}^N \sum_{i_3=1}^N (V_\Lambda)_{n_1 \dots n_4}(i_1, i_2, i_3) \mathbb{1}(\mathbf{p}_1 \in \mathcal{B}_{i_1}) \mathbb{1}(\mathbf{p}_2 \in \mathcal{B}_{i_2}) \mathbb{1}(\mathbf{p}_3 \in \mathcal{B}_{i_3}), \quad (7.65)$$

where we denote by

$$(V_\Lambda)_{\ell_1 \dots \ell_4}(i_1, i_2, i_3) \equiv (V_\Lambda)_{\ell_1 \dots \ell_4}(\boldsymbol{\pi}_{i_1}, \boldsymbol{\pi}_{i_2}, \boldsymbol{\pi}_{i_3}) \quad (7.66)$$

the values of the interaction vertex at each combination of the three representative momenta. Note, in particular, that the representative momentum $\boldsymbol{\pi}_{i_1}$ may lie on *any* Fermi surface—of *any* band, not necessarily only of the band labeled by n_1 —and the same applies to $\boldsymbol{\pi}_{i_2}$ and $\boldsymbol{\pi}_{i_3}$ as well. Hence, if L denotes the number of bands, there are in total $N^3 \times L^4$ complex numbers which parametrize the interaction vertex. We call our ansatz (7.65)–(7.66) the *refined projection scheme* (for a comparison with other projection schemes, see Ref. [Sch+16a, Sct. III]). Next, we state the RGE which the finitely many parameters (7.66) fulfill within the refined projection scheme.

Theorem 7.3 (RGE for discretized interaction vertex). *Under the discretization (7.65)–(7.66), the RGE for the static interaction vertex approximately reduces to*

$$\frac{d}{d\Lambda} (V_\Lambda)_{n_1 n_2 n_3 n_4}(i_1, i_2, i_3) = [\Phi_\Lambda^{\text{pp}} + \Phi_\Lambda^{\text{ph,c}} + \Phi_\Lambda^{\text{ph,d}}]_{n_1 n_2 n_3 n_4}(i_1, i_2, i_3), \quad (7.67)$$

where the three terms on the right-hand side are given by [Sch+16a]

$$(\Phi_\Lambda^{\text{pp}})_{n_1 n_2 n_3 n_4}(i_1, i_2, i_3) = \quad (7.68)$$

$$- \sum_{\ell_1, \ell_2} \sum_{j_1=1}^N \sum_{j_2=1}^N \sum_{\mathbf{K}} \mathbb{1}(\mathbf{K} + \boldsymbol{\pi}_{i_1} + \boldsymbol{\pi}_{i_2} - \boldsymbol{\pi}_{j_1} \in \mathcal{B}_{j_2}) (L_\Lambda^-)_{\ell_1 \ell_2}(i_1, i_2, j_1) \\ \times \left[(V_\Lambda)_{n_1 n_2 \ell_1 \ell_2}(i_1, i_2, j_1) (V_\Lambda)_{\ell_1 \ell_2 n_3 n_4}(j_1, j_2, i_3) + (j_1, \ell_1) \leftrightarrow (j_2, \ell_2) \right],$$

$$(\Phi_\Lambda^{\text{ph,c}})_{n_1 n_2 n_3 n_4}(i_1, i_2, i_3) = \quad (7.69)$$

$$-2 \sum_{\ell_1, \ell_2} \sum_{j_1=1}^N \sum_{j_2=1}^N \sum_{\mathbf{K}} \mathbb{1}(\mathbf{K} + \boldsymbol{\pi}_{i_1} - \boldsymbol{\pi}_{i_3} + \boldsymbol{\pi}_{j_1} \in \mathcal{B}_{j_2}) \\ \times (L_\Lambda^+)_{\ell_1 \ell_2}(i_1, i_3, j_1) (V_\Lambda)_{\ell_1 n_1 \ell_2 n_3}(j_1, i_1, j_2) (V_\Lambda)_{n_2 \ell_2 \ell_1 n_4}(i_2, j_2, j_1) \\ -2 \sum_{\ell_1, \ell_2} \sum_{j_1=1}^N \sum_{j_2=1}^N \sum_{\mathbf{K}} \mathbb{1}(\mathbf{K} + \boldsymbol{\pi}_{i_3} - \boldsymbol{\pi}_{i_1} + \boldsymbol{\pi}_{j_1} \in \mathcal{B}_{j_2}) \\ \times (L_\Lambda^+)_{\ell_1 \ell_2}(i_3, i_1, j_1) (V_\Lambda)_{\ell_2 n_1 \ell_1 n_3}(j_2, i_1, j_1) (V_\Lambda)_{n_2 \ell_1 \ell_2 n_4}(i_2, j_1, j_2),$$

$$(\Phi_\Lambda^{\text{ph,d}})_{n_1 n_2 n_3 n_4}(i_1, i_2, i_3) = -(\Phi_\Lambda^{\text{ph,c}})_{n_2 n_1 n_3 n_4}(i_2, i_1, i_3). \quad (7.70)$$

Here, we have defined the loop terms

$$(L_{\Lambda}^{\mp})_{\ell_1 \ell_2}(i_1, i_2, j_1) = \frac{1}{|\mathcal{B}|} \int_{\mathcal{B}_{j_1}} d^3 \mathbf{k} \dot{\chi}_{\Lambda}(e_{\ell_1}(\mathbf{k})) \chi_{\Lambda}(e_{\ell_2}(\mathbf{K} + \boldsymbol{\pi}_{i_1} \pm \boldsymbol{\pi}_{i_2} \mp \mathbf{k})) F_{\ell_1 \ell_2}^{\mp}(\mathbf{k}, \mathbf{K} + \boldsymbol{\pi}_{i_1} \pm \boldsymbol{\pi}_{i_2} \mp \mathbf{k}), \quad (7.71)$$

with the functions F^{\mp} given by Eqs. (7.55) and (7.56), respectively.

Remark. In the particle-particle term (7.68), the reciprocal lattice vector \mathbf{K} is fixed by the condition

$$\mathbf{K} + \boldsymbol{\pi}_{i_1} + \boldsymbol{\pi}_{i_2} - \boldsymbol{\pi}_{j_1} \in \mathcal{B}, \quad (7.72)$$

and hence, \mathbf{K} depends on only three patch indices i_1 , i_2 , and j_1 . The stricter condition

$$\mathbf{K} + \boldsymbol{\pi}_{i_1} + \boldsymbol{\pi}_{i_2} - \boldsymbol{\pi}_{j_1} \in \mathcal{B}_{j_2} \quad (7.73)$$

then also fixes the patch index j_2 . Therefore, the right-hand side of Eq. (7.68) effectively requires only a summation over two band indices ℓ_1, ℓ_2 and over one patch index j_1 , and the same applies also to the particle-hole terms.

Proof. See [Sch+16a, Appendix C.1]. □

8. Mean-field theory without SU(2) symmetry

While the RGE derived in the previous chapter can in principle be applied to any model with one or several energy bands, our main focus in this thesis is on the tight-binding Rashba model of Sct. 2.3. This model is given by a (2×2) Hamiltonian matrix $H_{ss'}(\mathbf{k})$, which corresponds to one spin-split energy band. In the next Ch. 9, we will use the fRG to study the superconducting phases and, in particular, to predict the *effective interactions* in this model (starting from an attractive, local initial interaction). After that, we will use *mean-field theory* to predict the *gap function* as well as the superconducting *order parameter*, and thereby obtain a more detailed characterization of these superconducting phases. The purpose of this chapter is therefore to explain mean-field theory and to derive the Bogoliubov transformation in a general setting without SU(2) spin rotation invariance. Our analysis is not restricted to the concrete Rashba model, but applies to any time-reversal invariant Hamiltonian $H_{ss'}(\mathbf{k})$ describing a spin-split energy band. Concretely, we proceed analogously to Ref. [SU91] and generalize the results presented there to the non-SU(2)-symmetric case.

8.1. Definitions

We consider an (effective) single-orbital model as described in Sct. 1.5, whose Hamiltonian is given by its matrix elements in a Bloch-like spin basis,

$$\langle \psi_{s,\mathbf{k}} | \hat{H}^0 | \psi_{s',\mathbf{k}'} \rangle = |\mathcal{B}| \delta^3(\mathbf{k} - \mathbf{k}') H_{ss'}^0(\mathbf{k}). \quad (8.1)$$

For technical reasons, we switch to the description of a *finite* crystal, where the allowed Bloch wavevectors \mathbf{k} are discrete owing to the Born-von-Karman boundary conditions, and the above equation turns into (see Ref. [SS16b, Appendix A.2])

$$\langle \psi_{s,\mathbf{k}} | \hat{H}^0 | \psi_{s',\mathbf{k}'} \rangle = \delta_{\mathbf{k},\mathbf{k}'} H_{ss'}^0(\mathbf{k}). \quad (8.2)$$

In particular, as the Dirac delta distribution is replaced by the Kronecker delta, we can evaluate this equation at $\mathbf{k} = \mathbf{k}'$ to obtain the simpler relation

$$H_{ss'}^0(\mathbf{k}) = \langle \psi_{s,\mathbf{k}} | \hat{H}^0 | \psi_{s',\mathbf{k}} \rangle. \quad (8.3)$$

In first quantization, the free Hamiltonian can now be written as

$$\hat{H}^0 = \sum_{\mathbf{k}} \sum_{s, s'} H_{ss'}^0(\mathbf{k}) |\psi_{s, \mathbf{k}}\rangle \langle \psi_{s', \mathbf{k}}|, \quad (8.4)$$

where the sum is over all allowed Bloch wavevectors. In second quantization, this operator translates into

$$\hat{H}^0 = \sum_{\mathbf{k}} \sum_{s, s'} H_{ss'}^0(\mathbf{k}) \hat{a}_s^\dagger(\mathbf{k}) \hat{a}_{s'}(\mathbf{k}), \quad (8.5)$$

where the operators $\hat{a}_s(\mathbf{k}) \equiv \hat{a}(|\psi_{s, \mathbf{k}}\rangle)$ and $\hat{a}_s^\dagger(\mathbf{k}) \equiv \hat{a}^\dagger(|\psi_{s, \mathbf{k}}\rangle)$ annihilate and create, respectively, a Bloch-like vector. In addition to this free Hamiltonian, we consider a *superconducting interaction*, which is defined as a two-particle interaction of the form

$$\hat{V} = \frac{1}{2} \sum_{\mathbf{k}, \mathbf{k}'} \sum_{s_1, \dots, s_4} V_{s_1 s_2 s_3 s_4}(\mathbf{k}, \mathbf{k}') \hat{a}_{s_1}^\dagger(-\mathbf{k}) \hat{a}_{s_2}^\dagger(\mathbf{k}) \hat{a}_{s_3}(\mathbf{k}') \hat{a}_{s_4}(-\mathbf{k}'), \quad (8.6)$$

with an interaction kernel depending on four spin indices but only two Bloch momenta.

Now, the mean-field ansatz consists in replacing the above quartic interaction operator by the quadratic *mean-field interaction*, which is given by

$$\begin{aligned} \hat{V}^{\text{mf}} = & \frac{1}{2} \sum_{\mathbf{k}, \mathbf{k}'} \sum_{s_1, \dots, s_4} V_{s_1 s_2 s_3 s_4}(\mathbf{k}, \mathbf{k}') \\ & \times \left(\hat{a}_{s_1}^\dagger(-\mathbf{k}) \hat{a}_{s_2}^\dagger(\mathbf{k}) \langle \hat{a}_{s_3}(\mathbf{k}') \hat{a}_{s_4}(-\mathbf{k}') \rangle + \langle \hat{a}_{s_1}^\dagger(-\mathbf{k}) \hat{a}_{s_2}^\dagger(\mathbf{k}) \rangle \hat{a}_{s_3}(\mathbf{k}') \hat{a}_{s_4}(-\mathbf{k}') \right). \end{aligned} \quad (8.7)$$

Consequently, the interacting Hamiltonian is replaced by the *mean-field Hamiltonian*,

$$\hat{H} = \hat{H}^0 + \hat{V} \mapsto \hat{H}^{\text{mf}} = \hat{H}^0 + \hat{V}^{\text{mf}}, \quad (8.8)$$

which is quadratic and can therefore be solved exactly. However, the expectation values in Eq. (8.7) are to be evaluated with respect to the mean-field Hamiltonian itself, i.e.,

$$\langle \hat{A} \rangle = \frac{1}{Z^{\text{mf}}} \text{Tr} \left(e^{-\beta(\hat{H}^{\text{mf}} - \mu \hat{N})} \hat{A} \right), \quad (8.9)$$

with

$$Z^{\text{mf}} = \text{Tr} \left(e^{-\beta(\hat{H}^{\text{mf}} - \mu \hat{N})} \right), \quad (8.10)$$

where μ denotes the chemical potential and β the inverse temperature. The self-consistent solution of Eqs. (8.7)–(8.10) is referred to as *mean-field theory*. Furthermore, the expectation value

$$\Psi_{ss'}(\mathbf{k}) = \langle \hat{a}_s(\mathbf{k}) \hat{a}_{s'}(-\mathbf{k}) \rangle \quad (8.11)$$

is called the *order parameter*, whereas the product

$$\Delta_{ss'}(\mathbf{k}) = - \sum_{\mathbf{k}'} \sum_{s_3, s_4} V_{s' s_3 s_4}(\mathbf{k}, \mathbf{k}') \langle \hat{a}_{s_3}(\mathbf{k}') \hat{a}_{s_4}(-\mathbf{k}') \rangle \quad (8.12)$$

is called the *gap function*. In the following, we will first study the general symmetries of these two (2×2) matrices, and then calculate them explicitly in the case of a *singlet* superconducting interaction (see Sect. 8.4).

8.2. Symmetries

We assume that the Hamiltonian $\hat{H} = \hat{H}^0 + \hat{V}$ is hermitean and invariant under time-reversal symmetry. The consequences of these symmetries for the free Hamiltonian matrix $H_{ss'}^0(\mathbf{k})$ have already been studied in Sect. 2.1 (see Table 2.2). In this section, we will derive the corresponding conditions on the interaction kernel, the gap function and the order parameter.

Superconducting interaction.—Without loss of generality, we may assume that the coefficient function $V_{s_1 \dots s_4}(\mathbf{k}, \mathbf{k}')$ in Eq. (8.6) is antisymmetric under the exchange of its first two and its last two arguments, i.e.,

$$V_{s_1 s_2 s_3 s_4}(\mathbf{k}, \mathbf{k}') = -V_{s_2 s_1 s_3 s_4}(-\mathbf{k}, \mathbf{k}') = -V_{s_1 s_2 s_4 s_3}(\mathbf{k}, -\mathbf{k}'). \quad (8.13)$$

The reason for this is that any symmetric contribution to the coefficient function would automatically cancel out in Eq. (8.6) due to the anticommutativity of the fermionic creation and annihilation operators. In addition, we assume that the interaction operator \hat{V} is hermitean,

$$\hat{V} = \hat{V}^\dagger, \quad (8.14)$$

and time-reversal invariant,

$$\hat{V} = \hat{\Theta}^{-1} \hat{V} \hat{\Theta}. \quad (8.15)$$

These conditions on the interaction operator translate into the following constraints on the interaction kernel: hermiticity,

$$V_{s_1 s_2 s_3 s_4}(\mathbf{k}, \mathbf{k}') = V_{s_4 s_3 s_2 s_1}^*(\mathbf{k}', \mathbf{k}), \quad (8.16)$$

and time-reversal symmetry,

$$V_{s_1 s_2 s_3 s_4}(\mathbf{k}, \mathbf{k}') = \sum_{t_1, \dots, t_4} [\mathrm{i}\sigma_y]_{s_1 t_1}^\dagger [\mathrm{i}\sigma_y]_{s_2 t_2}^\dagger V_{t_1 t_2 t_3 t_4}^*(-\mathbf{k}, -\mathbf{k}') [\mathrm{i}\sigma_y]_{t_3 s_3} [\mathrm{i}\sigma_y]_{t_4 s_4}. \quad (8.17)$$

In fact, these constraints can be derived similarly as the corresponding constraints on the free Hamiltonian matrix (see Sect. 2.1, and Ref. [Sch+16a, Appendix A.4]). In particular, the derivation of these constraints requires again the assumption (2.22) that the orbital $\varphi_s(\mathbf{x})$ —with respect to which the single-orbital model is defined—is real-valued.

Gap function.—The hermiticity of the mean-field Hamiltonian,

$$\hat{H}^{\mathrm{mf}} = (\hat{H}^{\mathrm{mf}})^\dagger, \quad (8.18)$$

implies by Eq. (8.9)–(8.10) the following property of the thermal expectation values,

$$\langle \hat{a}_{s_3}(\mathbf{k}') \hat{a}_{s_4}(-\mathbf{k}') \rangle = \langle \hat{a}_{s_4}^\dagger(-\mathbf{k}') \hat{a}_{s_3}^\dagger(\mathbf{k}') \rangle^*. \quad (8.19)$$

By using this property as well as Eq. (8.16), we can transform Eq. (8.12) into

$$\Delta_{ss'}(\mathbf{k}) = - \sum_{\mathbf{k}'} \sum_{s_3, s_4} V_{s_4 s_3 s s'}^*(\mathbf{k}', \mathbf{k}) \langle \hat{a}_{s_4}^\dagger(-\mathbf{k}') \hat{a}_{s_3}^\dagger(\mathbf{k}') \rangle^*, \quad (8.20)$$

and further, by taking the complex conjugate and substituting $\mathbf{k} \mapsto -\mathbf{k}$, into

$$\Delta_{ss'}^*(-\mathbf{k}) = - \sum_{\mathbf{k}'} \sum_{s_3, s_4} V_{s_4 s_3 s s'}(\mathbf{k}', -\mathbf{k}) \langle \hat{a}_{s_4}^\dagger(-\mathbf{k}') \hat{a}_{s_3}^\dagger(\mathbf{k}') \rangle, \quad (8.21)$$

which agrees with Ref. [SU91, Eq. (2.2)]. Moreover, one can show that the antisymmetry (8.13) of the interaction kernel implies the *antisymmetry* of the gap function,

$$\Delta(\mathbf{k}) = -\Delta^T(-\mathbf{k}), \quad (8.22)$$

while the time-reversal symmetry (8.17) leads to

$$\Delta(\mathbf{k}) = [\mathrm{i}\sigma_y]^\dagger \Delta^*(-\mathbf{k}) [\mathrm{i}\sigma_y]. \quad (8.23)$$

If we define the matrix $\tilde{\Delta}(\mathbf{k})$ by

$$\Delta(\mathbf{k}) = \tilde{\Delta}(\mathbf{k}) \mathrm{i}\sigma_y, \quad (8.24)$$

then the above conditions on the gap function translate into the following conditions on this transformed matrix: *hermiticity*,

$$\tilde{\Delta}(\mathbf{k}) = \tilde{\Delta}^\dagger(\mathbf{k}), \quad (8.25)$$

and time-reversal symmetry,

$$\tilde{\Delta}(\mathbf{k}) = [\mathrm{i}\sigma_y]^\dagger \tilde{\Delta}^*(-\mathbf{k}) [\mathrm{i}\sigma_y]. \quad (8.26)$$

Thus, we conclude that the matrix $\tilde{\Delta}(\mathbf{k})$ has exactly the same symmetries as the free Hamiltonian matrix $H(\mathbf{k})$. In particular, we can also expand the former in terms of the Pauli matrices as

$$\tilde{\Delta}(\mathbf{k}) = \psi(\mathbf{k}) \mathbb{1} + \mathbf{d}(\mathbf{k}) \cdot \boldsymbol{\sigma}, \quad (8.27)$$

where the functions $\psi(\mathbf{k})$ and $\mathbf{d}(\mathbf{k})$ have the same symmetries as the functions $f(\mathbf{k})$ and $\mathbf{g}(\mathbf{k})$ (see Table 2.2). We hence obtain the representation

$$\Delta(\mathbf{k}) = [\psi(\mathbf{k}) \mathbb{1} + \mathbf{d}(\mathbf{k}) \cdot \boldsymbol{\sigma}] \mathrm{i}\sigma_y \quad (8.28)$$

of the gap function, which is standard in the literature (see Ref. [SU91]).

Order parameter.—Similarly as for the gap function, one can derive the following constraints on the order parameter matrix: antisymmetry,

$$\Psi(\mathbf{k}) = -\Psi^T(-\mathbf{k}), \quad (8.29)$$

and time-reversal symmetry,

$$\Psi(\mathbf{k}) = [i\sigma_y]^\dagger \Psi^*(-\mathbf{k}) [i\sigma_y]. \quad (8.30)$$

Thus, the order parameter has the same symmetries as the gap function, which is indeed well-known [Poo+07]. In particular, we can expand also the order parameter as

$$\Psi(\mathbf{k}) = [\chi(\mathbf{k}) + \mathbf{c}(\mathbf{k}) \cdot \boldsymbol{\sigma}] i\sigma_y, \quad (8.31)$$

where the functions $\chi(\mathbf{k})$ and $\mathbf{c}(\mathbf{k})$ have the same symmetries as the functions $f(\mathbf{k})$ and $\mathbf{g}(\mathbf{k})$. Of course, the fact that the matrices $\Delta(\mathbf{k})$ and $\Psi(\mathbf{k})$ have the same symmetries does *not* imply that they are of the same form, because the functions $\chi(\mathbf{k})$ and $\mathbf{c}(\mathbf{k})$ may be different from $\psi(\mathbf{k})$ and $\mathbf{d}(\mathbf{k})$.

8.3. Mean-field Hamiltonian

We now rewrite the mean-field Hamiltonian (8.8) in a form which will allow for its straightforward diagonalization. For this purpose, consider first the mean-field interaction in Eq. (8.7). In the second term, we interchange the integration variables $\mathbf{k} \leftrightarrow \mathbf{k}'$ and relabel the spin variables as $(s_1, s_2, s_3, s_4) \mapsto (s_4, s_3, s_1, s_2)$. Then, we obtain

$$\begin{aligned} \hat{V} = & \frac{1}{2} \sum_{\mathbf{k}, \mathbf{k}'} \sum_{s_1, \dots, s_4} V_{s_1 s_2 s_3 s_4}(\mathbf{k}, \mathbf{k}') \langle \hat{a}_{s_3}(\mathbf{k}') \hat{a}_{s_4}(-\mathbf{k}') \rangle \hat{a}_{s_1}^\dagger(-\mathbf{k}) \hat{a}_{s_2}^\dagger(\mathbf{k}) \\ & + \frac{1}{2} \sum_{\mathbf{k}, \mathbf{k}'} \sum_{s_1, \dots, s_4} V_{s_4 s_3 s_1 s_2}(\mathbf{k}', \mathbf{k}) \langle \hat{a}_{s_4}^\dagger(-\mathbf{k}') \hat{a}_{s_3}^\dagger(\mathbf{k}') \rangle \hat{a}_{s_1}(\mathbf{k}) \hat{a}_{s_2}(-\mathbf{k}). \end{aligned} \quad (8.32)$$

By substituting $\mathbf{k} \mapsto -\mathbf{k}$ and using the antisymmetry of the interaction kernel, we can further write this in terms of the gap function (see Eqs. (8.12) and (8.21)) as

$$\hat{V} = \frac{1}{2} \sum_{\mathbf{k}} \sum_{s_1, s_2} \left(\Delta_{s_1 s_2}(\mathbf{k}) \hat{a}_{s_1}^\dagger(\mathbf{k}) \hat{a}_{s_2}^\dagger(-\mathbf{k}) - \Delta_{s_1 s_2}^*(-\mathbf{k}) \hat{a}_{s_1}(-\mathbf{k}) \hat{a}_{s_2}(\mathbf{k}) \right). \quad (8.33)$$

Next, we bring also the free part of the Hamiltonian as given by Eq. (8.5) into a more symmetric form: Its hermiticity implies that

$$\hat{H}^0 = (\hat{H}^0)^\dagger = \sum_{\mathbf{k}} \sum_{s_1, s_2} (H_{s_1 s_2}^0)^*(\mathbf{k}) \hat{a}_{s_2}^\dagger(\mathbf{k}) \hat{a}_{s_1}(\mathbf{k}). \quad (8.34)$$

Furthermore, by employing the anticommutation relation

$$[\hat{a}_{s_1}(\mathbf{k}), \hat{a}_{s_2}^\dagger(\mathbf{k}')]_+ = \delta_{s_1 s_2} \delta_{\mathbf{k}, \mathbf{k}'}, \quad (8.35)$$

and by dropping the constant term of the Hamiltonian, we obtain

$$\hat{H}^0 = - \sum_{\mathbf{k}} \sum_{s_1, s_2} (H_{s_1 s_2}^0)^* (\mathbf{k}) \hat{a}_{s_1}(\mathbf{k}) \hat{a}_{s_2}^\dagger(\mathbf{k}). \quad (8.36)$$

By combining this formula with Eq. (8.5), we can write the Hamiltonian as

$$\hat{H}^0 = \frac{1}{2} \left(\hat{H}^0 + (\hat{H}^0)^\dagger \right) \quad (8.37)$$

$$= \frac{1}{2} \sum_{\mathbf{k}} \sum_{s_1, s_2} \left(H_{s_1 s_2}^0(\mathbf{k}) \hat{a}_{s_1}^\dagger(\mathbf{k}) \hat{a}_{s_2}(\mathbf{k}) - (H_{s_1 s_2}^0)^*(-\mathbf{k}) \hat{a}_{s_1}(-\mathbf{k}) \hat{a}_{s_2}^\dagger(-\mathbf{k}) \right), \quad (8.38)$$

where in the second term, we have substituted $\mathbf{k} \mapsto -\mathbf{k}$. Taking into account also the particle number operator

$$\hat{N} = \sum_{\mathbf{k}} \sum_s \hat{a}_s^\dagger(\mathbf{k}) \hat{a}_s(\mathbf{k}) = \frac{1}{2} \sum_{\mathbf{k}} \sum_s \left(\hat{a}_s^\dagger(\mathbf{k}) \hat{a}_s(\mathbf{k}) - \hat{a}_s(-\mathbf{k}) \hat{a}_s^\dagger(-\mathbf{k}) \right), \quad (8.39)$$

the mean-field Hamiltonian (8.8) can finally be written in matrix form as

$$\begin{aligned} \hat{H}^{\text{mf}} - \mu \hat{N} &= \frac{1}{2} \sum_{\mathbf{k}} \sum_{s_1, s_2} \left(\hat{a}_{s_1}^\dagger(\mathbf{k}), \hat{a}_{s_1}(-\mathbf{k}) \right) \\ &\times \begin{pmatrix} H_{s_1 s_2}^0(\mathbf{k}) - \mu \delta_{s_1 s_2} & \Delta_{s_1 s_2}(\mathbf{k}) \\ -\Delta_{s_1 s_2}^*(-\mathbf{k}) & -(H_{s_1 s_2}^0)^*(-\mathbf{k}) + \mu \delta_{s_1 s_2} \end{pmatrix} \begin{pmatrix} \hat{a}_{s_2}(\mathbf{k}) \\ \hat{a}_{s_2}^\dagger(-\mathbf{k}) \end{pmatrix}. \end{aligned} \quad (8.40)$$

In the next section, we will explicitly diagonalize this operator for a special form of the superconducting interaction.

8.4. Solution for singlet interaction

A superconducting interaction of *singlet form* is defined by Eq. (8.6) together with the particular form of the interaction kernel

$$V_{s_1 s_2 s_3 s_4}(\mathbf{k}, \mathbf{k}') = \frac{g}{2} \left(\delta_{s_1 s_3} \delta_{s_2 s_4} - \delta_{s_1 s_4} \delta_{s_2 s_3} \right). \quad (8.41)$$

This can be written equivalently as (see Ref. [Ede89, Eq. (10)])

$$V_{s_1 s_2 s_3 s_4}(\mathbf{k}, \mathbf{k}') = \frac{g}{2} [\mathrm{i}\sigma_y]_{s_1 s_2} [\mathrm{i}\sigma_y]_{s_3 s_4} = -\frac{g}{2} [\mathrm{i}\sigma_y]_{s_2 s_1} [\mathrm{i}\sigma_y]_{s_3 s_4} \quad (8.42)$$

in terms of the Pauli matrix σ_y . As we will see in Ch. 9, this form of the interaction comes indeed out as the *effective interaction at the critical scale* in the two-dimensional Rashba model with an onsite attractive interaction [Sch+16a]. Note that mean-field theory itself cannot be used predict the form of the superconducting interaction, but requires this to be given as an input. However, given the superconducting interaction, mean-field theory allows one to predict the gap function and the order parameter.

8.4.1. Gap function

By assuming a superconducting interaction of singlet form, the gap function can be inferred immediately from its defining equation (8.12): we find

$$\Delta_{ss'}(\mathbf{k}) = \frac{g}{2} [\mathrm{i}\sigma_y]_{ss'} \sum_{\mathbf{k}'} \sum_{s_3, s_4} [\mathrm{i}\sigma_y]_{s_3 s_4} \langle \hat{a}_{s_3}(\mathbf{k}') \hat{a}_{s_4}(-\mathbf{k}') \rangle. \quad (8.43)$$

In matrix form, this can be written as

$$\Delta(\mathbf{k}) = \Delta_0 [\mathrm{i}\sigma_y], \quad (8.44)$$

where we have defined the scalar *gap parameter*

$$\Delta_0 = \frac{g}{2} \sum_{\mathbf{k}} \sum_{s_3, s_4} [\mathrm{i}\sigma_y]_{s_3 s_4} \langle \hat{a}_{s_3}(\mathbf{k}) \hat{a}_{s_4}(-\mathbf{k}) \rangle. \quad (8.45)$$

In order to determine this parameter, we first have to calculate the order parameter, which in turn depends on the gap function. Therefore, Δ_0 must be determined self-consistently as the solution of the *gap equation* (see Sct. 8.4.5). Up to this parameter, however, the form of the gap function is already fixed by Eq. (8.44): it is independent of the Bloch momentum \mathbf{k} and of the chemical potential μ , and it is of a purely singlet form (see Sct. 8.4.4).

8.4.2. Bogoliubov transformation

In order to calculate the order parameter, we have to diagonalize the mean-field Hamiltonian (8.40). For this purpose, we proceed analogously as in Ref. [SU91] by introducing the (4×4) matrix

$$\mathcal{H}_{\mathbf{k}} = \begin{pmatrix} h_{\mathbf{k}}^0 & \Delta_{\mathbf{k}} \\ -\Delta_{-\mathbf{k}}^* & -(h_{-\mathbf{k}}^0)^* \end{pmatrix}, \quad (8.46)$$

where we have defined (similarly as in Eq. (7.5))

$$h_{\mathbf{k}}^0 := H_{\mathbf{k}}^0 - \mu. \quad (8.47)$$

Here and in the following, we denote the momentum dependencies as subscripts in order to lighten the notation. Note that by Eq. (8.22), we have

$$-\Delta_{-\mathbf{k}}^* = \Delta_{\mathbf{k}}^\dagger, \quad (8.48)$$

and hence $\mathcal{H}_{\mathbf{k}}$ is a hermitean matrix. The diagonalization of the mean-field Hamiltonian is performed by means of a *Bogoliubov transformation*, which reads

$$\hat{a}_s(\mathbf{k}) = X_{sn}(\mathbf{k}) \hat{b}_n(\mathbf{k}) + Y_{sn}(\mathbf{k}) \hat{b}_n^\dagger(-\mathbf{k}), \quad (8.49)$$

$$\hat{a}_s^\dagger(-\mathbf{k}) = Y_{sn}^*(-\mathbf{k}) \hat{b}_n(\mathbf{k}) + X_{sn}^*(-\mathbf{k}) \hat{b}_n^\dagger(-\mathbf{k}). \quad (8.50)$$

We seek $X_{\mathbf{k}} \equiv X(\mathbf{k})$ and $Y_{\mathbf{k}} \equiv Y(\mathbf{k})$ such that the 4×4 matrix

$$\mathcal{U}_{\mathbf{k}} = \begin{pmatrix} X_{\mathbf{k}} & Y_{\mathbf{k}} \\ Y_{-\mathbf{k}}^* & X_{-\mathbf{k}}^* \end{pmatrix} \quad (8.51)$$

has the following properties: (i) it is unitary, i.e.,

$$\mathcal{U}_{\mathbf{k}}^\dagger \mathcal{U}_{\mathbf{k}} = 1, \quad (8.52)$$

and (ii) it diagonalizes $\mathcal{H}_{\mathbf{k}}$, i.e.,

$$\mathcal{U}_{\mathbf{k}}^\dagger \mathcal{H}_{\mathbf{k}} \mathcal{U}_{\mathbf{k}} = \mathcal{E}_{\mathbf{k}}, \quad (8.53)$$

where $\mathcal{E}_{\mathbf{k}}$ is the diagonal matrix of eigenvalues, which turns out to be of the form

$$\mathcal{E}_{\mathbf{k}} = \begin{pmatrix} \varepsilon_{\mathbf{k}} & 0 \\ 0 & -\varepsilon_{-\mathbf{k}} \end{pmatrix} \equiv \begin{pmatrix} \varepsilon_{-}(\mathbf{k}) & 0 & 0 & 0 \\ 0 & \varepsilon_{+}(\mathbf{k}) & 0 & 0 \\ 0 & 0 & -\varepsilon_{-}(-\mathbf{k}) & 0 \\ 0 & 0 & 0 & -\varepsilon_{+}(-\mathbf{k}) \end{pmatrix}. \quad (8.54)$$

With this, the mean-field Hamiltonian (8.40) is diagonalized as

$$\hat{H}^{\text{mf}} - \mu \hat{N} = \frac{1}{2} \sum_{\mathbf{k}} \sum_n (\hat{b}_n^\dagger(\mathbf{k}), \hat{b}_n(-\mathbf{k})) \begin{pmatrix} \varepsilon_n(\mathbf{k}) & 0 \\ 0 & -\varepsilon_n(-\mathbf{k}) \end{pmatrix} \begin{pmatrix} \hat{b}_n(\mathbf{k}) \\ \hat{b}_n^\dagger(-\mathbf{k}) \end{pmatrix}, \quad (8.55)$$

or equivalently, by substituting $\mathbf{k} \mapsto -\mathbf{k}$,

$$\hat{H}^{\text{mf}} - \mu \hat{N} = \sum_{\mathbf{k}} \sum_n \varepsilon_n(\mathbf{k}) \hat{b}_n^\dagger(\mathbf{k}) \hat{b}_n(\mathbf{k}). \quad (8.56)$$

In order to find the eigenvalues $\varepsilon_{\mathbf{k}}$ and the unitary matrix $\mathcal{U}_{\mathbf{k}}$, we first note that Eq. (8.53) can be written equivalently as

$$\mathcal{H}_{\mathbf{k}} \mathcal{U}_{\mathbf{k}} = \mathcal{U}_{\mathbf{k}} \mathcal{E}_{\mathbf{k}}, \quad (8.57)$$

or more explicitly as

$$\begin{pmatrix} h_{\mathbf{k}}^0 & \Delta_{\mathbf{k}} \\ \Delta_{\mathbf{k}}^\dagger & -(h_{-\mathbf{k}}^0)^* \end{pmatrix} \begin{pmatrix} X_{\mathbf{k}} & Y_{\mathbf{k}} \\ Y_{-\mathbf{k}}^* & X_{-\mathbf{k}}^* \end{pmatrix} = \begin{pmatrix} X_{\mathbf{k}} & Y_{\mathbf{k}} \\ Y_{-\mathbf{k}}^* & X_{-\mathbf{k}}^* \end{pmatrix} \begin{pmatrix} \varepsilon_{\mathbf{k}} & 0 \\ 0 & -\varepsilon_{-\mathbf{k}} \end{pmatrix}. \quad (8.58)$$

This yields the conditions

$$h_{\mathbf{k}}^0 X_{\mathbf{k}} + \Delta_{\mathbf{k}} Y_{-\mathbf{k}}^* = X_{\mathbf{k}} \varepsilon_{\mathbf{k}}, \quad (8.59)$$

$$\Delta_{\mathbf{k}}^\dagger X_{\mathbf{k}} - (h_{-\mathbf{k}}^0)^* Y_{-\mathbf{k}}^* = Y_{-\mathbf{k}}^* \varepsilon_{\mathbf{k}}, \quad (8.60)$$

as well as

$$h_{\mathbf{k}}^0 Y_{\mathbf{k}} + \Delta_{\mathbf{k}} X_{-\mathbf{k}}^* = -Y_{\mathbf{k}} \varepsilon_{-\mathbf{k}}, \quad (8.61)$$

$$\Delta_{\mathbf{k}}^\dagger Y_{\mathbf{k}} - (h_{-\mathbf{k}}^0)^* X_{-\mathbf{k}}^* = -X_{-\mathbf{k}}^* \varepsilon_{-\mathbf{k}}. \quad (8.62)$$

By substituting $\mathbf{k} \mapsto -\mathbf{k}$ and by complex conjugation, one can convince oneself that Eqs. (8.59) and (8.60) are actually equivalent to Eqs. (8.62) and (8.61), respectively. Thus, we only have to consider two equations, say, Eqs. (8.59) and (8.60). Next, we choose $X_{\mathbf{k}}$ such that it diagonalizes the free Hamiltonian,

$$h_{\mathbf{k}}^0 X_{\mathbf{k}} = X_{\mathbf{k}} e_{\mathbf{k}}, \quad (8.63)$$

with $e_{\mathbf{k}} = E_{\mathbf{k}} - \mu$. Then, Eq. (8.59) yields

$$X_{\mathbf{k}} (\varepsilon_{\mathbf{k}} - e_{\mathbf{k}}) = \Delta_{\mathbf{k}} Y_{-\mathbf{k}}^*. \quad (8.64)$$

Multiplying both sides of this equation with $\Delta_{\mathbf{k}}^\dagger$ and using that by Eq. (8.44),

$$\Delta_{\mathbf{k}}^\dagger \Delta_{\mathbf{k}} = \Delta_0^2, \quad (8.65)$$

we obtain the explicit expression of $Y_{-\mathbf{k}}^*$ in terms of $X_{\mathbf{k}}$:

$$Y_{-\mathbf{k}}^* = \frac{1}{\Delta_0^2} \Delta_{\mathbf{k}}^\dagger X_{\mathbf{k}} (\varepsilon_{\mathbf{k}} - e_{\mathbf{k}}). \quad (8.66)$$

Furthermore, putting this result into Eq. (8.60) and applying $\Delta_{\mathbf{k}}$ on both sides of the equation yields

$$-\frac{1}{\Delta_0^2} \Delta_{\mathbf{k}} (h_{-\mathbf{k}}^0)^* \Delta_{\mathbf{k}}^\dagger X_{\mathbf{k}} (\varepsilon_{\mathbf{k}} - e_{\mathbf{k}}) = X_{\mathbf{k}} ((\varepsilon_{\mathbf{k}} - e_{\mathbf{k}}) \varepsilon_{\mathbf{k}} - \Delta_0^2). \quad (8.67)$$

The time-reversal symmetry of $h_{\mathbf{k}}^0$ (see Eq. (2.43)) implies that

$$\frac{1}{\Delta_0^2} \Delta_{\mathbf{k}} (h_{-\mathbf{k}}^0)^* \Delta_{\mathbf{k}}^\dagger = [\mathrm{i}\sigma_y] (h_{-\mathbf{k}}^0)^* [\mathrm{i}\sigma_y]^\dagger = h_{\mathbf{k}}^0, \quad (8.68)$$

and hence, Eq. (8.67) simplifies to

$$-h_{\mathbf{k}}^0 X_{\mathbf{k}} (\varepsilon_{\mathbf{k}} - e_{\mathbf{k}}) = X_{\mathbf{k}} ((\varepsilon_{\mathbf{k}} - e_{\mathbf{k}}) \varepsilon_{\mathbf{k}} - \Delta_0^2). \quad (8.69)$$

Now, a comparison with Eq. (8.63) yields the condition

$$-E_{\mathbf{k}} (\varepsilon_{\mathbf{k}} - e_{\mathbf{k}}) = (\varepsilon_{\mathbf{k}} - e_{\mathbf{k}}) \varepsilon_{\mathbf{k}} - \Delta_0^2, \quad (8.70)$$

from which we obtain the eigenvalue matrix as

$$\varepsilon_{\mathbf{k}}^2 = e_{\mathbf{k}}^2 + \Delta_0^2. \quad (8.71)$$

We shall employ a convention by which for $\Delta_0 \rightarrow 0$, the mean-field eigenvalues $\varepsilon_{\mp}(\mathbf{k})$ approach the respective eigenvalues $e_{\mp}(\mathbf{k})$ of the non-interacting system. Thus, we define

$$\varepsilon_{\mathbf{k}} = \mathrm{sgn}(e_{\mathbf{k}}) \sqrt{e_{\mathbf{k}}^2 + \Delta_0^2}, \quad (8.72)$$

where $\mathrm{sgn}(x) = x/|x|$ denotes the sign function. Note that this is an identity between

two diagonal matrices. In particular, using Eq. (1.175), we also obtain the condition

$$\varepsilon_{-\mathbf{k}} = \varepsilon_{\mathbf{k}} \quad (8.73)$$

as a consequence of the time reversal-symmetry.

It remains to calculate the matrices $X_{\mathbf{k}}$ and $Y_{\mathbf{k}}$. By Eq. (8.63), the column vectors of $X_{\mathbf{k}}$ are the eigenvectors of the free Hamiltonian $h_{\mathbf{k}}^0$, hence each of them coincides up to a constant factor with the respective column vector of the matrix $U_{\mathbf{k}}$ as given by Eq. (1.163). Thus, we may write

$$X_{\mathbf{k}} = U_{\mathbf{k}} (\varepsilon_{\mathbf{k}} + e_{\mathbf{k}}) N_{\mathbf{k}}, \quad (8.74)$$

with a yet to be determined diagonal matrix

$$N_{\mathbf{k}} = \begin{pmatrix} N_{\mathbf{k}-} & 0 \\ 0 & N_{\mathbf{k}+} \end{pmatrix}. \quad (8.75)$$

Next, by putting Eq. (8.74) into Eq. (8.66) and using that

$$(\varepsilon_{\mathbf{k}} + e_{\mathbf{k}})(\varepsilon_{\mathbf{k}} - e_{\mathbf{k}}) = \varepsilon_{\mathbf{k}}^2 - e_{\mathbf{k}}^2 = \Delta_0^2, \quad (8.76)$$

we also obtain

$$Y_{-\mathbf{k}}^* = \Delta_{\mathbf{k}}^\dagger U_{\mathbf{k}} N_{\mathbf{k}}. \quad (8.77)$$

Now, the matrix $N_{\mathbf{k}}$ is determined from the condition that $U_{\mathbf{k}}$ is unitary: in fact, Eq. (8.52) is equivalent to the two identities

$$X_{\mathbf{k}}^\dagger X_{\mathbf{k}} + Y_{-\mathbf{k}}^{\text{T}} Y_{-\mathbf{k}}^* = 1, \quad (8.78)$$

$$X_{\mathbf{k}}^\dagger Y_{\mathbf{k}} + Y_{-\mathbf{k}}^{\text{T}} X_{-\mathbf{k}}^* = 0. \quad (8.79)$$

Using Eqs. (8.74) and (8.77), we find

$$X_{\mathbf{k}}^\dagger X_{\mathbf{k}} = N_{\mathbf{k}}^\dagger (\varepsilon_{\mathbf{k}} + e_{\mathbf{k}}) U_{\mathbf{k}}^\dagger U_{\mathbf{k}} (\varepsilon_{\mathbf{k}} + e_{\mathbf{k}}) N_{\mathbf{k}} = N_{\mathbf{k}}^\dagger N_{\mathbf{k}} (\varepsilon_{\mathbf{k}} + e_{\mathbf{k}})^2, \quad (8.80)$$

and respectively,

$$Y_{-\mathbf{k}}^{\text{T}} Y_{-\mathbf{k}}^* = N_{\mathbf{k}}^\dagger U_{\mathbf{k}}^\dagger \Delta_{\mathbf{k}} \Delta_{\mathbf{k}}^\dagger U_{\mathbf{k}} N_{\mathbf{k}} = N_{\mathbf{k}}^\dagger N_{\mathbf{k}} \Delta_0^2. \quad (8.81)$$

Therefore, Eq. (8.78) yields the condition

$$N_{\mathbf{k}}^\dagger N_{\mathbf{k}} ((\varepsilon_{\mathbf{k}} + e_{\mathbf{k}})^2 + \Delta_0^2) = 1, \quad (8.82)$$

which in turn implies (by choosing $N_{\mathbf{k}}$ real-valued)

$$N_{\mathbf{k}} = \frac{1}{\sqrt{(\varepsilon_{\mathbf{k}} + e_{\mathbf{k}})^2 + \Delta_0^2}}. \quad (8.83)$$

Hence, it remains to check that Eq. (8.79) is also fulfilled:

$$X_{\mathbf{k}}^\dagger Y_{\mathbf{k}} + Y_{-\mathbf{k}}^T X_{-\mathbf{k}}^* = N_{\mathbf{k}}^\dagger \left(-(\varepsilon_{\mathbf{k}} + e_{\mathbf{k}}) U_{\mathbf{k}}^\dagger \Delta_{\mathbf{k}} U_{-\mathbf{k}}^* + U_{\mathbf{k}}^\dagger \Delta_{\mathbf{k}} U_{-\mathbf{k}}^* (\varepsilon_{\mathbf{k}} + e_{\mathbf{k}}) \right) N_{-\mathbf{k}}^*, \quad (8.84)$$

where we have used that $\Delta_{-\mathbf{k}}^T = -\Delta_{\mathbf{k}}$, while $e_{\mathbf{k}}$ and $\varepsilon_{\mathbf{k}}$ are even in \mathbf{k} . Furthermore, the property (1.176) implies that

$$\Delta_{\mathbf{k}} U_{-\mathbf{k}}^* = \Delta_0 [i\sigma_y] U_{-\mathbf{k}}^* = \Delta_0 U_{\mathbf{k}} e^{-i\varphi_{\mathbf{k}}} \sigma_z, \quad (8.85)$$

and hence the above expression simplifies to

$$X_{\mathbf{k}}^\dagger Y_{\mathbf{k}} + Y_{-\mathbf{k}}^T X_{-\mathbf{k}}^* = N_{\mathbf{k}}^\dagger \left(-\Delta_0 (\varepsilon_{\mathbf{k}} + e_{\mathbf{k}}) e^{-i\varphi_{\mathbf{k}}} \sigma_z + \Delta_0 e^{-i\varphi_{\mathbf{k}}} \sigma_z (\varepsilon_{\mathbf{k}} + e_{\mathbf{k}}) \right) N_{-\mathbf{k}}^*, \quad (8.86)$$

which vanishes because any two diagonal matrices commute with each other. In summary, the (4×4) Hamiltonian matrix $\mathcal{H}_{\mathbf{k}}$ as defined in Eq. (8.46) is diagonalized by the unitary matrix $\mathcal{U}_{\mathbf{k}}$ in Eq. (8.51), where $X_{\mathbf{k}}$ and $Y_{\mathbf{k}}$ are given explicitly by

$$X_{\mathbf{k}} = U_{\mathbf{k}} (\varepsilon_{\mathbf{k}} + e_{\mathbf{k}}) \frac{1}{\sqrt{(\varepsilon_{\mathbf{k}} + e_{\mathbf{k}})^2 + \Delta_0^2}}, \quad (8.87)$$

$$Y_{\mathbf{k}} = -\Delta_{\mathbf{k}} U_{-\mathbf{k}}^* \frac{1}{\sqrt{(\varepsilon_{\mathbf{k}} + e_{\mathbf{k}})^2 + \Delta_0^2}}. \quad (8.88)$$

These formulae generalize the results presented in Ref. [SU91, Eq. (2.13)] to the case without SU(2) spin rotation invariance. Note, in particular, that $e_{\mathbf{k}}$ and $\varepsilon_{\mathbf{k}}$ are diagonal matrices, which contain the eigenvalues of the free Hamiltonian (subtracted by the chemical potential) and respectively of the mean-field Hamiltonian, where the latter eigenvalues are given by Eq. (8.72).

8.4.3. Order parameter

Having diagonalized the mean-field Hamiltonian, it is no more difficult to calculate the order parameter (8.11). In terms of the new annihilation and creation operators $\hat{b}_n(\mathbf{k})$ and $\hat{b}_n^\dagger(\mathbf{k})$, we can write this as

$$\begin{aligned} \Psi_{ss'}(\mathbf{k}) = \sum_{n,n'} \left\langle \left(X_{sn}(\mathbf{k}) \hat{b}_n(\mathbf{k}) + Y_{sn}(\mathbf{k}) \hat{b}_n^\dagger(-\mathbf{k}) \right) \right. \\ \left. \times \left(X_{s'n'}(-\mathbf{k}) \hat{b}_{n'}(-\mathbf{k}) + Y_{s'n'}(-\mathbf{k}) \hat{b}_{n'}^\dagger(\mathbf{k}) \right) \right\rangle. \end{aligned} \quad (8.89)$$

Using the anticommutation relation between these operators,

$$[\hat{b}_{n_1}(\mathbf{k}), \hat{b}_{n_2}^\dagger(\mathbf{k}')]_{+} = \delta_{n_1 n_2} \delta_{\mathbf{k}, \mathbf{k}'}, \quad (8.90)$$

we obtain the identities

$$\langle \hat{b}_n(\mathbf{k}) \hat{b}_{n'}^\dagger(\mathbf{k}) \rangle = \delta_{nn'} (1 - f_n(\mathbf{k})), \quad (8.91)$$

$$\langle \hat{b}_n^\dagger(-\mathbf{k}) \hat{b}_{n'}(-\mathbf{k}) \rangle = \delta_{nn'} f_n(-\mathbf{k}) = \delta_{nn'} f_n(\mathbf{k}), \quad (8.92)$$

with the Fermi distribution function $f_n(\mathbf{k}) \equiv f(e_n(\mathbf{k}))$ given by Eq. (7.10). With these relations, Eq. (8.89) simplifies to

$$\Psi_{ss'}(\mathbf{k}) = \sum_n X_{sn}(\mathbf{k}) Y_{s'n}(-\mathbf{k}) (1 - f_n(\mathbf{k})) + \sum_n Y_{sn}(\mathbf{k}) X_{s'n}(-\mathbf{k}) f_n(\mathbf{k}), \quad (8.93)$$

which can be written more compactly in matrix form as

$$\Psi_{\mathbf{k}} = X_{\mathbf{k}} (1 - f_{\mathbf{k}}) Y_{-\mathbf{k}}^T + Y_{\mathbf{k}} f_{\mathbf{k}} X_{-\mathbf{k}}^T. \quad (8.94)$$

We now put the matrices $X_{\mathbf{k}}$ and $Y_{\mathbf{k}}$ as given by Eqs. (8.87)–(8.88) into this formula. Then, we obtain for the first term,

$$X_{\mathbf{k}} (1 - f_{\mathbf{k}}) Y_{-\mathbf{k}}^T = U_{\mathbf{k}} (\varepsilon_{\mathbf{k}} + E_{\mathbf{k}}) N_{\mathbf{k}} (1 - f_{\mathbf{k}}) N_{\mathbf{k}} U_{\mathbf{k}}^\dagger \Delta_{\mathbf{k}}, \quad (8.95)$$

where we have used again Eq. (8.22). Furthermore, by Eqs. (8.72) and (8.83), we have

$$N_{\mathbf{k}}^2 = \frac{1}{(\varepsilon_{\mathbf{k}} + e_{\mathbf{k}})^2 + \Delta_0^2} = \frac{1}{2\varepsilon_{\mathbf{k}}(\varepsilon_{\mathbf{k}} + e_{\mathbf{k}})}, \quad (8.96)$$

and consequently,

$$X_{\mathbf{k}} (1 - f_{\mathbf{k}}) Y_{-\mathbf{k}}^T = U_{\mathbf{k}} \frac{1 - f_{\mathbf{k}}}{2\varepsilon_{\mathbf{k}}} U_{\mathbf{k}}^\dagger \Delta_{\mathbf{k}}. \quad (8.97)$$

Similarly, we obtain for the second term in Eq. (8.94),

$$Y_{\mathbf{k}} f_{\mathbf{k}} X_{-\mathbf{k}}^T = -\Delta_{\mathbf{k}} U_{-\mathbf{k}}^* \frac{f_{\mathbf{k}}}{2\varepsilon_{\mathbf{k}}} U_{-\mathbf{k}}^T = -U_{\mathbf{k}} \frac{f_{\mathbf{k}}}{2\varepsilon_{\mathbf{k}}} U_{\mathbf{k}}^\dagger \Delta_{\mathbf{k}}, \quad (8.98)$$

where we have used the explicit form of $\Delta_{\mathbf{k}}$, Eq. (8.44), and the property (1.176) of $U_{\mathbf{k}}$. By combining Eqs. (8.97) and (8.98), we arrive at

$$\Psi_{\mathbf{k}} = U_{\mathbf{k}} \frac{1 - 2f_{\mathbf{k}}}{2\varepsilon_{\mathbf{k}}} U_{\mathbf{k}}^\dagger \Delta_{\mathbf{k}}. \quad (8.99)$$

To obtain an even more concrete expression for the order parameter, let us define the function

$$\gamma(\varepsilon) = \frac{1 - 2f(\varepsilon)}{2\varepsilon} = \frac{1}{2\varepsilon} \tanh\left(\frac{\beta\varepsilon}{2}\right), \quad (8.100)$$

which in the zero-temperature limit reduces to

$$\lim_{\beta \rightarrow \infty} \gamma(\varepsilon) = \frac{1}{2|\varepsilon|}. \quad (8.101)$$

With this, we can write Eq. (8.99) as

$$\Psi_{\mathbf{k}} = U_{\mathbf{k}} \gamma(\varepsilon_{\mathbf{k}}) U_{\mathbf{k}}^\dagger \Delta_0 [\mathrm{i}\sigma_y]. \quad (8.102)$$

Next, we split the diagonal matrix into two terms,

$$\gamma(\varepsilon_{\mathbf{k}}) \equiv \begin{pmatrix} \gamma(\varepsilon_-(\mathbf{k})) & 0 \\ 0 & \gamma(\varepsilon_+(\mathbf{k})) \end{pmatrix} \quad (8.103)$$

$$= \frac{\gamma(\varepsilon_-(\mathbf{k})) + \gamma(\varepsilon_+(\mathbf{k}))}{2} \mathbb{1} + \frac{\gamma(\varepsilon_-(\mathbf{k})) - \gamma(\varepsilon_+(\mathbf{k}))}{2} \sigma_z. \quad (8.104)$$

Using the unitarity as well as the property (1.170) of $U_{\mathbf{k}}$, this yields

$$\Psi_{\mathbf{k}} = \Delta_0 \frac{\gamma(\varepsilon_-(\mathbf{k})) + \gamma(\varepsilon_+(\mathbf{k}))}{2} \mathrm{i}\sigma_y - \Delta_0 \frac{\gamma(\varepsilon_-(\mathbf{k})) - \gamma(\varepsilon_+(\mathbf{k}))}{2} [-\hat{\mathbf{g}}(\mathbf{k}) \cdot \boldsymbol{\sigma}] \mathrm{i}\sigma_y, \quad (8.105)$$

where we have introduced the notation

$$\hat{\mathbf{g}}(\mathbf{k}) = \frac{\mathbf{g}(\mathbf{k})}{|\mathbf{g}(\mathbf{k})|} \quad (8.106)$$

for the normalized vector $\mathbf{g}(\mathbf{k})$, which appears in the free Hamiltonian (1.157). The above Eq. (8.105) is our general result for the order parameter matrix $\Psi_{\mathbf{k}} \equiv \Psi_{ss'}(\mathbf{k})$. In contrast to the gap function (8.44), the order parameter depends nontrivially on the Bloch momentum \mathbf{k} and on the chemical potential μ , and it is not of a pure singlet form.

8.4.4. Singlet and triplet amplitudes

Next, we define the (*spin*) *singlet and triplet amplitudes* $\Psi_s(\mathbf{k})$ and $\Psi_t(\mathbf{k})$ of the order parameter through the expansion

$$\Psi(\mathbf{k}) = \Psi_s(\mathbf{k}) \mathrm{i}\sigma_y + \Psi_t(\mathbf{k}) [\hat{\mathbf{g}}(\mathbf{k}) \cdot \boldsymbol{\sigma}] \mathrm{i}\sigma_y. \quad (8.107)$$

In fact, we can compare this expansion with Eq. (8.31), which was deduced from symmetry considerations only. Obviously, the singlet and triplet amplitudes are related to the functions $\chi(\mathbf{k})$ and $\mathbf{c}(\mathbf{k})$ in the latter expansion by

$$\chi(\mathbf{k}) = \Psi_s(\mathbf{k}), \quad (8.108)$$

$$\mathbf{c}(\mathbf{k}) = \Psi_t(\mathbf{k}) \hat{\mathbf{g}}(\mathbf{k}). \quad (8.109)$$

Concretely, from our result (8.105), we read off the singlet and triplet amplitudes as

$$\Psi_s(\mathbf{k}) = \Delta_0 \frac{\gamma(\varepsilon_+(\mathbf{k})) + \gamma(\varepsilon_-(\mathbf{k}))}{2}, \quad (8.110)$$

$$\Psi_t(\mathbf{k}) = \Delta_0 \frac{\gamma(\varepsilon_+(\mathbf{k})) - \gamma(\varepsilon_-(\mathbf{k}))}{2}. \quad (8.111)$$

In the zero-temperature limit, these formulae reduce to

$$\Psi_s(\mathbf{k}) = \frac{\Delta_0}{4} \left(\frac{1}{|\varepsilon_+(\mathbf{k})|} + \frac{1}{|\varepsilon_-(\mathbf{k})|} \right), \quad (8.112)$$

$$\Psi_t(\mathbf{k}) = \frac{\Delta_0}{4} \left(\frac{1}{|\varepsilon_+(\mathbf{k})|} - \frac{1}{|\varepsilon_-(\mathbf{k})|} \right). \quad (8.113)$$

For comparison, consider the corresponding singlet and triplet amplitudes of the gap function, which can be defined analogously through

$$\Delta(\mathbf{k}) = \Delta_s(\mathbf{k}) i\sigma_y + \Delta_t(\mathbf{k}) [\hat{\mathbf{g}}(\mathbf{k}) \cdot \boldsymbol{\sigma}] i\sigma_y. \quad (8.114)$$

In fact, the result (8.44) for the gap function is equivalent to

$$\Delta_s(\mathbf{k}) = \Delta_0, \quad \Delta_t(\mathbf{k}) = 0, \quad (8.115)$$

and for this reason, we have called Eq. (8.44) a *purely singlet-type* gap function.

8.4.5. Gap equation and critical temperature

So far, we have calculated the gap function $\Delta_{ss'}(\mathbf{k})$ and the order parameter $\Psi_{ss'}(\mathbf{k})$ up to the scalar gap parameter Δ_0 . The latter was defined in Eq. (8.45), which can be written equivalently in terms of the order parameter and a trace over the spin indices as

$$\Delta_0 = \frac{g}{2} \sum_{\mathbf{k}} \text{Tr}(\Psi(\mathbf{k}) [i\sigma_y]^\dagger). \quad (8.116)$$

By inserting our result for the order parameter, Eqs. (8.107) and (8.110)–(8.111), and by using that the Pauli matrices are traceless,

$$\text{Tr}(\hat{\mathbf{g}}(\mathbf{k}) \cdot \boldsymbol{\sigma}) = 0, \quad (8.117)$$

we obtain immediately

$$\Delta_0 = \frac{g}{2} \sum_{\mathbf{k}} 2\Psi_s(\mathbf{k}) = \frac{g}{2} \Delta_0 \sum_{\mathbf{k}} (\gamma(\varepsilon_+(\mathbf{k})) + \gamma(\varepsilon_-(\mathbf{k}))), \quad (8.118)$$

which is equivalent to the scalar *gap equation*

$$1 = \frac{g}{2} \sum_{\mathbf{k}} \sum_n \frac{1}{2\varepsilon_n(\mathbf{k})} \tanh\left(\frac{\beta\varepsilon_n(\mathbf{k})}{2}\right). \quad (8.119)$$

Note that this agrees with the standard form of the gap equation in the SU(2)-symmetric case (see Ref. [VW90]). If combined with the expression (8.72) for the mean-field energies $\varepsilon_n(\mathbf{k})$, the gap equation constitutes an implicit equation for determining the gap parameter Δ_0 as a function of the inverse temperature β , the chemical potential μ and the coupling constant g . Furthermore, the gap equation allows one to estimate the critical temperature for the onset of superconductivity, which is defined as the temperature where the gap vanishes (for a short discussion, see Ref. [Sch+16a, Sct. IV.D]).

9. Application to the Rashba model

In this chapter, we apply the combined fRG and mean-field approach described in the previous chapters to the tight-binding Rashba model of Sect. 2.3. We first specify the model parameters and briefly explain our numerical implementation, and after that summarize our results for the effective interaction, the order parameter and the gap function. For a more detailed discussion, we refer the interested reader to the original publication [Sch+16a] (parts of which are reproduced in this chapter).

9.1. Model parameters and numerical implementation

We start from the two-dimensional tight-binding Rashba model as described by the Hamiltonian matrix $H_{ss'}(\mathbf{k})$ given by Eq. (2.105), where the functions $f(\mathbf{k})$ and $\mathbf{g}(\mathbf{k})$ are defined in Eqs. (2.151) and (2.163)–(2.168), respectively, and where the parameters α/t and γ/t are specified in Eq. (2.170). The corresponding Hamiltonian operator is given in second quantization by Eq. (8.5). To this quadratic part of the Hamiltonian, we now add a quartic (two-body) interaction term of the general form

$$\hat{V} = -\frac{1}{2} \sum_{\mathbf{k}_1, \mathbf{k}_2, \mathbf{k}_3} \sum_{s_1, \dots, s_4} V_{s_1 \dots s_4}(\mathbf{k}_1, \mathbf{k}_2, \mathbf{k}_3) \hat{a}_{s_1}^\dagger(\mathbf{k}_1) \hat{a}_{s_2}^\dagger(\mathbf{k}_2) \hat{a}_{s_3}(\mathbf{k}_3) \hat{a}_{s_4}(\mathbf{k}_4). \quad (9.1)$$

In this expression, \mathbf{k}_4 is fixed by the “Bloch momentum conservation”, i.e.,

$$\mathbf{k}_4 = \mathbf{K} + \mathbf{k}_1 + \mathbf{k}_2 - \mathbf{k}_3, \quad (9.2)$$

where the reciprocal lattice vector \mathbf{K} ensures that \mathbf{k}_4 lies in the first Brillouin zone (see Ref. [Sch+16a, Eq. (A147)]). Concretely, we choose a momentum-independent interaction kernel given by

$$V_{s_1 \dots s_4}(\mathbf{k}_1, \mathbf{k}_2, \mathbf{k}_3) = \frac{U}{2} (\delta_{s_1 s_3} \delta_{s_2 s_4} - \delta_{s_1 s_4} \delta_{s_2 s_3}), \quad (9.3)$$

such that Eq. (9.1) coincides with the normal-ordered operator

$$\hat{V} = U \sum_{\mathbf{R}} : \hat{n}_\uparrow(\mathbf{R}) \hat{n}_\downarrow(\mathbf{R}) : \equiv U \sum_{\mathbf{R}} \hat{a}_\uparrow^\dagger(\mathbf{R}) \hat{a}_\downarrow^\dagger(\mathbf{R}) \hat{a}_\downarrow(\mathbf{R}) \hat{a}_\uparrow(\mathbf{R}), \quad (9.4)$$

where the spin-resolved density operator is defined as

$$\hat{n}_s(\mathbf{R}) = \hat{a}_s^\dagger(\mathbf{R}) \hat{a}_s(\mathbf{R}). \quad (9.5)$$

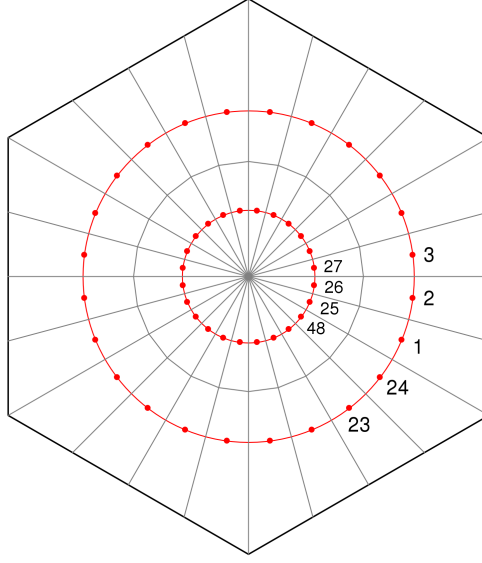


Figure 9.1: Division of the Brillouin zone into 48 patches and representative momenta on the two Fermi lines. The latter are only schematically represented here as perfect circles, which is indeed a good approximation for small Fermi energies (near the band crossing, see Fig. 2.1). The patches are labeled counterclockwise, with patches on the outer Fermi line having smaller indices than those on the inner Fermi line.

An interaction of this form is called *local*, because it contains only products of electronic density operators at the same lattice site. Furthermore, we define the parameter

$$U/t = -2, \quad (9.6)$$

which, by its negative sign, implies an *attractive* interaction between electrons. In the framework of the fRG, the electron-electron interaction determines the *initial condition* for the one-line-irreducible four-point function (see Eqs. (7.21)–(7.23)).

For the concrete implementation of the RGE, we use the non-strict regulator function

$$\chi_\Lambda(e) = \left(10^{(\Lambda - |e|)/(0.05\Lambda)} + 1 \right)^{-1} \quad (9.7)$$

in the denominator of the scale-dependent covariance (7.12). This regulator function is always greater than zero and smaller than one, hence all momenta inside a shell of thickness Λ around the Fermi lines are *suppressed* (but not cut off). However, we perform our calculations at a tiny positive temperature (such that $\beta t = 10^{10}$), where χ_Λ can be used down to scales $\Lambda \approx 10^{-10}t$. Next, we choose the initial scale Λ_0 much larger than the bandwidth of the model (given by Eq. (2.172)), i.e.,

$$\Lambda_0/t = 40. \quad (9.8)$$

Thus, the condition (7.15) is approximately fulfilled for any band index n and any Bloch momentum \mathbf{k} , which implies that the covariance essentially vanishes at the initial scale.

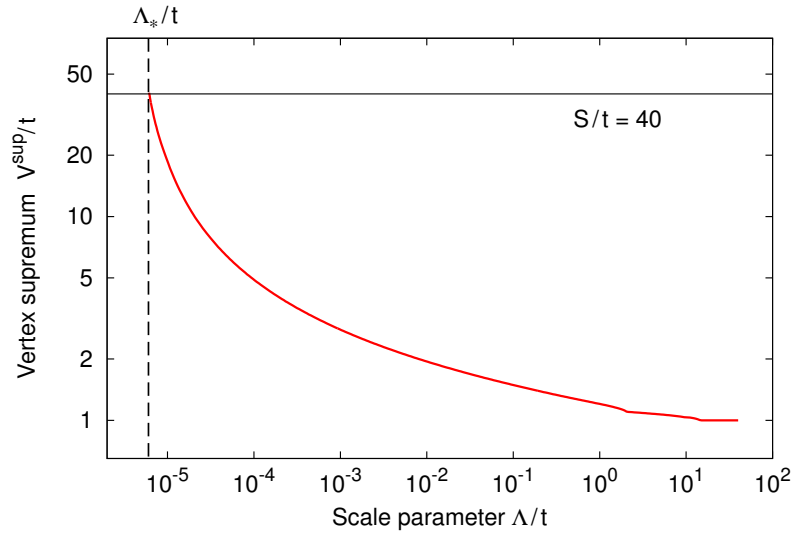


Figure 9.2: Double-logarithmic plot of the scale-dependent vertex supremum $V^{\text{sup}}(\Lambda)$ as obtained for a chemical potential of $\mu/t = -2$. The RG flow is stopped at the scale Λ_* where V^{sup} exceeds the threshold parameter S .

Furthermore, the RG flow is stopped at the *stopping scale* Λ_* defined by

$$V^{\text{sup}}(\Lambda_*) = S, \quad (9.9)$$

with the scale-dependent *vertex supremum*

$$V^{\text{sup}}(\Lambda) := \sup\{|(V_\Lambda)_{n_1 \dots n_4}(\mathbf{k}_1, \mathbf{k}_2, \mathbf{k}_3)|\}. \quad (9.10)$$

The threshold parameter S is chosen more than an order of magnitude larger than the initial interaction (9.6), i.e.,

$$S/t = 40. \quad (9.11)$$

By this choice, the stopping scale Λ_* is always close to, but slightly above the *critical scale* Λ_c where the interaction vertex diverges (see Ref. [Sch+16a]). In the following, we will not distinguish explicitly between these two scales.

In our numerical implementation, we solve directly the RGE for the discretized interaction vertex as given by Theorem 7.3. For this purpose, we divide the Brillouin zone into 48 patches, which are shown schematically in Fig. 9.1. The solution V_Λ with the given initial interaction $V_{\Lambda_0} \equiv V$ can be written formally as

$$V_\Lambda = V_{\Lambda_0} + \int_{\Lambda_0}^{\Lambda} d\Lambda \frac{d}{d\Lambda} V_\Lambda = V_{\Lambda_0} + \int_{\Lambda_0}^{\Lambda} d\Lambda [\Phi_\Lambda^{\text{pp}} + \Phi_\Lambda^{\text{ph,c}} + \Phi_\Lambda^{\text{ph,d}}]. \quad (9.12)$$

This scale integral can be performed numerically by starting at the initial scale Λ_0 , and by stepwise determining $V_{\Lambda+d\Lambda}$ from the previously calculated V_Λ . Here, we dynamically

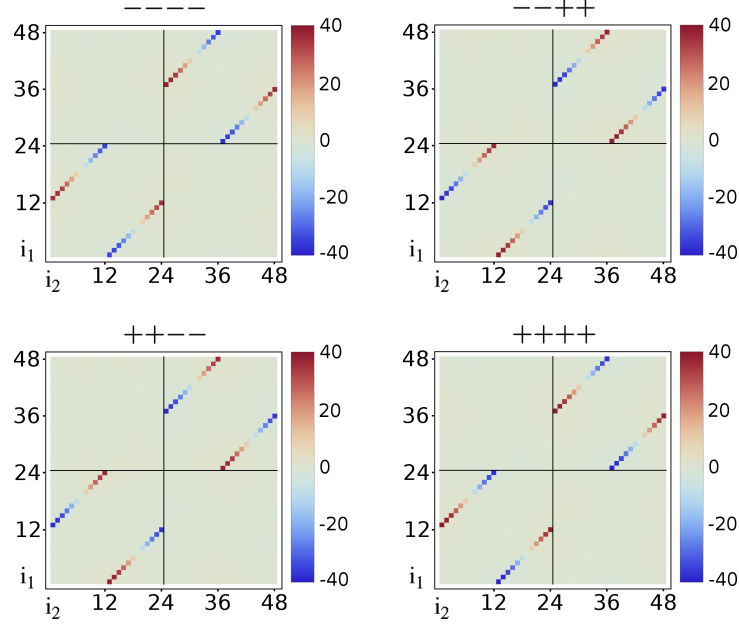


Figure 9.3: Real part of the interaction vertex in the band basis, $\text{Re}(V_\Lambda)_{n_1 n_2 n_3 n_4}(i_1, i_2, i_3)/t$, after following the RG flow down to the stopping scale $\Lambda = \Lambda_*$ (for $\mu/t = -2$). Shown are the four non-vanishing contributions with band indices $n_1 n_2 n_3 n_4$ and the dependence on two patch indices i_1 and i_2 (while the third patch index is fixed as $i_3 = 1$). The patches are labeled as shown in Fig. 9.1.

adjust the integration steps $d\Lambda$ depending on how fast the interaction vertex changes in the flow. In this way, the divergence at the critical scale can be approached numerically by gradually decreasing the step size.

9.2. Effective interaction and critical scale

Our numerical result for the vertex supremum $V^{\text{sup}}(\Lambda)$ as a function of the scale parameter Λ is shown in Fig. 9.2. One clearly sees that the interaction vertex grows with decreasing Λ and eventually approaches a divergence at the critical scale. This is interpreted as a signal for “an instability leading to an ordered phase via spontaneous symmetry breaking” [RRM07] (see also Ref. [KL65, footnote 2]). The divergence of the effective interaction is due to the truncation, which in particular restricts to the symmetric phase. It has been shown [Ger+05; Sal+04] that the flow can be continued into the symmetry-broken phase and down to $\Lambda = 0$ if the symmetry-breaking terms indicated by the effective interaction above Λ_c are included. The numerical result for the effective interaction at the stopping scale is shown in the band basis in Fig. 9.3 and in the spin basis in Fig. 9.4. We have fixed the third patch index as $i_3 = 1$ and analyzed the dependence of the effective interaction on i_1 and i_2 for all possible band and spin

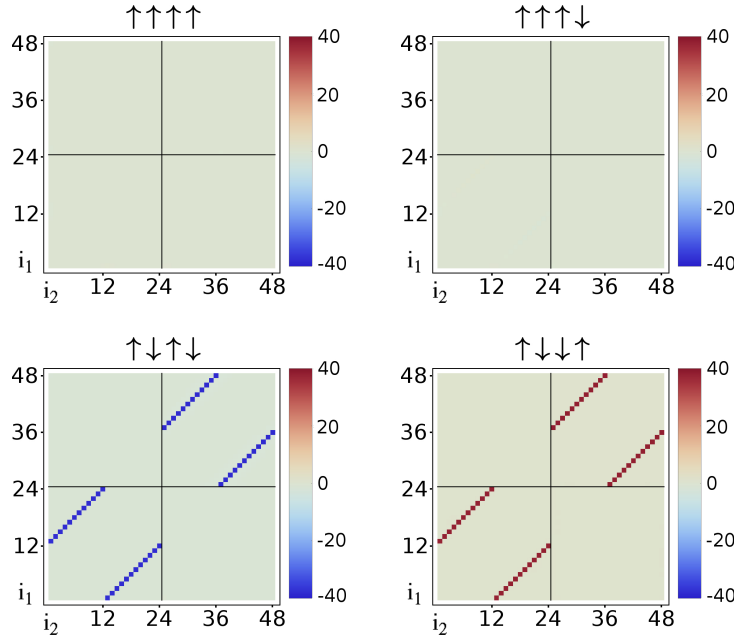


Figure 9.4: Interaction vertex $(V_\Lambda)_{s_1 s_2 s_3 s_4}(i_1, i_2, i_3)/t$ in the spin basis at the stopping scale $\Lambda = \Lambda_*$ (for $\mu/t = -2$). Shown are four representative spin configurations $s_1 s_2 s_3 s_4$ and the dependence on two patch indices i_1 and i_2 (while $i_3 = 1$). The patches are labeled again as shown in Fig. 9.1.

combinations (of which four representative ones are shown in Figs. 9.3 and 9.4, respectively). The result clearly signals a superconducting instability, where pairing occurs between opposite momenta on the same Fermi line. The discretized effective interaction at the stopping scale is well represented in the band basis by

$$(V_{\Lambda_*})_{n_1 \dots n_4}(i_1, i_2, i_3) = \mathbb{1}(\boldsymbol{\pi}_{i_1} = -\boldsymbol{\pi}_{i_2}) S \delta_{n_1 n_2} \delta_{n_3 n_4} n_2 n_3 e^{i\varphi(\boldsymbol{\pi}_{i_3}) - i\varphi(\boldsymbol{\pi}_{i_2})}, \quad (9.13)$$

and in the spin basis by

$$(V_{\Lambda_*})_{s_1 \dots s_4}(i_1, i_2, i_3) = \mathbb{1}(\boldsymbol{\pi}_{i_1} = -\boldsymbol{\pi}_{i_2}) (-S) (\delta_{s_1 s_3} \delta_{s_2 s_4} - \delta_{s_1 s_4} \delta_{s_2 s_3}), \quad (9.14)$$

where S is the threshold parameter (see Eq. (9.11)). The corresponding interaction operator (which is obtained by first putting Eq. (9.14) into the projection ansatz (7.65) and then inserting the resulting interaction kernel into Eq. (9.1)) is approximately given by

$$\hat{V}_{\Lambda_*} = \frac{S}{2N} \sum_{\mathbf{k}_2, \mathbf{k}_3} \sum_{s_1, \dots, s_4} (\delta_{s_1 s_3} \delta_{s_2 s_4} - \delta_{s_1 s_4} \delta_{s_2 s_3}) \hat{a}_{s_1}^\dagger(-\mathbf{k}_2) \hat{a}_{s_2}^\dagger(\mathbf{k}_2) \hat{a}_{s_3}(\mathbf{k}_3) \hat{a}_{s_4}(-\mathbf{k}_3), \quad (9.15)$$

where N is the number of patches (in our case, $N = 48$). The factor $1/N$ corresponds to the area of a single \mathbf{k} -space patch, which arises because our effective interaction (9.14) turns out to have a $\mathbf{k}_1 = -\mathbf{k}_2$ restriction on the level of patches (see the derivation in

Ref. [Sch+16a, Appendix C.2]). By explicitly performing the spin sums and using the canonical anticommutation relations, we further obtain the equivalent expression

$$\hat{V}_{\Lambda_*} = -g \sum_{\mathbf{k}, \mathbf{k}'} \hat{a}_{\uparrow}^{\dagger}(-\mathbf{k}) \hat{a}_{\downarrow}^{\dagger}(\mathbf{k}) \hat{a}_{\downarrow}(\mathbf{k}') \hat{a}_{\uparrow}(-\mathbf{k}'), \quad (9.16)$$

where we have defined the coupling constant

$$g := \frac{2S}{N} > 0. \quad (9.17)$$

An interaction of the form (9.16) is called *singlet* superconducting interaction (see Sect. 8.4). We have obtained this result for the effective interaction independently of the chemical potential μ , whether it is above ($\mu > 0$) or below ($\mu < 0$) the band crossing of the Rashba dispersion.

We stress here that the form of the effective interaction depends crucially on the projection scheme used to discretize the scale-dependent interaction vertex. Our result given by Eqs. (9.13)–(9.14) is obtained by using the refined projection scheme (see Sect. 7.3), whereas a qualitatively different result would be obtained in the projection scheme of Ref. [PHT13] (see the discussion in Ref. [Sch+16a]). In particular, our numerical implementation of the RGE shows that the scale-dependent interaction vertex V_{Λ} has relevant contributions from both bands of the model at any scale Λ , even if the Fermi level lies in the lower band (such that the upper band is empty at zero temperature). This is most clearly seen in Fig. 9.3, which shows the four contributions

$$(V_{\Lambda})_{----}, \quad (V_{\Lambda})_{--++}, \quad (V_{\Lambda})_{++--}, \quad (V_{\Lambda})_{++++} \quad (9.18)$$

of the interaction vertex in the band basis at the stopping scale $\Lambda = \Lambda_*$ (for $\mu < 0$, where the Fermi level lies in the lower band). The four contributions are of equal magnitude, and the momentum dependence is well described by Eq. (9.13). The unexpected result that even in this case, contributions to the interaction vertex with an upper band index cannot be neglected in RG flow, has been explained further by means of an analytical resummation of the particle-particle ladder in Ref. [Sch+16a, Sect. III.E]. In fact, we have provided there a general, analytical solution of the particle-particle flow in the spin basis, which applies to the case where the single-particle Hamiltonian is not SU(2) invariant. This analytical solution is completely consistent with our numerical results.

Next, we show our results for the critical scale as well as the phase diagram: The RG flow is stopped at the scale Λ_* , where the interaction vertex exceeds the threshold S and hence a divergence is approached, which signals the breakdown of the Fermi liquid description. Figure 9.5 shows Λ_* as a function of the chemical potential μ . The numerical data turn out to be well represented by the formula

$$\Lambda_*/t = 5.0 \exp\left(-\frac{2}{|U|D(\mu)}\right), \quad (9.19)$$

where U is the initial interaction strength (given by Eq. (9.6)), and $D(\mu)$ is the density of states of the minimal tight-binding model (see Fig. 2.2). The exponent in the above

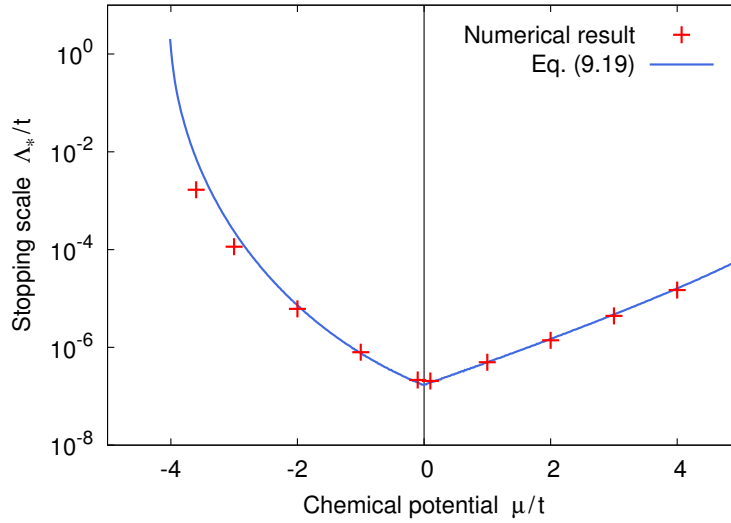


Figure 9.5: Logarithmic plot of the stopping scale Λ_* as a function of the chemical potential μ , for an initial interaction of $U/t = -2$. The vertical line (where $\mu = 0$) marks the position of the band crossing of the Rashba dispersion. The red points show the stopping scales obtained from the numerical implementation of the RG flow. The blue curve corresponds to Eq. (9.19), which can be motivated by an analytical resummation of the particle-particle ladder.

formula can in fact be motivated by an analytical resummation of the particle-particle ladder, as we have shown in Ref. [Sch+16a, Sct. III.E]. In particular, the sharp increase of Λ_* for small μ reflects the diverging density of states at the band minimum of the Rashba dispersion, and the kink at $\mu = 0$ corresponds to the kink in the density of states at the band crossing. Finally, concerning the interpretation of Fig. 9.5 as a “phase diagram” (in particular in relation to the Mermin–Wagner theorem), we refer the interested reader to the discussion in Ref. [Sch+16a, Sct. III.D].

9.3. Solving the gap equation

Our result for the effective interaction at the critical scale, Eq. (9.15), represents a superconducting interaction of the form (8.6), with a singlet interaction kernel as defined in Eq. (8.41). Therefore, we can employ the mean-field solution derived in Sct. 8.4 for the general case of a time-reversal invariant Hamiltonian $H_{ss'}(\mathbf{k})$ (where here, we specialize to the tight-binding Rashba Hamiltonian defined in Sct. 2.3). In particular, we thus obtain the order parameter in terms of the singlet and triplet amplitudes, Eqs. (8.110)–(8.111), or Eqs. (8.112)–(8.113) in the zero-temperature limit.

For small energies, i.e., in the vicinity of the band crossing, the dispersion of our tight-binding model is approximately described by the ideal Rashba model (see Sct. 3.2). Therefore, near $\mu = 0$, the singlet and triplet amplitudes of the order parameter essen-

tially depend only on the modulus $|\mathbf{k}|$. Figure 9.6 shows these amplitudes as a function of k_x for three different values of the chemical potential μ (above, at, and below the band crossing), where we assume a small value of the scalar gap parameter, $\Delta_0/t = 0.1$. We can qualitatively understand these results as follows: First, we restrict ourselves to such momenta \mathbf{k} which satisfy the condition $|e_n(\mathbf{k})| \equiv |E_n(\mathbf{k}) - \mu| < \Lambda_*$. For small enough Δ_0 , we may then estimate using Eq. (8.72),

$$\begin{cases} |\varepsilon_-(\mathbf{k})| \ll |\varepsilon_+(\mathbf{k})|, & \text{if } |e_-(\mathbf{k})| < \Lambda_*, \\ |\varepsilon_+(\mathbf{k})| \ll |\varepsilon_-(\mathbf{k})|, & \text{if } |e_+(\mathbf{k})| < \Lambda_*. \end{cases} \quad (9.20)$$

From Eqs. (8.112)–(8.113), we therefore obtain

$$\begin{cases} \Psi_s(\mathbf{k}) \approx \frac{\Delta_0}{4|\varepsilon_-(\mathbf{k})|} \approx -\Psi_t(\mathbf{k}), & \text{if } |e_-(\mathbf{k})| < \Lambda_*, \\ \Psi_s(\mathbf{k}) \approx \frac{\Delta_0}{4|\varepsilon_+(\mathbf{k})|} \approx \Psi_t(\mathbf{k}), & \text{if } |e_+(\mathbf{k})| < \Lambda_*. \end{cases} \quad (9.21)$$

This means, if \mathbf{k} is close to the Fermi line of the lower or the upper band, then the singlet and triplet amplitudes are of equal magnitude, and they have the opposite or the same sign, respectively. In particular, if the Fermi level is above the band crossing ($\mu > 0$), then there is one Fermi line for each band, and hence the ratio between Ψ_s and Ψ_t changes sign in the Brillouin zone as seen in the uppermost panel of Fig. 9.6.

Furthermore, we have solved the scalar gap equation (8.119) both analytically (in the asymptotic regime) and numerically. For $\beta \rightarrow \infty$, this gap equation reduces to

$$1 = \frac{g}{4} \sum_{\mathbf{k}} \sum_n \frac{1}{\sqrt{(E_n(\mathbf{k}) - \mu)^2 + \Delta_0^2}}. \quad (9.22)$$

In terms of the density of states (2.171), we can write this equivalently as

$$1 = \frac{g}{4} \int_{\mu-\Lambda_*}^{\mu+\Lambda_*} dE \frac{D(E)}{\sqrt{(E - \mu)^2 + \Delta_0^2}}. \quad (9.23)$$

For $E < 0$ (i.e., below the band crossing), the dispersion of the tight-binding model can be approximated by the ideal Rashba model, whose density of states can be calculated explicitly (see Ref. [Sch+16a, Eq. (29)]). By putting the result for $D(E)$ into Eq. (9.23), we obtain

$$1 = g \frac{\sqrt{3}}{16\pi} \frac{(a_0 k_R)^2}{E_R} \int_{\mu-\Lambda_*}^{\mu+\Lambda_*} dE \frac{1}{\sqrt{1 + E/E_R}} \frac{1}{\sqrt{(E - \mu)^2 + \Delta_0^2}}, \quad (9.24)$$

where a_0 denotes the lattice constant, while k_R and E_R denote the Rashba wavevector and the Rashba energy, respectively (see Sect. 3.2). Note that μ and E are measured relatively to the band crossing, and hence the minimum of the lower band has the negative energy $E = -E_R$. For simplicity, we now ignore the integration boundaries depending

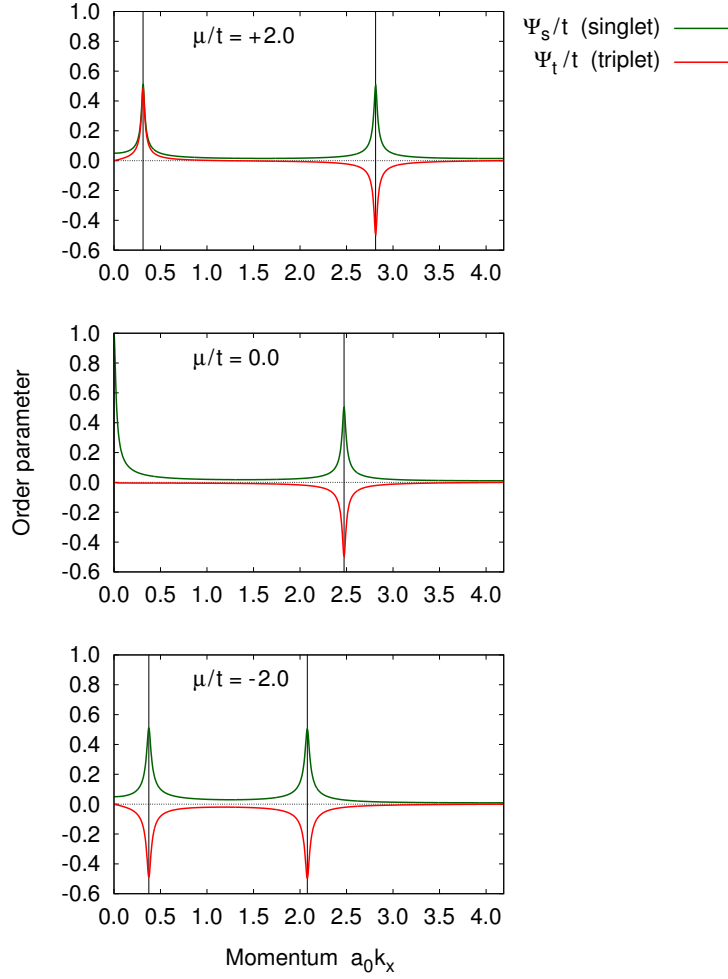


Figure 9.6: Spin singlet and triplet amplitudes of the order parameter, for $\Delta_0/t = 0.1$. Vertical lines mark the positions of the two Fermi lines for the respective values of μ .

on Λ_* and instead integrate over the whole interval $-E_R \leq E \leq 0$. Furthermore, as we are interested in the case where $\mu \approx -E_R$, we define the dimensionless variables

$$\bar{\mu} \equiv \frac{\mu + E_R}{E_R}, \quad \bar{E} \equiv \frac{E + E_R}{E_R}, \quad \bar{\Delta} \equiv \frac{\Delta_0}{E_R}, \quad (9.25)$$

as well as the dimensionless coupling constant

$$\bar{g} \equiv g \frac{\sqrt{3}}{16\pi} \frac{(a_0 k_R)^2}{E_R}. \quad (9.26)$$

In terms of these new variables, we can write the gap equation (9.24) compactly as

$$1 = \bar{g} \int_0^1 d\bar{E} \frac{1}{\sqrt{\bar{E}}} \frac{1}{\sqrt{(\bar{E} - \bar{\mu})^2 + \bar{\Delta}^2}}. \quad (9.27)$$

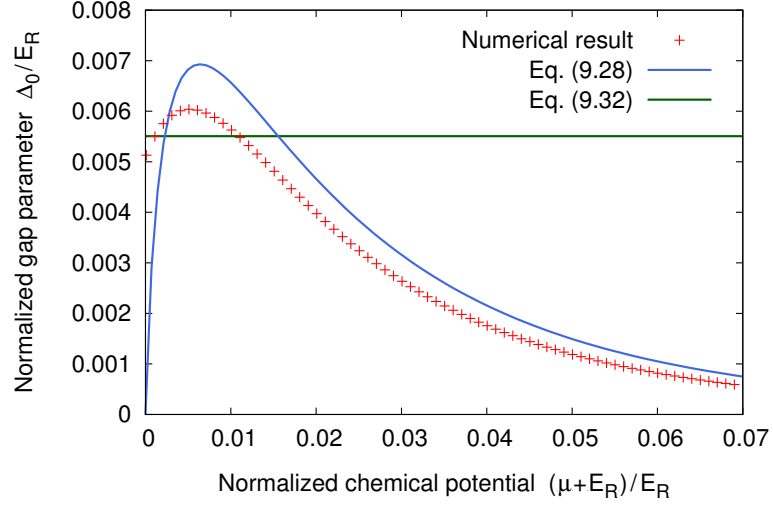


Figure 9.7: Numerical solution of the scalar gap equation (9.27) for $\bar{g} = 0.02$, and comparison with the analytical results for the asymptotics, Eqs. (9.28) and (9.32).

Next, we summarize our analytical results for the asymptotics of the solution: On the one hand, for $1 \gg \bar{\mu} \gg \bar{g}^2$, we find

$$\bar{\Delta} = 8\bar{\mu} \exp\left(-\frac{\sqrt{\bar{\mu}}}{2\bar{g}}\right). \quad (9.28)$$

Using that the density of states [Sch+16a, Eq. (29)] is given for $\bar{\mu} < 1$ by

$$D_R(\bar{\mu}) = \frac{4\bar{g}}{g} \frac{1}{\sqrt{\bar{\mu}}}, \quad (9.29)$$

the above result is equivalent to

$$\bar{\Delta} = 8\bar{\mu} \exp\left(-\frac{2}{gD_R(\bar{\mu})}\right), \quad (9.30)$$

or in terms of the original parameters,

$$\Delta_0 = 8(\mu + E_R) \exp\left(-\frac{2}{gD_R(\mu)}\right). \quad (9.31)$$

Note in particular the exponent, which coincides with the usual exponent in the SU(2)-symmetric case. On the other hand, for $\bar{\mu} = 0$, we find

$$\bar{\Delta} = (\bar{g}C)^2, \quad (9.32)$$

or in terms of the original parameters,

$$\Delta_0 = \frac{g^2}{E_R} \left(\frac{\sqrt{3}C}{16\pi}\right)^2 (a_0 k_R)^4. \quad (9.33)$$

This solution is valid for sufficiently small coupling parameters, i.e., for $\bar{g} \ll 1$.

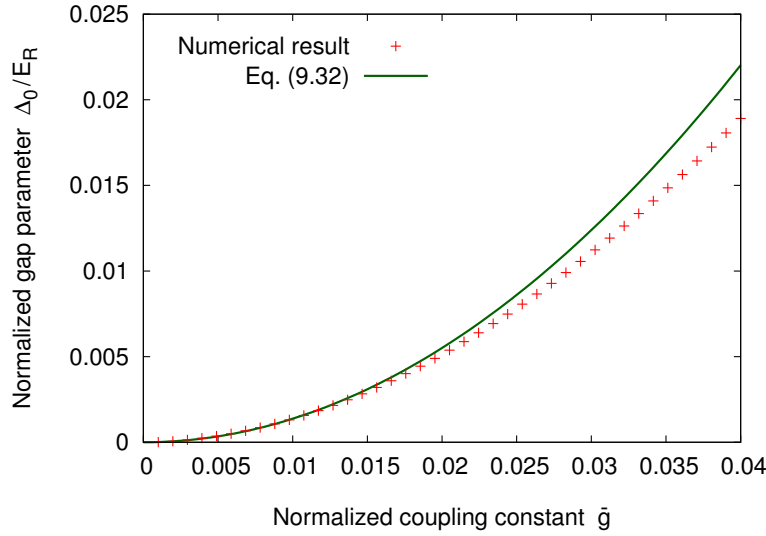


Figure 9.8: Numerical solution of the scalar gap equation (9.27) for $\bar{\mu} = 0.001$, and comparison with the analytical result for $\bar{\mu} = 0$, Eq. (9.32).

Finally, for the numerical solution of Eq. (9.27), we have used the function `fzero` from *GNU Octave* [Eat+14]. We have fixed the coupling parameter to a small value, $\bar{g} = 0.02$, and solved the implicit equation for the gap parameter $\bar{\Delta}$. Fig. 9.7 shows the resulting dependence of $\bar{\Delta}$ on the chemical potential $\bar{\mu}$. The characteristic features of the asymptotic solution are clearly reproduced in the numerical result: (i) the positive value of $\bar{\Delta}(\bar{\mu} = 0)$, (ii) the maximum of $\bar{\Delta}(\bar{\mu})$ at small $\bar{\mu}$, and (iii) the exponential decay for large $\bar{\mu}$. Even quantitatively, there is a good agreement between the numerical data and the analytical results as given by Eqs. (9.28) and (9.32). Finally, we have fixed the chemical potential to a tiny value ($\bar{\mu} = 0.001$) and plotted the dependence of the gap parameter $\bar{\Delta}$ on the coupling constant \bar{g} . The result is shown in Fig. 9.8. One clearly sees the quadratic dependence on \bar{g} , and the agreement with the analytical result (9.32) becomes perfect for small coupling constants.

Part IV.

Summary of further work

10. Electrodynamic properties of BiTeI

In this chapter, we briefly summarize the theoretical results published in Refs. [Dem+12; Lee+11; Sch+12; Sch+16b], which concern the electrodynamic and optical properties of the Rashba semiconductor BiTeI as well as related bismuth tellurohalides. (Parts of these publications are reproduced in this chapter.)

10.1. Optical conductivity

First, in Ref. [Lee+11], we have calculated the optical conductivity of BiTeI from the 18-band model of Ref. [Ish+11] (see Sect. 3.1). For this purpose, we have employed the Kubo formula [Kub57] (see also Refs. [GV05; Mah90]), which implies in particular that the conductivity tensor can be written as a sum of two contributions,

$$\overleftrightarrow{\sigma}(\omega) = \overleftrightarrow{\sigma}^{\text{inter}}(\omega) + \overleftrightarrow{\sigma}^{\text{intra}}(\omega), \quad (10.1)$$

an *interband* and an *intraband* contribution. The former is given by [Lee+11]

$$\sigma_{ij}^{\text{inter}}(\omega) = \frac{e^2 \hbar}{iV} \sum_{\mathbf{k}} \sum_{n \neq m} \frac{f(E_{n\mathbf{k}}) - f(E_{m\mathbf{k}})}{E_{m\mathbf{k}} - E_{n\mathbf{k}}} \frac{v_{i,nm}(\mathbf{k}) v_{j,mn}(\mathbf{k})}{E_{m\mathbf{k}} - E_{n\mathbf{k}} - (\hbar\omega + i\Gamma)}, \quad (10.2)$$

where $E_{n\mathbf{k}}$ is the eigenenergy corresponding to the n th eigenstate $|n\mathbf{k}\rangle$, and the velocity matrix elements are defined as [Wan+06]

$$v_{i,nm}(\mathbf{k}) = \frac{1}{\hbar} \left\langle n\mathbf{k} \left| \frac{\partial \hat{H}(\mathbf{k})}{\partial k_i} \right| m\mathbf{k} \right\rangle. \quad (10.3)$$

Furthermore, $f(E) = (e^{\beta(E-\mu)} + 1)^{-1}$ denotes the Fermi distribution function, and Γ the “carrier damping” constant. On the other hand, the intraband contribution is formally obtained by setting $n = m$ in Eq. (10.2), hence it is given by [All06]

$$\sigma_{ij}^{\text{intra}}(\omega) = \frac{1}{\hbar\omega + i\Gamma} \frac{e^2 \hbar}{iV} \sum_{\mathbf{k}} \sum_n f'(E_{n\mathbf{k}}) v_{i,nn}(\mathbf{k}) v_{j,nn}(\mathbf{k}), \quad (10.4)$$

where $f'(E)$ denotes the derivative of the Fermi distribution function. As the 18-band model is given in the basis of maximally localized Wannier functions, special care is required for evaluating the velocity matrix elements. In this respect, we have followed the procedure described in Ref. [Wan+06] (see, in particular, Eq. (31) therein).

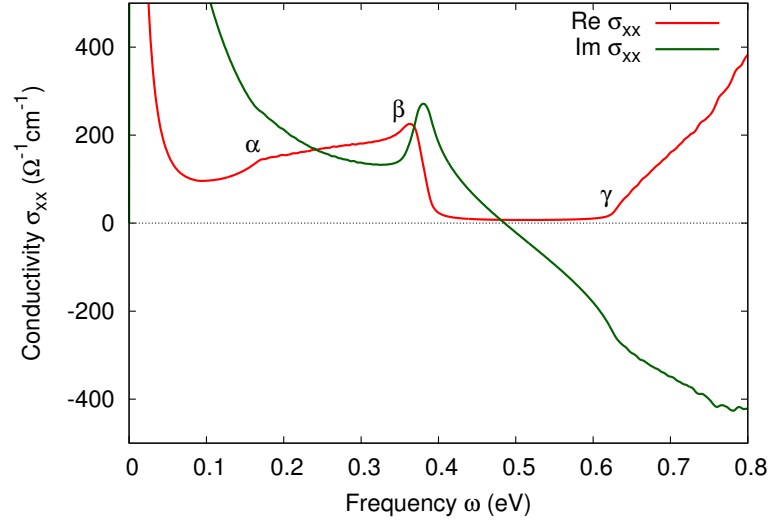


Figure 10.1: Longitudinal conductivity of BiTeI. The characteristic energies α , β and γ can be assigned to the interband transitions as shown in Fig. 10.2.

The result for the *longitudinal* optical conductivity σ_{xx} is shown in Fig. 10.1 for the following parameters: chemical potential $\mu = 90$ meV (above the crossing of the lowest conduction bands), temperature $T = 10$ K, and carrier damping $\Gamma = 5$ meV. (The last parameter can be chosen such as to optimally fit the experimental data, see Ref. [Lee+11]). Apart from the Drude-Lorentz part at low frequencies, which results from the intraband contribution, one can clearly see the onset of the interband contribution at ~ 0.6 eV, which corresponds to the *optical gap* γ (see Fig. 10.2). In addition, there is a contribution below the optical gap, which can be attributed to optical transitions *within* the Rashba spin-split conduction bands, and whose lower and upper edges correspond to the transitions α and β indicated by arrows in Fig. 10.2. Note that at zero temperature, optical transitions can occur only between occupied states (below the Fermi energy) and empty states (above the Fermi energy). We also remark that optical transitions between bands with different spin polarizations are theoretically expected to occur as a consequence of the spin-orbit coupling [Sch+16b] (see also Refs. [Lee+11; Sak+13]).

Furthermore, we have investigated in Ref. [Lee+11] the systematic change of the characteristic transition energies by varying the chemical potential (which corresponds to the carrier density). Experimentally, the carrier density could be controlled by doping Ag, Cu and Mn, as well as by changing the composition ratio between Te and I. Overall, the conductivity spectra obtained theoretically show an excellent agreement with the experimental results. Thus, the optical transitions within the spin-split energy bands confirm the bulk nature of the Rashba spin splitting (the skin depth of the midinfrared light is around 10–30 μm), and they manifest the relativistic nature of the electron dynamics in the semiconductor BiTeI [Lee+11].

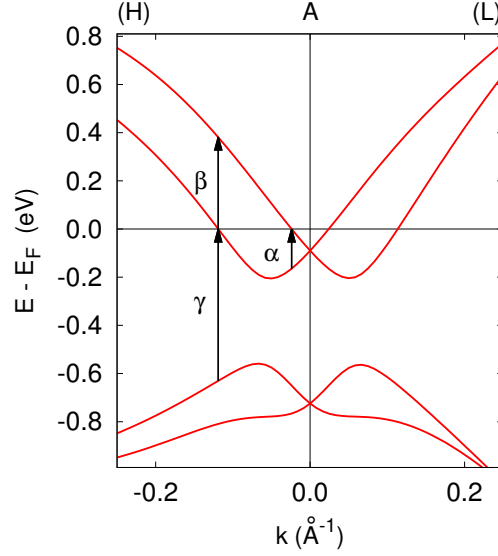


Figure 10.2: Band structure of BiTeI near the A point of the Brillouin zone (cf. Fig. 3.2; here, the two highest valence and two lowest conduction bands are shown). The arrows indicate transitions between these bands which correspond to characteristic features in the optical spectrum (see Figs. 10.1 and 10.4).

Finally, in the more recent work [Sch+16b], we have extended the optical conductivity calculations to the whole class of bismuth tellurohalides (BiTeX with X = I, Br, Cl). In particular, we have computed the entire conductivity tensor from first-principles density functional theory, and we have thus obtained the conductivity spectra for a wide energy range up to 12 eV. Furthermore, we have compared our theoretical results systematically with the recent measurements of Akrap *et al.* [Akr+14], Makhnev *et al.* [Mak+14] and Rusinov *et al.* [Rus+15], whereby we have found an excellent agreement. Moreover, we have calculated the dielectric constants and refractive indices, which in turn agree well with the experimental values as reported by Rusinov *et al.* [Rus+15].

10.2. Magneto-optical conductivity

Next, in Ref. [Dem+12], we have calculated the magneto-optical conductivity of BiTeI, i.e., the transverse conductivity σ_{xy} in the presence of a perpendicular magnetic field B_z (parallel to the crystal's principal axis). For this purpose, we have employed Fukuyama's formula [FFK10; Fuk69a; Fuk69b], which can be written in SI units as

$$\sigma_{xy}(\omega) = \frac{e^3 \hbar B_z}{2\omega} \frac{1}{V} \sum_{\mathbf{k}} \frac{1}{\beta} \sum_{\ell} \mathcal{S}(\mathbf{k}, i\hbar\omega_n, i\hbar\varepsilon_{\ell}) \Big|_{i\omega_n \rightarrow \omega}. \quad (10.5)$$

Here, we sum over all fermionic Matsubara frequencies, $\varepsilon_{\ell} = (2\ell + 1)\pi/(\hbar\beta)$, $\ell \in \mathbb{Z}$, while $\omega_n = 2n\pi/(\hbar\beta)$, $n \in \mathbb{Z}$, denotes a bosonic Matsubara frequency (see Ref. [Mah90]). The

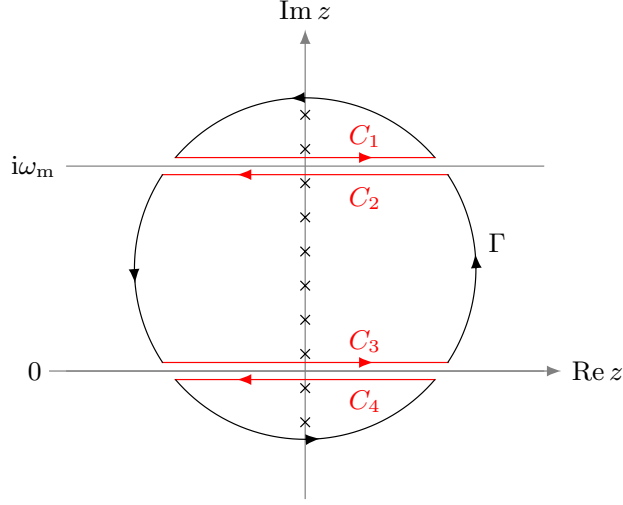


Figure 10.3: Contour integral used to evaluate the Matsubara frequency sum in Fukuyama’s formula for the Hall conductivity (see Ref. [Fuk69a]).

function \mathcal{S} is given explicitly by

$$\begin{aligned}
 \mathcal{S}_{\mathbf{k}, i\hbar\omega_n}(i\hbar\varepsilon_\ell) = & \frac{1}{m} \text{Tr} \left[F v_x G v_x G - F v_x F v_x G \right] \\
 & + \text{Tr} \left[F v_x G v_x G v_y G v_y - F v_x G v_y G v_x G v_y \right] \\
 & + \text{Tr} \left[F v_y F v_x G v_x G v_y - F v_x F v_x G v_y G v_y \right] \\
 & + \text{Tr} \left[F v_x F v_y F v_x G v_y - F v_y F v_x F v_x G v_y \right],
 \end{aligned} \tag{10.6}$$

where G denotes the thermal Green function

$$G \equiv G_{\mathbf{k}}(i\hbar\varepsilon_\ell) = (i\hbar\varepsilon_\ell + i\Gamma \text{sgn}(\varepsilon_\ell) - H_{\mathbf{k}} + \mu)^{-1} \tag{10.7}$$

with the “spectrum broadening” Γ [FFK10], and F is defined as

$$F \equiv F_{\mathbf{k}, i\hbar\omega_n}(i\hbar\varepsilon_\ell) = G_{\mathbf{k}}(i\hbar\varepsilon_\ell - i\hbar\omega_n). \tag{10.8}$$

Furthermore, the prefactor $1/m$ in Eq. (10.12) denotes the inverse electron mass, and v_i the velocity matrix as given by Eq. (10.3). After evaluating the Matsubara frequency sum in Eq. (10.5), the result should be analytically continued to the real axis.

Before proceeding with the evaluation of Eq. (10.5), we note that the analytic continuation of the Green function G has a branch cut at $\text{Im } z = 0$,

$$G_{\mathbf{k}}(z) = \begin{cases} (z + i\Gamma - H_{\mathbf{k}} + \mu)^{-1}, & \text{if } \text{Im } z > 0, \\ (z - i\Gamma - H_{\mathbf{k}} + \mu)^{-1}, & \text{if } \text{Im } z < 0, \end{cases} \tag{10.9}$$

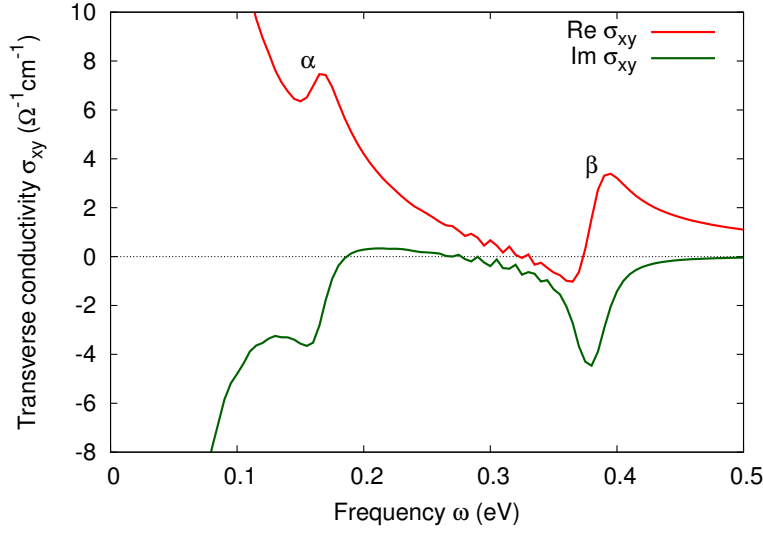


Figure 10.4: Transverse conductivity of BiTeI in the presence of a perpendicular magnetic field of $B_z = 3$ T. The characteristic energies α and β can be assigned to the interband transitions indicated in Fig. 10.2.

whereas F has a branch cut at $\text{Im } z = \hbar\omega_n$,

$$F_{\mathbf{k}, i\hbar\omega_n}(z) = \begin{cases} (z - i\hbar\omega_n + i\Gamma - H_{\mathbf{k}} + \mu)^{-1}, & \text{if } \text{Im } z > \hbar\omega_n, \\ (z - i\hbar\omega_n - i\Gamma - H_{\mathbf{k}} + \mu)^{-1}, & \text{if } \text{Im } z < \hbar\omega_n. \end{cases} \quad (10.10)$$

Therefore, the analytic continuation of the function \mathcal{S} is given by

$$\mathcal{S}_{\mathbf{k}, i\hbar\omega_n}(z) = \begin{cases} \mathcal{T}_{\mathbf{k}}(z - i\hbar\omega_n + i\Gamma, z + i\Gamma), & \text{if } \text{Im } z > \hbar\omega_n, \\ \mathcal{T}_{\mathbf{k}}(z - i\hbar\omega_n - i\Gamma, z + i\Gamma), & \text{if } \hbar\omega_n > \text{Im } z > 0, \\ \mathcal{T}_{\mathbf{k}}(z - i\hbar\omega_n - i\Gamma, z - i\Gamma), & \text{if } \text{Im } z < 0, \end{cases} \quad (10.11)$$

where we have defined

$$\begin{aligned} \mathcal{T}_{\mathbf{k}}(z_1, z_0) = & \frac{1}{m} \text{Tr} \left[G_1 v_x G_0 v_x G_0 - G_1 v_x G_1 v_x G_0 \right] \\ & + \text{Tr} \left[G_1 v_x G_0 v_x G_0 v_y G_0 v_y - G_1 v_x G_0 v_y G_0 v_x G_0 v_y \right] \\ & + \text{Tr} \left[G_1 v_y G_1 v_x G_0 v_x G_0 v_y - G_1 v_x G_1 v_x G_0 v_y G_0 v_y \right] \\ & + \text{Tr} \left[G_1 v_x G_1 v_y G_1 v_x G_0 v_y - G_1 v_y G_1 v_x G_1 v_x G_0 v_y \right], \end{aligned} \quad (10.12)$$

in terms of the analytic function ($i = 0, 1$)

$$G_i \equiv (z_i - H_{\mathbf{k}} + \mu)^{-1}. \quad (10.13)$$

Next, we perform the frequency sum in Eq. (10.5) by means of the residue theorem (see Ref. [Fuk69a]). By integrating over the contour shown schematically in Fig. 10.3, we obtain the identity

$$-\frac{1}{\beta} \sum_{\ell} \mathcal{S}_{\mathbf{k}, i\hbar\omega_n}(i\hbar\varepsilon_{\ell}) = \int_{\Gamma} \frac{dz}{2\pi i} f(z) \mathcal{S}_{\mathbf{k}, i\hbar\omega_n}(z) + \sum_{\ell=1}^4 \int_{C_{\ell}} \frac{dz}{2\pi i} f(z) \mathcal{S}_{\mathbf{k}, i\hbar\omega_n}(z), \quad (10.14)$$

where $f(z) = (e^{\beta z} + 1)^{-1}$ denotes the analytic continuation of the Fermi distribution function. The first term on the right-hand side of this equation vanishes as the radius of the circle Γ goes to infinity. Furthermore, by using Eq. (10.12), the four integrals over C_1, \dots, C_4 can be transformed into integrals over the real axis as

$$\begin{aligned} -\frac{1}{\beta} \sum_{\ell} \mathcal{S}_{\mathbf{k}, i\hbar\omega_n}(i\hbar\varepsilon_{\ell}) &= \frac{1}{2\pi i} \int_{-\infty}^{\infty} dE f(E) \left\{ \begin{aligned} &\mathcal{T}_{\mathbf{k}}(E + i\Gamma, E + i\hbar\omega_n + i\Gamma) \\ &- \mathcal{T}_{\mathbf{k}}(E - i\Gamma, E + i\hbar\omega_n + i\Gamma) \\ &+ \mathcal{T}_{\mathbf{k}}(E - i\hbar\omega_n - i\Gamma, E + i\Gamma) \\ &- \mathcal{T}_{\mathbf{k}}(E - i\hbar\omega_n - i\Gamma, E - i\Gamma) \end{aligned} \right\}. \end{aligned} \quad (10.15)$$

After performing the analytic continuation ($i\omega_n \mapsto \omega$) in Eq. (10.5), we thus arrive at

$$\begin{aligned} \sigma_{xy}(\omega) &= \frac{e^3 \hbar B_z}{2\omega} \frac{i}{2\pi} \frac{1}{V} \sum_{\mathbf{k}} \int_{-\infty}^{\infty} dE f(E) \left\{ \begin{aligned} &\mathcal{T}_{\mathbf{k}}(E + i\Gamma, E + \hbar\omega + i\Gamma) \\ &- \mathcal{T}_{\mathbf{k}}(E - i\Gamma, E + \hbar\omega + i\Gamma) \\ &+ \mathcal{T}_{\mathbf{k}}(E - \hbar\omega - i\Gamma, E + i\Gamma) \\ &- \mathcal{T}_{\mathbf{k}}(E - \hbar\omega - i\Gamma, E - i\Gamma) \end{aligned} \right\}. \end{aligned} \quad (10.16)$$

Finally, the sum over Bloch wavevectors \mathbf{k} can be approximated by an integral over the Brillouin zone, which together with the integral over E can be evaluated numerically.

The result for the transverse optical conductivity is shown in Fig. 10.4 for the following parameters: chemical potential $\mu = 90$ meV (above the conduction band crossing), temperature $T = 10$ K, carrier damping $\Gamma = 6.5$ meV, and magnetic field $B = 3$ T. The interpretation of this spectrum is similar as in the case of the longitudinal conductivity: Apart from the Drude-Lorentz contribution (which is only indicated in Fig. 10.4 by the sharp increase at low frequencies), one can clearly see a contribution resulting from optical transitions *within* the spin-split conduction bands. In particular, the characteristic energies α and β correspond again to the transitions shown in Fig. 10.2. In Ref. [Dem+12], we have also studied the systematic change of these characteristic energies by varying the chemical potential, and our results are again in excellent agreement with the experimental data. We further remark that the magneto-optical response of BiTeI in the infrared region is extraordinarily large for a non-ferromagnetic material, and this is a direct consequence of the giant Rashba spin splitting of the bulk energy bands [Dem+12].

10.3. Magnetic susceptibility

Finally, we have investigated the magnetic susceptibility of BiTeI in Ref. [Sch+12]. Usually, one distinguishes between the *orbital* and the *spin* contribution to the magnetic susceptibility, although cross contributions are generally also possible (see Ref. [SS16c, Sect. 3.2.5]). The orbital magnetic susceptibility can be calculated in at least three different ways: (i) from its thermodynamic definition as the second derivative of the free energy, (ii) from the Kubo formalism, and (iii) from Fukuyama's formula. In the following, we will briefly explain these three methods and show that they yield exactly the same result for the Rashba model of Sect. 3.2. For a general statement about the equivalence of these approaches, we refer the interested reader to Ref. [SS16c, Sect. 4.4]. Furthermore, we remark that in Ref. [Sch+12], we have also calculated the orbital magnetic susceptibility in the 18-band model of Ref. [Ish+11] and thereby obtained a good agreement with the experimental results for BiTeI.

10.3.1. Thermodynamic calculation

In the presence of a perpendicular magnetic field $\mathbf{B} = -B\mathbf{e}_z$, the Rashba Hamiltonian (3.1) is modified as [She+04]

$$\hat{H} = \frac{1}{2m^*} (\hat{\mathbf{p}} + e\mathbf{A})^2 + \frac{\alpha}{\hbar} \mathbf{e}_z \cdot ((\hat{\mathbf{p}} + e\mathbf{A}) \times \boldsymbol{\sigma}) - \frac{1}{2} g_s \mu_B B \sigma_z, \quad (10.17)$$

where $\mathbf{A} = yB\mathbf{e}_x$ is the vector potential in the Landau gauge, g_s the electron's Landé g-factor, and $\mu_B = e\hbar/2m_e$ the Bohr magneton (with m_e the electron mass). The eigenvalues of this Hamiltonian—i.e., the *Landau levels* of the two-dimensional electron gas in the presence of the spin-orbit coupling—can be calculated explicitly [She+04]. They are labeled by $N \in \mathbb{N}_0$ and $s \in \{-1, +1\}$, and they are given as follows: for $N = 0$,

$$E_0 = \hbar\omega_B \frac{1}{2} (1 - g), \quad (10.18)$$

and for $N \geq 1$,

$$E_{Ns} = \hbar\omega_B \left(N + \frac{s}{2} \sqrt{(1 - g)^2 + 8N\eta^2} \right). \quad (10.19)$$

Here, we have defined the *cyclotron frequency*

$$\omega_B = \frac{eB}{m^*}, \quad (10.20)$$

the *effective g-factor*

$$g = g_s \frac{m^*}{2m_e}, \quad (10.21)$$

the *magnetic length*

$$\ell_B = \sqrt{\frac{\hbar}{eB}}, \quad (10.22)$$

and the dimensionless constant (with k_R the Rashba wavevector)

$$\eta = \ell_B k_R = \frac{\ell_B m^* \alpha}{\hbar^2}, \quad (10.23)$$

whose square equals the quotient (with E_R the Rashba energy)

$$\eta^2 = \frac{2E_R}{\hbar\omega_B}. \quad (10.24)$$

The corresponding eigenvectors can also be calculated explicitly (see Ref. [She+04]). In particular, due to the invariance of the Hamiltonian (10.17) under translations in the x direction, each eigenvalue has a degeneracy of $L^2/(2\pi\ell_B^2)$, where L denotes the linear dimension of the sample (hence L^2 is the area of the two-dimensional sample).

Having diagonalized the Rashba Hamiltonian in the presence of the magnetic field, we can compute the thermodynamic *grand potential* as [Sch06, Eq. (4.1.7)]

$$\Phi = -\frac{1}{\beta} \ln Z = -\frac{1}{\beta} \frac{L^2}{2\pi\ell_B^2} \sum_{N,s} \ln \left(1 + e^{-\beta(E_{Ns}-\mu)} \right), \quad (10.25)$$

where $\beta = 1/k_B T$ denotes the inverse temperature and μ the chemical potential. From this, we obtain the magnetic susceptibility as

$$\chi_m = -\mu_0 \frac{1}{L^2} \frac{\partial^2 \Phi}{\partial B^2}. \quad (10.26)$$

For a strictly two-dimensional system, this quantity has the unit of a length (m). In order to compare our results to the measured magnetic susceptibility of BiTeI, however, we multiply it by A_{mol} , the surface area per mol of one BiTeI layer. This is given by

$$A_{\text{mol}} = N_A \det(\mathbf{a}_1, \mathbf{a}_2) \approx 9.82 \times 10^4 \text{ m}^2 \text{ mol}^{-1}, \quad (10.27)$$

where N_A denotes Avogadro's constant, and $\mathbf{a}_1, \mathbf{a}_2$ are the primitive vectors of the two-dimensional hexagonal lattice (see Sct. 1.2). The resulting *molar* magnetic susceptibility

$$\chi_{m,\text{mol}} = A_{\text{mol}} \chi_m \quad (10.28)$$

has the unit m^3/mol (SI units), or emu/mol (Gaussian units), where [IEEE16]

$$1 \frac{\text{emu}}{\text{mol}} = 4\pi \times 10^{-6} \frac{\text{m}^3}{\text{mol}}. \quad (10.29)$$

We have chosen the parameters of the Rashba model as in Eqs. (3.17)–(3.18) and performed the calculation at a temperature of $T = 30$ K. Our result for the orbital magnetic susceptibility is shown in Fig. 10.5 as a function of the chemical potential μ . We see that (i) if the chemical potential is above the band crossing ($\mu > 0$), χ_m approaches the *Landau diamagnetism* of free electrons with the effective mass m^* (see the original article [Lan30], or [GV05, Sct. 4.5]), i.e.,

$$\chi_{m,\text{Landau}} = -\frac{\mu_0 e^2}{12\pi m^*}. \quad (10.30)$$

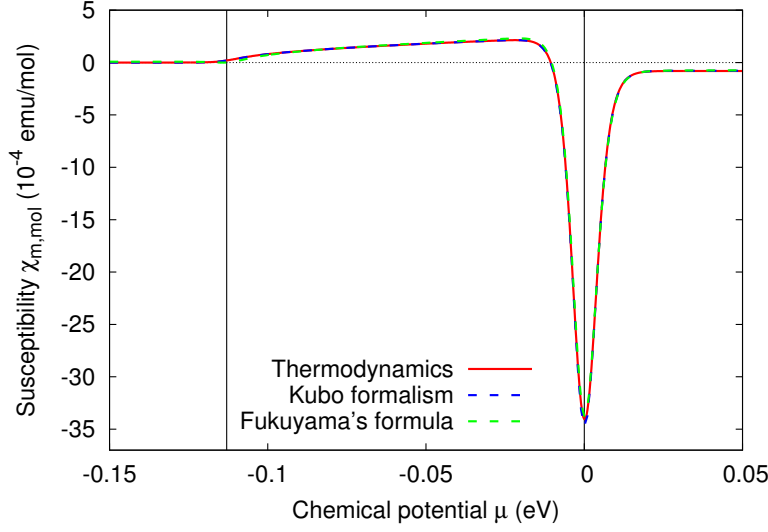


Figure 10.5: Orbital magnetic susceptibility of the Rashba model (see Sct. 3.2). The vertical lines mark the band minimum ($E = -E_R$) and the band crossing ($E = 0$), respectively. Our results obtained from the thermodynamic calculation, the Kubo formalism and Fukuyama's formula coincide exactly.

Furthermore, (ii) near the band crossing ($\mu \simeq 0$), the orbital diamagnetism is enhanced and in fact diverges as $-1/T$ for the temperature $T \rightarrow 0$. Finally, (iii) below the band crossing ($\mu < 0$), an *orbital paramagnetism* (i.e., $\chi_m > 0$) occurs as a consequence of the Rashba spin-orbit coupling [Sch+12]. Such an effect had been considered before by only a few theoretical studies [BI98; BR60; KO56; Pri+10; Vig91]. In Ref. [Sch+12], we have also predicted this effect to occur in BiTeI based on a calculation in the 18-band model of Ref. [Ish+11]. In fact, after subtracting the *Larmor diamagnetism* originating from the ionic cores, the *orbital paramagnetism* of the conduction electrons has been observed experimentally for the first time in this material [Sch+12].

10.3.2. Calculation in the Kubo formalism

We start again from the Rashba Hamiltonian (3.1), which reads in second quantization

$$\hat{H} = \sum_{\mathbf{k}} \sum_{s,s'} H_{ss'}(\mathbf{k}) \hat{a}_{\mathbf{k},s}^\dagger \hat{a}_{\mathbf{k},s'}, \quad (10.31)$$

where the (2×2) Hamiltonian matrix $H_{ss'}(\mathbf{k})$ is given by Eq. (3.5). To diagonalize this Hamiltonian, we define the new annihilation and creation operators (cf. Eq. (3.7))

$$\hat{a}_{\mathbf{k},n} = \sum_s U_{sn}^*(\mathbf{k}) \hat{a}_{\mathbf{k},s}, \quad (10.32)$$

$$\hat{a}_{\mathbf{k},n}^\dagger = \sum_s U_{sn}(\mathbf{k}) \hat{a}_{\mathbf{k},s}^\dagger, \quad (10.33)$$

where $n \in \{+, -\}$ labels the two branches of the Rashba dispersion, and $U(\mathbf{k}) \equiv U_{sn}(\mathbf{k})$ is the unitary matrix given by Eq. (3.8). Thus, we obtain the representation

$$\hat{H} = \sum_{\mathbf{k}} \sum_n E_n(\mathbf{k}) \hat{a}_{\mathbf{k},n}^\dagger \hat{a}_{\mathbf{k},n}, \quad (10.34)$$

where the eigenvalues $E_n(\mathbf{k})$ are given by Eq. (3.14). Next, the velocity operator is obtained from the classical relation $v_i = \partial H / \partial p_i$ ($i = x, y$), which yields for the Rashba model (3.1) the first-quantized expressions

$$\hat{v}_x = \frac{1}{m^*} \hat{p}_x + \frac{\alpha}{\hbar} \sigma_y, \quad \hat{v}_y = \frac{1}{m^*} \hat{p}_y - \frac{\alpha}{\hbar} \sigma_x. \quad (10.35)$$

From this, we deduce the *paramagnetic current density* operator [GV05, Appendix 2],

$$\hat{j}_p(\mathbf{q}) = -\frac{e}{2} \left(\hat{\mathbf{v}} e^{-i\mathbf{q} \cdot \hat{\mathbf{r}}} + e^{-i\mathbf{q} \cdot \hat{\mathbf{r}}} \hat{\mathbf{v}} \right), \quad (10.36)$$

where $\hat{\mathbf{r}} = (\hat{x}, \hat{y})$ denotes the two-dimensional position operator. Restricting ourselves to the x component, we obtain

$$\hat{j}_{p,x}(\mathbf{q}) = e^{-i\mathbf{q} \cdot \hat{\mathbf{r}}} \left\{ -\frac{e}{m^*} \left(\hat{p}_x - \frac{\hbar q_x}{2} \right) - \frac{e\alpha}{\hbar} \sigma_y \right\}. \quad (10.37)$$

In second quantization, this operator turns into

$$\hat{j}_{p,x}(\mathbf{q}) = \sum_{\mathbf{k}} \sum_{s,s'} \left\{ -\frac{e\hbar}{m^*} \left(k_x - \frac{q_x}{2} \right) \delta_{ss'} - \frac{e\alpha}{\hbar} (\sigma_y)_{ss'} \right\} \hat{a}_{\mathbf{k}-\mathbf{q},s}^\dagger \hat{a}_{\mathbf{k},s'}. \quad (10.38)$$

In the following, we will consider only the case where $\mathbf{q} \equiv q\mathbf{e}_y$ (with \mathbf{e}_y the unit vector in the y direction). Then, we can write

$$\hat{j}_{p,x}(q\mathbf{e}_y) = \sum_{\mathbf{k}} \sum_{s,s'} (j_{p,x})_{ss'}(\mathbf{k}) \hat{a}_{\mathbf{k}-\mathbf{q},s}^\dagger \hat{a}_{\mathbf{k},s'}, \quad (10.39)$$

with the \mathbf{q} -independent (2×2) matrix

$$j_{p,x}(\mathbf{k}) = -\frac{e\hbar}{m^*} k_x \mathbb{1} - \frac{e\alpha}{\hbar} \sigma_y = -\frac{e\alpha}{\hbar} \begin{pmatrix} k_x/k_R & -i \\ i & k_x/k_R \end{pmatrix}, \quad (10.40)$$

where $k_R = m^*\alpha/\hbar^2$ denotes the Rashba wavevector. In the basis of the energy eigenvectors, the same operator can be written as

$$\hat{j}_{p,x}(q\mathbf{e}_y) = \sum_{\mathbf{k}} \sum_{n,n'} (j_{p,x})_{nn'}(\mathbf{k} - \mathbf{q}, \mathbf{k}) \hat{a}_{\mathbf{k}-\mathbf{q},n}^\dagger \hat{a}_{\mathbf{k},n'}, \quad (10.41)$$

where we have defined the matrix elements

$$(j_{p,x})_{nn'}(\mathbf{k} - \mathbf{q}, \mathbf{k}) = \sum_{s,s'} (j_{p,x})_{ss'}(\mathbf{k}) U_{sn}^*(\mathbf{k} - \mathbf{q}) U_{s'n'}(\mathbf{k}) \quad (10.42)$$

$$= [U^\dagger(\mathbf{k} - \mathbf{q}) j_{p,x}(\mathbf{k}) U(\mathbf{k})]_{nn'}. \quad (10.43)$$

Now, for a magnetic field applied in the z direction (perpendicular to the two-dimensional electron gas), the orbital magnetic susceptibility χ_m can be calculated from linear response theory as (see Refs. [GV05, Eq. (3.183)] or [SS15a, Eq. (7.38)])

$$\chi_m \equiv (\chi_m)_{zz} = \mu_0 \lim_{q \rightarrow 0} \frac{\chi_{xx}(q\mathbf{e}_y, \omega = 0)}{q^2}, \quad (10.44)$$

where the *current response function* χ_{xx} is given by the Kubo formula (see Refs. [GV05, Eq. (4.46)] or [SS16c, Appendix C]), which reads

$$\chi_{xx}(q\mathbf{e}_y, \omega) = -\frac{e^2 n_e}{m^*} + \frac{i}{\hbar L^2} \int_0^\infty dt e^{i\omega t} e^{-\eta t} \left\langle \left[\hat{j}_{p,x}(q\mathbf{e}_y, t), \hat{j}_{p,x}(-q\mathbf{e}_y) \right] \right\rangle. \quad (10.45)$$

Here, the first term comes from the *diamagnetic current density* [GV05, Appendix 2], which is proportional to the electron density

$$n_e = \frac{N_e}{L^2} = \frac{1}{L^2} \sum_{\mathbf{k}} \sum_n f(E_n(\mathbf{k})), \quad (10.46)$$

where f denotes the Fermi distribution function. The second term in Eq. (10.45) involves the commutator of the paramagnetic current operators, whose time evolution is given in the interaction picture, and the expectation value is taken with respect to the grand canonical ensemble. By neglecting electron-electron interactions, this expression can be evaluated as follows (using Eq. (10.41), and abbreviating $\mathbf{q} \equiv q\mathbf{e}_y$):

$$\begin{aligned} \left\langle \left[\hat{j}_{p,x}(\mathbf{q}, t), \hat{j}_{p,x}(-\mathbf{q}) \right] \right\rangle &= \sum_{\mathbf{k}} \sum_{n, n'} \sum_{\mathbf{k}'} \sum_{\ell, \ell'} (j_{p,x})_{nn'}(\mathbf{k} - \mathbf{q}, \mathbf{k}) (j_{p,x})_{\ell\ell'}(\mathbf{k}' + \mathbf{q}, \mathbf{k}') \\ &\times \left\langle \left[\hat{a}_{\mathbf{k}-\mathbf{q}, n}^\dagger(t) \hat{a}_{\mathbf{k}, n'}(t), \hat{a}_{\mathbf{k}'+\mathbf{q}, \ell}^\dagger \hat{a}_{\mathbf{k}', \ell'} \right] \right\rangle. \end{aligned} \quad (10.47)$$

Here, the time dependence of the annihilation and creation operators is given by

$$\hat{a}_{\mathbf{k}, n}(t) = \hat{a}_{\mathbf{k}, n} e^{-it(E_{\mathbf{k}, n} - \mu)/\hbar}, \quad (10.48)$$

$$\hat{a}_{\mathbf{k}, n}^\dagger(t) = \hat{a}_{\mathbf{k}, n}^\dagger e^{it(E_{\mathbf{k}, n} - \mu)/\hbar}, \quad (10.49)$$

and hence, the expectation value of the commutator yields [GV05, Eq. (4.7)]

$$\left\langle \left[\hat{a}_{\mathbf{k}-\mathbf{q}, n}^\dagger \hat{a}_{\mathbf{k}, n'}, \hat{a}_{\mathbf{k}'+\mathbf{q}, \ell}^\dagger \hat{a}_{\mathbf{k}', \ell'} \right] \right\rangle = \delta_{\mathbf{k}-\mathbf{q}, \mathbf{k}'} \delta_{n\ell'} \delta_{n'\ell} (f(E_{\mathbf{k}-\mathbf{q}, n}) - f(E_{\mathbf{k}, n'})). \quad (10.50)$$

Thus, we obtain from Eq. (10.47),

$$\begin{aligned} \left\langle \left[\hat{j}_{p,x}(\mathbf{q}, t), \hat{j}_{p,x}(-\mathbf{q}) \right] \right\rangle &= \sum_{\mathbf{k}} \sum_{n, n'} (j_{p,x})_{nn'}(\mathbf{k} - \mathbf{q}, \mathbf{k}) (j_{p,x})_{n'n}(\mathbf{k}, \mathbf{k} - \mathbf{q}) \\ &\times (f(E_{\mathbf{k}-\mathbf{q}, n}) - f(E_{\mathbf{k}, n'})) e^{it(E_{\mathbf{k}-\mathbf{q}, n} - E_{\mathbf{k}, n'})/\hbar}. \end{aligned} \quad (10.51)$$

From the definition (10.43), we further deduce that

$$(j_{p,x})_{n'n}(\mathbf{k}, \mathbf{k} - \mathbf{q}) = (j_{p,x})_{nn'}^*(\mathbf{k} - \mathbf{q}, \mathbf{k}), \quad (10.52)$$

where we have used that $j_{p,x}(\mathbf{k})$ is hermitean and that $j_{p,x}(\mathbf{k} - \mathbf{q}) = j_{p,x}(\mathbf{k})$ holds for $q_x = 0$. Therefore, the product of the two matrix elements in Eq. (10.51) can be replaced by the squared absolute value of the first matrix element. By putting this result into the Kubo formula (10.45) and by performing the frequency integral explicitly, we obtain the (non-interacting) current response function as

$$\chi_{xx}(q\mathbf{e}_y, \omega) = -\frac{e^2 n_e}{m^*} - \frac{1}{L^2} \sum_{\mathbf{k}} \sum_{n, n'} \frac{f(E_{\mathbf{k}-\mathbf{q}, n}) - f(E_{\mathbf{k}, n'})}{\hbar(\omega + i\eta) + E_{\mathbf{k}-\mathbf{q}, n} - E_{\mathbf{k}, n'}} |(j_{p,x})_{nn'}(\mathbf{k} - \mathbf{q}, \mathbf{k})|^2. \quad (10.53)$$

Furthermore, by evaluating this expression at zero frequency and taking into account also Eq. (10.46), we arrive at the following formula for the orbital magnetic susceptibility (in the non-interacting case; with $\mathbf{q} \equiv q\mathbf{e}_y$):

$$\begin{aligned} \chi_m = -\mu_0 \lim_{q \rightarrow 0} \frac{1}{q^2} & \left\{ \frac{e^2}{m^*} \frac{1}{L^2} \sum_{\mathbf{k}} \sum_n f(E_{\mathbf{k}, n}) \right. \\ & \left. + \frac{1}{L^2} \sum_{\mathbf{k}} \sum_{n, n'} \frac{f(E_{\mathbf{k}-\mathbf{q}, n}) - f(E_{\mathbf{k}, n'})}{E_{\mathbf{k}-\mathbf{q}, n} - E_{\mathbf{k}, n'}} |(j_{p,x})_{nn'}(\mathbf{k} - \mathbf{q}, \mathbf{k})|^2 \right\}. \end{aligned} \quad (10.54)$$

This formula can be evaluated numerically for the Rashba model. The resulting magnetic susceptibility as a function of the chemical potential coincides precisely with the result obtained from the thermodynamic calculation, which is shown in Fig. 10.5.

We remark that the advantages of calculating the magnetic susceptibility in the Kubo formalism are that this method does not require knowledge of the precise form of the Landau levels, and that it can be generalized straightforwardly to take into account electron-electron interaction effects (see Ref. [Pri+10]). In fact, following a suggestion of Giovanni Vignale, we have also calculated the first-order interaction contribution to the orbital magnetic susceptibility in the Rashba model. For this purpose, we have assumed a local density-density interaction as given by the normal-ordered operator

$$\hat{V} = \frac{U}{2} \sum_{\mathbf{q} \neq 0} : \hat{n}_{\mathbf{q}} \hat{n}_{-\mathbf{q}} : , \quad (10.55)$$

where $U > 0$ (corresponding to a repulsive interaction), and where the density operator reads in the spin or in the energy eigenbasis as

$$\hat{n}_{\mathbf{q}} = \sum_{\mathbf{k}} \sum_s \hat{a}_{\mathbf{k}-\mathbf{q}, s}^\dagger \hat{a}_{\mathbf{k}, s} = \sum_{\mathbf{k}} \sum_{n, n'} [U^\dagger(\mathbf{k} - \mathbf{q}) U(\mathbf{k})]_{nn'} \hat{a}_{\mathbf{k}-\mathbf{q}, n}^\dagger \hat{a}_{\mathbf{k}, n'}. \quad (10.56)$$

Our result for the interaction correction to the orbital magnetic susceptibility is shown in Fig. 10.6 for $U = 5$ eV. We see that for $\mu < 0$, the orbital paramagnetism is further enhanced, and the first-order contribution grows linearly with the energy difference to the band minimum. On the other hand, for $\mu > 0$, the magnetic susceptibility remains unaffected by the electron-electron interaction.

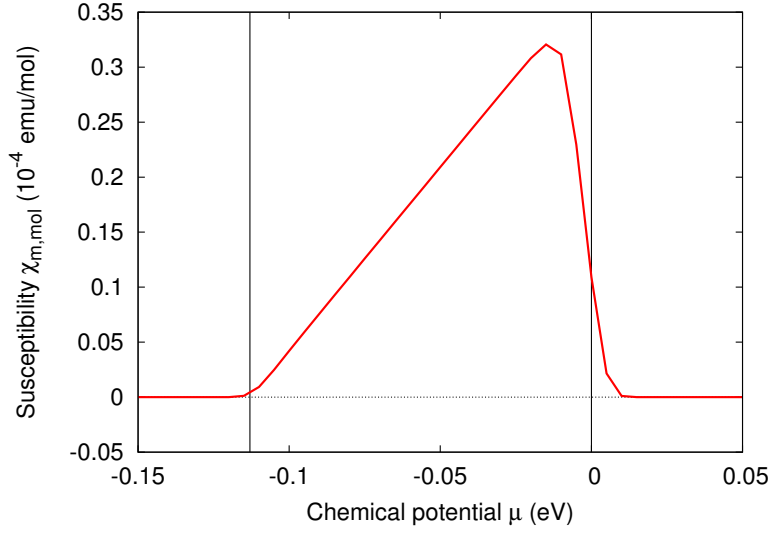


Figure 10.6: First-order contribution to the orbital magnetic susceptibility at $T = 30$ K, assuming a repulsive contact interaction of $U = 5$ eV. The vertical lines mark the band minimum and respectively the crossing point of the Rashba model dispersion.

10.3.3. Calculation from Fukuyama's formula

Finally, we have calculated the orbital magnetic susceptibility in the Rashba model from Fukuyama's formula [FFK10; Fuk70], which reads in SI units

$$\chi_m = \frac{\mu_0 e^2 \hbar^2}{2} \frac{1}{V} \sum_{\mathbf{k}} \frac{1}{\beta} \sum_{\ell} \text{Tr} [G v_x G v_y G v_x G v_y], \quad (10.57)$$

where

$$G \equiv G(\mathbf{k}, \varepsilon_{\ell}) = (i\hbar\varepsilon_{\ell} + \mu - H_0(\mathbf{k}))^{-1} \quad (10.58)$$

is the thermal Green function depending on the momentum \mathbf{k} and the fermionic Matsubara frequency ε_{ℓ} . Furthermore, $v_i(\mathbf{k}) = \partial H(\mathbf{k})/(\hbar k_i)$ denotes the velocity matrix, which is given for the Rashba model (3.5) by

$$v_x = \frac{\hbar k_x}{m^*} \mathbb{1} + \frac{\alpha}{\hbar} \sigma_y, \quad v_y = \frac{\hbar k_y}{m^*} \mathbb{1} - \frac{\alpha}{\hbar} \sigma_x. \quad (10.59)$$

The advantage of using Fukuyama's formula for evaluating the orbital magnetic susceptibility is that this formula does not require us to perform the $q \rightarrow 0$ limit numerically as in Eq. (10.54). Our result obtained from Fukuyama's formula agrees again precisely with the one obtained before from the thermodynamic calculation and from the Kubo formalism, as can be seen in Fig. 10.5 (see also Ref. [Sch+12]).

11. Functional Approach to electrodynamics of media

In this last chapter, we describe in desperate brevity the Functional Approach to electrodynamics of media, which has been developed systematically in Refs. [SS15a; SS15b; SS16a; SS16b; SS16c] (parts of these publications are reproduced in this chapter).

11.1. Introduction

The Functional Approach [SS15a; SS15b; SS16a; SS16b; SS16c] denotes a microscopic field theory of electromagnetic material properties, which operates in accordance with the common practice in *ab initio* physics. In particular, it resolves the following *conceptual problems* of the Standard Approach (where the latter is described in the traditional textbook literature, such as [Gri99; Jac99; LL84])—for a more detailed discussion, see Ref. [SS16c]:

- (i) *Incomplete field equations*: The well-established equation $\nabla \cdot \mathbf{P} = \rho_b$ for the polarization in terms of the “bound” charge density determines only the longitudinal part of the polarization, but leaves its transverse part undefined. Correspondingly, the equation $\nabla \cdot \mathbf{D} = \rho_f$ for the displacement field in terms of the “free” charge density leaves the transverse part of the displacement field undefined. In particular, this implies that even electromagnetic response functions—such as the (relative) dielectric tensor $\overset{\leftrightarrow}{\varepsilon}_r$, which should be defined through the relation $\mathbf{D} = \varepsilon_0 \overset{\leftrightarrow}{\varepsilon}_r \mathbf{E}$ —are underdetermined in the Standard Approach.
- (ii) *Ambiguous source splitting*: At present, there is no consensus about the precise meaning of “bound” and “free” charges or currents. In particular, this distinction is usually based on *a priori* assumptions about the material, which cannot be upheld microscopically. In other words, this traditional splitting cannot be justified on the level of the many-body Schrödinger equation, which (together with the microscopic Maxwell equations) forms the basis of modern *ab initio* calculations.

Apart from this, the Standard Approach also leads to *practical problems*, which regard in particular the description of bianisotropic materials (Sct. 11.2) and the relativistic covariance (Sct. 11.3). Moreover, the Standard Approach implies a wrong formula for the refractive index (Sct. 11.4).

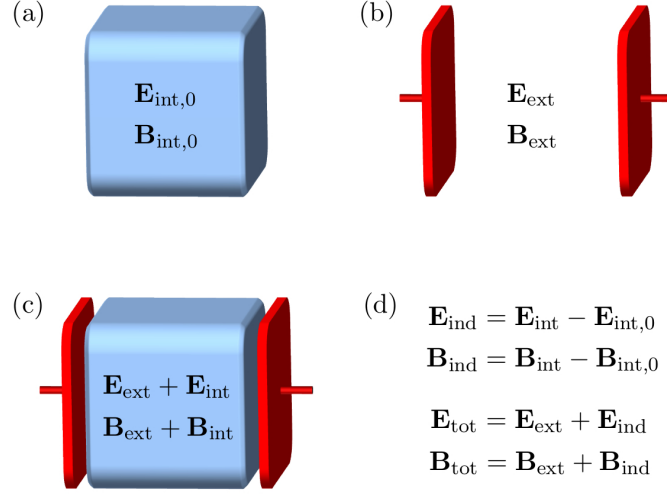


Figure 11.1: Definition of internal, external, induced and total fields (see Ref. [SS15a, Fig. 2]).

By contrast, the Functional Approach to electrodynamics of materials is *conceptually based* on the following fundamental principles [SS15a; SS16c]:

- (i) *Splitting into internal and external contributions:* on a microscopic level, all field quantities (i.e., electric and magnetic fields, potentials, charges and currents) are split into *internal* and *external* contributions. The former correspond to the degrees of freedom which constitute the medium, whereas the latter correspond to an external perturbation. The internal quantities are further split into their values in the absence of the perturbation and the *induced* contributions (i.e., induced under the action of the external perturbation). Finally, the *total* fields are defined as the respective sums of the external and the induced quantities (see Fig. 11.1). The so-defined external and induced fields are related to their counterparts in the Standard Approach by the Fundamental Field Identifications:

$$\mathbf{P}(\mathbf{x}, t) = -\varepsilon_0 \mathbf{E}_{\text{ind}}(\mathbf{x}, t), \quad (11.1)$$

$$\mathbf{D}(\mathbf{x}, t) = \varepsilon_0 \mathbf{E}_{\text{ext}}(\mathbf{x}, t), \quad (11.2)$$

$$\mathbf{E}(\mathbf{x}, t) = \mathbf{E}_{\text{tot}}(\mathbf{x}, t), \quad (11.3)$$

and

$$\mathbf{M}(\mathbf{x}, t) = \mathbf{B}_{\text{ind}}(\mathbf{x}, t)/\mu_0, \quad (11.4)$$

$$\mathbf{H}(\mathbf{x}, t) = \mathbf{B}_{\text{ext}}(\mathbf{x}, t)/\mu_0, \quad (11.5)$$

$$\mathbf{B}(\mathbf{x}, t) = \mathbf{B}_{\text{tot}}(\mathbf{x}, t). \quad (11.6)$$

In particular, in the Functional Approach, all electric and magnetic fields are uniquely defined by the microscopic Maxwell equations in terms of their respective charge and current densities (compare [SS16c, Table 1 and Table 3]).

- (ii) *Functional dependence of induced on external fields:* The Functional Approach postulates a functional dependence of the induced fields on the external perturbation, where the concrete form of this functional characterizes the material under consideration. In particular, the functional dependence of the induced four-current on the external four-potential,

$$j_{\text{ind}}^\mu = j_{\text{ind}}^\mu[A_{\text{ext}}^\nu], \quad (11.7)$$

completely determines the electromagnetic response of any material. The reason for this is that the external four-potential contains the whole information about the applied electromagnetic perturbation, and the induced four-current contains the whole information about the induced electromagnetic fields. Furthermore, *linear* response theory corresponds to the first-order expansion of this functional,

$$j_{\text{ind}}^\mu(x) = \int d^4x' \chi^\mu{}_\nu(x, x') A_{\text{ext}}^\nu(x'), \quad (11.8)$$

where $x = (\mathbf{x}, t)$ and $d^4x = d^3\mathbf{x} c dt$, and where the integral kernel $\chi^\mu{}_\nu$ is called *fundamental response tensor*. The above equation constitutes the most general first-order response relation, which incorporates all effects of inhomogeneity, anisotropy and relativistic retardation [SS15a].

On the other hand, the *practical basis* of the Functional Approach is the Kubo formalism, which gives the concrete formulae for the actual calculation of linear response functions (in particular of the fundamental response tensor, see Ref. [SS16c, Sect. 3.2.4]).

11.2. Universal Response Relations

By the continuity equation and the gauge invariance of the induced current, the fundamental response tensor of any physical system has to obey the following constraints (see Refs. [AS10] or [SS15a, Eqs. (5.5)–(5.6)]):

$$\partial_\mu \chi^\mu{}_\nu(x, x') = 0, \quad (11.9)$$

$$\partial^\nu \chi^\mu{}_\nu(x, x') = 0. \quad (11.10)$$

These can be used to deduce the general form of the Lorentz-covariant response tensor, which is given in Fourier space by [SS15a, Eq. (5.12)]

$$\chi^\mu{}_\nu(\mathbf{k}, \mathbf{k}'; \omega) = \begin{pmatrix} -\frac{c^2}{\omega^2} \mathbf{k}^T \overset{\leftrightarrow}{\chi} \mathbf{k}' & \frac{c}{\omega} \mathbf{k}^T \overset{\leftrightarrow}{\chi} \\ -\frac{c}{\omega} \overset{\leftrightarrow}{\chi} \mathbf{k}' & \overset{\leftrightarrow}{\chi} \end{pmatrix}. \quad (11.11)$$

Therefore, *there are at most 9 independent linear electromagnetic response functions for any material*, and the (3×3) *current response tensor* $\overset{\leftrightarrow}{\chi}$ already describes the linear response of any material completely. Furthermore, by the universal relation (for its

derivation, see Ref. [SS16c, Sct. 3.2.3])

$$\overleftrightarrow{\sigma}(\mathbf{k}, \mathbf{k}'; \omega) = i\omega \overleftrightarrow{\chi}(\mathbf{k}, \mathbf{k}'; \omega), \quad (11.12)$$

it follows that the conductivity tensor also contains the complete information about the linear response of any material. Consequently, all linear electromagnetic response functions (including magneto-electric cross couplings) can be expressed analytically in terms of the conductivity tensor by means of universal (i.e., material-independent) relations. These Universal Response Relations have been derived explicitly in Ref. [SS15a]. In the Fourier domain, they read as follows:

$$\frac{dE_{\text{ind}}^i(\mathbf{k}, \omega)}{dE_{\text{ext}}^j(\mathbf{k}', \omega)} = -\frac{1}{\varepsilon_0 \omega^2} \frac{\omega^2 \delta_{im} - c^2 k_i k_m}{\omega^2 - c^2 |\mathbf{k}|^2} i\omega \sigma_{mj}(\mathbf{k}, \mathbf{k}'; \omega), \quad (11.13)$$

$$\frac{1}{c} \frac{dE_{\text{ind}}^i(\mathbf{k}, \omega)}{dB_{\text{ext}}^j(\mathbf{k}', \omega)} = -\frac{1}{\varepsilon_0 \omega^2} \frac{\omega^2 \delta_{im} - c^2 k_i k_m}{\omega^2 - c^2 |\mathbf{k}|^2} i\omega \sigma_{mn}(\mathbf{k}, \mathbf{k}'; \omega) \frac{\epsilon_{nlj} \omega c k'_\ell}{-c^2 |\mathbf{k}'|^2}, \quad (11.14)$$

$$c \frac{dB_{\text{ind}}^i(\mathbf{k}, \omega)}{dE_{\text{ext}}^j(\mathbf{k}', \omega)} = -\frac{1}{\varepsilon_0 \omega^2} \frac{\epsilon_{ikm} \omega c k_k}{\omega^2 - c^2 |\mathbf{k}|^2} i\omega \sigma_{mj}(\mathbf{k}, \mathbf{k}'; \omega), \quad (11.15)$$

$$\frac{dB_{\text{ind}}^i(\mathbf{k}, \omega)}{dB_{\text{ext}}^j(\mathbf{k}', \omega)} = -\frac{1}{\varepsilon_0 \omega^2} \frac{\epsilon_{ikm} \omega c k_k}{\omega^2 - c^2 |\mathbf{k}|^2} i\omega \sigma_{mn}(\mathbf{k}, \mathbf{k}'; \omega) \frac{\epsilon_{nlj} \omega c k'_\ell}{-c^2 |\mathbf{k}'|^2}. \quad (11.16)$$

where ϵ_{ijk} is the Levi-Civita symbol, and we sum over all doubly appearing indices. Importantly, in the above formulae (using a symbolic vector notation),

$$\overleftrightarrow{\chi}_{EE}(\mathbf{k}, \mathbf{k}'; \omega) \equiv \frac{d\mathbf{E}_{\text{ind}}(\mathbf{k}, \omega)}{d\mathbf{E}_{\text{ext}}(\mathbf{k}', \omega)} \quad (11.17)$$

$$= \frac{\delta \mathbf{E}_{\text{ind}}(\mathbf{k}, \omega)}{\delta \mathbf{E}_{\text{ext}}(\mathbf{k}', \omega)} + \frac{\delta \mathbf{E}_{\text{ind}}(\mathbf{k}, \omega)}{\delta \mathbf{B}_{\text{ext}}(\mathbf{k}', \omega)} \frac{\delta \mathbf{B}_{\text{ext}}(\mathbf{k}', \omega)}{\delta \mathbf{E}_{\text{ext}}(\mathbf{k}', \omega)} \quad (11.18)$$

denotes the *total functional derivative* [SS15a, Sct. 4.2] of the induced electric field with respect to the external electric field. Similarly,

$$\overleftrightarrow{\chi}_{EB}(\mathbf{k}, \mathbf{k}'; \omega) \equiv \frac{1}{c} \frac{d\mathbf{E}_{\text{ind}}(\mathbf{k}, \omega)}{d\mathbf{B}_{\text{ext}}(\mathbf{k}', \omega)} \quad (11.19)$$

$$= \frac{1}{c} \frac{\delta \mathbf{E}_{\text{ind}}(\mathbf{k}, \omega)}{\delta \mathbf{B}_{\text{ext}}(\mathbf{k}', \omega)} + \frac{1}{c} \frac{\delta \mathbf{E}_{\text{ind}}(\mathbf{k}, \omega)}{\delta \mathbf{E}_{\text{ext}}(\mathbf{k}', \omega)} \frac{\delta \mathbf{E}_{\text{ext}}(\mathbf{k}', \omega)}{\delta \mathbf{B}_{\text{ext}}(\mathbf{k}', \omega)} \quad (11.20)$$

denotes the total functional derivative with respect to the external magnetic field, etc. These total functional derivatives directly correspond to the physical response functions (see the discussion in Ref. [SS15a, Sct. 6.1]). For example, the dielectric tensor and the (relative) magnetic permeability can be expressed in terms of these as

$$(\overleftrightarrow{\varepsilon}_r)^{-1} = \overleftrightarrow{1} + \overleftrightarrow{\chi}_{EE}, \quad (11.21)$$

$$\overleftrightarrow{\mu}_r = \overleftrightarrow{1} + \overleftrightarrow{\chi}_{BB}. \quad (11.22)$$

We stress again that the above relations between linear electromagnetic response functions are valid for any material, and they include all possible effects of inhomogeneity, anisotropy, relativistic retardation and magneto-electric cross coupling. On the other hand, all standard relations between linear electromagnetic response functions can be rederived in special cases from the Universal Response Relations (see Ref. [SS15a, Sct. 7]). Hence, if combined with the Kubo formalism, the Universal Response Relations lend themselves to the *ab initio* calculation of all linear electromagnetic response functions.

We close this section with the following remark [SS16c]: As the physical response functions necessarily correspond to total functional derivatives, part of the *magnetic* reaction is already contained in the *electric* response function, and vice versa. A naive expression of the induced electric and magnetic fields in terms of the external fields, as often used in the context of bianisotropic media, therefore leads to an overcounting. This raises the delicate question of how the induced electric and magnetic fields can actually be expanded in terms of the physical response functions. For the answer to this question, the interested reader is referred to Ref. [SS15a, Sct. 6.6], where it is shown that there exist three different but equivalent field expansions on the fundamental level.

11.3. Relativistic covariance

On a macroscopic scale, Ohm's law relates the induced electric current density through the *direct conductivity* σ to an externally applied electric field by

$$\mathbf{j}_{\text{ind}} = \sigma \mathbf{E}_{\text{ext}}, \quad (11.23)$$

or through the *proper conductivity* $\tilde{\sigma}$ to the total electric field by

$$\mathbf{j}_{\text{ind}} = \tilde{\sigma} \mathbf{E}_{\text{tot}}. \quad (11.24)$$

In the following, this difference does not play any role, because the transformation properties of the direct and the proper conductivities coincide (for a comparison between direct and proper response functions, see [SS15b, Sct. 2.3]). Microscopically, however, Ohm's law has to be interpreted as a non-local convolution (see e.g. [GV05, Eqs. (3.167) and (3.185)]), i.e.,

$$j_{\text{ind}}^i(x) = \int d^4x' \sigma_{ij}(x, x') E_{\text{ext}}^j(x'). \quad (11.25)$$

From the relativistic point of view, the problem with Ohm's law apparently is that it relates the spatial part \mathbf{j} of the four-vector $j^\mu = (c\rho, \mathbf{j})$ to the spatial three vector $E_i = cF^{0i}$, which is part of the second-rank field strength tensor $F^{\mu\nu} = \partial^\mu A^\nu - \partial^\nu A^\mu$. Hence, it is not obvious how Eq. (11.25) squares with the usual relativistic transformation laws.

To clarify this issue on a fundamental level, we start from the linear relation (11.8) in terms of the fundamental response tensor. This relation is relativistically covariant

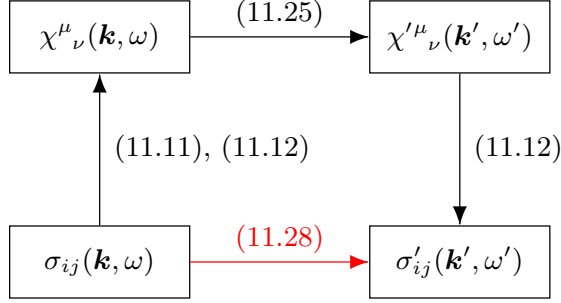


Figure 11.2: Universal relations and transformation laws. The arrow labels refer to equation numbers in the text.

per constructionem, because it relates the relativistic four-vectors j^μ and A^ν . In Ref. [SS16a], we have shown that Ohm's law in the form (11.25) can be *derived* covariantly from Eq. (11.8) and, consequently, Ohm's law holds in every inertial frame. Thereby it is understood that σ_{ij} (just as $\chi^\mu{}_\nu$) obeys a relativistic transformation law itself. This transformation law of the conductivity tensor has been derived explicitly in Ref. [SS16a] from the procedure shown in Fig. 11.2 (assuming homogeneity in space and time): (i) By means of Eq. (11.12), one obtains the spatial part of the fundamental response tensor from the conductivity tensor $\sigma_{ij}(\mathbf{k}, \omega)$ in the unprimed coordinate system, and by Eq. (11.11) one reconstructs from this the whole fundamental response tensor $\chi^\mu{}_\nu(\mathbf{k}, \omega) \equiv \chi(\mathbf{k}, \omega)$. (ii) The fundamental response tensor transforms under a general Lorentz transformation $\Lambda \equiv \Lambda^\mu{}_\nu \in \text{O}(1, 3)$ according to

$$\chi'(\mathbf{k}', \omega') = \Lambda \chi(\mathbf{k}, \omega) \Lambda^{-1}, \quad k' = \Lambda k, \quad (11.26)$$

where $k \equiv k^\mu = (\omega/c, \mathbf{k})^T$ denotes the relativistic four-momentum. (iii) In the primed coordinate system, one invokes again Eq. (11.12) to read out the conductivity tensor $\sigma'_{ij}(\mathbf{k}', \omega')$. The concatenation of these operations leads to a complicated (i.e., non-tensorial) transformation law for the microscopic conductivity tensor under general Lorentz transformations. In particular, for a boost of the form

$$\Lambda(\mathbf{v}) = \begin{pmatrix} \gamma & -\gamma \mathbf{v}^T/c \\ -\gamma \mathbf{v}/c & \overset{\leftrightarrow}{\Lambda} \end{pmatrix}, \quad (11.27)$$

where \mathbf{v} is the velocity of the primed coordinate frame relative to the unprimed frame, $\gamma = 1/\sqrt{1 - |\mathbf{v}|^2/c^2}$, and

$$\overset{\leftrightarrow}{\Lambda} = \overset{\leftrightarrow}{1} + (\gamma - 1) \frac{\mathbf{v} \mathbf{v}^T}{|\mathbf{v}|^2}, \quad (11.28)$$

this transformation law reads as follows:

$$\overset{\leftrightarrow}{\sigma}'(\mathbf{k}', \omega') = \frac{1}{\gamma} \left(1 - \frac{\mathbf{v} \cdot \mathbf{k}}{\omega}\right)^{-1} \overset{\leftrightarrow}{\Lambda} \left(\overset{\leftrightarrow}{1} - \frac{\mathbf{v} \mathbf{k}^T}{\omega}\right) \overset{\leftrightarrow}{\sigma}(\mathbf{k}, \omega) \left(\overset{\leftrightarrow}{1} - \frac{\mathbf{k} \mathbf{v}^T}{\omega}\right) \overset{\leftrightarrow}{\Lambda}. \quad (11.29)$$

This is the most general transformation law for the conductivity tensor, which incorporates all effects of anisotropy and relativistic retardation. In Ref. [SS16a], we have shown that in the special case of a constant, scalar conductivity, this transformation law can be used to rederive the standard textbook generalization of Ohm's law (see e.g. Refs. [Reb12, Sct. 5.3], [Jac99, Problem 11.16], or [Tsa97, Problem 9-15]). Finally, we remark that by a similar logic, one can also derive the relativistic transformation behavior of all other linear electromagnetic response functions (see Ref. [SS17b]).

11.4. Refractive index

Within an *ab initio* context, the standard formula for the refractive index n in terms of the relative permittivity ε_r and the relative permeability μ_r (see e.g. Refs. [BW99; Gri99; Hec02; LL84])

$$n^2 \stackrel{?}{=} \varepsilon_r \mu_r, \quad (11.30)$$

cannot be upheld. This formula is usually deduced from the alleged wave equation for the electric field in the medium (see Refs. [Fox10, Appendix A.2] or [Nol07, Sct. 4.3.1]),

$$\left(\varepsilon_0 \varepsilon_r \mu_0 \mu_r \frac{\partial^2}{\partial t^2} - \Delta \right) \mathbf{E}(\mathbf{x}, t) \stackrel{?}{=} 0. \quad (11.31)$$

However, both this wave equation and the ensuing standard formula for the refractive index have been refuted in Ref. [SS15b]. Instead, it turns out that the fundamental, Lorentz-covariant wave equation for the electromagnetic four-potential as used in plasma physics (see Refs. [Mel08; MM91], and [SS15b, Eq. (4.7)]),

$$\left(\left(-\frac{\omega^2}{c^2} + |\mathbf{k}|^2 \right) \eta^\mu{}_\nu - k^\mu k_\nu - \mu_0 \tilde{\chi}^\mu{}_\nu(\mathbf{k}, \omega) \right) A^\nu(\mathbf{k}, \omega) = 0, \quad (11.32)$$

is equivalent [SS15b] to the simple condition

$$\overleftrightarrow{\varepsilon}_r(\mathbf{k}, \omega) \mathbf{E}(\mathbf{k}, \omega) = 0, \quad (11.33)$$

which means that the electric field component of the wave in the medium lies in the kernel (null-space) of the dielectric tensor. (Note that in Eq. (11.32), $\tilde{\chi}^\mu{}_\nu$ denotes the *proper* fundamental response tensor, which relates the induced four-current to the *total* four-potential; see [SS15b, Eq. (2.50)].) In the *isotropic limit*, the longitudinal and transverse oscillations decouple, and hence we obtain

$$\varepsilon_{r,L}(\mathbf{k}, \omega) \mathbf{E}_L(\mathbf{k}, \omega) = 0, \quad (11.34)$$

$$\varepsilon_{r,T}(\mathbf{k}, \omega) \mathbf{E}_T(\mathbf{k}, \omega) = 0. \quad (11.35)$$

Here, the *longitudinal* and *transverse dielectric functions* are defined by the equality

$$\overleftrightarrow{\varepsilon}_r(\mathbf{k}, \omega) = \varepsilon_{r,L}(\mathbf{k}, \omega) \overleftrightarrow{P}_L(\mathbf{k}) + \varepsilon_{r,T}(\mathbf{k}, \omega) \overleftrightarrow{P}_T(\mathbf{k}), \quad (11.36)$$

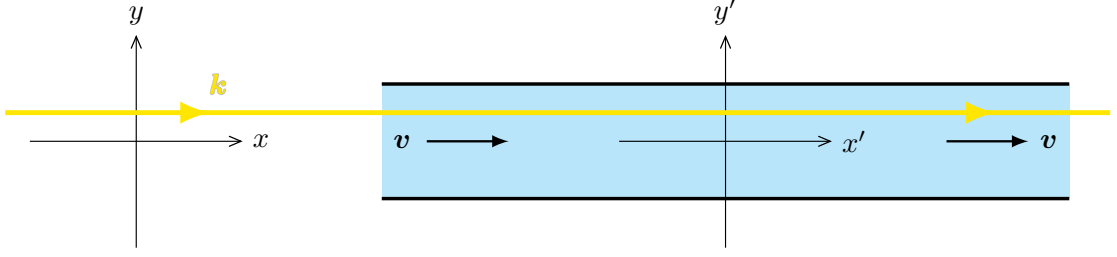


Figure 11.3: Schematic representation of the Fizeau experiment, which established that the speed of light u' in a moving medium is related to the speed u in the medium at rest by $u' = u - v(1 - 1/n^2)$. Here, v denotes the speed of the medium and n its refractive index.

where $P_L(\mathbf{k})$ and $P_T(\mathbf{k})$ denote the longitudinal and transverse projection operators, respectively (see [SS15a, Sct. 2.1]). While Eq. (11.34) describes transverse light waves in the medium, Eq. (11.35) describes the so-called plasmons (see Ref. [MR02, Eq. (4.92)]). Thus, the theory of plasmons combines with the theory of transverse electromagnetic waves in media into one unified wave equation in materials, which is given by Eq. (11.33).

Furthermore, in an *ab initio* context the refractive index is defined from the *dispersion relation* $\omega = \omega_{\mathbf{k}\lambda}$ of the medium. The latter is obtained from the condition

$$\det \overset{\leftrightarrow}{\varepsilon}_r(\mathbf{k}, \omega_{\mathbf{k}\lambda}) = 0, \quad (11.37)$$

which is necessary for having a nontrivial solution of Eq. (11.33). Concretely, the speed of light in materials, $u = u_{\mathbf{k}\lambda}$, is defined as

$$u_{\mathbf{k}\lambda} = \frac{\omega_{\mathbf{k}\lambda}}{|\mathbf{k}|}, \quad (11.38)$$

which generalizes the vacuum relation $c = \omega/|\mathbf{k}|$, and the refractive index is given by

$$n_{\mathbf{k}\lambda} = \frac{c}{u_{\mathbf{k}\lambda}} = \frac{c|\mathbf{k}|}{\omega_{\mathbf{k}\lambda}}. \quad (11.39)$$

In particular, we have shown in Ref. [SS15b, Appendix A] that this definition allows for a straightforward rederivation of the Fizeau result for the refractive index of moving media (see Fig. 11.3).

Conclusion

Thus the Coulomb correlation energy is too big, and can therefore be neglected. If this reason for neglecting Coulomb effects seems odd, remember that we are not trying to explain and predict everything about the solid. We are just trying to understand superconductivity.

R. P. Feynman [[Fey72](#), p. 269]

In this thesis, we have further developed and improved (quantum) field theoretical techniques as they are presently used in materials physics, and we have applied them to models describing the Rashba spin splitting of the bismuth tellurohalides. We consider the main achievements of this thesis—for the articles on which this thesis is based, see p. [xi](#)—to be the following:

Part I (Chapters 1–3).

1. The systematic derivation of the relations between plane-wave functions, Bloch functions, Bloch-like functions, Wannier functions and atomic orbitals in the general case including the spin-orbit coupling (Scts. [1.3–1.4](#)).
2. The straightforward derivation of the Rashba Hamiltonian from symmetry conditions (Sct. [2.2](#), which is in accordance with Ref. [[BAN11](#)]), and the construction of a minimal tight-binding model on the hexagonal lattice which reproduces the Rashba spin splitting near the center of the Brillouin zone (Sct. [2.3](#)).
3. The construction of the “effective single-orbital model” in Sct. [3.3](#), which as a two-band tight-binding model accurately reproduces the spin-split lowest conduction bands of BiTeI.

Part II (Chapters 4–5).

4. The definition of lattice Green functions and the clarification of their relation to the fundamental Green functions (Sct. [4.3](#)).
5. The derivation of the Green function perturbation theory (for temperature Green functions in imaginary time) from their fundamental equations of motion, in particular the straightforward proof of Wick’s theorem (Theorem [4.8](#); Ref. [[SS17a](#)]).

6. The development of Universal Feynman Graphs as a simple and efficient graphical representation which can be universally used for various Green function techniques (Sct. 4.5; for the advantages of these graphs, see p. 106).
7. The simple proof of the Grassmann field integral representation of fermionic Green functions, which uses only the factorization property of the Grassmann–Gaussian integral (Theorem 5.3; Ref. [SS17a]).
8. The detailed and transparent proofs of the Feynman graph expansion of the connected and the one-line-irreducible temperature Green functions, i.e., Theorem 5.7 and Theorem 5.17 (building on the proofs given in Refs. [NO98] and [Zin02]).

Part III (Chapters 6–9).

9. The detailed derivation of the renormalization group equations for the connected and the one-line-irreducible Green functions in Scts. 6.2–6.3 (following the lines of Ref. [SH01] with only very slight simplifications, see the remark on p. 168).
10. The derivation of the explicit renormalization group equations for the momentum-discretized interaction vertex in the refined projection scheme (see the projection ansatz (7.65) and Theorem 7.3, as well as the discussion in Ref. [Sch+16a]).
11. The general solution of the mean-field theory for a time-reversal invariant Hamiltonian $H_{ss'}(\mathbf{k})$ with a singlet superconducting interaction, which generalizes results of Ref. [SU91] to the non-SU(2)-symmetric case (see Sct. 8.4, in particular the Bogoliubov transformation defined by Eqs. (8.87)–(8.88)).
12. The application of the combined functional renormalization and mean-field approach to the Rashba model with an attractive local interaction, and the ensuing prediction of the superconducting interaction, the gap function and the order parameter (Ch. 9 and Ref. [Sch+16a]).

Part IV, Chapter 10. The theoretical description of the following effects in the Rashba semiconductor BiTeI:

13. Optical transitions within the spin-split conduction bands, which are allowed due to the spin-orbit coupling (Sct. 10.1 and Ref. [Lee+11]).
14. The enhanced infrared magneto-optical response, which also results from transitions within the spin-split conduction bands (Sct. 10.2 and Ref. [Dem+12]).
15. The orbital paramagnetic response, which has been predicted in the Rashba model already in Ref. [BR60] and which has been observed experimentally for the first time in BiTeI (Sct. 10.3 and Ref. [Sch+12]).

Part IV, Chapter 11. The systematic development of the Functional Approach to electrodynamics of media in Refs. [SS15a; SS15b; SS16a; SS16b; SS16c]. This approach

constitutes a microscopic field theory of electromagnetic material properties which sits in accordance with *ab initio* physics. In particular, this approach comprises:

16. The Universal Response Relations, which constitute model- and material-independent relations between linear electromagnetic response functions (Sct. 11.2).
17. The proof that Ohm's law is Lorentz covariant, and the ensuing relativistic transformation law for the conductivity tensor (Sct. 11.3).
18. The refutation of the standard formula for the refractive index, $n^2 = \epsilon_r \mu_r$, and its replacement by a microscopic theory of the refractive index, which is based on the dispersion relation as derived from microscopic wave equations for the electromagnetic field in materials (Sct. 11.4).

Finally, we provide a view of a possible first-principles study of the low-temperature properties of BiTeI, which combines several techniques developed in this thesis. One may start from the effective single-orbital model of Sect. 3.3, which accurately describes the dispersion of the two lowest conduction bands of BiTeI. One may add to this an electron-electron interaction obtained from the cRPA method [Ari12; Ary+04] and/or a phonon-mediated interaction as derived in Ref. [SS16b]. This model may be investigated using the combined functional renormalization and mean-field approach developed in Ref. [Sch+16a], which allows one in particular to predict the low-temperature phase diagram and (for a superconducting phase) the gap function as well as the order parameter. Furthermore, from the resulting effective Hamiltonian one may deduce the (wavevector- and frequency-dependent) conductivity tensor by employing the Kubo formalism. This quantity can in turn be used to compute all other linear electromagnetic response properties via the Universal Response Relations [SS15a; SS16c], and in this way to characterize in detail the (possibly superconducting) phases of the material. In summary, we expect the field theoretical techniques developed in this thesis to be useful for an unbiased theoretical description of the low-temperature properties of spin-based correlated materials.

References

- [Akr+14] A. Akrap et al., *Optical properties of BiTeBr and BiTeCl*, [Phys. Rev. B **90**, 035201 \(2014\)](#).
- [All06] P. B. Allen, *Electron transport*, in: S. G. Louie and M. L. Cohen (eds.), *Conceptual foundations of materials: A standard model for ground- and excited-state properties*, Elsevier, Amsterdam, 2006.
- [AM76] N. W. Ashcroft and N. D. Mermin, *Solid state physics*, Harcourt, Inc., Orlando, 1976.
- [Ari12] R. Arita, personal communication, 2012.
- [Ary+04] F. Aryasetiawan et al., *Frequency-dependent local interactions and low-energy effective models from electronic structure calculations*, [Phys. Rev. B **70**, 195104 \(2004\)](#).
- [AS10] A. Altland and B. Simons, *Condensed matter field theory*, 2nd ed., Cambridge University Press, Cambridge, 2010.
- [Ast+07] C. R. Ast et al., *Giant spin splitting through surface alloying*, [Phys. Rev. Lett. **98**, 186807 \(2007\)](#).
- [Bah+12] M. S. Bahramy et al., *Emergence of non-centrosymmetric topological insulating phase in BiTeI under pressure*, [Nat. Commun. **3**, 679 \(2012\)](#).
- [BAN11] M. S. Bahramy, R. Arita, and N. Nagaosa, *Origin of giant bulk Rashba splitting: Application to BiTeI*, [Phys. Rev. B **84**, 041202 \(2011\)](#).
- [BF04] H. Bruus and K. Flensberg, *Many-body quantum theory in condensed matter physics: An introduction*, Oxford University Press, Oxford, 2004.
- [BI98] C. Bruder and Y. Imry, *Orbital paramagnetism of electrons in proximity to a superconductor*, [Phys. Rev. Lett. **80**, 5782 \(1998\)](#).
- [BIPM06] Bureau International des Poids et Mesures, *A concise summary of the international system of units, the SI*, 2006, URL: http://www.bipm.org/utis/common/pdf/si_summary_en.pdf (visited on 2016-08-27).
- [Bla+01] P. Blaha et al., *WIEN2k, an augmented plane wave + local orbitals program for calculating crystal properties*, Karlheinz Schwarz, Techn. Universität Wien, Austria, 2001.

- [Bor+13] S. Bordács et al., *Landau level spectroscopy of Dirac electrons in a polar semiconductor with giant Rashba spin splitting*, *Phys. Rev. Lett.* **111**, 166403 (2013).
- [BR60] I. I. Boiko and E. I. Rashba, *Properties of semiconductors with an extremum loop. II. Magnetic susceptibility in a field perpendicular to the plane of the loop*, *Sov. Phys.–Solid State* **2**, 1692 (1960) [*Fiz. Tverd. Tela* **2**, 1874 (1960)].
- [BTW02] J. Berges, N. Tetradis, and C. Wetterich, *Non-perturbative renormalization flow in quantum field theory and statistical physics*, *Phys. Rep.* **363**, 223 (2002).
- [BW99] M. Born and E. Wolf, *Principles of optics: Electromagnetic theory of propagation, interference and diffraction of light*, 7th ed., Cambridge University Press, Cambridge, 1999.
- [Che+13] Y. L. Chen et al., *Discovery of a single topological Dirac fermion in the strong inversion asymmetric compound BiTeCl*, *Nat. Phys.* **9**, 704 (2013).
- [DD90] S. Datta and B. Das, *Electronic analog of the electro-optic modulator*, *Appl. Phys. Lett.* **56**, 665 (1990).
- [DDJ08] M. S. Dresselhaus, G. Dresselhaus, and A. Jorio, *Group theory. Application to the physics of condensed matter*, Springer-Verlag, Berlin/Heidelberg, 2008.
- [Dem+12] L. Demkó et al., *Enhanced infrared magneto-optical response of the non-magnetic semiconductor BiTeI driven by bulk Rashba splitting*, *Phys. Rev. Lett.* **109**, 167401 (2012).
- [Dir47] P. A. M. Dirac, *The principles of quantum mechanics*, 3rd ed., Oxford University Press, Oxford, 1947.
- [Eat+14] J. W. Eaton et al., *GNU Octave version 3.8.1 manual: A high-level interactive language for numerical computations*, CreateSpace Independent Publishing Platform, 2014, URL: <http://www.gnu.org/software/octave/doc/interpreter>.
- [Ede89] V. M. Edel'shtein, *Characteristics of the Cooper pairing in two-dimensional noncentrosymmetric electron systems*, *Sov. Phys.–JETP* **68**, 1244 (1989) [*ZhETF* **95**, 2151 (1989)].
- [Fey72] R. P. Feynman, *Statistical mechanics: A set of lectures*, W. A. Benjamin, Inc., Reading, 1972.
- [FFK10] H. Fukuyama, Y. Fuseya, and A. Kobayashi, *Transport currents and persistent currents in solids: Orbital magnetism and Hall effect of Dirac electrons*, in: A. Aharony and O. Entin-Wohlman (eds.), *Perspectives of mesoscopic physics: Dedicated to Yoseph Imry's 70th birthday*, World Scientific Publishing Co. Pte. Ltd., Singapore, 2010.

- [FMW95] R. P. Feynman, F. B. Morinigo, and W. G. Wagner, *Feynman lectures on gravitation*, Addison-Wesley Publishing Company, Reading, 1995.
- [Fox10] M. Fox, *Optical properties of solids*, 2nd ed., Oxford University Press, Oxford, 2010.
- [Fuk69a] H. Fukuyama, *Theory of Hall effect. I: Nearly free electron*, *Prog. Theor. Phys.* **42**, 494 (1969).
- [Fuk69b] H. Fukuyama, *Theory of Hall effect. II: Bloch electrons*, *Prog. Theor. Phys.* **42**, 1284 (1969).
- [Fuk70] H. Fukuyama, *A formula for the orbital magnetic susceptibility of Bloch electrons in weak fields*, *Phys. Lett. A* **32**, 111 (1970).
- [FW71] A. L. Fetter and J. D. Walecka, *Quantum theory of many-particle systems*, McGraw-Hill, San Francisco, 1971.
- [Ger+05] R. Gersch et al., *Fermionic renormalization group flow into phases with broken discrete symmetry: Charge-density wave mean-field model*, *Eur. Phys. J. B* **48**, 349 (2005).
- [Gia+09] P. Giannozzi et al., *QUANTUM ESPRESSO: A modular and open-source software project for quantum simulations of materials*, *J. Phys. Condens. Matter* **21**, 395502 (2009).
- [Gri99] D. J. Griffiths, *Introduction to electrodynamics*, 3rd ed., Prentice-Hall, Inc., Upper Saddle River, 1999.
- [GV05] G. F. Giuliani and G. Vignale, *Quantum theory of the electron liquid*, Cambridge University Press, Cambridge, 2005.
- [Hec02] E. Hecht, *Optics*, 4th ed., Addison Wesley, San Francisco, 2002.
- [Hel+11] K. Held et al., *Hedin equations, GW, GW+DMFT, and all that*, in: E. Pavarini et al. (eds.), *The LDA+DMFT approach to strongly correlated materials*, lecture notes of the Autumn School 2011 Hands-on LDA+DMFT, vol. 1 of Schriften des Forschungszentrums Jülich, Reihe Modeling and Simulation, Forschungszentrum Jülich GmbH, Jülich, 2011.
- [ID89] C. Itzykson and J.-M. Drouffe, *Statistical field theory*, vol. 1: From Brownian motion to renormalization and lattice gauge theory, Cambridge University Press, Cambridge, 1989.
- [IEEE16] IEEE Magnetics Society, *Magnetic units*, URL: http://www.ieeemagnetics.org/index.php?option=com_content&view=article&id=118&Itemid=107 (visited on 2016-08-27).
- [Ish+11] K. Ishizaka et al., *Giant Rashba-type spin splitting in bulk BiTeI*, *Nat. Mater.* **10**, 521 (2011).

- [IUCr05] International Union of Crystallography, *International tables for crystallography*, vol. A: Space-group symmetry, Springer, Dordrecht, 2005.
- [Jac99] J. D. Jackson, *Classical electrodynamics*, 3rd ed., John Wiley & Sons, Inc., Hoboken, 1999.
- [Kat04] Y. Katznelson, *An introduction to harmonic analysis*, 3rd ed., Cambridge University Press, 2004.
- [KF96] G. Kresse and J. Furthmüller, *Efficient iterative schemes for ab initio total-energy calculations using a plane-wave basis set*, *Phys. Rev. B* **54**, 11169 (1996).
- [KL65] W. Kohn and J. M. Luttinger, *New mechanism for superconductivity*, *Phys. Rev. Lett.* **15**, 524 (1965).
- [KO56] R. Kubo and Y. Obata, *Note on the paramagnetic susceptibility and the gyromagnetic ratio in metals*, *J. Phys. Soc. Jpn.* **11**, 547 (1956).
- [Koo+09] H. C. Koo et al., *Control of spin precession in a spin-injected field effect transistor*, *Science* **325**, 1515 (2009).
- [Kub57] R. Kubo, *Statistical-mechanical theory of irreversible processes. I. General theory and simple applications to magnetic and conduction problems*, *J. Phys. Soc. Jpn.* **12**, 570 (1957).
- [Kun+10] J. Kuneš et al., *Wien2wannier: From linearized augmented plane waves to maximally localized Wannier functions*, *Comput. Phys. Commun.* **181**, 1888 (2010).
- [Lan30] L. Landau, *Diamagnetismus der Metalle*, *Z. Phys.* **64**, 629 (1930).
- [Lee+11] J. S. Lee et al., *Optical response of relativistic electrons in the polar BiTeI semiconductor*, *Phys. Rev. Lett.* **107**, 117401 (2011).
- [LL84] L. D. Landau and E. M. Lifshitz, *Electrodynamics of continuous media*, 2nd ed., vol. 8 of Course of Theoretical Physics, Pergamon Press Ltd., Oxford, 1984.
- [LMJ96] S. LaShell, B. A. McDougall, and E. Jensen, *Spin splitting of an Au(111) surface state band observed with angle resolved photoelectron spectroscopy*, *Phys. Rev. Lett.* **77**, 3419 (1996).
- [Löw50] P.-O. Löwdin, *On the non-orthogonality problem connected with the use of atomic wave functions in the theory of molecules and crystals*, *J. Chem. Phys.* **18**, 365 (1950).
- [Mah90] G. D. Mahan, *Many-particle physics*, Plenum Press, New York, 1990.

- [Mak+14] A. A. Makhnev et al., *Optical properties of BiTeI semiconductor with a strong Rashba spin-orbit interaction*, *Opt. Spectrosc.* **117**, 764 (2014) [*Optika i Spektroskopiya* **117**, 789 (2014)].
- [Mel08] D. B. Melrose, *Quantum plasmadynamics: Unmagnetized plasmas*, vol. 735 of *Lecture Notes in Physics*, Springer, New York, 2008.
- [Mes62] A. Messiah, *Quantum mechanics*, vol. 2, North Holland Publishing Company, Amsterdam, 1962.
- [Met+12] W. Metzner et al., *Functional renormalization group approach to correlated fermion systems*, *Rev. Mod. Phys.* **84**, 299 (2012).
- [MM91] D. B. Melrose and R. C. McPhedran, *Electromagnetic processes in dispersive media: A treatment based on the dielectric tensor*, Cambridge University Press, Cambridge, 1991.
- [Mos+08] A. A. Mostofi et al., *wannier90: A tool for obtaining maximally-localised Wannier functions*, *Comput. Phys. Commun.* **178**, 685 (2008).
- [MR02] P. A. Martin and F. Rothen, *Many-body problems and quantum field theory: An introduction*, Springer-Verlag, Berlin/Heidelberg, 2002.
- [Mue+16] L. Muechler et al., *Topological metals from band inversion* (2016), arXiv: [1604.01398v2](https://arxiv.org/abs/1604.01398v2) [[cond-mat.mes-hall](https://arxiv.org/archive/cond-mat)].
- [Nit+97] J. Nitta et al., *Gate control of spin-orbit interaction in an inverted In_{0.53}Ga_{0.47}As/In_{0.52}Al_{0.48}As heterostructure*, *Phys. Rev. Lett.* **78**, 1335 (1997).
- [NO98] J. W. Negele and H. Orland, *Quantum many-particle systems*, Westview Press, Boulder, 1998.
- [Nol07] W. Nolting, *Grundkurs Theoretische Physik 3: Elektrodynamik*, 8th ed., Springer-Verlag, Berlin/Heidelberg, 2007.
- [PG15] O. Passon and J. Grebe-Ellis, *Was ist eigentlich ein Photon?*, *Praxis der Naturwissenschaften – Physik in der Schule* **64**, 46 (2015). See also the comments at https://www.researchgate.net/publication/282574316_Was_ist_eigentlich_ein_Photon.
- [PHT13] C. Platt, W. Hanke, and R. Thomale, *Functional renormalization group for multi-orbital Fermi surface instabilities*, *Adv. Phys.* **62**, 453 (2013).
- [Pic12] W. E. Pickett, *“Tight binding” method: Linear combination of atomic orbitals (LCAO)*, lecture notes, UC Davis, 2012, URL: <http://yclept.ucdavis.edu/course/240C/Notes/tb.pdf> (visited on 2016-08-28).
- [Poo+07] C. P. Poole et al., *Superconductivity*, 2nd ed., Elsevier Ltd., Amsterdam, 2007.

- [Pri+10] A. Principi et al., *Many-body orbital paramagnetism in doped graphene sheets*, *Phys. Rev. Lett.* **104**, 225503 (2010).
- [Ras12] E. I. Rashba, *Quantum nanostructures in strongly spin-orbit coupled two-dimensional systems*, *Phys. Rev. B* **86**, 125319 (2012).
- [Ras60] E. I. Rashba, *Properties of semiconductors with an extremum loop. I. Cyclotron and combinational resonance in a magnetic field perpendicular to the plane of the loop*, *Sov. Phys.–Solid State* **2**, 1109 (1960) [*Fiz. Tverd. Tela* **2**, 1224 (1960)].
- [Reb12] E. Rebban, *Theoretische Physik: Relativitätstheorie und Kosmologie*, Springer-Verlag, Berlin/Heidelberg, 2012.
- [RRM07] J. Reiss, D. Rohe, and W. Metzner, *Renormalized mean-field analysis of antiferromagnetism and d-wave superconductivity in the two-dimensional Hubbard model*, *Phys. Rev. B* **75**, 075110 (2007).
- [Rus+15] I. P. Rusinov et al., *Role of anisotropy and spin-orbit interaction in the optical and dielectric properties of BiTeI and BiTeCl compounds*, *JETP Letters* **101**, 507 (2015) [*Pis'ma v Zhurnal Eksperimental'noi i Teoreticheskoi Fiziki* **101**, 563 (2015)].
- [Sak+13] M. Sakano et al., *Strongly spin-orbit coupled two-dimensional electron gas emerging near the surface of polar semiconductors*, *Phys. Rev. Lett.* **110**, 107204 (2013).
- [Sal+04] M. Salmhofer et al., *Renormalization group flows into phases with broken symmetry*, *Prog. Theor. Phys.* **112**, 943 (2004).
- [Sal99] M. Salmhofer, *Renormalization: An introduction*, Springer-Verlag, Berlin/Heidelberg/New York, 1999.
- [Sch+12] G. A. H. Schober et al., *Mechanisms of enhanced orbital dia- and paramagnetism: Application to the Rashba semiconductor BiTeI*, *Phys. Rev. Lett.* **108**, 247208 (2012).
- [Sch+16a] G. A. H. Schober et al., *Functional renormalization and mean-field approach to multiband systems with spin-orbit coupling: Application to the Rashba model with attractive interaction*, *Phys. Rev. B* **93**, 115111 (2016). See also arXiv: [1409.7087 \[cond-mat.str-el\]](#).
- [Sch+16b] S. Schwalbe et al., *Ab initio electronic structure and optical conductivity of bismuth tellurohalides* (2016), arXiv: [1607.06693 \[physics.comp-ph\]](#).
- [Sch06] F. Schwabl, *Statistical mechanics*, 2nd ed., Springer-Verlag, Berlin/Heidelberg, 2006.
- [SH01] M. Salmhofer and C. Honerkamp, *Fermionic renormalization group flows: Technique and theory*, *Prog. Theor. Phys.* **105**, 1 (2001).

- [She+04] S.-Q. Shen et al., *Resonant spin Hall conductance in two-dimensional electron systems with a Rashba interaction in a perpendicular magnetic field*, *Phys. Rev. Lett.* **92**, 256603 (2004).
- [SK12] R. Starke and G. Kresse, *Self-consistent Green function equations and the hierarchy of approximations for the four-point propagator*, *Phys. Rev. B* **85**, 075119 (2012).
- [SK54] J. C. Slater and G. F. Koster, *Simplified LCAO method for the periodic potential problem*, *Phys. Rev.* **94**, 1498 (1954).
- [SMV01] I. Souza, N. Marzari, and D. Vanderbilt, *Maximally localized Wannier functions for entangled energy bands*, *Phys. Rev. B* **65**, 035109 (2001).
- [SS15a] R. Starke and G. A. H. Schober, *Functional approach to electrodynamics of media*, *Phot. Nano. Fund. Appl.* **14**, 1 (2015). See also https://www.researchgate.net/publication/275208133_Functional_Approach_to_Electrodynamics_of_Media.
- [SS15b] R. Starke and G. A. H. Schober, *Microscopic theory of the refractive index*, 2015, arXiv: 1510.03404 [cond-mat.mtrl-sci]. See also https://www.researchgate.net/publication/282843974_Microscopic_Theory_of_the_Refractive_Index.
- [SS16a] R. Starke and G. A. H. Schober, *Relativistic covariance of Ohm's law*, *Int. J. Mod. Phys. D* (2016). See also https://www.researchgate.net/publication/265644297_Relativistic_covariance_of_Ohm%27s_law.
- [SS16b] R. Starke and G. A. H. Schober, *Response theory of the electron-phonon coupling*, 2016, arXiv: 1606.00012 [cond-mat.mtrl-sci]. See also https://www.researchgate.net/publication/303747580_Response_Theory_of_the_Electron-Phonon_Coupling.
- [SS16c] R. Starke and G. A. H. Schober, *Ab initio materials physics and microscopic electrodynamics of media*, 2016, arXiv: 1606.00445 [cond-mat.mtrl-sci]. See also https://www.researchgate.net/publication/303755035_Ab_initio_materials_physics_and_microscopic_electrodynamics_of_media.
- [SS17a] G. A. H. Schober and R. Starke (in preparation).
- [SS17b] R. Starke and G. A. H. Schober (in preparation).
- [SU91] M. Sigrist and K. Ueda, *Phenomenological theory of unconventional superconductivity*, *Rev. Mod. Phys.* **63**, 239 (1991).
- [Tsa97] T. Tsang, *Classical electrodynamics*, World Scientific Publishing Co. Pte. Ltd., Singapore, 1997.

-
- [Vig91] G. Vignale, *Orbital paramagnetism of electrons in a two-dimensional lattice*, *Phys. Rev. Lett.* **67**, 358 (1991).
- [VW90] D. Vollhardt and P. Wölfle, *The superfluid phases of Helium 3*, Taylor & Francis, London, 1990.
- [Wan+06] X. Wang et al., *Ab initio calculation of the anomalous Hall conductivity by Wannier interpolation*, *Phys. Rev. B* **74**, 195118 (2006).
- [Wik16] *Crystal system* – Wikipedia, the free encyclopedia, URL: https://en.wikipedia.org/wiki/Crystal_system (visited on 2016-08-27).
- [Win03] R. Winkler, *Spin-orbit coupling effects in two-dimensional electron and hole systems*, vol. 191 of Springer Tracts in Modern Physics, Springer-Verlag, Berlin/Heidelberg/New York, 2003.
- [Zin02] J. Zinn-Justin, *Quantum field theory and critical phenomena*, 4th ed., Oxford University Press, Oxford, 2002.

Acknowledgments

It is a great pleasure to thank all those who have made the writing of this thesis possible.

First and foremost, I am much obliged to my doctoral supervisor, Manfred Salmhofer, for his continuous support and encouragement through all stages of my study. In addition to his meticulous and thoroughgoing advice to me in this work, I have enjoyed the great benefit of the time he offered me in order to discuss various questions, even if they were not directly related to this thesis.

I am also indebted to Naoto Nagaosa for giving me the opportunity to study as part of his group in the University of Tokyo, and for his tireless enthusiasm and guidance during my stay there. I would also like to thank my student tutor, Atsuo Shitade, for helping me to organize my study and for always being ready to answer my questions.

During recent years, I have benefited greatly from the joint work undertaken with my colleagues, and I am particularly grateful to Ryotaro Arita, Mohammad Saeed Bahramy, Kay-Uwe Giering, Carsten Honerkamp, and Michael Scherer for sharing their knowledge and expertise with me. I further appreciate the helpful suggestions received from Giovanni Vignale during the APS March Meeting 2012.

Special thanks are additionally due to my friend and colleague Ronald Starke for his productive collaboration over the years. In addition, I thank him as well as Elizabeth Corrao and Jonathan Griffiths for critical proofreading of certain parts of this thesis.

I am also exceptionally grateful to Elmar Bittner and Kambis Veschgini for the excellent computer support. Further thanks go to Sonja Bartsch, Cornelia Merkel, Melanie Steiert, and Tae Tokuyoshi for their organizational, administrative and logistic help on any issue.

I have always enjoyed the friendly atmosphere at the Institute “Phil19”, the motivating discussions during the lunch breaks as well as the emotional physics debates with my office mates. For this I would like to thank, in particular, Martin Braß, Tilman Enss, Kay-Uwe Giering, Long Lu, Sabiha Tokus, and Kambis Veschgini.

Grateful acknowledgment is further necessary for the German Academic Exchange Service (DAAD), the Japanese Ministry of Education, Culture, Sports, Science and Technology (MEXT), and the DFG Research Unit FOR723 for their generous financial support.

On a personal note, I wish to thank my parents, my sister, my brother, and Nino for their moral support and understanding, as well as for their distractions necessary for me to maintain my well-being.